

IS AGE JUST A NUMBER?
ACCOUNTING FOR AGE WHEN DESIGNING
VIRAL VECTORS FOR PARKINSON'S DISEASE

By

Nicole Kathleen Polinski

A DISSERTATION

Submitted to
Michigan State University
in partial fulfillment of the requirements
for the degree of

Neuroscience—Doctor of Philosophy

2016

ABSTRACT

IS AGE JUST A NUMBER? ACCOUNTING FOR AGE WHEN DESIGNING VIRAL VECTORS FOR PARKINSON'S DISEASE

By

Nicole Kathleen Polinski

Parkinson's disease (PD) is the second most common neurodegenerative disease with no disease-modifying therapy currently available. Viral vector-mediated gene therapy, however, is being tested in clinical trials as a method to slow disease progression. Although multiple clinical trials have tested the efficacy of this therapy for PD, all strategies have failed to provide adequate relief. Although possibly due to a variety of reasons, failing to consider aging as a covariate in preclinical trials could have contributed to these results. The importance of accounting for age when designing viral vectors for PD stems from the fact that age is the greatest risk factor for developing PD and age-related impairments in cellular processes overlap with steps of viral vector transduction. As a result, I sought to test whether advanced age impacts viral vector transduction efficiency.

In the present dissertation, I tested the efficiency of four viral vector constructs in two systems of the brain involved in PD. Three pseudotypes of recombinant adeno-associated virus (rAAV2/2, rAAV2/5, rAAV2/9) and a lentiviral vector (LV) were chosen due to their use in clinical trials for PD, preclinical trials in PD animal models, or proposed use in clinical trials for PD. These viral vectors were injected into the substantia nigra pars compacta (SNpc) to transduce the nigrostriatal system—the system that degenerates in PD—or the striatum to transduce the striatonigral system—the system most often targeted in viral vector-mediated gene therapy clinical trials for PD.

The first evidence for an age-related transduction deficiency came from observations that rAAV2/5 expressing green fluorescent protein (rAAV2/5 GFP) was deficient in transducing the aged as compared

to young adult rat midbrain and nigrostriatal system two weeks post-injection. I continued this investigation by systematically characterizing the ability of rAAV2/2, rAAV2/5, rAAV2/9, and LV, all expressing GFP, to transduce the aged as compared to young adult rat nigrostriatal and striatonigral systems at one month post-injection when expression levels asymptote. I observed robust age-related deficiencies in the ability of rAAV2/2 and rAAV2/5 to transduce the nigrostriatal and striatonigral systems. Age-related deficiencies were also observed in rAAV2/9 and LV transduction; however, deficiencies were observed in the nigrostriatal but not striatonigral system with LV and vice versa with rAAV2/9. Taken together, these results indicate robust age-related transduction deficiencies that are structure- and vector-specific. The clinical relevance of this finding was investigated to determine whether the viral vector construct used in an upcoming clinical trial is similarly deficient in the aged striatonigral system. I found robust deficiencies in rAAV2/2 overexpressing glial cell line-derived neurotrophic factor (rAAV2/2 GDNF) in the injected striatum as well as in the ipsilateral anterograde structures, suggesting age may negatively impact an upcoming PD clinical trial. Finally, I sought to determine the mechanism of the age-related transduction deficiency of rAAV2/2 in the nigrostriatal system and uncovered a role for cell surface receptors in the deficiency.

Taken together, the results of my experiments highlight the need to account for age when developing therapies for age-related neurodegenerative diseases. Specifically, age can greatly impact the ability of viral vectors to transduce brain systems involved in PD, with robust age-related deficiencies observed across multiple viral vectors, target structures, transgenes expressed, rat strains, and durations of expression. Furthermore, the mechanism of this deficiency may involve virion interactions with cell surface receptors. With this information, future clinical and preclinical studies using viral vectors in the aged brain may be able to circumvent age-related transduction deficiencies and develop a disease-modifying treatment for neurodegenerative diseases like PD.

I would like to dedicate this work
to the two strongest women I know,
June Cummins and Peggy Cummins.
May I continue the legacy you have begun.

ACKNOWLEDGEMENTS

I would first and foremost like to thank my advisor, Caryl Sortwell, for her unfaltering support and guidance during my graduate career. Regardless of the activity, Caryl has always given me her support and help from start to finish and I am forever grateful for her role in shaping me into the scientist and individual that I am today. The members of my committee—Jack Lipton, Fredric Manfredsson, Tim Collier, and Cindy Jordan—also deserve a special thanks for their invaluable advice and feedback that has been incorporated into this work. I would also like to extend my sincere gratitude to the members of the Sortwell lab—Chris Kemp, Luke Fischer, and Megan Duffy—for sharing their knowledge and supporting me through my graduate career. I must also acknowledge the collaborators outside of my committee and lab for their help with these different experiments, especially Matt Benskey, Kathy Steece-Collier, Allyson Cole-Strauss, Joseph Zaia, R. Jude Samulski, and Katrina Paumier. I would like to thank my friends in the TSMC department. It was my friends within the department that kept my spirits up in hard times and made me look forward to coming to work each day.

Finally, I would like to thank the members from the many sides of my family—the Cummins', Polinski's, and Holtzman's. I am the person I am today because of you. Notably, I would like to thank my fiancé, Alex Holtzman. You have always grounded me and when my view became too myopic in my studies, you pushed me to expand my viewpoint to see where I fit in this world and how my work and my person are part of a bigger picture.

PREFACE

At the time of writing this dissertation, one chapter has been published, one chapter is in the submission process, and two chapters are in preparation for submission. Chapter 2 was published in 2015 in *Neurobiology of Aging*. Chapter 1, or a similar review, will be submitted as a chapter for the book entitled “Handbook for Models of Human Aging” published by Academic Press/Elsevier. Chapter 3 was submitted to *Molecular Therapy* and is being edited for resubmission to this journal with the inclusion of the data in Chapter 5.

TABLE OF CONTENTS

LIST OF TABLES	xii
LIST OF FIGURES	xiii
KEY TO ABBREVIATIONS	xv
Chapter 1: Introduction	1
Parkinson’s Disease	1
I. Clinical Description of Parkinson’s Disease	1
II. Parkinson’s Disease Neuropathology.....	2
III. Current Treatment Strategies for Parkinson’s Disease – Addressing PD Symptoms	5
i. Levodopa Treatment.....	6
ii. Dopamine Agonist Treatment	9
iii. Monoamine Oxidase-B Inhibitors.....	9
iv. Deep Brain Stimulation	9
v. Disease Modification in Currently Used Therapies.....	11
Viral Vector-Mediated Gene Therapy	13
I. Recombinant Adeno-Associated Viral Vectors.....	14
i. Steps of AAV Transduction	15
II. Lentiviral Vectors	21
i. Steps of LV Transduction	22
III. Neurotransmitter Replacement Gene Therapy Clinical Trials for PD.....	24
i. GAD Gene Therapy Clinical Trial	25
Mechanism and Preclinical Trials.....	25
Clinical Trial Design and Outcomes.....	29
ii. hAADC-2 Clinical Trial	31
Mechanism and Preclinical Trials.....	31
Clinical Trial Design and Outcomes.....	33
iii. ProSavin Gene Therapy Clinical Trial	34
Mechanism and Preclinical Trials.....	34
Clinical Trial Design and Outcomes.....	37
IV. Trophic Factor Gene Therapy Clinical Trials for PD.....	38
i. Trophic Factors for Neuroprotection in PD	38
Trophic Factor Signaling.....	38
Delivery of Recombinant GDNF	44
Delivery of Recombinant NTN.....	46
Issues with Direct Infusion of Recombinant GDNF/NTN	47
ii. CERE-120 Gene Therapy Clinical Trial	47
Mechanism and Preclinical Trials.....	47
Clinical Trial Design and Outcomes.....	49
iii. Glial Cell Line-Derived Neurotrophic Factor Gene Therapy Clinical Trial	51
Mechanism and Preclinical Trials.....	51
Clinical Trial Design and Outcomes.....	54
Viral Vector Transduction and the Aged Brain	55

I. Potential Impact of Age-Related Changes in the Brain on Viral Vector Transduction	57
i. Changes in the Aged Brain Related to Steps of AAV and LV Transduction.....	57
II. Age-Related Deficits in Transduction Efficiency	60
III. Importance of Accounting for Age in Viral Vector-Mediated Gene Therapy	62
Overarching Conclusions	63
LITERATURE CITED.....	65

Chapter 2: Recombinant adeno-associated virus 2/5-mediated gene transfer is reduced in the aged rat midbrain

Abstract	84
Introduction.....	84
Methods	86
I. Experimental overview.....	86
II. Animals.....	87
III. Viral vectors	87
IV. rAAV2/5 GFP injections.....	88
V. Sacrifice and tissue preparation.....	88
VI. Microdissections	89
i. SD Striatal Tissue for Protein Analyses.	89
ii. F344 Striatal Tissue for Protein Analyses and SN Tissue for RNA Analyses.....	89
VII. Immunohistochemistry.....	90
i. Immunohistochemistry.....	90
ii. TH and GFP Double Label Immunofluorescence	91
VIII. Western blot.....	91
IX. RNA isolation and cDNA synthesis	92
X. GFP qPCR	92
XI. RNAscope <i>in situ</i> hybridization for GFP mRNA	93
XII. Stereology	94
XIII. Counts of GFP and TH immunoreactive cells	94
XIV. Volume of GFPir Mesencephalic Expression	95
XV. Statistical analyses	95
Results.....	96
I. Aging and rAAV2/5 GFP injection do not impact SN pars compacta (SNpc) tyrosine hydroxylase immunoreactive (THir) neuron number	96
II. Aged rats exhibit decreased numbers of transduced cells as compared to young adult rats....	96
III. Reduced exogenous transgene expression in the aged brain spans the entire rostral-caudal mesencephalic axis	100
IV. Aged rats display decreased GFP protein expression in the striatum as compared to young adult rats.....	101
V. Aged rats exhibit decreased levels of GFP mRNA expression as compared to young adult rats....	103
Discussion	103
LITERATURE CITED.....	111

Chapter 3: Impact of Age and Vector Construct on Striatal and Nigral Transduction Efficiency

Abstract	116
Introduction.....	116

Methods	119
I. Experimental Overview	119
II. Animals.....	121
III. Viral Vectors.....	121
IV. Viral Vector Injections.....	122
V. Euthanasia and Tissue Preparation	122
VI. Microdissections	123
i. Striatal Tissue for Protein Analyses (SN-Injected GFP Vectors).....	123
ii. SNpc Tissue for RNA Analyses (SN-Injected rAAV2/2 GFP and rAAV2/9 GFP)	123
iii. SNpr Tissue for Protein Analyses (STR-Injected GFP Vectors)	124
VII. Western Blot.....	124
VIII. Immunohistochemistry	126
i. Immunohistochemistry.....	126
ii. TH and GFP Double Label Immunofluorescence	127
iii. TH and GFP Double Label Near-Infrared Staining.....	127
iv. GFP/NeuN/Glia Immunofluorescence	128
IX. RNA Isolation and cDNA Synthesis.....	129
X. GFP qPCR	129
XI. RNAscope <i>in situ</i> Hybridization for GFP or CBA mRNA	130
XII. Stereology	131
XIII. Counts of GFP and TH Immunoreactive Cells	131
XIV. Counts of GFP/NeuN, GFP/GFAP, and GFP/Iba-1 Immunoreactive Cells	132
XV. Near-Infrared Signal Intensity and Striatal Transduction Area Measurements	132
XVI. Comparisons Between Vectors.....	133
XVII. Statistical Analyses	133
Results	134
I. Transduction efficiency in the nigrostriatal system and midbrain following intranigral injections to the young adult and aged rat	136
i. Age-related decreases in exogenous GFP protein in the nigrostriatal system are observed with rAAV2/2, rAAV2/5, and LV, but not rAAV2/9 intranigral injections	136
ii. Age-related nigrostriatal transduction deficiencies are not reflected by differences in total GFP-positive cells within the mesencephalon	138
iii. Quantification of GFP+/TH+ SNpc neurons reveals fewer GFP+ nigrostriatal dopamine neurons in aged rats injected with rAAV2/2 GFP and LV GFP	138
iv. Age-related decreases in GFP mRNA are observed following intranigral injection with rAAV2/2, rAAV2/5, and LV, but not with rAAV2/9	142
II. Transduction efficiency in the striatonigral system following intrastriatal injections to the young adult and aged rat.....	144
i. Age-related decreases in exogenous GFP protein in the striatonigral system are observed following intrastriatal rAAV2/2, rAAV2/5, and rAAV2/9, but not LV injections	144
ii. Age-related changes in striatonigral transduction efficiency are not detectable by quantitation of GFP+ cells in the striatum.....	146
iii. Evaluation of GFP mRNA expression following intrastriatal injection.....	146
iv. Astrocytes display limited tropism for viral particles in the young adult and aged rat striatum	149
III. Comparisons between rAAV pseudotype transduction efficiency in young adult and aged rat... ..	152

i. rAAV2/9 delivers the most exogenous GFP protein to the nigrostriatal system of both young adult and aged rats	152
ii. rAAV2/5 and rAAV2/9 transduce the greatest numbers of mesencephalic neurons in both young adult and aged rats	154
iii. rAAV2/5 and rAAV2/9 transduce the greatest numbers of TH+ SNpc neurons in young adult and aged rats	154
iv. rAAV2/9 delivers the most exogenous GFP protein to the striatonigral system of both young adult and aged rats	155
i. rAAV2/9 transduces the greatest number of striatal cells in both young adult and aged rats....	155
.....	155
ii. Following intrastriatal vector injections, GFP intensity in the striatum parallels GFP levels in the SNpr	157
iii. rAAV2/9 results in the largest area of striatal transduction in both young adult and aged rats	158
Discussion	159
LITERATURE CITED.....	164

Chapter 4. Age-related deficiencies exist in rAAV2/2 GDNF transduction of the basal ganglia following intrastriatal injection in rats. 171

Abstract	171
Introduction.....	172
Methods	175
I. Experimental Overview	175
II. Animals.....	176
III. Viral Vectors.....	176
IV. Viral Vector Injections.....	178
V. Sacrifice and Tissue Preparation	178
VI. Microdissections	179
i. Tissue for GDNF ELISA (Left Striatum, GP, EP, and SNpr)	179
ii. Tissue for GDNF RNA Analyses (Right Striatum).....	179
iii. Tissue for pS6 Protein Analyses (Left SNpc)	180
VII. GDNF ELISA	180
VIII. RNA Isolation and cDNA Synthesis	181
IX. GDNF qPCR.....	181
X. pS6 Western Blot.....	182
XI. Immunofluorescence	182
i. VMAT2 and pS6 Double Label Immunofluorescence	183
ii. TH/Total S6/pS6 Triple Label Immunofluorescence	183
XII. Intensity Measures for Immunofluorescent Staining	184
XIII. Statistical Analyses	185
Results	185
I. GDNF protein overexpression is lower in the aged vs young adult basal ganglia following intrastriatal rAAV2/2 GDNF injection	186
II. GDNF mRNA overexpression is equivalent between ages.....	188
III. Measures of GDNF downstream signaling activation are greater in the aged versus young adult brain regardless of rAAV2/2 GDNF injection.....	188
Discussion	192
LITERATURE CITED.....	197

Chapter 5: Age-Related Transduction Deficiencies are Rescued by Altered Receptor Binding in the Rat Nigrostriatal System	202
Abstract	202
Introduction	202
Methods	205
I. Experimental Overview	205
II. Animals.....	206
III. Viral Vectors.....	206
IV. Viral Vector Injections.....	207
V. Euthanasia and Tissue Preparation	207
VI. Microdissections	208
VII. Western Blot.....	208
VIII. Immunohistochemistry	209
i. Immunohistochemistry.....	209
ii. TH and GFP Double Label Immunofluorescence	210
IX. Stereology	210
X. Counts of GFP and TH Immunoreactive Cells.....	211
XI. Statistical Analyses.....	211
Results	212
I. No age-related differences occur in total numbers of GFP+ midbrain cells	213
II. rAAV2 GFP transduction is deficient in the aged nigrostriatal system	213
III. rAAV2G9 GFP transduction is not deficient in the aged nigrostriatal system.....	216
Discussion	216
LITERATURE CITED.....	223
Chapter 6. Discussion	226
Conclusions, In Brief	226
Future Directions and Implications for Use of Viral Vectors in Aged Brains	227
I. Characterization of Age-Related Transduction Deficiencies	227
i. Defining Transduction Efficiency	227
ii. Expanding Investigation to other Viral Vector Constructs	230
iii. Expanding Investigation to other Brain Systems and Structures	231
iv. Expanding Investigation to other Species, Ages, and Sexes	233
v. Investigating the Impact of Age and Parkinson’s Disease Pathology on Transduction	234
II. rAAV2/2 GDNF Transduction after Intrastriatal Injection.....	235
III. Mechanism of the Transduction Deficiency	237
i. Receptors.....	237
ii. Downstream Steps of Transduction	245
Final Remarks.....	246
LITERATURE CITED.....	247

LIST OF TABLES

Table 1. List of Receptors and Co-Receptors for Adeno-Associated Virus Serotypes 1-9	16
Table 2. Viral Vector-Mediated Gene Therapy Clinical Trials for Parkinson's Disease	26
Table 3. Percent of GFP+ Transduced Cells Classified by Phenotype following Intraneuronal or Intrastriatal Injection of rAAV2/2, rAAV2/5, rAAV2/9, or LV GFP.....	141
Table 4. AAV2 Mutant Viral Constructs and Implications of Efficient Transduction in the Aged Brain.	232
Table 5. Potential Mechanisms of the AAV Age-Related Transduction Deficiency.....	238
Table 6. Catalogued Attempts at Quantifying AAV2, AAV5, and AAV9 Receptor Levels.....	241

LIST OF FIGURES

Figure 1. Diagram of basal ganglia pathways.....	4
Figure 2. Diagram of AAV transduction mechanism	17
Figure 3. Diagram of LV transduction mechanism	23
Figure 4. Diagram of GDNF/NTN signaling cascades	42
Figure 5. Schematic of experimental design and rAAV2/5 viral vector construct.....	97
Figure 6. GFP immunoreactivity reveals fewer transduced cells in aged rats following rAAV2/5 GFP injection	98
Figure 7. Decreases in exogenous transgene expression in the aged brain span the anterior-posterior (AP) mesencephalic axis.....	99
Figure 8. rAAV2/5-mediated GFP protein expression is diminished in the aged striatum.....	102
Figure 9. rAAV2/5-mediated GFP mRNA expression is diminished in the aged SN.....	104
Figure 10. Steps of recombinant adeno-associated virus (rAAV) transduction and potential impact of the aged brain environment	108
Figure 11. Schematic of experimental design for nigrostriatal and striatonigral rAAV2/2, rAAV2/5, rAAV2/9, or LV GFP transduction experiments	120
Figure 12. Validation of SNpr tissue punch for analysis of anterograde transport in the striatonigral system	125
Figure 13. No age- or vector-related toxicity is observed in the SNpc following injection of rAAV2/2, rAAV2/5, rAAV2/9, or LV.....	135
Figure 14. Viral vector-mediated expression of GFP is reduced in the aged nigrostriatal system with rAAV2/2, rAAV2/5, and LV, but not rAAV2/9	137
Figure 15. Quantitation of GFP-positive cells after intranigral injection does not consistently reveal age-related nigrostriatal transduction deficiencies.....	139
Figure 16. The ratio of neurons and glia expressing GFP does not change with age in the SNpc following intranigral injection.....	140
Figure 17. Evidence for decreased GFP mRNA expression in the aged as compared to the young adult rat midbrain and SNpc following rAAV2/2, rAAV2/5, and LV, but not rAAV2/9 GFP injection to the SNpc..	143

Figure 18. Viral vector-mediated expression of GFP is reduced in the aged striatonigral system with rAAV2/2, rAAV2/5, and rAAV2/9, but not LV	145
Figure 19. Quantitation of GFP-positive cells after intrastriatal injection does not reveal an age-related decrease in striatonigral transduction efficiency.....	147
Figure 20. The ratio of neurons and glia expressing GFP does not change with age in the striatum following intrastriatal injection.....	148
Figure 21. GFP mRNA expression in the aged as compared to the young adult rat striatum following rAAV2/2, rAAV2/9, rAAV2/5, and LV GFP injection to the striatum.....	150
Figure 22. <i>In situ</i> hybridization combined with immunohistochemistry reveals viral particles located within neurons and largely absent within astrocytes in the striatum	151
Figure 23. Comparisons between rAAV2/2, rAAV2/5, and rAAV2/9 in the young adult or aged rat nigrostriatal system	153
Figure 24. Comparisons between rAAV2/2, rAAV2/5, and rAAV2/9 in the young adult or aged rat striatonigral system	156
Figure 25. Schematic of experimental design of rAAV2/2 GDNF striatonigral transduction experiments	177
Figure 26. GDNF protein overexpression is lower in the aged versus young adult rat basal ganglia.....	187
Figure 27. GDNF mRNA levels do not differ between ages one month after rAAV2/2 GDNF injection...	189
Figure 28. pS6 levels are greater in aged versus young adult rat SNpc dopaminergic neurons regardless of rAAV2/2 GDNF injection	191
Figure 29. No age-related differences are observed in total number of GFP+ cells following rAAV2 or rAAV2G9 injection.....	214
Figure 30. rAAV2 is deficient in transducing the aged nigrostriatal system at the injection site, whereas rAAV2G9 is equally as efficient between ages.....	215
Figure 31. Viral vector-mediated expression of GFP is reduced in the aged nigrostriatal system with rAAV2, but not rAAV2G9, in the anterograde structure.....	217
Figure 32. Workflow of the LC-MS proteomics and glycomics analyses by Dr. Joseph Zaia	244

KEY TO ABBREVIATIONS

PD.....	Parkinson's disease
α -syn	alpha synuclein
SNpc	substantia nigra pars compacta
DA.....	dopamine
MRI.....	magnetic resonance imaging
PET	positron emission tomography
SPECT.....	single-photon emission computed tomography
DAT.....	dopamine transporter
VMAT2	vesicular monoamine transporter 2
DDC	DOPA decarboxylase
UPDRS	united Parkinson's disease rating scale
MDS-UPDRS	Movement Disorders Society united Parkinson's disease rating scale
L-dopa	levodopa
TH.....	tyrosine hydroxylase
AADC	aromatic l-amino acid decarboxylase
COMT	catechol-O-methyltransferase
MAO-B.....	monoamine oxidase B
DBS.....	deep brain stimulation
VIM.....	ventral intermedius nucleus
STN	subthalamic nucleus
GPi.....	globus pallidus interna
CoQ10	coenzyme Q10

LV lentivirus
 AAV..... adeno-associated virus
 rAAV recombinant adeno-associated virus
 CMV..... cytomegalovirus
 ITR inverted terminal repeat
 PRE post-transcriptional regulatory elements
 WPRE..... woodchuck hepatitis virus post-transcriptional regulatory elements
 polyA polyadenylation
 CLIC/GEEC clathrin-independent carriers/GPI-enriched endocytic compartment
 HSPG..... heparan sulfate proteoglycan
 PI3K phosphatidylinositol-3 kinase
 PLA phospholipase A2
 PIP₂..... phosphatidylinositol-3,4-biphosphate
 PIP₃..... phosphatidylinositol-3,4,5-triphosphate
 MOTC microtubule organizing center
 NPC..... nuclear pore complex
 ssDNA..... single stranded DNA
 dsDNA double stranded DNA
 LTR..... long terminal repeats
 VSV-G vesicular stomatitis virus glycoprotein G
 GABA gamma-aminobutyric acid
 GAD glutamic acid decarboxylase
 SNpr..... substantia nigra pars reticulata
 6-OHDA 6-hydroxydopamine

NHP non-human primate
 MPTP 1-methyl-4-phenyl-1,2,3,6-tetrahydropyridine
 hAADC human aromatic l-amino acid decarboxylase
 CH1 GTP cyclohydrolase 1
 GDNF glial cell line-derived neurotrophic factor
 NTN neurturin
 TGF β transforming growth factor beta
 GFR α GDNF receptor alpha
 FRS2 fibroblast growth factor receptor substrate 2
 Src tyrosine-kinase Src
 Shc Src-homologous and collagen-like protein
 STAT signal transducers and activators of transcription
 GRB growth factor receptor-bound protein
 MAPK mitogen-activated protein kinase
 Akt protein kinase B
 NF- κ B nuclear factor kappa B
 Bcl-2 B cell lymphoma 2
 JNK c-Jun N terminal kinase
 pS6 phosphorylated ribosomal protein S6
 MNK mitogen-activated protein kinase
 RSK ribosomal protein S6 kinase
 CREB cAMP response element binding protein
 ERK extracellular signal-regulating kinase
 MEK mitogen extracellular signal-regulated kinase

IP3 inositol tri-phosphate 3

AD.....Alzheimer’s disease

IACUCinstitutional animal care and use committee

F344.....Fischer344

CβA.....chicken beta actin

GFPir/GFP+green fluorescent protein immunoreactive

THir/TH+tyrosine hydroxylase immunoreactive

MTN.....medial terminal nucleus of the optic chiasm

APanterior-posterior

DV.....dorsal-ventral

MLmedial-lateral

NGF.....nerve growth factor

PDGFRplatelet derived growth factor receptor

CNS.....central nervous system

vg.....vector genomes

NeuNneuronal nuclei

GFAP.....glia fibrillary acidic protein

Iba-1ionized calcium-binding adapter molecule 1

S100BS100 calcium-binding protein B

MOImultiplicity of infection

EPentopeduncular nucleus

S6.....ribosomal protein S6

ROI.....region of interest

N-GalN-linked galactose

Chapter 1: Introduction

Parkinson's Disease

Dr. James Parkinson first described Parkinson's disease (PD) in 1817 as a "shaking palsy" that exhibits progressive motor impairments in patients [Parkinson, 2002; Goetz, 2011]. Today, PD is the second most common neurodegenerative disease after Alzheimer's disease. PD affects approximately 1 million Americans with only about 10% of cases linked to a genetic cause [de Lau and Breteler, 2006; Klein and Westenberger, 2012; Parkinson's Disease Foundation, 2016]. The remaining 90% of cases are considered sporadic and can sometimes be attributed to environmental toxins such as herbicides, synthetic neurotoxins, or pesticides, but mostly are of unknown origin [de Lau and Breteler, 2006]. For all suspected cases of PD, clinical diagnosis is primarily based on the motor symptoms that manifest in this disease.

I. Clinical Description of Parkinson's Disease

Although not solely a motor disease, a clinical diagnosis of PD is heavily reliant on the motor impairments that present. The most common motor impairments in PD are bradykinesia (slowness of movement), akinesia (difficulty initiating movement), resting tremor, rigidity, and postural instability [Hughes et al, 1993; Gelb et al, 1999]. Although these symptoms are all associated with PD, presentation differs between individuals and the main issues associated with quality of life impairment in PD patients is quite heterogeneous.

In addition to motor impairments, non-motor symptoms are associated with PD as well. These symptoms can appear decades before onset of motor impairments and include sleep disturbances, gastrointestinal dysfunction, orthostatic hypotension, and lost sense of smell, among others [Lee and

Koh, 2015; Visanji and Marras, 2015]. Furthermore, cognitive issues can also be associated with PD. These issues include confusion, memory impairments, depression, slowed thinking, and at advanced stages, dementia [Cooney and Stacy, 2016]. Similar to the heterogeneity of motor impairments in PD patient populations, non-motor and cognitive impairments also vary greatly based on individual.

II. Parkinson's Disease Neuropathology

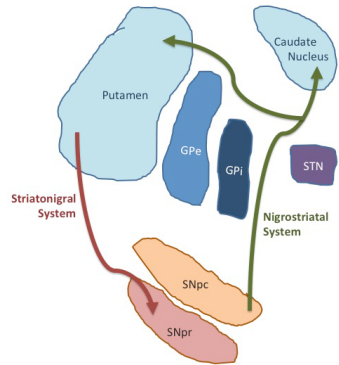
Confirmation of PD diagnosis is made *post mortem* and rests on two key pathological hallmarks in the brain. The first hallmark of PD is the presence of Lewy bodies in surviving neurons within brain regions implicated in PD [Olanow et al, 2009]. Lewy bodies are large intracellular proteinaceous inclusions that contain neurofilaments, ubiquitin, alpha synuclein (α -syn), and other proteins [Goldman et al, 1983; Lowe et al, 1988; Pollanen et al, 1993; Spillantini et al, 1997]. Aggregated α -syn is the protein most often related to PD pathology due to its presence in Lewy bodies and the identification of duplications and triplications in the α -syn gene, *SNCA*, leading to genetic forms of PD [Polymeropoulos et al, 1997; Spillantini et al, 1997; Singleton et al, 2003]. Similarly, Lewy neurites are dystrophic dendrites and axons characterized by proteinaceous inclusions similar to those in Lewy bodies [Braak et al, 1999]. Although commonly thought to be pathogenic, Lewy bodies and Lewy neurites may be a consequence rather than a cause of degeneration in PD; furthermore, some individuals are beginning to investigate the possibility that these inclusions may even be neuroprotective [Gertzel et al, 1994; Kanaan and Manfredsson, 2012].

The second pathological hallmark is the loss of dopaminergic projections in the nigrostriatal system. The nigrostriatal system consists of dopaminergic neurons with cell bodies in the substantia nigra pars compacta (SNpc) projecting to the caudate nucleus and putamen, which are collectively termed the striatum (Figure 1). This system is responsible for supplying dopamine (DA) to the striatum to facilitate desired movements. In PD, the nigrostriatal system degenerates, leading to an imbalance in the basal

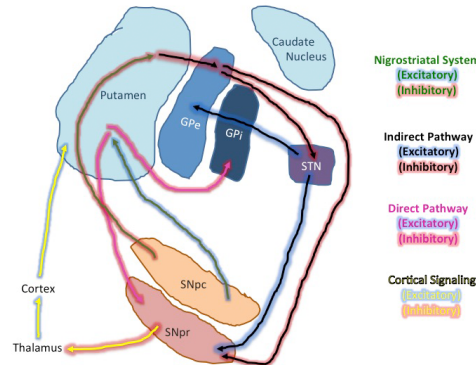
ganglia and the motor symptoms described above. The degeneration of the nigrostriatal system begins with the dying-back of axons of the nigrostriatal system projecting to the striatum and later leads to death of the cell bodies in the SNpc [Burke and O'Malley, 2013]. Importantly, motor symptoms present when 50-60% of the nigrostriatal dopaminergic neurons have already degenerated and the striatum is depleted of 70-80% of the resulting DA [Agid, 1991; Schapira and Obeso, 2006]. Responsiveness of motor symptoms to pharmacological DA replacement therapies consequently forms another basis for diagnosis of PD *in vivo*. However, early stage PD may not respond to DA replacement therapies due to compensatory mechanisms in the striatum and may cause problems with early diagnosis [Schapira and Obeso, 2006]. As a result, focus is now turning towards methods of early diagnosis for PD when striatal innervation remains and before half of the nigrostriatal system has degenerated and motor symptom responsiveness to DA replacement therapies appear.

Advances in brain imaging technologies have allowed more precise and earlier *in vivo* diagnosis of PD. This method is beneficial in that it can allow for earlier diagnosis of PD *in vivo* based on nigral and striatal abnormalities and allow better treatment of PD based on improved accuracy from the 83% accuracy of diagnosis based on motor symptoms [Brooks, 2012; Rizzo et al, 2016]. 7 tesla magnetic resonance imaging (MRI) can detect midbrain structural changes that differentiate between PD and other motor diseases. Positron emission tomography (PET) and single-photon emission computed tomography (SPECT) ligands that target dopamine transporters (DAT), vesicular monoamine transporter 2 (VMAT2), and DOPA decarboxylase (DDC) are currently in development for *in vivo* diagnosis of PD based on structural changes in the brain. Decreased striatal uptake of these markers indicates functional dopaminergic loss and can allow for differentiation between PD, other movement disorders, and healthy controls with as great as 95% specificity [Brooks, 2012].

a Nigrostriatal and Striatonigral System



b Normal Basal Ganglia



c Parkinson's Disease Basal Ganglia

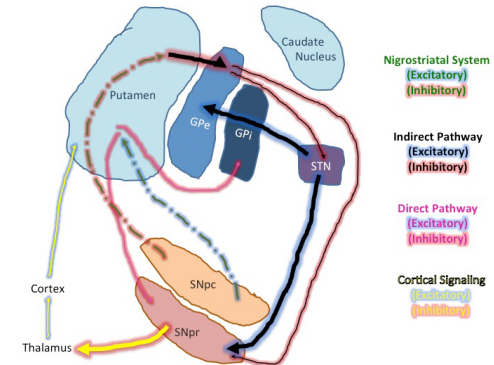


Figure 1. Diagram of basal ganglia pathways. a) Diagram of nigrostriatal system (green) and striatonigral system (red). The nigrostriatal system is composed of excitatory dopaminergic neuron cell bodies in the SNpc that project to the caudate nucleus and putamen (collectively termed striatum). The striatonigral system is composed of inhibitory gamma amino butyric acid (GABA) producing medium spiny neurons (MSNs) that project from the striatum to the SNpr. In later chapters, the nigrostriatal system will be targeted through viral vector injection into the SNpc and quantitation of exogenous protein in the striatum, and the striatonigral will be targeted through viral vector injection into the striatum and quantitation of exogenous protein in the SNpr. b) A simplified, incomplete diagram of the basal ganglia in the normal brain. The nigrostriatal system projects from the SNpc to the striatum (green arrows) and excites the direct (pink arrows) pathway and inhibits the indirect (black arrows) pathway. The direct pathway excites the inhibitory projections from the striatum directly to the GPi and SNpr whereas the indirect pathway inhibits the projects from the striatum to the GPe-STN-SNpr or GPe-SNpr. The SNpr then sends projects to the thalamus, which synapses on the cortex to control movement. Under normal conditions, the direct (excitatory) and indirect (inhibitory) pathways are balanced to allow for controlled movement. c) A modified diagram of the basal ganglia that shows the result of Parkinson's disease degeneration of the nigrostriatal system and resulting basal ganglia signaling dysregulation. In Parkinson's disease, the degenerating nigrostriatal system reduces dopaminergic signaling to the striatum. This reduces inhibitory feedback to the SNpr through the direct pathway (and thus more activation through less inhibition) and increases excitatory feedback from the STN or reduced inhibitory feedback from the GPe through the indirect pathway (and thus more direct activation or more activation through less inhibition). This leads to more activation of the inhibitory projections from the SNpr to the thalamus and the presence of motor symptoms like akinesia and bradykinesia. Abbreviations: SNpr, substantia nigra pars reticulata; SNpc, substantia nigra pars compacta; GPe, globus pallidus externa; GPi, globus pallidus interna; STN, subthalamic nucleus. Blue halos around the arrows designate excitatory effects whereas red halos designate inhibitory effects.

Although diagnosis of PD is made based on motor symptoms and nigrostriatal degeneration, pathology related to PD also occurs in brain regions outside of the SNpc and basal ganglia. The catecholaminergic systems of the brain are subject to degeneration in PD, including catecholaminergic neurons of the locus coeruleus, raphe nucleus, and nucleus basalis of Meynert [Jellinger, 1999; Braak *et al*, 2003].

Importantly, the progression of PD has been proposed to follow specific stages of advancing pathology in various brain regions [Braak *et al*, 2003]. This progression, called the Braak Staging Hypothesis, involves PD pathology beginning in the dorsal motor nucleus and progressing upwards to involve the coeruleus, substantia nigra, temporal mesocortex, premotor and sensory areas, and finally the high-order sensory association and prefrontal areas [Braak *et al*, 2003]. The progressive degeneration of these various non-motor areas are thought to underlie the numerous non-motor symptoms of PD that begin before motor symptoms and continue to develop with disease severity.

III. Current Treatment Strategies for Parkinson's Disease – Addressing PD Symptoms

Although many new therapeutic strategies for PD are currently undergoing research and development, a few standard treatment options exist based on the patient's demographics and chief symptoms.

Importantly, all of these therapies are only able to provide symptomatic treatment and do not slow or halt disease progression. Disease progression and efficacy of treatments are quantified using the United Parkinson's Disease Rating Scale (UPDRS), with lower scores indicating less motor impairment [Movement Disorder Society Task Force on Rating Scales for Parkinson's Disease, 2003]. The UPDRS has four subscales that assess I) mood and behavior, II) activities of daily living, III) motor performance, and IV) complications of therapy [Movement Disorder Society Task Force on Rating Scales for Parkinson's Disease, 2003; Shulman *et al*, 2016]. Although UPDRS does not adequately assess all non-motor symptoms of PD, the modified Movement Disorders Society UPDRS (MDS-UPDRS) or coupling the UPDRS with additional questionnaires and exams for non-motor symptoms such as depression can provide a

good indication of disease progression, treatment efficacy, and unintended consequences of treatments [Movement Disorder Society Task Force on Rating Scales for Parkinson's Disease, 2003; Goetz et al, 2008; Shulman et al, 2016].

Importantly, the placebo effect is a very common influential factor in PD. Many patients experience the placebo effect as determined by a significant improvement in UPDRS scores following placebo administration. In a meta-analysis of PD clinical trials, the overall placebo response rate was approximately 16% as determined by patients experiencing at least 50% improvement in the motor UPDRS subsection as compared to baseline [Goetz *et al*, 2008]. Furthermore, stronger interventions, such as surgical sham treatments, result in greater placebo effects than less-invasive interventions [Lidstone, 2014]. The placebo effect of PD is not only present in UPDRS scores—which could be influenced by subjective self-rating of motor function, activities of daily living, and cognitive/emotional experiences—but can also be observed through increased dopamine responsiveness in the striatum [de la Fuente-Fernandez *et al*, 2001; de la Fuente-Fernandez *et al*, 2004; Lidstone *et al*, 2010]. These increases in striatal dopamine are due to activation of reward pathways and result from expectation of clinical benefit as well as physiological dopamine depletion in the motor striatum and can lead to motor improvements with placebo treatment [Lidstone *et al*, 2010; Lidstone, 2014]. This creates a need to determine the impact of the placebo effect in treatments and clinical trials for PD.

i. Levodopa Treatment

Since the discovery of reduced DA in the striatum of PD patients in 1960 and the subsequent test of the DA precursor levodopa (L-dopa) to replenish DA levels in PD patients in 1967, L-dopa has been the gold standard for symptomatic treatment of PD motor symptoms for nearly 50 years [Lees et al, 2015]. L-dopa (L-3,4-dihydroxyphenylalanine) has long been considered the most efficacious drug in eliminating

the motor symptoms of PD. L-dopa is most often administered orally, but can also take the form of an injection, nasal spray, or intestinal gel [Jankovic and Aguilar, 2008].

Endogenous L-dopa is produced through the conversion of tyrosine to L-dopa by tyrosine hydroxylase (TH). L-dopa is then converted to DA by aromatic acid decarboxylase (AADC) and is packaged into vesicles for release. Oral L-dopa is absorbed through the gut and crosses the blood brain barrier through the large neutral amino acid transporter. Once in the brain, L-dopa is converted to DA in AADC-containing neurons such as the SNpc dopaminergic neurons or serotonergic neurons of the raphe nucleus. Various additional drugs are commonly administered with L-dopa to increase the efficiency of this process. These include AADC inhibitors to block peripheral DA decarboxylase (e.g. Benserazide and Carbidopa) or catechol-O-methyltransferase (COMT) inhibitors to increase L-dopa bioavailability to cross the blood brain barrier, delay degradation, and reduce L-dopa dosage (e.g. Tolcapone and Entacapone) [Jankovic, 2002; Jankovic and Aguilar, 2008].

Although L-dopa greatly reduces the motor symptoms of PD and is the most commonly prescribed PD symptomatic drug, debate exists on when to start L-dopa treatment [Aminoff, 2006; Schapira and Obeso, 2006]. Traditionally, physicians advised delaying administration of L-dopa until PD-related motor impairments significantly interfered with activities of daily life, especially in cases of early onset PD (<50 years of age). The rationale behind this recommendation stems from the loss of effectiveness of L-dopa treatment with time and the significant motor side effects associated with this drug [Aminoff, 2006; Schapira and Obeso, 2006]. Within 5 years of beginning L-dopa treatment, the majority of PD patients will experience significant motor complications and fluctuations resulting from this drug [Ahlskog and Muenter, 2001; Jankovic, 2002]. This complication is due to the natural progression of PD and continued loss of striatal DA terminals that are needed for successful conversion of L-dopa to DA.

Major side effects of L-dopa treatment include levodopa-induced dyskinesias, psychiatric problems, and wearing-off effects. Dyskinesias are involuntary movements such as chorea, dystonia, and myoclonus. Although these motor complications can be debilitating and painful, many PD patients prefer L-dopa-induced motor complications to the PD-related motor symptoms [Jankovic, 2002]. Psychiatric problems associated with L-dopa treatment include punding (intense fascination with repetitive examining or sorting objects), hallucinations, delusions, and hypersexuality [Jankovic, 2002]. Wearing-off effects of chronic L-dopa treatment are also caused by the continued loss of striatal dopaminergic terminals in PD or changes in peripheral pharmacokinetics. Wearing-off is characterized by a shorter window of treatment benefit, the need to increase L-dopa dose, and more unpredictability between times on L-dopa and off L-dopa [Jankovic, 2002]. These fluctuating motor responses, however, can be reduced by switching from oral administration of L-dopa to levodopa-carbidopa intestinal gel (DuoDOPA) [Wirdefeldt *et al*, 2016].

Furthermore, some hesitation to prescribe L-dopa in early stages of PD stems from a claim that L-dopa may be toxic to the basal ganglia. This theory is based on the increased DA levels caused by L-dopa which may be excitotoxic if not properly packaged and metabolized. These claims, however, have never been substantiated in patients. In fact, in the clinical ELLDOPA study, patients who were naïve to PD treatment were assigned treatment with a placebo or three escalating doses of L-dopa for nine months. Following treatment and a two-week washout period, patients assigned L-dopa therapy displayed better UPDRS scores than patients treated with the placebo [Fahn, 2005; Fahn, 2006]. Although this could indicate L-dopa has neuroprotective effects in PD, it is most likely due to the fact that two weeks is an inadequate amount of time for washout of L-dopa and the UPDRS score benefit is due to lingering effects of the drug [Fahn, 2005; Fahn, 2006; Chan *et al*, 2007].

ii. Dopamine Agonist Treatment

In place of L-dopa, DA agonists are usually the preferred strategy for treatment of early stage PD. DA agonists directly activate DA receptors rather than requiring the additional step of DA synthesis.

Although DA agonists alone do not improve PD motor impairments as well as L-dopa, these drugs are preferred for early stages of dopaminergic therapy due to the concern that L-dopa might be neurotoxic and duration of treatment with L-dopa might increase negative side effects like dyskinesias [Jankovic and Aguilar, 2008; Connolly and Lang, 2014]. In addition, DA agonists may be combined with L-dopa to allow for a reduction in the dose of L-dopa required and, consequently, a reduction in L-dopa-related motor impairments.

iii. Monoamine Oxidase-B Inhibitors

Similar to DA agonists, monoamine oxidase-B (MAO-B) inhibitors are sometimes prescribed in early stages of PD [Yuan et al, 2010]. MAO-B inhibitors work by preventing the breakdown of DA by MAO-B and increasing synaptic DA levels. Unfortunately, MAO-B inhibitors only provide modest benefits for PD motor symptoms and do not impact L-dopa-resistant motor and non-motor symptoms [Yuan et al, 2010]. As a result, MAO-B inhibitors are oftentimes used as an adjunct therapy with L-dopa to decreased breakdown of DA and consequently reduce the required dose of L-dopa [Olanow, 2009; Yuan et al, 2010].

iv. Deep Brain Stimulation

Deep brain stimulation (DBS) is the preferred surgical method of treating PD. First performed in the 1980s, DBS is now preferred over other neurosurgical techniques that were once used for PD, like thalamotomy or pallidotomy [Jankovic and Aguilar, 2008; Moldovan et al, 2015]. In the past, DBS was

only recommended for patients in later stages of disease who did not respond to DA pharmacotherapy or had severe motor complications from L-dopa treatment [Williams et al., 2010; Moldovan et al., 2015]. Today, however, DBS is considered a good treatment strategy for younger patients with shorter disease duration, high response to L-dopa therapy, and the absence of dementia and severe comorbidities [Bronstein et al, 2011; Moldovan et al., 2015].

DBS involves the application of a stimulating electrode to the basal ganglia circuitry to correct aberrant activity. Common targets for high-frequency stimulation include the ventral intermedialis nucleus (VIM) of the thalamus, subthalamic nucleus (STN), and internal globus pallidus (GPi), with the STN targeted most frequently. STN DBS is the most common neurosurgical procedure for PD, leading to improvement in many PD motor symptoms and often a reduction in the need for L-dopa or other DA pharmacotherapies. Targeting the STN and GPi are relatively comparable. A benefit to targeting the STN is that it requires lower electrical power and thus conserves battery lifespans of the stimulation device [Moldovan et al, 2015]. Stimulation of the GPi, however, is more beneficial than STN stimulation in regards to decreasing dyskinesias and appears to reduce depression scores as well [Follett et al, 2010; Moldovan et al, 2015]. Furthermore, VIM stimulation has no effect on dyskinesias, rigidity, or bradykinesia; rather, VIM stimulation greatly reduces tremor symptoms and is thus a good choice for tremor-dominant PD [Moldovan et al, 2015].

The mechanism of action of DBS is still under debate. Some mechanisms that have been speculated include disrupting the basal ganglia network to “jam” the feedback loop from the periphery, acting as a depolarization block, preferentially activating inhibitory neurons, and functionally ablating the region by desynchronizing pathological beta oscillations [Jankovic and Aguilar, 2008; Moldovan et al, 2015; Herrington et al, 2016]. It has also been postulated that the different latencies in symptom relief exerted

by DBS implicates multiple mechanisms of action in the treatment [Herrington et al, 2016]. For instance, the almost instantaneous benefit of DBS on tremor and rigidity could indicate a neuromodulation mechanism, followed by a synaptic plasticity mechanism that targets bradykinesia symptoms hours after stimulation begins, and an anatomical reorganization mechanism as axial symptoms are reduced days to weeks after stimulation begins [Herrington et al, 2016].

There are, however, drawbacks to the use of DBS to treat PD. Some clinical studies have indicated a possible worsening of depressive symptoms and fatigue after STN DBS [Follett et al, 2010; Okun et al, 2012], although other studies have reported a decrease in depressive symptoms following DBS [Combs et al, 2015]. In addition, STN stimulation-related complications in speech and cognition can occur but may be controlled by altering stimulation parameters [Benabid et al, 2009; Combs et al, 2015].

Furthermore, elective neurosurgery for the treatment of PD should be performed by a surgeon and hospital experienced in this technique, causing limited availability.

v. Disease Modification in Currently Used Therapies

Although the FDA-approved treatments for PD can greatly reduce PD symptomatology, no approved therapy has been able to unequivocally demonstrate neuroprotection [Olanow, 2009; de la Fuente-Fernandez et al, 2010]. Numerous clinical trials have tried to elucidate potential neuroprotective effects of L-dopa, DA agonists, and MAO-B inhibitors. The first of these studies was the DATATOP study that investigated the potential neuroprotective effects of two MAO-B inhibitors in patients [Shoulson, 1989]. In this study, patients naïve to PD treatment received either deprenyl, tocopherol, deprenyl and tocopherol, or a placebo for nine months with UPDRS scores obtained after a one month washout period [Shoulson, 1989]. Although the authors concluded that deprenyl was neuroprotective due to better UPDRS scores compared to placebo [Shoulson, 1989], the benefit was actually due to the short

washout period and the symptomatic effects of the MAO-B inhibitor [Jankovic and Aguilar, 2008; Olanow, 2009; de la Fuente-Fernandez et al, 2010; Lew, 2011]. A revised version of this study was the ADAGIO study in 2009 to test the possible neuroprotective effects of the MAO-B inhibitor rasagiline [Olanow et al, 2009]. Although this study did benefit from a delayed-start design to parse out symptomatic from neuroprotective effects, the design was not blinded in the second phase and the improvement in UPDRS scores can be explained by the placebo effect [de la Fuente-Fernandez et al, 2010].

Two other clinical trials were completed in 2002 and 2003 to investigate the neuroprotective effects of DA agonists. The first of these was the CALM-PD-CIT study in 2002 that used DAT neuroimaging to assess the progression of PD following treatment with the DA agonist pramipexole or L-dopa as a control [Parkinson Study Group, 2002]. Similarly, in 2003 the REAL-PET study compared fluorodopa uptake as a marker of striatal impairment after treatment with the DA agonist ropinirole or L-dopa as a control [Whone et al, 2003]. In both cases, authors concluded that the DA agonist was neuroprotective as it was associated with slower rates of PD progression. However, neither group contained a placebo control and later analyses of these studies indicate differences in drug interactions with the imaging biomarkers causing a false-positive [Olanow, 2009; de la Fuente-Fernandez et al, 2010].

Furthermore, L-dopa and DBS have also been evaluated for neuroprotective effects. As mentioned previously, the ELLDOPA study in 2005 investigated the neurotoxic or neuroprotective effects of L-dopa treatment versus placebo after nine weeks of treatment and two weeks washout [Fahn, 2005]. Although UPDRS scores were better following L-dopa as compared to placebo, this is likely due to symptomatic effects of the drug that would have been eliminated after a longer washout period [Fahn, 2005; Fahn, 2006; Chan et al, 2007]. DBS is also thought to have symptomatic rather than neuroprotective effects in

PD patients [Olanow, 2009]. Although no clinical trials have investigated the neuroprotective effects of DBS, comparative studies and prediction models of DBS effects do not show and modification of disease progression in either motor or non-motor symptoms of PD [Tsai et al, 2009; Yuan et al, 2010].

This lack of a treatment that can slow, halt, or reverse the progression of PD has led to continued efforts to develop new therapeutics that are disease-modifying. These include targeting oxidative stress with antioxidants like coenzyme Q10 (CoQ10) [NINDS NET-PD Investigators, 2007; Parkinson Study Group QE3 Investigators, 2014; Yoritaka et al, 2015] and inosine [Parkinson Study Group SURE-PD Investigators, 2014], stem cell therapy [Freed et al, 2003; Venkataramana et al, 2010], viral vector-mediated gene therapy (see below), and others.

Viral Vector-Mediated Gene Therapy

Viral vector-mediated gene therapy is currently being tested in a variety of neurodegenerative diseases [O'Connor and Boulis, 2015, Choudhury *et al*, 2016]. This therapy uses a virus' innate ability to infect cells and introduce foreign genes. However, viral vectors for gene therapy are "guttled" to remove pathogenic and replicative portions of the virus to merely create a vehicle to deliver a transgene of interest. The most common viral vectors used in the central nervous system are lentivirus (LV) and adeno-associated virus (AAV) as these vectors can transduce dividing and non-dividing cells [O'Connor and Boulis, 2015, Choudhury *et al*, 2016]. Although concerns surround the immune response generated by the infusion of viral vectors, the inflammation triggered by these viral constructs is generally short-lived and limited [O'Connor and Boulis, 2015, Choudhury *et al*, 2016]. As a result, viral vectors are considered safe and well-tolerated in multiple species and have been approved for use in patients.

I. Recombinant Adeno-Associated Viral Vectors

Recombinant AAV (rAAV) is a “guttled” form of the parvovirus AAV in which the replicative and pathogenic portions of the virus are removed and a gene of interest is inserted [Choudhury *et al*, 2016]. rAAV is composed of an icosahedral capsid approximately 22-26nm in diameter containing a linear single-stranded DNA genome [Nonnenmacher and Weber, 2012]. The genome is composed of the gene of interest, promoter to drive gene expression, and is flanked by two inverted terminal repeats (ITRs) that are T-shaped portions of the viral genome required for packaging the genome into capsids, stabilizing the genome, and efficient transcription [Schultz and Chamberlain, 2008; Nonnenmacher and Weber, 2012]. Additional elements can be added to improve transduction efficiency as well. Enhancing elements like cytomegalovirus (CMV) increase expression by improving transcription with additional transcription binding sites, post-transcriptional regulatory elements (PREs) like that of the Woodchuck Hepatitis Virus (WPRE) can increase expression by improving nuclear export and preventing silencing of transgenes, or polyadenylation (polyA) signal upstream enhancers to improve transduction efficiency by improving nuclear export, translation, and mRNA stability [Powell *et al*, 2015].

Numerous different rAAVs have been isolated in nature, each with a distinct capsid and ITR sequence. These different rAAVs, denoted as serotypes, display different tissue tropism based on capsid shape, residue, and binding sites [Schultz and Chamberlain, 2008]. Furthermore, combining the ITR sequence from one rAAV subtype with the capsid of a different rAAV subtype can alter the tropism further, producing what is called a viral pseudotype [Schultz and Chamberlain, 2008]. Numerous viral vector serotypes and pseudotypes have been tested in the central nervous system, with differences in tropism for different cell types and brain regions reported [Burger *et al*, 2004; Paterna *et al*, 2004; McFarland *et al*, 2009; Dodiya *et al*, 2010; Markakis *et al*, 2010; van der Perren *et al*, 2011]. These differences in

tropism can be attributed to the fact that the capsids of each rAAV serotype bind to different receptors and co-receptors on cells (Table 1) [Schultz and Chamberlain, 2008; Nonnenmacher and Weber, 2012].

rAAV is commonly used for viral vector-mediated gene therapy due to the tropism of the various serotypes and favorable safety profile. As mentioned previously, choosing the appropriate promoter and rAAV serotype/pseudotype can control the spread of transduction and types of cells transduced. In addition, rAAV is suitable for viral vector-mediated gene therapy and *in vivo* gene delivery due to its ability to transduce mitotic and post-mitotic cells, low immunogenicity, and lack of integration into the host chromosome which can have unintended consequences such as gene disruption or oncogenicity. Furthermore, rAAV can be produced in large quantities and high titers, further improving the practical utility of this viral construct. Unfortunately, the small packaging capacity (4.5kb) of rAAV can hinder some applications of this virus as the gene of interest may exceed this capacity. Current efforts are underway to overcome this challenge by producing functional, condensed versions of the transgene or using a dual rAAV system that splits an oversized transgene between two vectors delivered simultaneously for reconstitution of the gene upon delivery [Choudhury *et al*, 2016].

i. Steps of AAV Transduction

The first step of AAV infection of cells is binding of the virion to cell surface receptors and co-receptors (Figure 2, Step 1). The capsid of each AAV serotype associates with specific receptors and co-receptors that vary based on the receptor-binding motifs on the capsid proteins of the different serotypes. A list of the receptors and co-receptors believed to be involved in the attachment and internalization of AAV1-9 are located in Table 1. In general, the primary receptor used by AAV is a proteoglycan-conjugated receptor (heparan sulfate proteoglycan (HSPG) for AAV2, AAV3, and AAV6) or an O-linked or N-linked sugar (O-linked for AAV4, N-linked for AAV1, AAV5, AAV6, and AAV9) [Nonnenmacher and Weber,

Table 1. List of Receptors and Co-Receptors for Adeno-Associated Virus Serotypes 1-9

AAV Serotype	Primary Receptors	Co-Receptors
AAV1	N-linked sialic acid [Wu <i>et al</i> , 2006]	Unknown
AAV2	HSPG [Summerford and Samulski, 1998]	FGFR1 [Qing <i>et al</i> , 1999]
		c-Met [Kashiwakura <i>et al</i> , 2005]
		α V β 5 integrin [Summerford <i>et al</i> , 1999]
		LamR [Akache <i>et al</i> , 2006]
		150kDa glycoprotein [Mizukami <i>et al</i> , 1996]
AAV3	HSPG [Rabinowitz <i>et al</i> , 2002]	FGFR1 [Blackburn <i>et al</i> , 2006]
		HGFR [Ling <i>et al</i> , 2010]
		LamR [Akache <i>et al</i> , 2006]
AAV4	O-linked sialic acid [Kaludov <i>et al</i> , 2001]	Unknown
AAV5	N-linked sialic acid [Walters <i>et al</i> , 2001]	PDGFR [Di Pasquale <i>et al</i> , 2003]
AAV6	N-linked sialic acid [Wu <i>et al</i> , 2006]	EGFR [Weller <i>et al</i> , 2010]
	HSPG [Ng <i>et al</i> , 2010]	
AAV7	Unknown	Unknown
AAV8	Unknown	LamR [Akache <i>et al</i> , 2006]
AAV9	N-linked galactose [Shen <i>et al</i> , 2012]	LamR [Akache <i>et al</i> , 2006]
All AAV1-9	AAVR [Pillay <i>et al</i> , 2016]	Unknown

Abbreviations: AAV, adeno-associated virus; HSPG, heparan sulfate proteoglycan; AAVR, adeno-associated virus receptor; FGFR1, fibroblast growth factor receptor 1; HGFR, hepatocyte growth factor receptor; c-Met, hepatocyte growth factor receptor c-Met; LamR, laminin receptor; HGFR, hepatocyte growth factor receptor; PDGFR, platelet-derived growth factor receptor; EGFR, epidermal growth factor receptor.

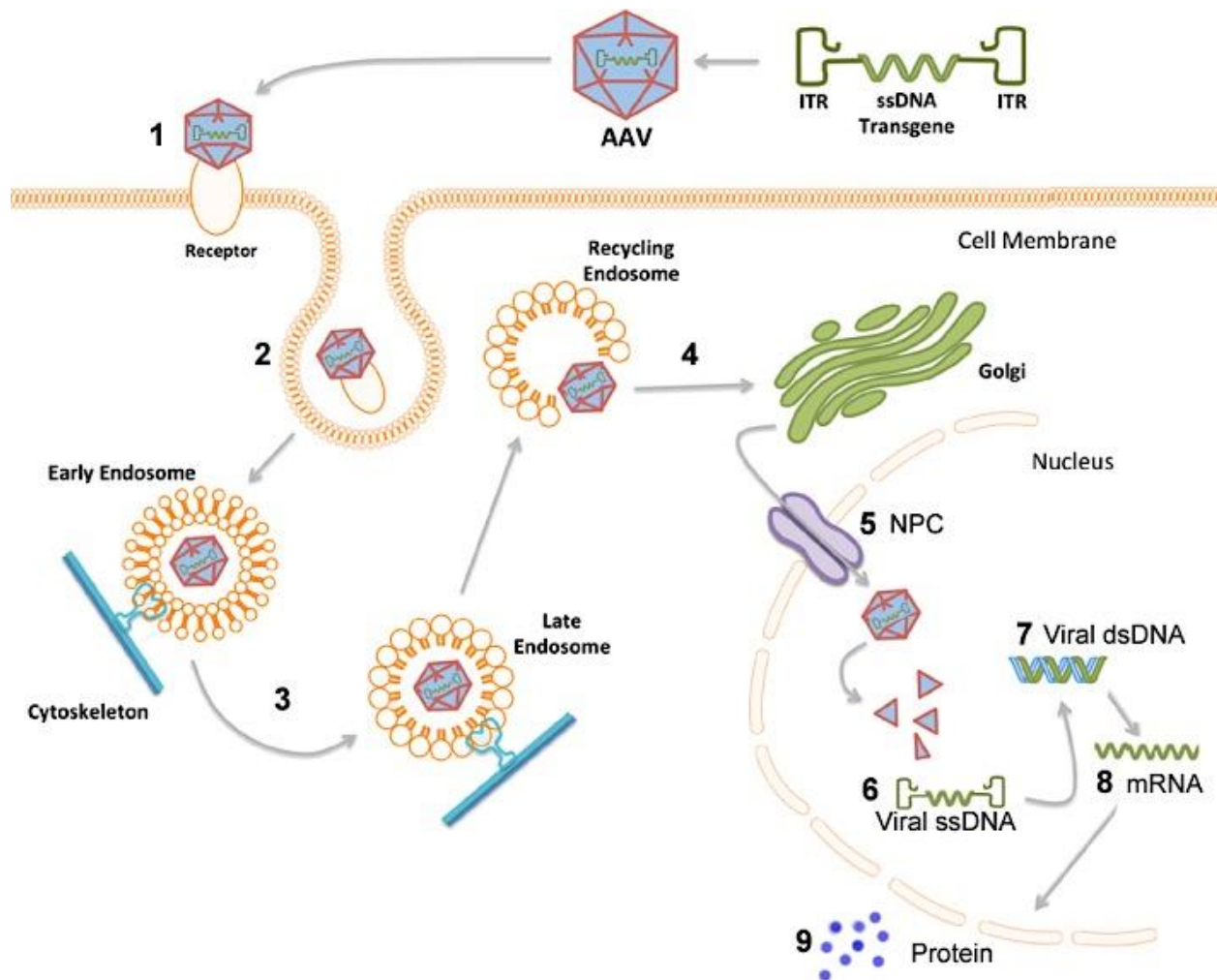


Figure 2. Diagram of AAV transduction mechanism. A single stranded DNA (ssDNA) expression cassette of interest is flanked by inverted terminal repeats (ITRs) to make up the recombinant genome is packaged into rAAV capsid. 1) Injected rAAV capsids bind to designated cell surface receptor and co-receptors. 2) Endocytosis of the viral particle occurs through clathrin coated pits or calveolar endocytosis. 3) The rAAV capsid is trafficked through the cytoskeleton by dynamin in early, late, and recycling endosomes; acidification processes within the endosomes initiate capsid breakdown and genome release. 4) The viral particle is released from the endosome into the cytoplasm for golgi-mediated capsid processing. 5) The viral particle is internalized into the nucleus through the nuclear pore complex (NPC). 6) The ssDNA genome is released from the viral capsid. 7) Viral ssDNA is converted to double stranded DNA (dsDNA) either by strand annealing or by second strand synthesis. 8) Viral dsDNA is converted into mRNA encoded by the transgene. 9) Transgene mRNA is translated into the protein encoded by the transgene. Adapted from the dissertation of Sara Gombash-Lampe.

2012]. The secondary receptor, conversely, is a proteinaceous receptor (Table 1). Although binding and competition assays implicated these receptors and co-receptors in the transduction of their respective AAV serotypes, the necessity of these specific receptors remains up for debate and appears to fluctuate based on experimental design, *in vitro* versus *in vivo* testing, and cell line used [Ding *et al*, 2005; Schultz and Chamberlain, 2008; Nonnenmacher and Weber, 2012]. It is most likely that these receptors and co-receptors are important in viral vector transduction, but alternate receptors and co-receptors may be used in specific instances [Nonnenmacher and Weber, 2012].

Once bound to cell surface receptors and co-receptors, viral particles undergo endocytosis to enter the cells (Figure 2, Step 2). The penetration efficiency, as defined by the number of viral-cell contacts versus internalization events, is approximately 13% [Seisenberger *et al*, 2001; Schultz and Chamberlain, 2008]. Regardless of this low number, AAV endocytosis into cells is very rapid and occurs within 100ms, with some reports estimating the totality of viral particles bound to the cell membrane able to be internalized within 30-60 min [Bartlett *et al*, 2000; Seisenberger *et al*, 2001]. A number of mechanisms have been proposed for the endocytosis of the different AAV serotypes. Internalization of AAV is thought to predominantly occur through clathrin-mediated endocytosis, although caveolae-mediated endocytosis, clathrin-independent carriers/GPI-enriched endocytic compartment (CLIC/GEEC) endocytosis, and phagocytosis have also been proposed [Sanlioglu *et al*, 2001; Nonnenmacher and Weber, 2012]. Studies on transduction mechanisms of AAV have primarily been performed using AAV2 as this was the first AAV cloned and it is able to efficiently transduce common cell lines *in vitro* [Nonnenmacher and Weber, 2012]. For these reasons, most of what is known about AAV transduction is based on AAV2 transduction and that will be the focus of the remainder of this section.

Although still under debate, AAV2 endocytosis is believed to primarily begin when AAV2 binds the HSPG primary receptor and $\alpha\text{V}\beta\text{5}$ integrin co-receptor [Ding *et al*, 2005; Sanlioglu *et al*, 2000]. This activates the intracellular small GTP-binding protein Rac1, which initiates endocytosis of receptor-bound AAV2 [Sanlioglu *et al*, 2000]. Activation of Rac1 subsequently activates phosphatidylinositol-3 kinase (PI3K) that allows the endocytosed virus to traffic along microtubules to the nucleus [Sanlioglu *et al*, 2000]. Dynamin has also been implicated in the endocytosis of AAV2 as a GTPase that regulates the pinching off of clathrin-coated vesicles from the cell membrane [Duan *et al*, 1999; Bartlett *et al*, 2000]. The involvement of these proteins in AAV2 endocytosis, however, is still under debate as studies have reported conflicting results on the impact of overexpressing or inhibiting these proteins [Nonnenmacher and Weber, 2012]. It is entirely possible that multiple mechanisms are available for virion endocytosis based on the viral receptors and co-receptors used, as well as the cell type being transduced. Nevertheless, it appears clathrin-mediated endocytosis is the most common mechanism of entry, with AAV2 binding to HSPG and $\alpha\text{V}\beta\text{5}$ activating Rac1 for endocytosis and PI3K for trafficking to the nucleus.

Once inside cells, viral particles are located inside of endosomes and undergo the necessary step of endosomal processing (Figure 2, Step 3). Endosomal processing is a key step in viral vector transduction. A paramount study by Sonntag and colleagues found that microinjecting viral particles into the cytoplasm or directly into the nucleus resulted in a clear lack of transduction [Sonntag *et al*, 2006]. Rather, AAV capsids undergo a conformational change in endosomes whereby the N-terminal domain of the VP1 and VP2 capsid proteins transition from inside the viral particle to outside the capsid [Sonntag *et al*, 2006]. These domains contain basic residues and a phospholipase A2 (PLA) domain that together act as nuclear localization signals and are necessary for endosomal escape, nuclear localization, and transduction [Kronenberg *et al*, 2005; Sonntag *et al*, 2006; Stahnke *et al*, 2011]. This viral processing in

endosomes is a result of endosomal acidification and processing by endosomal proteins such as cathepsins [Sonntag *et al*, 2006; Akache *et al*, 2007].

Viral particles are also trafficked to the golgi complex and then nucleus when inside endosomes (Figure 2, Step 4). This transportation occurs in early (Rab5-positive), late (Rab7-positive), and recycling (Rab11-positive) endosomes which are characterized by their associated Rab protein that controls endosome budding, sorting, movement, and fusion within cells [Pfeffer, 2001; Zerial and McBride, 2001]. Studies have shown that trafficking occurs primarily in late and recycling endosomes [Ding *et al*, 2005; Ding *et al*, 2006]. Although the mechanism is still unclear, it appears that AAV traffics to the Golgi apparatus, possibly through Rab 9 interactions [Diaz *et al*, 1997; Barbero *et al*, 2002], and undergoes Golgi-mediated processing prior to nuclear import [Bantel-Schall *et al*, 2002]. This is thought to be the result of PI3K signaling generating phosphatidylinositol-3,4-biphosphate (PIP₂) and phosphatidylinositol-3,4,5-triphosphate (PIP₃), known mediators of vesicular trafficking involved in rearrangement of the cytoskeleton [Kapeller and Cantley, 1994; Sanlioglu *et al*, 2001]. This theory is supported by studies that find disrupting microtubules can disrupt transduction [Seisenberger *et al*, 2001], but other studies have found no impact of microtubule disruption on transduction [Hirosue *et al*, 2007]. Nevertheless, following golgi-mediated processing, viral particles escape endosomes and accumulate near the Golgi compartment and microtubule organizing center (MTOC) [Bantel-Schall *et al*, 2002; Ding *et al*, 2006; Xiao and Samulski, 2012].

Nuclear import of viral particles is thought to occur through signaling between the nuclear localization motifs in the N-terminal of VP1 and VP2 viral capsid proteins and the nuclear pore complex (NPC) proteins (Figure 2, Step 5) [Sonntag *et al*, 2006]. In this process, intact viral particles that have undergone endosomal processing are located at the perinuclear region associated with the MTOC where

they accumulate and await nuclear import [Sanlioglu *et al*, 2000; Sanlioglu *et al*, 2001; Hauck *et al*, 2004]. Here, importin- β binds to the exposed N-terminal basic residues and transports the viral particles through the NPC with energy provided by the small GTPase Ran which also dissociates importin- β from the virion in the nucleus [Nicolson and Samulski, 2014]. Once inside the nucleus, AAV is transported to the nucleolus, possibly by interactions with the protein nucleolin [Qui and Brown, 1999; Johnson and Samulski, 2009].

Once in the nucleus, the single stranded DNA (ssDNA) AAV genome is released from the capsid (Figure 2, Step 6) [Bartlett *et al*, 2000]. The viral ssDNA is then converted to double stranded DNA (dsDNA) by strand annealing or second strand synthesis (Figure 2, Step 7) [Schultz and Chamberlain, 2008]. Strand annealing occurs when two complimentary ssDNA vector genomes that were trafficked into the nucleus anneal to form a single dsDNA genome. This appears to be the most common method of converting ssDNA to dsDNA [Nakai *et al*, 2000; Hauck *et al*, 2004]. Second-strand synthesis using host cell polymerases and DNA repair mechanisms also converts ssDNA to dsDNA in cells, although to a lesser extent than strand annealing [Nakai *et al*, 2000; Zhou *et al*, 2008]. Once the viral genome takes the form of dsDNA, it is then transcribed into mRNA (Figure 2, Step 8) and translated into protein (Figure 2, Step 9).

II. Lentiviral Vectors

LV is a modified form of HIV-1 and a member of the retrovirus family and relies on reverse transcription for transgene expression [Sakuma *et al*, 2012]. LV is much larger than rAAV, at approximately 100nm in diameter with a packaging capacity of 7-9kDa [Choudhury *et al*, 2016]. The LV genome is an RNA genome that consists of the promoter, gene of interest, and long terminal repeats (LTRs) that are required for integration into the host genome, reverse transcription, and viral transcription [Sakuma *et*

al, 2012]. Similar to rAAV, additional elements can be added to the LV construct to drive high levels of expression in the target cell population. LV is also often pseudotyped with the capsid viral attachment proteins of vesicular stomatitis virus glycoprotein G (VSV-G) which results in a more stable LV with greater tropism for numerous cell types as it attaches to the ubiquitous phosphatidylserine component on cell membranes [Carneiro *et al*, 2002; Shin *et al*, 2010]. These characteristics allow LV to transduce dividing and non-dividing cells for long-term expression of a transgene of interest [Blomer *et al*, 1997].

A few safety concerns surround the use of LV *in vivo*. The first of these concerns involves LV integration into the host genome. Unlike AAV that remains episomal in the nucleus, LV preferentially integrates into introns of transcriptionally active genes, leading to oncogenic potential [Choudhury *et al*, 2016]. This concern is being addressed through the development of self-inactivating designs or integration-deficient LV constructs that could be used when targeting post-mitotic cells [Sakuma *et al*, 2012]. There is also concern that lentiviral vectors could remain replication-competent and inadvertently contaminate replication-incompetent LV batches. Self-inactivating designs also help combat this issue, as well as the development of a number of vector “generations” that continually remove HIV-1 proteins that could allow for replication [Sakuma *et al*, 2012]. Other drawbacks of LV include the low vector yield in LV production limiting maximum titer and the limited volumetric spread of LV in the brain parenchyma, presumably due to the larger size of LV [Choudhury *et al*, 2016]. These concerns have likely impacted the limited use of LV clinically in the United States and perpetuated the use of rAAV2 in clinical trials.

i. Steps of LV Transduction

Similar to rAAV, the first step of LV transduction is binding to cell surface receptors to initiate attachment and endocytosis (Figure 3, Step 1). As mentioned previously, VSV-G pseudotyped LV is the most common LV used due to its wide range of tropism [Sakuma *et al*, 2012]. The pseudotyped VSV-G

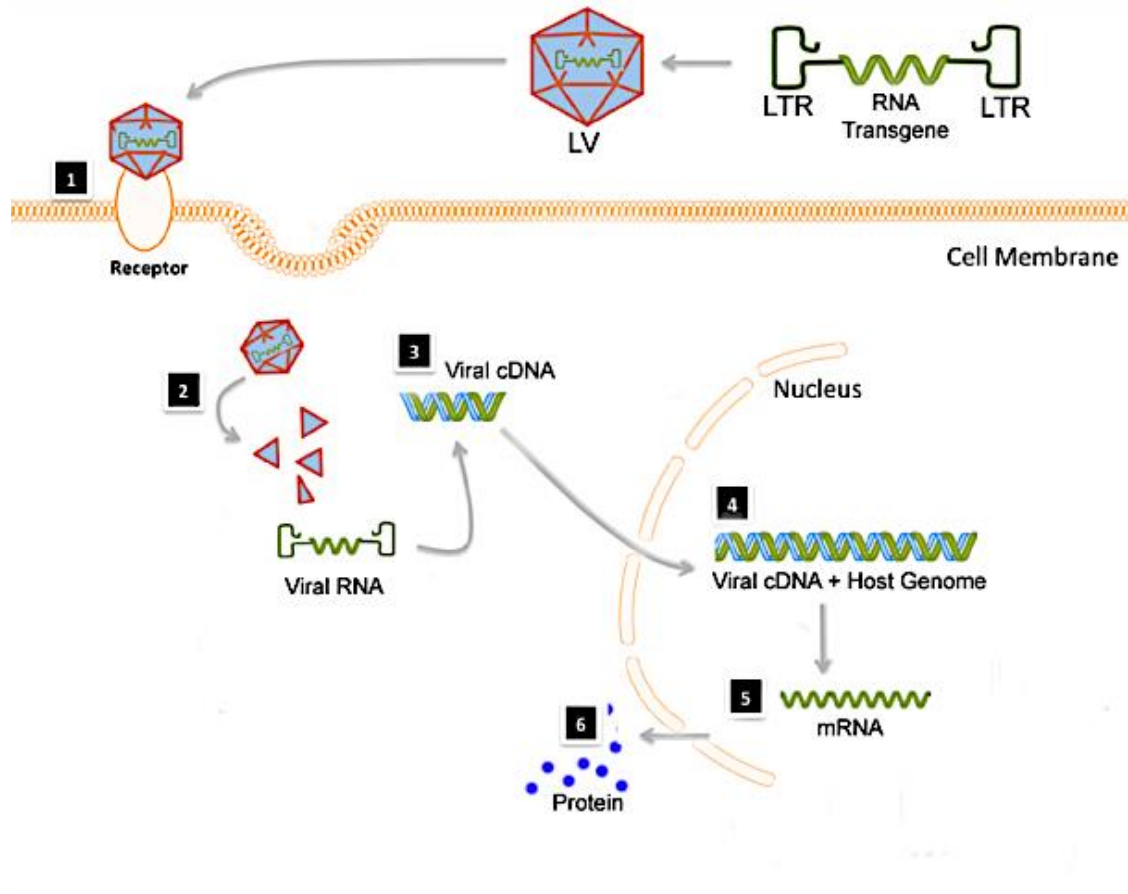


Figure 3. Diagram of LV transduction mechanism. An RNA expression cassette of interest is flanked by long terminal repeats (LTRs) to make up the recombinant genome is packaged into the VSV-G pseudotyped LV capsid. 1) Injected LV capsids bind to phosphatidylserine on the cell surface. 2) Endocytosis of the viral particle occurs whereby the virus is endocytosed and briefly located within an endosome; acidification of the virus in the endosome induces a conformational change, releasing the viral genome from its viral envelope. 3) the viral RNA genome is converted into a dsDNA genome through reverse transcription. 4) The viral dsDNA is imported into the nucleus where it is incorporated into the host genome. 5) Viral dsDNA is converted into mRNA encoded by the transgene. 9) Transgene mRNA is translated into the protein encoded by the transgene.

capsid binds to phosphatidylserine residues on cells to initiate binding and endocytosis [Carneiro *et al*, 2002; Shin *et al*, 2010; Sakuma *et al*, 2012]. Once bound to the receptor, endocytosis is initiated as an endosome is formed by a pinching off of the cell membrane. Inside this endosome, the viral capsid undergoes a conformational change due to the acidic environment and the viral envelope fuses with the endosome, releasing the vector genome (Figure 3, Step 2) [Carneiro *et al*, 2002].

Once inside the cell, the RNA vector genome is reverse transcribed into dsDNA by reverse transcriptase (Figure 3, Step 3) [Ramezani and Hawley, 2002]. This dsDNA vector genome is then translocated into the nucleus by interactions between the dsDNA and nuclear import pathway [Trono, 1995]. Inside the nucleus the dsDNA is integrated into the host genome by the viral protein integrase (Figure 3, Step 4) [Bushman and Craigie, 1991; LaFemina *et al*, 1991] where it can undergo transcription and translation to overexpress the protein encoded by the viral genome (Figure 3, Steps 5 and 6).

III. Neurotransmitter Replacement Gene Therapy Clinical Trials for PD

As depleted striatal dopamine and subsequent dysregulated basal ganglia signaling lead to the motor symptoms of PD, early viral vector-mediated gene therapy clinical trials aimed at replenishing neurotransmitter signaling and basal ganglia functioning. This can come in the form of overexpressing genes involved in dopamine synthesis in the striatum or gamma-aminobutyric acid (GABA) synthesis in the STN. A summary of the gene, viral vector, injection site, patient population, trial code, and status can be found in Table 2.

i. GAD Gene Therapy Clinical Trial

Mechanism and Preclinical Trials

As the first viral vector-mediated gene therapy clinical trial for PD, glutamic acid decarboxylase (GAD) gene therapy sought to intervene in the dysregulated basal ganglia functioning as a method for combating the motor symptoms of PD. This therapeutic strategy does not attempt to directly increase dopamine synthesis due to the risk that side effects (*e.g.* dyskinesias) from pharmacological treatments like L-dopa would be worsened with increased dopamine synthesized through the gene therapy strategies. Rather, this therapy aimed at lessening the PD motor symptoms by attempting to balance the dysregulated basal ganglia.

As mentioned previously, the healthy basal ganglia balances between the excitatory direct pathway and inhibitory indirect pathway. In PD, however, degeneration of the nigrostriatal system results in less excitation of the excitatory direct pathway (leading to less excitation) and less inhibition of the inhibitory indirect pathway (leading to more inhibition) (Figure 1). To re-establish balance of the basal ganglia signaling in PD, Kaplitt and colleagues sought to convert neurons of the STN from excitatory to inhibitory. They did this by overexpressing GAD in the STN, which catalyzes the synthesis of GABA [Kaplitt *et al*, 2007]. Thereby, the increased activation from STN signals to the substantia nigra pars reticulata (SNpr) would also include inhibitory signaling to counteract the activation, leading to less inhibition of the thalamus by the SNpr, more activation in the primary motor cortex from the thalamus, and a more normal basal ganglia signaling (Figure 1b & c) with a reduction in PD motor symptoms. Furthermore, proof-of-principle for this strategy can be found from other PD treatments reducing the activity of the STN with electrical activity in DBS, physical lesions, or direct infusions of GABA restoring motor function [Hamani *et al*, 2004].

Table 2. Viral Vector-Mediated Gene Therapy Clinical Trials for Parkinson's Disease

Name	Gene	Vector	Injection	Mechanism of Action	Sponsor	Phase	Goal of Trial	Trial Code	Success?
AAV GAD	GAD	AAV2	Unilateral STN	To correct basal ganglia functioning by inhibiting the over-stimulated STN	Neurologix, Inc.	Phase I, open label, no placebo	Assess safety and tolerability of AAV GAD in idiopathic PD (1 dose)	NCT 00195143 (completed)	Yes – safe with preliminary efficacy
AAV GAD	GAD	AAV2	Bilateral STN	To correct basal ganglia functioning by inhibiting the over-stimulated STN	Neurologix, Inc.	Phase II, double blind, placebo controlled	Assess effectiveness of AAV GAD in idiopathic PD (1 dose)	NCT 00643890 (terminated)	No – benefits no better than current therapies
AAV hAADC	hAADC	AAV2	Bilateral Putamen	Increase the conversion of L-dopa to dopamine in the striatum	Genzyme, a Sanofi Company	Phase I, open label, no placebo	Assess safety and possible efficacy of AAV hAADC in idiopathic PD (2 doses)	NCT 00229736 (completed)	No – benefits not long-term
AAV hAADC	hAADC	AAV2	Bilateral Putamen	Increase the conversion of L-dopa to dopamine in the striatum	Voyager Therapeutics	Phase I, open label, no placebo	Assess safety and possible efficacy of MRI-guided convective infusion of AAV hAADC (4 doses)	NCT 01973543 (recruiting)	Unknown
AAV hAADC	hAADC	AAV2	Bilateral Putamen	Increase the conversion of L-dopa to dopamine in the striatum	Jichi Medical University	Phase I/II, open label, no placebo	Assess safety and efficacy of AAV hAADC (2 doses)	NCT 02418598 (recruiting)	Unknown

Abbreviations: AAV, adeno-associated virus; GAD, glutamic acid decarboxylase; AAV2, AAV serotype 2; STN, subthalamic nucleus; PD, Parkinson's disease; hAADC, aromatic acid decarboxylase; L-dopa, levodopa; MRI, magnetic resonance imaging; TH, tyrosine hydroxylase; CH1, GTP cyclohydrolase 1; LV, lentivirus; NTN, neurturin; SNpc, substantia nigra pars compacta; GDNF, glial cell line-derived neurotrophic factor; NINDS, National Institute of Neurological Disorders and Stroke.

Table 2 (cont'd). Viral Vector-Mediated Gene Therapy Clinical Trials for Parkinson's Disease

Name	Gene	Vector	Injection	Mechanism of Action	Sponsor	Phase	Goal of Trial	Trial Code	Success?
ProSavin	TH, AADC, CH1	LV	Bilateral Putamen	Increase the conversion of tyrosine and L-dopa to dopamine in the striatum	Oxford BioMedica	Phase I/II, open label, no placebo	Assess safety, efficacy, and dose evaluation of ProSavin (3 doses)	NCT 00627588 (completed)	Yes – safe with preliminary efficacy
Cere-120	NTN	AAV2	Bilateral Putamen	Introduce neurotrophic factors for nigrostriatal neuroprotection or neurorestoration	Ceregene	Phase I, open label, no placebo	Assess safety and preliminary efficacy of AAV2-NTN in idiopathic PD (2 doses)	NCT 00252850 (completed)	Yes – safe with preliminary efficacy
Cere-120	NTN	AAV2	Bilateral Putamen	Introduce neurotrophic factors for nigrostriatal neuroprotection or neurorestoration	Ceregene	Phase II, double blind, placebo controlled	Assess effectiveness of AAV2-NTN in idiopathic PD (1 dose)	NCT 00400634 (completed)	No – primary outcome measure not met
Cere-120	NTN	AAV2	Bilateral SNpc and Putamen	Introduce neurotrophic factors for nigrostriatal neuroprotection or neurorestoration	Ceregene	Phase I/II, double blind, placebo controlled	Assess effectiveness of AAV2-NTN in idiopathic PD (1 dose)	NCT 00985517 (completed)	No – primary outcome measure not met
AAV GDNF	GDNF	AAV2	Bilateral Putamen	Introduce neurotrophic factors for nigrostriatal neuroprotection or neurorestoration	NINDS	Phase I, open label, no placebo	Assess safety and preliminary efficacy of AAV2-GDNF in idiopathic PD (4 doses)	NCT 01621581 (recruiting)	Unknown

Preclinical studies investigating AAV-GAD indicated promise for this gene therapy strategy. In one such study, AAV GAD was tested in a 6-hydroxydopamine (6-OHDA) rat model of PD [Luo *et al*, 2002]. Rats were injected with the AAV GAD, or AAV GFP as a control, in the STN and then received the 6-OHDA lesion to induce PD-like degeneration of the nigrostriatal system or a saline injection for an unlesioned control [Luo *et al*, 2002]. AAV GAD injection significantly increased neurotransmitter release following STN stimulation, with increased inhibitory signaling from the STN to the SNpr following AAV GAD, but not AAV GFP administration [Luo *et al*, 2002]. In addition, overexpression of AAV GAD in the STN protected against a medial forebrain bundle 6-OHDA lesion and significantly reduced motor symptoms and SNpc cell loss in this PD model over AAV GFP-treated control animals [Luo *et al*, 2002]. Other independent groups later replicated this study, with results suggesting the degree of the functional and anatomical improvement correlates with the level of AAV GAD expression in the STN [Lee *et al*, 2005].

The efficacy of AAV GAD was further corroborated in a non-human primate (NHP) model of PD. In one such study, rhesus monkeys were injected with 1-methyl-4-phenyl-1,2,3,6-tetrahydropyridine (MPTP) in the right carotid artery to render them hemiparkinsonian [Emborg *et al*, 2007]. All monkeys were then injected with AAV GAD or AAV GFP into the ipsilateral STN after validation of the lesion. As compared to AAV GFP injection, AAV GAD decreased motor deficits such as bradykinesia, gross motor deficits, and tremor [Emborg *et al*, 2007]. One year post-MPTP and AAV administration, robust GFP or GAD expression was observed in the injected hemisphere; however, no evidence of nigrostriatal recovery was observed with measures of the numbers of SNpc dopaminergic neurons in AAV2 GAD- versus AAV2 GFP-treated animals [Emborg *et al*, 2007]. These results indicate that AAV2 GAD does not generate a detrimental immune response or movement side effects and may result in functional recovery.

Clinical Trial Design and Outcomes

AAV2 GAD was tested in a Phase I clinical trial for safety and tolerability in the mid-2000s. This clinical trial was designed as a single-arm, open label, dose-escalation study in which AAV2 GAD was injected into the STN of PD patients and effects were examined one year post-injection [Kaplitt *et al*, 2007].

Twelve patients with idiopathic PD were recruited, with a mean age around 58 years, disease duration of at least 5 years, motor complications with L-dopa use, and no signs of cognitive or psychiatric conditions. AAV2 GAD was unilaterally injected into the right STN, with each patient receiving a low, medium, or high dose of the virus. Patients were then examined 1, 3, 6, and 12 months post-surgery to assess adverse effects of the therapy. AAV2 GAD proved safe and tolerable. No adverse side effects of AAV2 GAD were seen in any of the twelve patients in the study for up to one year after surgery when examined routinely as part of the clinical trial, or up to three years post-surgery when examined further [Kaplitt *et al*, 2007]. Furthermore, no evidence for a developed immunity to AAV2 was found, and pre-existing neutralizing antibodies to AAV2 or GAD did not seem to develop or influence therapy effectiveness.

Preliminary measures of effectiveness of AAV2 GAD treatment were also collected during this Phase I clinical trial. A significant effect of unilateral STN AAV2 GAD was uncovered in UPDRS motor scores at 3, 6, and 12 months post-injection in both “on” and “off” states (states when taking L-dopa and states when L-dopa is absent, respectively). These benefits were seen in the limbs controlled by the treated STN, whereas no benefits were observed in limbs corresponding to the untreated STN. No significant changes were seen in measures of activities of daily living, dyskinesias, or neuropsychological tests; however, trends towards benefits were seen in activities of daily living and dyskinesias at 12 months post-injection [Kaplitt *et al*, 2007]. Furthermore, PET scans for glucose metabolism were taken for each

patient and raters were blinded to treatment side and patient. Glucose metabolism was reduced in the thalamus and increased in the cortex of the treated hemisphere at 12 months post-injection as compared to baseline scans. No changes were observed in the untreated hemisphere. These increases in cortical activity highly correlated with UPDRS ratings, indicating that AAV2 GAD reduced STN activity, leading to an inhibition of anterograde structures and increased activity in the cortex [Kaplitt *et al*, 2007].

Although promising, this Phase I clinical trial was not designed to assess clinical effectiveness of AAV2 GAD treatment. The open label nature of this safety and tolerability trial lends itself to placebo effects. To directly examine efficacy, a Phase II AAV2 GAD clinical trial was initiated. This Phase II clinical trial had similar inclusion and exclusion criteria as the Phase I trial, including patients that were at least 5 years post-PD diagnosis with responsiveness to L-dopa and no cognitive or neuropsychiatric issues [LeWitt *et al*, 2011]. A total of 45 patients received a bilateral STN injection of AAV2 GAD or saline. All patients, caregivers, investigators, and raters were blind to the treatment group of the patients until the conclusion of the study. A significant improvement was found in UPDRS scores in AAV2 GAD-treated patients as compared to sham-treated patients at the 6 month endpoint of the study [LeWitt *et al*, 2011]. Similar to the Phase I trial, no adverse side effects were reported, and no differences were seen in activities of daily living, dyskinesias, or neuropsychological tests [Kaplitt *et al*, 2007; LeWitt *et al*, 2011]. This Phase II clinical trial using bilateral STN infusion of AAV2 GAD did meet the primary outcome measure of improved UPDRS scores at 6 months post-surgery [LeWitt *et al*, 2011]. However, these benefits of treatment were no greater than the benefits received from conventional treatment. As a result, this therapy did not move on to further testing [O'Connor and Boulis, 2015].

ii. hAADC-2 Clinical Trial

Mechanism and Preclinical Trials

As mentioned previously, the most common treatment for PD is dopamine replacement therapy, with L-dopa as the gold standard. However, with time L-dopa becomes less effective and exhibits worsening side effects such as dyskinesias. Although the reason for this is not entirely known, it is postulated that the progressive loss of dopaminergic nigrostriatal nerve terminals in PD leads to a loss of dopamine-synthesizing enzymes important for the conversion of L-dopa to dopamine. Loss of these synthesizing enzymes, like AADC, could then lead to decreased dopamine storage in synaptic vesicles, postsynaptic changes in striatal output neurons, or dysregulation of other neurotransmitter systems [Fahn *et al*, 2008]. Restoring these enzymes selectively in the striatum, however, could combat these issues and lead to more normalized basal ganglia functioning and a lower required dose of L-dopa that would decrease the side effects experienced with high doses.

Restoring dopamine-synthesizing enzymes using viral vector-mediated gene therapy was therefore investigated as a potential mechanism to treat PD symptoms. Delivering AADC directly to the striatum would bypass the need for functioning dopaminergic nigrostriatal terminals by allowing non-degenerating striatal neurons to convert exogenously delivered L-dopa to DA with AADC. The level of DA produced could then be adjusted based on the dosage of L-dopa administered, allowing better control of the treatment effect. The benefits of this treatment *in vivo* were demonstrated in preclinical work in rat and NHP models of PD.

In one study by the Bankiewicz lab in 2001, rats received a unilateral lesion to the nigrostriatal system through an injection of 6-OHDA to the medial forebrain bundle, followed by an injection of rAAV2 expressing GFP or human AADC (hAADC) about one month post-lesion induction and treatment with L-

dopa [Sanchez-Pernaute *et al*, 2001]. AAV2 hAADC significantly decreased measures of PD-like behaviors, such as contralateral rotations, as compared to post-lesion baseline. These improvements in behavior correlated with DA levels, which most likely resulted from the hAADC treatment as endogenous levels of DA in this lesion paradigm are extremely low [Sanchez-Pernaute *et al*, 2001]. Furthermore, comparisons in levels of L-dopa and DA following L-dopa administration in AAV2 hAADC and AAV2 GFP injected hemispheres and uninjected hemispheres of rats indicated the exogenous L-dopa was being rapidly decarboxylated into DA and the DA was released to act on DA receptors [Sanchez-Pernaute *et al*, 2001]. Overall, the introduction of hAADC with AAV2 was able to restore the decarboxylating capacity to about half that of the normal striatum.

The long-term benefits of AAV2 hAADC have also been explored in NHP preclinical trials. In another study by the Bankiewicz group, rhesus monkeys were injected in the right carotid artery to induce a unilateral, hemiparkinsonian model followed by an intrastriatal injection of AAV2 hAADC, or AAV2 LacZ as a control, 2-4 months later [Bankiewicz *et al*, 2006]. PET imaging for AADC revealed near-normal levels of AADC following AAV2 hAADC, but not AAV2 LacZ injection in the lesioned hemisphere. These levels of AADC remained stable for the two-year duration of the study and were on par with levels seen in the contralateral, unlesioned hemisphere [Bankiewicz *et al*, 2006]. Behaviorally, monkeys receiving AAV2 hAADC displayed functional recovery with few side effects after a low dose of L-dopa that was not beneficial in AAV2 LacZ monkeys or monkeys before gene therapy. Furthermore, advancements in convection-enhanced delivery of AAV2 hAADC allowed for high levels of expression in a larger tissue volume, allowing for even greater restoration of dopamine production [Bankiewicz *et al*, 2000].

Clinical Trial Design and Outcomes

A Phase I clinical trial for AAV2 hAADC began as a result of the favorable preclinical trial data. In this trial, the safety, tolerability, and potential efficacy of AAV2 hAADC were investigated in patients with mid- to late-stage PD [Muramatsu *et al*, 2010]. In the first arm of this study, six patients with a mean age of 60 years and a mean disease duration of 10 years received AAV2 hAADC injections to the putamen. All patients tolerated the treatment well, with side effects and increased titers of AAV2 neutralizing antibodies being only mild and transient in nature. AAV2 hAADC significantly improved the UPDRS “off” scores of patients at six months post-injection and many patients who received AAV2 hAADC went on to decrease their L-dopa dose [Muramatsu *et al*, 2010]. Furthermore, AADC levels were increased in patients following AAV2 hAADC injection, with increases persisting months after injection.

In the second arm of the AAV2 hAADC Phase I clinical trial, two doses of AAV2 hAADC were used to test the dose-response and potential efficacy of this treatment in mid-stage PD patients. In this arm of the study, ten patients with a mean age of 63 years and a mean disease duration of about 10 years received AAV2 hAADC injections to the putamen [Christine *et al*, 2009]. Again, side effects of this therapy were mainly mild and transient, with a few instances of hemorrhages resulting from the surgical procedure. Increases in striatal AADC signal in PET scan imaging indicated an increase in AADC expression following AAV2 hAADC administration that is dose-responsive. At six months post-injection, significant improvements were seen in UPDRS scores in the “off” and “on” states, with an additional reduction in dyskinesias and lowering of L-dopa dosage in some patients [Christine *et al*, 2009]. Although promising, these improvements in UPDRS score could be due to the placebo effect resulting from the open-label design of the study.

A long-term follow-up of the sixteen patients who received AAV2 hAADC was performed four years post-injection. The increased AADC levels, as measured by PET scans, at six months post-injection were sustained for the four-year duration of the study [Christine *et al*, 2009; Muramatsu *et al*, 2010; Mittermeyer *et al*, 2012]. Furthermore, no major side effects were reported during these evaluations. Unfortunately, the improvement in UPDRS scores in the “on” and “off” states reported one year post-injection [Christine *et al*, 2009; Muramatsu *et al*, 2010] were not sustained at four years post-injection. Rather, improvements slowly deteriorated during the subsequent years, with no persistent differences between low- and high-dose patients. Both the degree of symptomatic improvement and the decrease in this improvement over time suggest it may be the result of the placebo effect rather than neurobiological benefits in the open-label study [Muramatsu *et al*, 2010]. A new Phase I clinical trial is currently being recruiting in which higher doses of AAV2 hAADC will be used and a larger volume (~60%) of the putamen will be transduced (Clinical Trial Number: NCT01973543), as well as another Phase I/II clinical trial to test the safety and efficacy of AAV2 hAADC (Clinical Trial Number: NCT02418598) (see Table 2).

iii. ProSavin Gene Therapy Clinical Trial

Mechanism and Preclinical Trials

Similar to the concept of the AAV hAADC clinical trials, the ProSavin clinical trial sought to treat PD by overexpressing machinery involved in dopamine synthesis. ProSavin is a tricistronic VSV-G-pseudotyped LV vector capable of simultaneously expressing three genes involved in the synthesis of DA—TH, AADC, and GTP cyclohydrolase 1 [Palfi *et al*, 2014]. TH is a rate-limiting enzyme in DA synthesis, AADC decarboxylates levodopa into DA, and GTP cyclohydrolase 1 (CH1) is required for the synthesis of tetrahydrobiopterin, an essential co-factor for AADC. Overexpression of the LV-TH-AADC-CH1 vector would enable transduced cells to convert both exogenous L-dopa and endogenous tyrosine into DA to

replenish the loss in PD. Furthermore, the TH gene in ProSavin is mutated to prevent the negative feedback loop that would normally inhibit the activity of TH in the presence of DA [Feng and McGuire-Zeiss, 2011]. As a result, injection of ProSavin into the putamen would enable non-degenerating striatal cells to produce the dopamine that is no longer supplied by the nigrostriatal terminals, re-balancing the basal ganglia signaling.

Although LV is seen as a potentially more dangerous virus to use *in vivo* due to its oncogenic potential by insertion into the host genome, multiple steps were taken to ensure the safety of ProSavin. ProSavin uses a self-inactivating vector configuration based on a non-primate LV that lacks the viral control signals from the LTRs, thereby reducing the risk of insertional mutagenesis [Sakuma *et al*, 2012; Palfi *et al*, 2014]. In addition, ProSavin has been shown to target mainly post-mitotic cells, which can also decrease the risk of oncogenesis [Palfi *et al*, 2014]. The preference of the ProSavin LV to integrate into active genes also decreases the risk of oncogenesis, as insertion near a proliferation or oncogene is unlikely [Palfi *et al*, 2014]. Finally, the fact that PD gene therapy patients are not treated with immunosuppressants and the TH, AADC, and CH1 genes do not impart a proliferative advantage makes the risk of oncogenesis low [Palfi *et al*, 2014]. These properties, coupled with the fact that preclinical trials did not demonstrate insertional mutagenesis, allowed ProSavin to advance for clinical testing.

The promise of ProSavin was validated in both rat and NHP preclinical studies. An early version of the ProSavin construct was tested in rats that received a unilateral medial forebrain bundle lesion with 6-OHDA [Azzouz *et al*, 2002]. The LV-TH-AADC-CH1 construct and a control LV-LacZ was injected into the striatum five weeks post-lesion and functional recovery was assessed with the apomorphine-induced rotational asymmetry test (comparing post-LV-injected turns to a baseline collected post-lesion and prior to LV injection). At 4 weeks after viral injection, the LV-TH-AADC-CH1 treated rats displayed about

50% fewer rotations than the LV-LacZ treated animals, with this reduction remaining stable from 4-10 weeks after viral injection [Azzouz *et al*, 2002]. Furthermore, immunohistochemical staining revealed that transduced cells displayed a neuronal morphology of both the medium spiny neurons and aspiny neurons of the striatum [Azzouz *et al*, 2002]. Expression of the delivered transgenes was detected at late time points as well, with robust expression up to 5 months post-vector injection [Azzouz *et al*, 2002]. Finally, HPLC measures of striatal dopamine indicated three-fold higher levels following LV-TH-AADC-CH1 treatment as compared to LV-LacZ, however, DA levels in the LV-TH-AADC-CH1 hemisphere were only about 4% of the intact striatum but were still able to induce behavioral changes in rotational measures [Azzouz *et al*, 2002]. These results showed promise for the LV-TH-AADC-CH1 treatment strategy, and preclinical testing was moved to NHPs.

In one such NHP study, adult macaque monkeys were rendered parkinsonian through a systemic injection of MPTP causing bilateral motor deficits [Jarraya *et al*, 2009]. Lesions were verified using behavioral assessments and *post mortem* analyses of dopamine levels and SNpc cell numbers. Nineteen weeks after MPTP injection, the macaques received either bilateral LV-TH-AADC-CH1 injection into the putamen, LV-LacZ control injection into the putamen, or no surgical intervention [Jarraya *et al*, 2009]. Beginning two weeks after vector treatment, macaques that received LV-TH-AADC-CH1 showed improvements in posture and akinesia, with a significant improvement in global movement score at six weeks post-injection and no dyskinesias following L-dopa administration. These improvements were sustained throughout the one-year duration of the study, with one macaque monitored for 44 months displayed sustained motor improvements [Jarraya *et al*, 2009]. LV-LacZ treated animals did not display any motor improvements. Furthermore, measures of DA concentrations in the putamen revealed significantly higher levels of DA in the LV-TH-AADC-CH1 group as compared to the LV-LacZ or uninjected control groups [Jarraya *et al*, 2009]. Levels of DA were also greater in the LV-TH-AADC-CH1 group than

the control groups following L-dopa administration, indicating a significantly greater conversion of L-dopa to DA following LV-TH-AADC-CH1 treatment [Jarraya *et al*, 2009]. These changes also corresponded to normalized basal ganglia functioning. This improvement, coupled with the lack of toxicity or side effects observed with treatment, led to the ProSavin clinical trial.

Clinical Trial Design and Outcomes

The clinical trial for ProSavin was designed as an open-label, dose-escalation Phase I/II study with a twelve-month follow-up point at the two participating sites in France and the UK [Palfi *et al*, 2014]. Fifteen patients (average age of 57 years and disease duration of 14 years) with bilateral, idiopathic PD received bilateral injections of ProSavin into the putamen. Although some adverse side effects were reported, the majority of side effects were mild with a few moderate instances. The most common side effect was increased dyskinesias or on-off phenomenon, which resolved when the L-dopa dose administered was decreased [Palfi *et al*, 2014]. Furthermore, some individuals did display an increased antibody response to the ProSavin capsid or other viral proteins. These antibody responses were mild and did not correspond to any increased inflammation or inflammatory damage. Overall, ProSavin demonstrated a favorable safety profile in patients.

Patients also demonstrated motor improvements after ProSavin administration. At 6 and 12 months post-injection, patients displayed a significant improvement in mean total UPDRS “off” and “on” motor scores [Palfi *et al*, 2014]. Although no differences were seen in UPDRS scores between doses, patients with the higher ProSavin dose did request a decrease in L-dopa dose more frequently than lower dose patients. PET imaging revealed no differences in L-dopa uptake in the putamen in any group before or after ProSavin [Palfi *et al*, 2014]. PET imaging for DA receptor binding potential, however, did reveal a significant difference before and after ProSavin treatment, with a dose response and greater changes in

the injected putamen as compared to the uninjected caudate nucleus. Finally, restoration of inhibitory control of the motor cortex at rest and increased activation of the motor cortex during voluntary movement was reported in patients following ProSavin treatment. These outcomes indicate an improvement in motor control following ProSavin treatment in patients with bilateral, idiopathic PD.

Unfortunately, the open-label nature of the ProSavin clinical trial lends itself to the placebo effect, and the authors of the study do note that the magnitude of the benefits observed were within the range of the placebo effect in previous gene therapy clinical trials [Palfi *et al*, 2014; O'Connor and Boulis, 2015].

The authors plan to undertake a long-term follow up of the patients that received ProSavin to determine whether the motor improvements and lack of toxicity observed at one year post-injection are sustained for up to nine years post-injection [Palfi *et al*, 2014]. Furthermore, the authors plan to optimize the ProSavin delivery method further and initiate a double-blinded, randomized, Phase II clinical trial to better investigate the efficacy of ProSavin in PD patients [Palfi *et al*, 2014].

IV. Trophic Factor Gene Therapy Clinical Trials for PD

i. Trophic Factors for Neuroprotection in PD

Trophic Factor Signaling

The goal of the AAV GAD, AAV hAADC, and ProSavin clinical trials are to circumvent the need for dopaminergic input from the SNpc nigrostriatal system by locally altering imbalanced neurotransmitter release in the direct and indirect pathways of the basal ganglia (Figure 1). Although these gene therapy clinical trials may increase dopamine synthesis or re-establish balance in the basal ganglia to decrease the motor symptoms associated with PD, this treatment strategy is purely symptomatic and does not alter the progression of nigrostriatal degeneration. In addition, it is hypothesized that the effectiveness

of these therapies could wane as the nigrostriatal dopaminergic neurons continue to degenerate and fail to project to the striatum [Choudhury *et al*, 2016].

To combat this issue and attempt to treat PD progression, clinical trials that aim to slow or halt nigrostriatal degeneration have developed. Neurotrophic growth factors are the prime tool to accomplish this goal. Neurotrophic factors are small, secretory proteins that promote survival and healthy development of neurons through their interactions with cell surface receptors and the activation of multiple intracellular signaling pathways [Kelly *et al*, 2015]. The two most common neurotrophic factors used in preclinical and clinical trials for PD are glial cell line-derived neurotrophic factor (GDNF) and neurturin (NTN). GDNF, and its homolog NTN, are members of the transforming growth factor- β (TGF β) superfamily and members of the GDNF family ligands [Lin *et al*, 1993; Saarma and Sariola, 1999]. Although GDNF and NTN exert similar effects through similar intracellular signaling mechanisms, their signaling pathways are slightly different.

GDNF was first isolated and described as a survival molecule for rat embryonic midbrain dopamine neurons in culture in the early 1990s [Lin *et al*, 1993]. GDNF is first produced in a precursor form that is later converted to the mature form of the protein through proteolytic cleavage. The precursor form of GDNF is a 211 amino acid residue pre-propeptide that is cleaved into a 134 residue mature protein with a molecular weight of 33-45kDa upon secretion [Lin *et al*, 1993]. The mature form of GDNF forms homodimers held together by three disulfide bridges in a motif called a “cysteine knot” and acts on its appropriate receptor, the GDNF receptor alpha 1 (GFR α 1) receptor [Saarma and Sariola, 1999].

NTN was first isolated as a GDNF-like factor that enables the survival of sympathetic neurons *in vitro* [Kotzbauer *et al*, 1996]. Similar to GDNF, NTN is first produced in a precursor form that is converted to the mature form of the protein through proteolytic cleavage. The precursor form of NTN is a pre-

propeptide that is cleaved into a 100 residue mature protein with a molecular weight of 25kDa upon secretion [Domanskyi *et al*, 2015]. The mature form of NTN also forms a “cysteine knot” motif that can act on its appropriate receptor, the GFR α 2 receptor [Domanskyi *et al*, 2015]. NTN was found to share many properties with GDNF such as downstream signaling pathways and biological activity promoting survival in many of the same neuronal subtypes [Kotzbauer *et al*, 1996].

GDNF and NTN bind to different members of the GFR α family. GDNF binds to GFR α 1 whereas NTN binds to GFR α 2 and at times GFR α 1 when NTN concentrations are high [Airaksinen *et al*, 1999]. GFR α 1 and GFR α 2 lack a transmembrane spanning domain and are anchored to the cell membrane through a covalent interaction with glycosylphosphatidylinositol [Treanor *et al*, 1996]. As a result, intracellular signaling of GDNF and NTN is dependent on other membrane-spanning receptors once the GDNF and NTN ligands are activated. Signaling of the GDNF or NTN molecule then occurs by activating the receptor tyrosine kinase Ret once GDNF or NTN are bound to their respective glycosylphosphatidylinositol-anchored GFR α s, forming a ligand-receptor complex [Treanor *et al*, 1996; Kelly *et al*, 2015]. The ligand-receptor complex can also interact with other intracellular proteins for Ret-independent signaling; however, RET-dependent signaling is important for midbrain dopamine neurons and will thus be the focus of this section. Ligand-receptor complex-activated Ret then forms a homodimer and is auto-phosphorylated at an intracellular tyrosine kinase domain to initiate intracellular signaling cascades.

It is the interaction of phosphorylated, activated Ret with other proteins that activates different intracellular signaling cascades [Kramer and Liss, 2015]. Examples of some intracellular proteins that bind to phosphorylated Ret include fibroblast growth factor receptor substrate 2 (FRS2), proto-oncogene tyrosine-protein kinase Src (Src), Src-homologous and collagen-like protein (Shc), signal transducers and activators of transcription (STAT), growth factor receptor-bound protein 7 (GRB7), and

GRB10 [Pandey *et al*, 1995; Pandey *et al*, 1996; Schuringa *et al*, 2001; Encinas *et al*, 2004]. The location of the ligand-GFR α complex inside or outside a lipid raft will influence which intracellular protein will bind to Ret, and therefore which downstream signaling pathway will be activated (Figure 4).

Phosphorylated Ret will bind with Src and trigger activation of the mitogen-activated protein kinase (MAPK) pathway that mediates cell survival, growth, differentiation, and neuritogenesis when the ligand-GFR α complex is anchored to a lipid raft. Conversely, when the ligand-GFR α complex is not lipid-anchored, phosphorylated Ret will bind with Shc and trigger the PI3K/Akt pathway that mediates cell survival, proliferation, and neurotransmission [Airaksinen and Saarma, 2002; Kramer and Liss, 2015].

These pathways are essential to the survival effects of GDNF and NTN in midbrain dopaminergic neurons [Kramer and Liss, 2015].

The PI3K/Akt is an essential pathway for activating pro-survival genes and inhibiting apoptosis (Figure 4) [d'Angelmont de Tassigny *et al*, 2015]. In this downstream GDNF/NTN pathway, a ligand-GFR α complex that is located outside of lipid rafts will activate Ret, causing it to homodimerize and auto-phosphorylate. This activated Ret will interact with Shc that then activates PI3K. PI3K will then activate protein kinase B (Akt) and nuclear factor kappa B (NF- κ B), as well as indirectly stimulate B cell lymphoma 2 (Bcl-2) which prevents apoptosis. Akt will then inhibit p38 and c-Jun N-terminal kinase (JNK) while also stimulating the phosphorylation of ribosomal protein S6 (pS6) indirectly and NF- κ B directly. NF- κ B will then translocate into the nucleus and initiate the transcription of pro-survival genes.

The MAPK pathway is also important for downstream pro-survival signals (Figure 4) [Airaksinen and Saarma, 2015]. In this downstream GDNF/NTN signaling pathway, a ligand-GFR α complex that is located inside a lipid raft will activate Ret, causing it to homodimerize and auto-phosphorylate. This activated Ret will interact with FRS2, which activates Ras. Activated Ras will bind to RAF, which phosphorylates

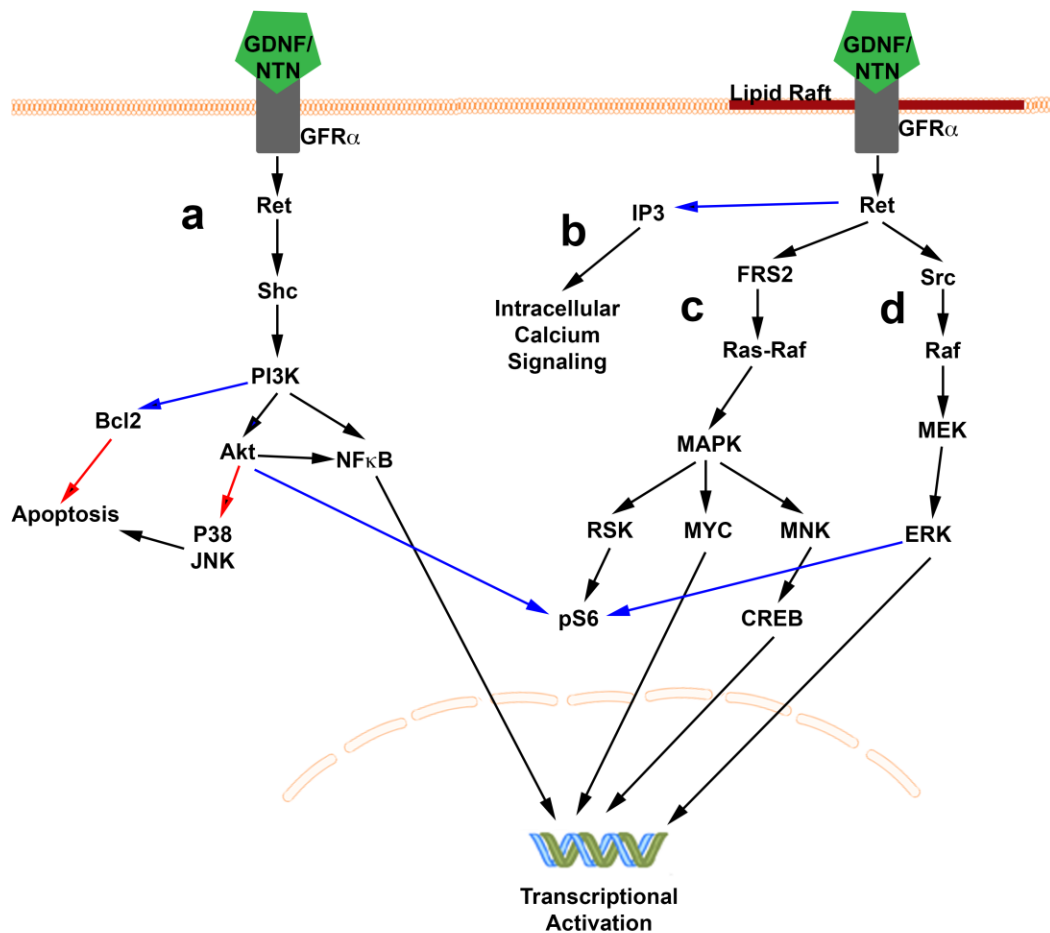


Figure 4. Diagram of GDNF/NTN signaling cascades. a) Diagram of the PI3K/Akt pathway. GDNF or NTN binds to the GFR α to form the ligand-receptor complex to activate Ret. When GFR α is not within a lipid raft, Ret activation goes on to activate Shc that activates PI3K. PI3K then indirectly activates Bcl2 (an apoptosis inhibitor), activates Akt to inhibit p38 and JNK (pro-apoptotic signaling), and Akt and PI3K both activate NF κ B which goes on to promote transcription of pro-survival genes. Akt can also indirectly lead to the phosphorylation of ribosomal protein S6 and activation of pS6. b-d) Diagram of the pathways controlled by GDNF or NTN when binding to the GFR α that is located within a lipid raft. b) Diagram of the IP3 signaling from Ret activation. Activated Ret indirectly activates IP3 which leads to increased intracellular calcium signaling. c) Diagram of the MAPK pathway. Activated Ret activates FRS2 which activates Ras to form the Ras-Raf complex. This then activates MAPK which activates the downstream kinases RSK, MYC and MNK. RSK phosphorylates S6 to form pS6, MYC provides transcriptional activation, and MNK phosphorylates CREB which then activates pro-survival genes. d) Diagram of the ERK pathway. In this pathway activated Ret activates Src. This then activates Raf which activates MEK. MEK will in turn phosphorylate ERK which will then activate pro-survival genes and indirectly lead to the activation of pS6. Abbreviations: GDNF, glial cell line-derived neurotrophic factor; NTN, neurturin; GFR α , GDNF receptor alpha; Ret, receptor tyrosine kinase Ret; Shc, Src-homologous and collagen-like protein; PI3K, phosphatidylinositide 3-kinase; Bcl2, B cell lymphoma 2; Akt, serine/threonine protein kinase Akt; JNK, c-Jun N-terminal kinase; NF κ B, nuclear factor kappa B; IP3, inositol trisphosphate 3; MAPK, mitogen-activated protein kinase; FRS2, fibroblast growth factor receptor substrate 2; MNK, mitogen-activated protein kinase; RSK, ribosomal protein S6 kinase; pS6, phosphorylated ribosomal protein S6; CREB, cAMP response element binding protein; Erk, extracellular signal-regulating kinase; Src, proto-oncogene tyrosine-protein kinase Src; MEK, mitogen extracellular signal-regulated kinase.

MAPK. MAPK will then phosphorylate mitogen-activated protein kinase (MNK), MYC, and ribosomal protein S6 kinase (RSK). Phosphorylated MNK phosphorylates cAMP response element binding protein (CREB), causing transcriptional activation. Phosphorylated RSK leads to S6 phosphorylation to activate pS6. Finally, phosphorylated MYC leads to transcriptional activation.

The MAPK pathway is also important for downstream pro-survival signals (Figure 4) [Airaksinen and Saarma, 2015]. In this downstream GDNF/NTN signaling pathway, a ligand-GFR α complex that is located inside a lipid raft will activate Ret, causing it to homodimerize and auto-phosphorylate. This activated Ret will interact with FRS2, which activates Ras. Activated Ras will bind to RAF, which phosphorylates MAPK. MAPK will then phosphorylate mitogen-activated protein kinase (MNK), MYC, and ribosomal protein S6 kinase (RSK). Phosphorylated MNK phosphorylates cAMP response element binding protein (CREB), causing transcriptional activation. Phosphorylated RSK leads to S6 phosphorylation to activate pS6. Finally, phosphorylated MYC leads to transcriptional activation.

Other pathways are also involved in downstream GDNF or NTN signaling (Figure 4). The extracellular signal-regulating kinase (ERK) pathway is one such pathway that is important for downstream pro-survival signals [d'Angelmont de Tassigny *et al*, 2015]. In this downstream GDNF/NTN signaling pathway, a lipid-bound ligand-GFR α complex will activate Ret, causing it to interact with Src. Src then activates Raf, which activates mitogen extracellular signal-regulated kinase (MEK), which activates ERK, and ERK indirectly activates pS6 and is also translocated into the nucleus where it initiates transcription of pro-survival genes. In addition, activated Ret indirectly activates inositol tris-phosphate 3 (IP3), which increases intracellular calcium signaling [d'Angelmont de Tassigny *et al*, 2015]. Using these pathways, GDNF and NTN are currently under consideration as a treatment for PD that would have the potential to modify disease progression.

Delivery of Recombinant GDNF

Recombinant GDNF protein has been shown to exhibit neuroprotective effects when delivered prior to inducing a parkinsonian lesion. GDNF prevented the loss of a significant portion of SNpc dopaminergic neurons when delivered to the SNpc at least 24 hours before nigral or striatal 6-OHDA lesions [Kearns and Gash, 1995]. In addition, delivery of recombinant GDNF protein to the SNpc one month after medial forebrain bundle lesion with 6-OHDA resulted in a rescue of motor behavior as assessed by the apomorphine-induced rotations test and DA levels in the SNpc that were not different from DA levels in the unlesioned hemisphere [Hoffer *et al*, 1994]. Furthermore, delivery of GDNF to the SNpc and lateral ventricle immediately before 6-OHDA lesion to the medial forebrain bundle prevented the 6-OHDA-induced decrease in DA reuptake in the striatum and loss of SNpc dopaminergic neurons in a 12 week, long-term study of GDNF neuroprotection [Sullivan *et al*, 1998]. Furthermore, GDNF was not only shown to be neuroprotective when administered prior to lesioning. When GDNF was administered to the striatum of pre-lesioned rat models of PD, neuroprotective/neurorestorative effects such as nigrostriatal axonal sprouting, reinnervation of the deafferented striatum, recovery of motor performance, and increased numbers of SNpc dopaminergic neurons were observed [Rosenblad *et al*, 1998; Aoi *et al*, 2000].

These promising studies in rat models of PD led to the investigation of the neuroprotective effects of GDNF in NHP models of PD. In one such case, GDNF was administered to the SNpc, caudate nucleus, or intracerebrally to hemiparkinsonian rhesus monkeys three months after MPTP injection [Gash *et al*, 1996]. Following GDNF treatment, monkeys displayed improvements in bradykinesia, rigidity, and postural instability. These improvements corresponded to greater DA levels in the midbrain and globus pallidus, larger SNpc dopaminergic neurons, and increased nigrostriatal fiber density

following GDNF treatment [Gash *et al*, 1996]. In another study, GDNF was chronically infused into the lateral ventricle or striatum of hemiparkinsonian rhesus monkeys for three months beginning one month after MPTP-lesion [Grondin *et al*, 2002]. The authors reported upregulation and regeneration of nigral dopaminergic neurons and their processes in the striatum, along with functional recovery and a lack of side effects from treatment. These promising results in NHP models of PD supported the move to human clinical trials using direct infusions of recombinant GDNF protein.

Multiple clinical trials sought to test the safety and efficacy of continuously infused recombinant GDNF in the brain of PD patients. In the first Phase I safety and tolerability clinical trial, one patient received monthly intracerebroventricular injections of recombinant GDNF [Kordower *et al*, 1999]. Numerous side effects were observed from this treatment, including hallucinations, loss of appetite, nausea, and depression, among others. In addition, no significant changes in PD symptom severity or regeneration of nigrostriatal neurons were observed [Kordower *et al*, 1999]. This led authors to conclude that alternate delivery methods should be explored as the frequency and location of delivery could have caused the observed issues [Kordower *et al*, 1999]. In a follow-up Phase I safety and tolerability trial, five patients with idiopathic PD received continuous delivery of GDNF through a pump and catheter inserted into the putamen [Gill *et al*, 2003]. No major adverse reactions were experienced in relation to GDNF infusion. In addition, preliminary efficacy investigations revealed a reduction in PD symptoms after three months of GDNF infusion, with significantly improved UPDRS scores in both the “on” and “off” phases [Gill *et al*, 2003]. Furthermore, these benefits were continued for two years when assessed in a follow-up study, and no serious clinical side effects were observed after long-term GDNF infusion [Patel *et al*, 2005]. These promising results led to the development of a Phase II efficacy trial.

One clinical trial involved monthly intracerebroventricular injection of varying doses of GDNF in twelve patients in a multicenter, randomized, double-blind, placebo-controlled Phase II clinical trial [Nutt *et al*, 2003]. Patients reported severe side effects from treatment, including nausea, anorexia, vomiting, weight loss, and parestesias (electric shocks). In addition, no benefits from GDNF were observed in either “on” or “off” UPDRS scores. This resulted in the termination of the clinical trial and the conclusion that GDNF was active (due to side effects) but possibly did not reach the structures involved in PD motor symptomatology [Nutt *et al*, 2003]. In another randomized, controlled Phase II clinical trial, 34 patients received bilateral continuous intraputamenal infusions of recombinant GDNF or placebo [Lang *et al*, 2006]. At six months, patients displayed a non-significant difference in UPDRS scores between GDNF and placebo groups. As a result, the study was concluded and were deemed unsuccessful.

Delivery of Recombinant NTN

In rat and NHP studies, NTN was found to provide neuroprotection in models of PD, albeit to a lesser extent than GDNF. In a study of striatal 6-OHDA lesioned rats, NTN or GDNF were injected intrastrially or intracerebroventricularly every third day starting one day after 6-OHDA injection [Rosenblad *et al*, 1999]. Intrastriatal, but not intracerebroventricular, injections of NTN resulted in lower dopaminergic nigral neuron death and increased axonal sprouting in the globus pallidus, but a loss of dopaminergic phenotype (as labeled by TH) in the remaining neurons. In addition, NTN did not reduce striatal denervation or PD behavioral phenotype and was less effective than GDNF in all outcome measures [Rosenblad *et al*, 1999]. In a separate study of NTN neuroregeneration in PD, rats were injected in the striatum with recombinant NTN twelve-weeks after an intrastriatal injection of 6-OHDA to induce a parkinsonian lesion [Oiwa *et al*, 2002]. Although no differences were observed in the number of dopaminergic neurons in the NTN- versus vehicle-treated groups, neurites of the SNpc dopaminergic neurons were more dense and abundant in the striatum following NTN treatment which corresponded

to higher DA levels in the striatum and reduced PD-like motor behaviors [Oiwa *et al*, 2002]. Similar neuroprotective effects of NTN were observed in a rhesus monkey MPTP-lesioned model of PD when injected directly into the putamen [Grondin *et al*, 2008]. Although promising, infusions or injections of recombinant NTN never progressed to clinical trials as the magnitude of benefit was consistently lower than recombinant GDNF.

Issues with Direct Infusion of Recombinant GDNF/NTN

The lack of efficacy in preclinical and clinical trials of recombinant GDNF and NTN injections could be due to the problematic delivery methods and diffusion properties of these neurotrophic factors. Neither GDNF nor NTN has the ability to cross the blood brain barrier, leading to the need for direct infusion in the brain [Domanskyi *et al*, 2015]. In addition, GDNF and NTN both bind with high affinity to HSPG in the extracellular matrix, causing very limited diffusion from the injection site [Domanskyi *et al*, 2015]. This could partially explain the lack of effects on PD symptoms when delivering GDNF or NTN intracerebroventricularly [Kordower *et al*, 1999; Rosenblad *et al*, 1999; Nutt *et al*, 2003]. In addition, infusion of recombinant GDNF or NTN does not allow for sustained expression of these trophic factors. These issues of delivery and diffusion are of vital importance when attempting to deliver a neurotrophic factor to a large structure like the striatum, leading to the investigation of other delivery methods like viral vectors for neurotrophic factors in PD.

ii. CERE-120 Gene Therapy Clinical Trial

Mechanism and Preclinical Trials

As discussed previously, preclinical work examined the effects of delivering recombinant NTN to the parkinsonian brain in an effort to protect and restore the remaining SNpc dopaminergic neurons and modify PD progression. However, the affinity for which NTN binds to HSPG greatly limits its spread

through the extracellular space and prevents its diffusion from the injection site, possibly leading to the underwhelming effects seen in the recombinant NTN infusion preclinical trials [Domanskyi *et al*, 2015]. To overcome this, efforts turned to using viral vectors to overexpress NTN once viral vectors were shown to be safe for use in the human brain. The advantage of viral vector-delivered NTN is that it would provide for sustained expression of the neurotrophic factor that would be controlled by the spread of the virus rather than the limited diffusion of the protein. In addition, the use of a viral vector to transduce neurons and stimulate *in vivo* production of NTN would generate a more biologically relevant form of the protein with proper cleavage and post-translational modifications rather than the form generated *in vitro* by *E.Coli* for infusion [Domanskyi *et al*, 2015].

The safety and efficacy of viral vector-mediated overexpression of NTN to the parkinsonian brain was first examined in a rat model of PD. The first attempt came in the form of a LV construct overexpressing NTN or GDNF to examine the role of the pre-pro-sequence in secretion of these neurotrophic factors [Fjord-Larsen *et al*, 2005]. In this study, the pre-pro-NTN form resulted in very little processing of the protein, whereas the pro-NTN form did not initiate the requisite GFR α 2-Ret mediated downstream signaling cascades required for neuroprotection. Deletion of the pro-region combined with addition of immunoglobulin heavy-chain signal peptide, however, provided a mature, active form of NTN that was highly secreted and activated downstream signaling cascades to provide neuroprotection in nigral dopaminergic neurons [Fjord-Larsen *et al*, 2005]. When this modified form of NTN was delivered via AAV2 in rats two weeks before 6-OHDA was injected into the striatum to induce a lesion, it prevented SNpc dopaminergic cell death, preserved fiber innervation of the striatum, and resulted in sustained behavioral recovery [Gasmi *et al*, 2007]. Furthermore, the AAV2-NTN, named CERE-120, demonstrated favorable safety and tolerability data, even at long time points [Gasmi *et al*, 2007].

CERE-120 was then tested in NHPs to examine efficacy in a higher-order species and again investigate safety and tolerability. In a key safety, tolerability, and efficacy study, rhesus monkeys were rendered hemiparkinsonian through a unilateral injection of MPTP [Kordower *et al*, 2006]. CERE-120 was then injected into the striatum and SNpc four days after MPTP injection. In this model, CERE-120 was able to significantly improve motor scores by 80-90% at four to ten months post-injection [Kordower *et al*, 2006]. Neuroanatomically, CERE-120 prevented the degeneration of a significant number of nigral dopaminergic neurons and preserved the axon terminals of the nigrostriatal system in the striatum. These neuroprotective and neurorestorative effects were the result of NTN activating the GFR α 2-Ret downstream signaling cascades, as assessed by increased levels of ERK following CERE-120 administration [Kordower *et al*, 2006]. Furthermore, CERE-120 administration did not appear to result in any negative side effects and no overt tissue pathology [Kordower *et al*, 2006].

Clinical Trial Design and Outcomes

The Phase I clinical trial for safety, tolerability, and preliminary efficacy was an open-label study that involved intraputaminial injections of CERE-120 in six patients receiving a low dose and six patients receiving a high dose of the vector (Table 2) [Marks *et al*, 2008]. Patients all had advanced idiopathic PD, with a mean age of 57 and a mean of 11 years post-diagnosis. No long-term side effects were reported as a result of the surgery or CERE-120, with no significant immune responses noted. Both dosage groups displayed improvements in “off” UPDRS scores at one year post-surgery [Marks *et al*, 2008]. Nigrostriatal function as measured by ¹⁸F-levodopa striatal uptake PET scans did not improve with CERE-120 treatment in either dose group [Marks *et al*, 2008]. These favorable safety results led to a Phase II clinical trial with intraputaminial CERE-120.

The Phase II clinical trial for intraputaminally delivered CERE-120 was designed as a placebo-controlled, double-blind, randomized trial (Table 2) [Marks *et al*, 2010]. In this trial, 58 patients with advanced idiopathic PD received either CERE-120 (38 patients) or a sham surgery (20 patients) with injections into the putamen. The average age of patients in both groups was about 60 years of age and about 10 years post-diagnosis for each group. At one year post-surgery, no significant differences were seen in primary outcome measure UPDRS scores between treated and placebo groups [Marks *et al*, 2010]. Some differences were observed in secondary outcome measures such as improvements in activities of daily living in the CERE-120 treated group. In a subset of patients assessed at 18 months post-surgery, CERE-120 resulted in slight improvements in the UPDRS “off” state, UPDRS “on” state without dyskinesias, and timed walking in the “off” state [Marks *et al*, 2010]. Several adverse effects were reported such as tumors, seizure, or hemorrhage, but most of these cases were either temporary or were not directly contributed to the intervention. As patients did not receive benefits from treatment in the primary outcome measure at one year post-surgery and the effects seen at 18 months post-surgery were modest, this trial was deemed unsuccessful [Marks *et al*, 2010]. However, the treatment was well tolerated and the slight differences at 18 months between CERE-120- and sham-treated patients may indicate a delayed neurotrophic effect [Marks *et al*, 2010; Kelly *et al*, 2015].

It is speculated that the lack of efficacy of the Phase II intraputaminally-delivered CERE-120 could be due to a lack transport of the neurotrophic factor to the nigrostriatal SNpc cell bodies. Following the Phase II clinical study, two patients died as a result of unrelated medical issues and their brains were then examined for the extent of NTN upregulation and spread [Marks *et al*, 2010; Bartus *et al*, 2011]. NTN-immunostaining revealed a pattern of robust NTN overexpression in about 15% of the putamen by volume. This volume was comparable to the volume covered by CERE-120 overexpression in young adult, aged, and parkinsonian NHPs [Bartus *et al*, 2011]. However, unlike the high levels of NTN

observed in SNpc dopaminergic neurons of NHPs, NTN overexpression in the patients was only rarely observed in the dopaminergic SNpc cell bodies of the nigrostriatal system [Bartus *et al*, 2011]. In addition, striatal NTN overexpression in NHPs induced robust TH expression in axonal fields of the nigrostriatal system whereas this was sparse and rarely observed in the CERE-120-injected patients [Bartus *et al*, 2011]. This led many to conclude that the lack of clinical efficacy was due to a lack of retrograde transport of NTN through the nigrostriatal system from the axon terminals in the striatum to the cell bodies in the SNpc [Marks *et al*, 2010; Bartus *et al*, 2011; Herzog *et al*, 2013].

To overcome this issue, a redesign of the CERE-120 was performed to involve delivery of the viral vector to the striatum as well as the SNpc (Table 2) [Herzog *et al*, 2013; Olanow *et al*, 2015]. In this second clinical study of efficacy, 51 patients were injected bilaterally in the putamen and SNpc with CERE-120 or sham and were assessed for functional recovery at 15- to 24-months after surgery in a double-blind, randomized Phase I/II clinical trial [Olanow *et al*, 2015]. No adverse side effects attributable to NTN or gene therapy were observed in any patients. At 15 months, no significant differences were observed in UPDRS scores between the CERE-120 and sham treated patients. In addition, no significant benefits were observed with CERE-120 in any of the secondary outcome measures for functional recovery [Olanow *et al*, 2015]. These disappointing outcomes led to the classification of the CERE-120 gene therapy clinical trials for PD a failure.

iii. Glial Cell Line-Derived Neurotrophic Factor Gene Therapy Clinical Trial

Mechanism and Preclinical Trials

Although recombinant GDNF infusion into the putamen showed promise in preclinical and Phase I clinical trials [Gash *et al*, 1996; Rosenblad *et al*, 1998; Aoi *et al*, 2000; Grondin *et al*, 2002; Gill *et al*, 2003; Patel *et al*, 2005], Phase II clinical trials showed a lack of efficacy and high prevalence of adverse

reactions [Nutt *et al*, 2003; Lang *et al*, 2006]. Similar with NTN, researchers sought to overcome the lack of diffusivity and provide sustained expression of a biologically relevant, post-translationally modified form of GDNF [Domanskyi *et al*, 2015]. As a result, viral vector-mediated gene therapy to overexpress GDNF is under development.

Even though viral vector-mediated gene therapy for NTN did not display clinical efficacy, gene therapy for GDNF is under development as GDNF has shown greater neuroprotective and neurorestorative properties than NTN [Rosenblad *et al*, 1999]. Preclinical studies testing viral vector-delivery of GDNF in rats and NHPs have shown promising neuroprotection and neurorestoration. LV-delivered GDNF was shown to be neurorestorative when administered four weeks after 6-OHDA injection to the SNpc to induce a rat model of early PD [Brizard *et al*, 2006]. In this model, authors claimed GDNF was able to preserve numbers of SNpc dopaminergic neurons, protect nigrostriatal fiber intensity in the striatum, stimulate axonal sprouting to reinnervate areas of the striatum that had lost dopaminergic projections, and reverse the development of PD-like motor behaviors [Brizard *et al*, 2006]. Similar results were observed when using LV, adenovirus, or AAV to introduce GDNF prior to or after induction of the PD model [Bilang-Bleuel *et al*, 1997; Kirik *et al*, 2000; Tereshchenko *et al*, 2014].

Notably, one study found LV-mediated GDNF delivery to the striatum and SNpc resulted in recovery of the nigrostriatal system from normal, unlesioned aged rhesus monkeys and MPTP-lesioned young adult rhesus monkeys [Kordower *et al*, 2000]. LV GDNF intrastriatal injection to aged, nonlesioned monkeys led to increased GDNF expression in the striatum and SNpr and markers of dopaminergic function in the striatum and SNpc. In young MPTP-lesioned monkeys, LV GDNF also led to increased GDNF expression in the striatum and SNpr and increased TH-immunoreactivity in the nigrostriatal system, and functional recovery. Importantly, the degree of striatal TH-immunoreactivity was variable between young adult

lesioned monkeys, and the degree of TH-immunoreactivity correlated strongly with the functional recovery observed in the hand-reach task [Kordower *et al*, 2000]. Although the LV GDNF results were promising, focus shifted to investigating the ability of AAV2 to delivery GDNF to the brain as this viral vector was already shown to be safe in clinical trials.

Preclinical trials using AAV2 GDNF in NHPs have also displayed promising results. The first NHP study using AAV2 GDNF used a unilateral MPTP-lesioned rhesus monkey model of PD [Eberling *et al*, 2009]. Four months after induction of the lesion, monkeys received bilateral infusions of AAV2 GDNF through convection-enhanced delivery. PET scans revealed a significant deficit in DA signaling in the lesioned striatum that was improved six months after AAV2 GDNF administration [Eberling *et al*, 2009]. This improved DA signaling corresponded to improved functional recovery that was sustained up to one year post-injection. In addition, AAV2 GDNF expression resulted in increased TH expression in the striatum [Eberling *et al*, 2009]. Furthermore, later experiments examined administration of AAV2 GDNF when delayed until full MPTP-lesioning of the nigrostriatal system in one hemisphere and a partial lesion of the nigrostriatal system in the contralateral hemisphere [Kells *et al*, 2011]. AAV2 GDNF resulted in significant improvement in motor scores that were sustained from three to 24 months after initiation of treatment. This study also found no adverse interactions between AAV2 GDNF and L-dopa treatment, with the concurrent treatments well tolerated in the vast majority of cases and only one instance of L-dopa induced dyskinesias [Kells *et al*, 2011]. These improvements in motor scores correlated with PET signaling of dopaminergic terminal integrity in the striatum and normal rates of DA turnover. GDNF expression in the striatum was mostly diffuse but did co-localize with striatal neurons, as well as evidence for anterograde transport observed with GDNF-positive neurons in the globus pallidus, STN, and SN. Dopaminergic fibers of the nigrostriatal system were also increased with AAV2 GDNF treatment, with these increases correlating with GDNF expression levels [Kells *et al*, 2011]. No evidence for long-

term AAV2 GDNF treatment-related toxicity was observed with the exception of one case of weight loss due to a misplaced cannula and infusion of the viral vector into the cerebrospinal fluid [Kells *et al*, 2011].

Clinical Trial Design and Outcomes

Based on the promising results of the preclinical AAV2 GDNF studies, a Phase I clinical trial for convection-enhanced, MRI-guided delivery of AAV2 GDNF is planned (Table 2). This trial is set up as a non-randomized, open label safety and efficacy study and is currently enrolling patients with idiopathic, advanced PD not controlled well by medications [clinicaltrials.gov, NCT01621581]. The primary outcome measure for this study will be the safety and tolerability of four different doses of AAV2 GDNF injected bilaterally into the putamen with the secondary outcome measure obtaining any preliminary information on clinical efficacy of treatment.

The putamen was the target structure of choice for the AAV2 GDNF clinical trial as preclinical work indicated high levels of anterograde transport of GDNF as well as a potential lack of efficacy upon delivery to the SNpc [Kirik *et al*, 2000; Kells *et al*, 2011; Kelly *et al*, 2015]. Injecting AAV2 GDNF into the putamen may result in the greatest functional and neuroanatomical benefits as it will provide GDNF locally to the remaining nigrostriatal system axon terminals in the striatum and transduce the largely intact striatonigral neurons that project to the SNpr where secretion of GDNF will bathe the nigrostriatal SNpc dopaminergic cell bodies in GDNF (Figure 1a) [Kelly *et al*, 2015]. In addition, as rAAV2 GDNF is primarily transported via anterograde transport, injection to the striatum allows robust overexpression in the striatum and SNpr, as well as distribution of the vector to other structures of the basal ganglia that are adversely affected in PD, such as the GP and STN [Ciesielska *et al*, 2011]. Furthermore, targeting the SNpc for gene therapy clinical trials is avoided when possible due to the depth of this structure and

its proximity to autonomic centers of the brain presenting added risks and potential for complication [Kelly *et al*, 2015].

Viral Vector Transduction and the Aged Brain

Although many of the viral vector-mediated gene therapy clinical trials for PD showed promise in early Phase I testing, all blinded and controlled Phase II efficacy trials have failed to meet the primary and secondary endpoints or show any improvements beyond the placebo effect or conventional treatments (Table 2) [Kelly *et al*, 2015; O'Connor and Boulis, 2015]. There are many possible reasons for these disappointing results. For instance, some speculate that the transduction volume mediated by AAV2 and LV is not adequate enough to impact the vast deficits in dopamine neurotransmission or nigrostriatal degeneration seen in PD [Choudhury *et al*, 2015]. Others argue that the clinical trial endpoints were too early and did not give enough time to see delayed effects [Marks *et al*, 2010]. The enrollment of advanced-stage PD patients in these trials could have also contributed to the disappointing outcomes, as targeting earlier stages in the disease could have enabled the rescue of a more intact basal ganglia and nigrostriatal system [Manfredsson *et al*, 2009]. Others argue that the structure injected was inappropriate for the study and should have included other structures to induce a more robust effect [Marks *et al*, 2010; Bartus *et al*, 2011]. Furthermore, it is possible that neurotrophic factors do not act as predicted in the PD brain based on preclinical animal studies as the animal models used to test the effects of neurotrophic factors do not model enough facets of the disease or are not suitable for modeling the effects of neurotrophic factors in aged PD patients [Manfredsson *et al*, 2009]. For instance, many believe the neurotoxin models of PD do not accurately model the neuropathology of this disease, favoring PD models generated with preformed α -syn fibrils [Paumier *et al*, 2015] or AAV-mediated overexpression of α -syn [Decressac *et al*, 2012].

In line with these opinions, the lack of modeling age-related diseases such as PD in an aged animal models may also be a factor leading to the unimpressive outcomes. Although age is the single greatest risk factor for developing PD [Collier *et al*, 2011; Reeve *et al*, 2014], preclinical therapeutic studies are almost exclusively conducted in young adult animals modeling this age-related disease [Azzouz *et al*, 2002; Lou *et al*, 2002; Bankiewicz *et al*, 2006; Brizard *et al*, 2006; Kordower *et al*, 2006; Gasmi *et al*, 2007; Eberling *et al*, 2009; Jarraya *et al*, 2009; among others]. Furthermore, the viral vector-mediated gene therapy preclinical trials that were performed in aged animals were mostly conducted in naïve aged NHPs that did not model PD [Kordower *et al*, 2000; Herzog *et al*, 2007; Su *et al*, 2009; Bartus *et al*, 2011]. In addition, aged non-human primates that were rendered parkinsonian were never directly compared to a young adult counterpart [Emborg *et al*, 2009], missing any important age-related changes in the efficacy of viral vector-mediated gene therapy between young adult and aged animals.

Failing to account for aging as a covariate in PD could ignore possible interactions between age and neurotrophic factor signaling, dopamine synthesis, or viral vector transduction. This, however, is important information to know as the degree of functional or neuroanatomical benefits correlates strongly with the level of transgene expression. In a 2009 study by Emborg and colleagues, aged rhesus monkeys were rendered hemiparkinsonian with an MPTP injection. One week later monkeys received an injection of LV GDNF or a control virus, LV LacZ, and monitored for three months post-injection. GDNF overexpression levels correlated significantly with behavioral, neuroimaging, and anatomical measures of nigrostriatal system neuroprotection [Emborg *et al*, 2009]. Expression levels of GDNF varied greatly between aged monkeys, elucidating a threshold of GDNF overexpression must be surpassed in order to display any behavioral or neuroanatomical benefit from treatment [Emborg *et al*, 2009]. Furthermore, the authors noted that—when compared to previous studies on young adult parkinsonian rhesus

monkeys—the magnitude of neuroprotection or neurorestoration was dependent on GDNF overexpression levels *as well as* age of the subject [Emborg *et al*, 2009]. Taken together, these results indicate a need to understand the impact of age on viral vector-mediated gene therapy.

I. Potential Impact of Age-Related Changes in the Brain on Viral Vector Transduction

With the vast number of changes that take place in neurons with advanced age, it is quite possible that age could alter the ability of viral vectors to transduce cells. As many steps of viral vector transduction are rate-limiting, deficiencies in cellular processes related to these steps in aged neurons could exacerbate already slow mechanisms, limiting the ability of viral vectors to efficiently transduce cells. This possibility applies both to AAV and LV transduction in the aged brain.

i. Changes in the Aged Brain Related to Steps of AAV and LV Transduction

Due to the overlap between AAV and LV transduction and the cellular processes impacted by aging, it is very possible that advanced age could impact the ability of these viral vectors to transduce cells. For instance, viral vectors must first diffuse through the extracellular matrix to infect a large volume and number of cells. However, changes in the extracellular space occur with advancing age such as increased presence of debris in the extracellular space due to decreased clearance mechanisms [Kang and Lichtman, 2013; Morawski *et al*, 2014] and increased presence of neutralizing antibodies towards AAV in aged as compared to young adult patients that could prevent the transduction of AAV [Mimuro *et al*, 2014]. In addition, diffusion parameters of the extracellular matrix are altered in the aged brain as a result of structural rebuilding of the tissue by astrocytes, astrocytic processes, or alterations in extracellular matrix molecules on neurons [Sykova *et al*, 2002]. Age-related changes in the brain extracellular space could prevent viral vectors from diffusing freely, thereby limiting their spread and the area of transduction.

In order for a viral vector to transduce a cell, it must first bind to its required receptor and co-receptor (Figure 2, Table 1), with some stating that the most significant factor influencing viral binding is the abundance of receptors [Ding *et al*, 2005]. In addition, with the AAV penetration efficiency (ratio of the number of virus-cell contacts compared to the number of internalization events) being only about 13% [Schultz and Chamberlain, 2008], decreases in factors affecting receptor binding and endocytosis could make this process even less efficient. It has been shown that some of the receptors involved in viral vector docking and endocytosis are downregulated in certain brain structures of aged as compared to young adult animals. For instance, rAAV5 requires the 2,3-linked sialic acid receptor as its primary receptor [Walters *et al*, 2001]. Age has been shown to impact levels of 2,3-linked sialic acid in various brain regions, with decreases in this receptor reported in the aged rat hippocampus [Sato and Endo, 1999; Sato *et al*, 2001] and cerebellum [Sasaki *et al*, 2002]. These decreases are of biological importance as previous studies have shown that decreasing 2,3-linked sialic acid receptor levels corresponds to a decrease in AAV5 transduction levels [Walters *et al*, 2001]. As a result, it is likely that age-related decreases, like those observed with 2,3-linked sialic acid, could occur with other receptors and co-receptors, thereby leading to a decrease in transduction in the aged brain.

Endocytosis of viral particles is another important step in transduction (Figure 2) that may be impacted by age-related changes in neurons. For example, clathrin-mediated endocytosis is believed to be the main method of endocytosis for AAV [Sanlioglu *et al*, 2001; Schultz and Chamberlain, 2008]. Aged neurons, however, have altered clathrin dynamics that make this process become less efficient with age [Park *et al*, 2001; Blanpied *et al*, 2003]. After endocytosis, AAV viral particles are trafficked along the cytoskeleton in endosomes where they undergo acidification to initiate intracellular localization and capsid breakdown (Figure 2) [Sanlioglu *et al*, 2000; Kronenberg *et al*, 2005; Ding *et al*, 2006].

Cytoskeletal trafficking, however, is highly energy-dependent and increased mitochondrial dysfunction with age [Bender *et al*, 2006; Kraytsberg *et al*, 2006] could lead to issues in energetics leaving a buildup of AAV particles in the cytoplasm unable to continue the transduction process due to a lack of energy for intracellular trafficking.

AAV particles that are successfully trafficked then purportedly undergo Golgi-mediated processing [Bantel-Schall *et al*, 2002] and enter the nucleus through the NPC [Nicolson and Samulski, 2014]. It is possible that steps that underlie AAV processing in the Golgi are altered with age. In addition, the NPC undergoes substantial age-related deterioration [D'Angelo *et al*, 2009]. The deterioration of the NPC results in the lack of turnover in some NPC scaffolding proteins, causing a more permissive NPC and an influx of obstructive proteins, such as tubulin, into the nucleus [D'Angelo *et al*, 2009]. This process could block influx of viral particles or interfere with downstream steps of transduction such as the uncoating of AAV particles or the conversion of AAV ssDNA to dsDNA, or integration of LV into the host genome [Schultz and Chamberlain, 2008; Sakuma *et al*, 2012]. Furthermore, conversion of ssDNA to dsDNA may involve DNA repair mechanisms that are impaired in aged cells [Lombard *et al*, 2005].

Aging also impacts the last steps of AAV and LV transduction—transcription and translation. Numerous groups have found changes in transcription in the aged as compared to young adult brain [Lee *et al*, 2000; Gao *et al*, 2013]. Consistently, approximately 5-10% of the genome experiences age-related changes in transcription [Glorioso and Sibille, 2011]. These changes occur in genes related to neurotrophic factor signaling, calcium signaling, synaptic density, neurotransmitter signaling, stress response, protein turnover, and inflammation [Lee *et al*, 2000; Glorioso and Sibille, 2011; Gao *et al*, 2013]. Most of the changes in the neuronal transcriptome are the result of down-regulating genes while the glial transcriptome conversely experiences up-regulation with age [Glorioso and Sibille, 2011]. These

changes in transcription may result from age-related changes in the expression of transcriptional regulators such as histones, transcription factors, or methylation-related proteins [Glorioso and Sibille, 2011]. These age-related changes have the potential to substantially influence the ability of viral vectors to transduce cells by altering the ability of cells to convert viral dsDNA to mRNA or impacting any other step of transduction that experiences a down-regulation of key factors involved in that process.

The process of translation is also altered in the aged brain. Studies have indicated that protein synthesis is decreased in the aged as compared to young adult brain [Smith *et al*, 1995; Ryazanov and Nefsky, 2002]. These decreases occur in multiple brain regions and result in a modest (approximately 17% lower) rate of protein synthesis in structures like the rat SN [Smith *et al*, 1995; Ryazanov and Nefsky, 2002]. Together, age-related changes in this and many other cellular processes used by AAV and LV vectors to successfully transduce cells could lead to an age-related deficiency in transduction of the brain.

II. Age-Related Deficits in Transduction Efficiency

Few studies have directly compared the efficiency of viral vector transduction in the aged versus young adult brain. One study by Wu *et al* (2004) found transduction deficiencies in the aged F344/Brown Norway rat when using rAAV2/2 to overexpress either GFP or nerve growth factor in the rat septum. A modest but non-significant decrease in the total number of transgene-expressing cells were observed in the aged as compared to young adult rat septum, with lighter immunostaining noted. In addition, protein quantitation showed a significant decrease in nerve growth factor overexpression in the aged as compared to young adult rat septum. These findings led authors to conclude that age-related decreases in exogenous protein expression were present within individual cells following rAAV2/2 administration to the septum [Wu *et al*, 2004].

Similarly, our group reported an age-related transduction deficiency when using rAAV2/5 to overexpress human wildtype α -syn (rAAV2/5 α -syn) in the SNpc [Fischer *et al*, 2016]. Regardless of rAAV2/5 titer or duration of expression, rAAV2/5 α -syn resulted in fewer α -syn-positive cells in the mesencephalon and lower levels of α -syn protein in the ipsilateral striatum indicating a robust transduction deficiency with age for rAAV2/5 in the SNpc [Fischer *et al*, 2016]. However, not all rAAV constructs are deficient in the aged brain. A study by Klein *et al* (2010) found rAAV2/9 to be equally as efficient in the aged as compared to young adult rat SNpc. In this study, rAAV2/9 overexpressing GFP or human wildtype tau was injected into the SNpc of young adult and aged Sprague Dawley rats. To compare transduction efficiency between young adult and aged rats, Western blots were performed for GFP protein in the microdissected SNpc two weeks after rAAV2/9 GFP injection in the SNpc. No significant differences were seen between GFP expression levels in young adult or aged rats [Klein *et al*, 2010]. Similar results were observed in a higher-order animal, the NHP. rAAV2/9 injected into the SNpc of young adult and aged marmoset monkeys resulted in identical patterns of transduction between ages as assessed by the volume of the SN expressing the virally-delivered transgene [Bourdenx *et al*, 2015].

Taken together, these studies investigating the impact of age on viral vector-mediated gene therapy indicate a potential age-related deficit in transduction by some [Wu *et al*, 2004; Fischer *et al*, 2016], but not all [Klein *et al*, 2010; Bourdenx *et al*, 2015] viral vectors. It is important to investigate and thoroughly characterize the impact of age on viral vector transduction as this technology is used in the creation of aged animal models for age-related neurodegenerative diseases [Klein *et al*, 2010; Bourdenx *et al*, 2015; Fischer *et al*, 2016] and to test different factors for gene therapy application in the aged brain [Wu *et al*, 2004].

III. Importance of Accounting for Age in Viral Vector-Mediated Gene Therapy

Parkinson's disease is the second most common neurodegenerative disease, after Alzheimer's disease (AD). The primary risk factor for developing both of these diseases is advanced age, with the average age of onset for PD being 65 years of age [Collier *et al*, 2011]. Currently there are no treatments available that can slow or halt the progression of PD or AD, with current treatments only providing modest symptomatic benefits [Cummings *et al*, 2013; Stocchi and Olanow, 2013]. As a result, viral vector-mediated gene therapy is being tested or proposed for use in both of these prevalent, age-related brain diseases.

Viral vector-mediated gene therapy has been tested in seven clinical trials for PD, with three more clinical trials currently recruiting patients (Table 2). These clinical trials all target the basal ganglia, mainly the putamen, for overexpression of genes involved in regulating basal ganglia neurotransmission or providing trophic support to the degenerating nigrostriatal system (Table 2). The clinical trials that have been completed have all resulted in early promising benefits in open-label Phase I trials followed by a lack of benefit observed in later, placebo-controlled Phase II testing [O'Connor and Boulis, 2015]. Similarly, viral vector-mediated clinical trials for AD are early in development, with clinical trials using AAV2 to overexpress a neurotrophic factor in the forebrain of patients demonstrating promise in open-label Phase I trials and a failure to meet primary endpoints in the subsequent Phase II trials [Rafii *et al*, 2014; O'Connor and Boulis, 2015; clinicaltrials.gov, NCT00876863].

Although this is most likely due to a variety of factors, the possibility that age could impact the efficiency of viral vector transduction needs to be investigated due to the overlap between mechanisms of viral vector transduction and the age-related changes that occur in different cellular processes. With the vast majority of the preclinical studies for viral vector-mediated gene therapy for PD and AD performed in

young adult animals, failing to account for the covariate of aging adds an additional hurdle when translating this therapy to the clinical. When translating work from preclinical animal models to human clinical trials, the titer of the virus must be extrapolated to account for differences in the brains between species. Failing to account for age in the preclinical trials creates another variable that needs to be accounted for, and failing to account for potential viral vector-mediated transduction deficiencies that come with advancing age may result in insufficient scaling for clinical trials. Understanding if age impacts viral vector transduction, which viral vectors are affected by advanced age, and the mechanism behind age-related transduction deficiencies will be an important step in designing future viral vector-mediated gene therapy clinical trials and interpreting the results of previous clinical trials using this technology.

Overarching Conclusions

- PD is the second most common neurodegenerative disease, after AD, and is primarily characterized by motor dysfunctions that arise from degeneration of the nigrostriatal system.
- Currently, no treatment is currently available that can slow or halt the progression of PD, and symptomatic treatments oftentimes lose efficacy after extended use.
- Viral vector-mediated gene therapy is being tested in multiple clinical trials for PD, none of which have resulted in benefits over the placebo effect or conventional treatment.
- Preclinical trials that led to the clinical trials were almost exclusively performed in young adult animals, therefore failing to account of advancing age as a covariate in treatment.
- Preliminary studies have shown an age-related deficiency in the ability of some, but not all, viral vectors to transduce various structures within the brain.
- A lack of understanding exists as to which viral vectors may be deficient in transducing the aged as compared to young adult brain and the mechanism behind these deficiencies.

- Characterizing which viral vectors are most efficient in the aged brain and the mechanism behind any age-related transduction deficiencies will lead to improved preclinical trials using viral vectors to induce or treat disease models in aged animals, as well as better informed clinical trials in the hopes of developing a disease-modifying treatment for PD.

LITERATURE CITED

LITERATURE CITED

- Agid, Y. (1991). Parkinson's disease: pathophysiology. *Lancet*, **337(8753)**: 1321-1324.
- Ahlskog, J.E., and M.D. Muentner. (2001). Frequency of levodopa-related dyskinesias and motor fluctuations as estimated from the cumulative literature. *Mov Disord*, **16**: 448-458.
- Airaksinen, M.S., A. Titievski, and M. Saarma. (1999). GDNF family neurotrophic factor signaling: four masters, one servant? *Mol Cell Neurosci*, **13(5)**: 313-325.
- Airaksinen, M.S., and M. Saarma. (2002). The GDNF family: Signalling, biological functions, and therapeutic value. *Nature Rev Neurosci*, **3**: 383-394.
- Akache, B., D. Grimm, K. Pandey, S.R. Yant, H. Xu, and M.A. Kay. (2006). The 37/67-kilodalton laminin receptor is a receptor for adeno-associated virus serotypes 8, 2, 3, and 9. *J Virol*, **80(19)**: 9831-9836.
- Akache, B., D. Grimm, X. Shen, S. Fuess, S.R. Yant, D.S. Glazer, J. Park, and M.A. Kay. (2007). A two-hybrid screen identifies cathepsins B and L as uncoating factors for adeno-associated virus 2 and 8. *Mol Ther*, **15(2)**: 330-339.
- Aminoff, M.J. (2006). Treatment should not be initiated too soon in Parkinson's disease. *Annal Neurol*, **59(3)**: 562-564.
- Aoi, M., I. Date, S. Tomita, and T. Ohmoto. (2000). The effect of intrastriatal single injection of GDNF on the nigrostriatal dopaminergic system in hemiparkinsonian rats: behavioral and histological studies using two different dosages. *Neurosci Res*, **36(4)**: 319-325.
- Azzouz, M., E. Martin-Rendon, R.D. Barber, K.A. Mitrophanous, E.E. Carter, J.B. Rohll, S.M. Kingsman, A.J. Kingsman, and N.M. Mazarakis. (2002). Multicistronic lentiviral vector-mediated striatal gene transfer of aromatic L-amino acid decarboxylase, tyrosine hydroxylase, and GTP cyclohydrolase I induces sustained transgene expression, dopamine production, and functional improvement in a rat model of Parkinson's disease. *J Neurosci*, **22(23)**: 10302-10312.
- Bankiewicz, K.S., J. Forsayeth, J.L. Eberling, R. Sanchez-Pernaute, P. Pivrotto, J. Bringas, P. Herscovitch, R.E. Carson, W. Eckelman, B. Reutter, and J. Cunningham. (2006). Long-term clinical improvement in MPTP-lesioned primates after gene therapy with AAV-hAADC. *Mol Ther*, **14**: 564-570.
- Bankiewicz, K.S., J.L. Eberling, M. Kohutnicka, W. Jagust, P. Pivrotto, J. Bringas, J. Cunningham, T.F. Budinger, and J. Harvey-White. (2000). Convection-enhanced delivery of AAV vector in parkinsonian monkeys; in vivo detection of gene expression and restoration of dopaminergic function using pro-drug approach. *Exp Neurol*, **164(1)**: 2-14.
- Bantel-Schall, U., B. Hubb, and J. Kartenbeck. (2002). Endocytosis of adeno-associated virus type 5 leads to accumulation of virus particles in the Golgi compartment. *J Virol*, **76**: 2340-2349.

- Barbero, P., L. Bittova, and S.R. Pfeffer. (2002). Visualization of Rab9-mediated vesicle transport from endosomes to the trans-Golgi in living cells. *J Cell Biol*, **156**: 511-518.
- Bartlett, J.S., R. Wilcher, and R.J. Samulski. (2000). Infectious entry pathway of adeno-associated virus and adeno-associated virus vectors. *J Virol*, **74**: 2777-2785.
- Bartus, R.T., C.D. Herzog, Y. Chu, A. Wilson, L. Brown, J. Siffert, E.M. Johnson Jr, C.W. Olanow, E.J. Mufson, and J.H. Kordower. (2011). Bioactivity of AAV2-neurturin gene therapy (CERE-120): differences between Parkinson's disease and nonhuman primate brains. *Mov Disord*, **26(1)**: 27-36.
- Benabid, A.L., S. Chabardes, J. Mitrofanis, and P. Pollak. (2009). Deep brain stimulation of the subthalamic nucleus for the treatment of Parkinson's disease. *Lancet Neurol*, **8(1)**: 67-81.
- Bender, A., K.J. Krishnan, C.M. Morris, G.A. Taylor, A.K. Reeve, R.H. Perry, E. Jaros, J.S. Hersheson, J. Betts, T. Klopstock, R.W. Taylor, and D.M. Turnbull. (2006). High levels of mitochondrial DNA deletions in substantia nigra neurons in aging and Parkinson's disease. *Nat Gen*, **38(5)**: 515-517.
- Bilang-Bleuel, A., F. Revah, P. Colin, I. Locquet, J.J. Robert, J. Mallet, and P. Horellou. (1997). Intrastriatal injection of an adenoviral vector expressing glial-cell-line-derived neurotrophic factor prevents dopaminergic neuron degeneration and behavioral impairment in a rat model of Parkinson disease. *Proc Natl Acad Sci USA*, **94(16)**: 8818-8823.
- Blackburn, S.D., R.A. Steadman, and F.B. Johnson. (2006). Attachment of adeno-associated virus type 3H to fibroblast growth factor receptor 1. *Arch Virol*, **151(3)**: 617-623.
- Blanpied, T.A., D.B. Scott, and M.D. Ehlers. (2003). Age-related regulation of dendritic endocytosis associated with altered clathrin dynamics. *Neurobiol Aging*, **24**: 1095-1104.
- Blomer, U., L. Naldini, T. Kafri, D. Trono, I.M. Verma, and F.H. Gage. (1997). Highly efficient and sustained gene transfer in adult neurons with a lentivirus vector. *J Virol*, **71(9)**: 6641-6649.
- Bourdenx, M., S. Dovero, M. Engeln, S. Bido, M.F. Bastide, N. Dutheil, I. Vollenweider, L. Baud, C. Piron, V. Grouthier, T. Boraud, G. Porras, Q. Li, V. Baekelandt, D. Scheller, A. Michel, P. Fernagut, F. Georges, G. Courtine, E. Bezard, and B. Dehay. (2015). Lack of additive role of ageing in nigrostriatal neurodegeneration triggered by alpha-synuclein overexpression. *Acta Neuropathol Commun*, **3**: 46.
- Braak, H., D. Sandmann-Keil, W. Gai, and E. Braak. (1999). Extensive axonal Lewy neurites in Parkinson's disease: a novel pathological feature revealed by α -synuclein immunocytochemistry. *Neuroscience letters*, **265 (1)**: 67-69.
- Brizard, M., C. Carcenac, A.P. Bemelmans, C. Feuerstein, J. Mallet, and M. Savasta. (2006). Functional reinnervation from remaining DA terminals induced by GDNF lentivirus in a rat model of early Parkinson's disease. *Neurobiol Dis*, **21(1)**: 90-101.
- Bronstein, J.M., M. Tagliati, R.L. Alterman, A.M. Lozano, J. Volkmann, A. Stefani, F.B. Horak, M.S. Okun, K.D. Foote, P. Krack, R. Pahwa, J.M. Henderson, M.I. Hariz, R.A. Bakay, A. Rezai, W.J. Marks Jr, E.

- Moro, J.L. Vitek, F.M. Weaver, R.E. Gross, and M.R. DeLong. (2011). Deep brain stimulation for Parkinson disease: an expert consensus and review of key issues. *Arch Neurol*, **68**: 165.
- Brooks, D.J. (2012). Parkinson's disease: diagnosis. *Parkinsonism Relat Disord*, **18 Suppl 1**: S31-S33.
- Burger, C., O.S. Gorbatyuk, M.J. Velardo, C.S. Peden, P. Williams, S. Zolotukhin, P.J. Reier, R.J. Mandel, and N. Muzyczka. (2004). Recombinant AAV viral vectors pseudotyped with viral capsids from serotypes 1, 2, and 5 display differential efficiency and cell tropism after delivery to different regions of the central nervous system. *Mol Ther*, **10(2)**: 302-317.
- Burke, R.E., and K. O'Malley. (2013). Axon degeneration in Parkinson's disease. *Exp Neurol*, **246**: 72-83.
- Bushman, F.D., and R. Craigie. (1991). Activities of human immunodeficiency virus (HIV) integration protein in vitro: specific cleavage and integration of HIV DNA. *Proc Natl Acad Sci USA*, **88(4)**: 1339-1343.
- Carneiro, F.A., M.L. Bianconi, G. Weissmuller, F. Stauffer, and A.T. da Poian. (2002). Membrane recognition by vesicular stomatitis virus involves enthalpy-driven protein-lipid interactions. *J Virol*, **76(8)**: 3756-3764.
- Chan, P.L., J.G. Nutt, and N.H. Holford. (2007). Levodopa slows progression of Parkinson's disease: external validation by clinical trial simulation. *Pharm Res*, **24(4)**: 791-802.
- Choudhury, S.R., E. Hudry, C.A. Maguire, M. Sena-Esteves, X.O. Breakefield, and P. Grandi. (2016). Viral vectors for therapy of neurologic diseases. *Neuropharmacology*, doi: 10.1016/j.neuropharm.2015.02.013.
- Christine, C.W., P.A. Starr, P.S. Larson, J.L. Eberling, W.J. Jagust, R.A. Hawkins, H.F. VanBrocklin, J.F. Wright, K.S. Bankiewicz, and M.J. Aminoff. (2009). Safety and tolerability of putaminal AADC gene therapy for Parkinson's disease. *Neurology*, **73(20)**: 1662-1669.
- Ciesielska, A., G. Mittermeyer, P. Hadaczek, A.P. Kells, J. Forsayeth and K.S. Bankiewicz. (2011). Anterograde axonal transport of AAV2-GDNF in rat basal ganglia. *Mol Ther*, **19(5)**: 922-927.
- Clinicaltrials.gov. (2016). AAV2-GDNF for advanced Parkinson's disease, NCT01621581. <https://clinicaltrials.gov/ct2/show/NCT01621581?term=aav2+gdnf+parkinson%27s&rank=1>
- Clinicaltrials.gov. (2016). Randomized, controlled study evaluating CERE-110 in subjects with mild to moderate Alzheimer's disease, NCT00876863. <https://clinicaltrials.gov/ct2/show/NCT00876863?term=00876863&rank=1>
- Collier, T.J., N.M. Kanaan, and J.H. Kordower. (2011). Ageing as a primary risk factor for Parkinson's disease: evidence from studies of non-human primates. *Nat Rev Neurosci*, **12(6)**: 359-366.
- Combs, H.L., B.S. Folley, D.T. Berry, S.C. Segerstrom, D.Y. Han, A.J. Anderson-Mooney, B.D. Walls, and C. van Horne. (2015). Cognition and depression following deep brain stimulation of the subthalamic nucleus and globus pallidus pars internus in Parkinson's disease: a meta-analysis. *Neuropsychol Rev*, **25(4)**: 439-454.

- Connolly, B.S., and A.E. Lang. (2014). Pharmacological treatment of Parkinson's disease: a review. *JAMA*, **311(16)**: 1670-1683.
- Cooney, J.W., and M. Stacy. (2016). Neuropsychiatric issues in Parkinson's disease. *Curr Neurol Neurosci Rep*, **16(5)**: 49.
- Cummings, J.L., S.J. Banks, R.K. Gary, J.W. Kinney, J.M. Lombardo, R.R. Walsh, and K. Zhong. (2013). Alzheimer's disease drug development: translational neuroscience strategies. *CNS Spectrums* **18(3)**: 128-138.
- D'Angelo, M. M. Raices, S.H. Panowski, and M.W. Hetzer. (2009). Age-dependent deterioration of nuclear pore complexes causes a loss of nuclear integrity in postmitotic cells. *Cell*, **136**: 284-295.
- D'Anglemont de Tassigny, X., A. Pascual, and J. Lopez-Barneo. (2015). GDNF-based therapies, GDNF-producing interneurons, and trophic support of the dopaminergic nigrostriatal pathway. Implications for Parkinson's disease. *Front Neuroanat*, **9**: 10.
- De la Fuente-Fernandez, R., T.J. Ruth, V. Sossi, M. Schulzer, D.B. Calne, and A.J. Stoessl. (2001). Expectation and dopamine release: mechanism of the placebo effect in Parkinson's disease. *Science*, **293(5532)**: 1164-1166.
- De la Fuente-Fernandez, R., M. Schulzer, and A.J. Stoessl. (2004). Placebo mechanisms and reward circuitry: clues from Parkinson's disease. *Biol Psychiatry*, **56(2)**: 67-71.
- De la Fuente-Fernandez, R., M. Schulzer, E. Mak, and V. Sossi. (2010). Trials of neuroprotective therapies for Parkinson's disease: problems and limitations. *Parkinsonism Relat Disord*, **16(6)**: 356-369.
- De Lau, L.M.L., and M.M.B. Breteler. (2006). Epidemiology of Parkinson's disease. *Lancet*, **5(6)**: 525-535.
- Di Pasquale, G., B.L. Davidson, C.S. Stein, I. Martins, D. Scudiero, A. Monks, and J.A. Chiorini. (2003). Identification of PDGFR as a receptor for AAV-5 transduction. *Nat Med*, **9**: 1306-1312.
- Decressac, M., B. Mattsson, and A. Bjorklund. (2012). Comparison of the behavioral and histological characteristics of the 6-OHDA and alpha-synuclein rat models of Parkinson's disease. *Exp Neurol*, **235(1)**: 306-315.
- Diaz, E., F. Schimmoller, and S.R. Pfeffer. (1997). A novel Rab9 effector required for endosome-to-TGN transport. *J Cell Biol*, **138**: 283-290.
- Ding, W., L. Zhang, Z. Yan, and J.F. Engelhardt. (2005). Intracellular trafficking of adeno-associated viral vectors. *Gene Ther*, **12**: 873-880.
- Ding, W., L.N. Zhang, C. Yeaman, and J.F. Engelhardt. (2006). rAAV2 traffics through both the late and the recycling endosomes in a dose-dependent fashion. *Mol Ther*, **13**: 671-682.
- Dodiya, H.B., T. Bjorklund, J. Stansell III, R.J. Mandel, D. Kirik, and J.H. Kordower. (2010). Differential transduction following basal ganglia administration of distinct pseudotyped AAV capsid serotypes in nonhuman primates. *Mol Ther*, **18(3)**: 579-587.

- Domanskyi, A., M. Saarma, and M. Airavaara. (2015). Prospects of neurotrophic factors for Parkinson's disease: comparison of protein and gene therapy. *Hum Gene Ther*, **26(8)**: 550-559.
- Duan, D., Q. Li, A.W. Kao, Y. Yue, J.E. Pessin, and J.F. Engelhardt. (1999). Dynamin is required for recombinant adeno-associated virus type 2 infection. *J Virol*, **73**: 10371-10376.
- Eberling, J.L., A.P. Kells, P. Pivrotto, J. Beyer, J. Bringas, H.J. Federoff, J. Forsayeth, and K.S. Bankiewicz. (2009). Functional effects of AAV2-GDNF on the dopaminergic nigrostriatal pathway in parkinsonian rhesus monkeys. *Hum Gene Ther*, **20(5)**: 511-518.
- Emborg, M.E., J. Moirano, J. Raschke, V. Bondarenko, R. Zufferey, S. Peng, A.D. Ebert, V. Joers, B. Roitberg, J.E. Holden, J. Koprach, J. Lipton, J.H. Kordower, and P. Aebischer. (2009). Response of aged parkinsonian monkeys to in vivo gene transfer of GDNF. *Neurobiol Dis*, **36(2)**: 303-311.
- Emborg, M.E., M. Carbon, J.E. Holden, M.J. During, Y. Ma, C. Tang, J. Moirano, H. Fitzsimons, B.Z. Roitberg, E. Tuccar, A. Roberts, M.G. Kaplitt, and D. Eidelberg. (2007). Subthalamic glutamic acid decarboxylase gene therapy: changes in motor function and cortical metabolism. *J Cereb Blood Flow Metab*, **27(3)**: 501-509.
- Encinas, M., R.J. Crowder, J. Milbrandt, and E.M. Johnson Jr. (2004). Tyrosine 981, a novel ret autophosphorylation site, binds to c-Src to mediate neuronal survival. *J Biol Chem*, **279(18)**: 18262-18269.
- Fahn, S. (2006). A new look at levodopa based on the ELLDOPA study. *J Neural Transm Suppl*, **70**: 419-426.
- Fahn, S. (2008). The history of dopamine and levodopa in the treatment of Parkinson's disease. *Mov Disord*, **Suppl 3**: S497-S508.
- Fahn, S. Parkinson Study Group. (2005). Does levodopa slow or hasten the rate of progression of Parkinson's disease? *J Neurol*, **252(Suppl 4)**: IV37-IV42.
- Feng, L.R., and K.A. McGuire-Zeiss. (2011). Gene therapy in Parkinson's disease: rationale and current status. *CNS Drugs*, **24(3)**: 177-192.
- Fischer, D.L., S.E. Gombash, C.J. Kemp, F.P. Manfredsson, N.K. Polinski, M.F. Duffy, and C.E. Sortwell. (2016). Viral vector-based modeling of neurodegenerative disorders: Parkinson's disease. *Methods Mol Biol*, **1382**: 367-382.
- Fjord-Larsen, L., J.L. Johansen, P. Kusk, J. Tornoe, M. Gronborg, C. Rosenblad, and L.U. Wahlberg. (2005). Efficient in vivo protection of nigral dopaminergic neurons by lentiviral gene transfer of a modified Neurturin construct. *Exp Neurol*, **195(1)**: 49-60.
- Follett, K.A., F.M. Weaver, M. Stern, K. Hur, C.L. Harris, P. Luo, W.J. Marks Jr, J. Rothlind, O. Sagher, C. Moy, R. Pahwa, K. Burchiel, P. Hogarth, E.C. Lai, J.E. Duda, K. Hollaway, A. Samii, S. Horn, J.M. Bronstein, G. Stoner, P.A. Starr, R. Simpson, G. Baltuch, A. De Salles, G.D. Huang, and D.J. Reda. (2010). Pallidal versus subthalamic deep-brain stimulation for Parkinson's disease. *N Engl J Med*, **362(22)**: 2077-2091.

- Freed, C.R., M.A. Leehey, M. Zawada, K. Bjugstad, L. Thompson, and R.E. Breeze. (2003). Do patients with Parkinson's disease benefit from embryonic dopamine cell transplantation? *J Neurol*, **250(Suppl 3)**: III44-III46.
- Gao, L., M. Hidalgo-Figueroa, L.M. Escudero, J. Diaz-Martin, J. Lopez-Barneo, and A. Pascual. (2013). Age-mediated transcriptomic changes in adult mouse substantia nigra. *PLoSone*, **9(4)**: e62456.
- Gash, D.M., Z. Zhang, A. Ovadia, W.A. Cass, A. Yi, L. Simmerman, D. Russell, D. Martin, P.A. Lapchak, F. Collins, B.J. Hoffer, and G.A. Gerhardt. (1996). Functional recovery in parkinsonian monkeys treated with GDNF. *Nature*, **380(6571)**: 252-255.
- Gasmi, M., E.P. Brandon, C.D. Herzog, A. Wilson, K.M. Bishop, E.K. Hofer, J.J. Cunningham, M.A. Printz, J.H. Kordower, and R.T. Bartus. (2007). AAV2-mediated delivery of human neurturin to the rat nigrostriatal system: Long-term efficacy and tolerability of CERE-120 for Parkinson's disease. *Neurobio Dis*, **27(1)**: 67-76.
- Gelb, D.J., E. Oliver, and S. Gilman. (1999). Diagnostic criteria for Parkinson disease. *Arch Neurol*, **56(1)**: 33-39.
- Gertz, H.J., A. Siegers, and J. Kuchinke. (1994). Stability of cell size and nucleolar size in Lewy body containing neurons of substantia nigra in Parkinson's disease. *Brain Res*, **637(1-2)**: 339-341.
- Gill, S.S., N.K. Patel, G.R. Hotton, K. O'Sullivan, R. McCarter, M. Bunnage, D.J. Brooks, C.N. Svendsen, and P. Heywood. (2003). Direct brain infusion of glial cell line-derived neurotrophic factor in Parkinson's disease. *Nature Med*, **9**: 589-595.
- Glorioso, C., and E. Sibille. (2011). Between density and disease: genetics and molecular pathways of human central nervous system aging. *Prog Neurobiol*, **93**: 165-181.
- Goetz, C.G. (2011). The history of Parkinson's disease: early clinical descriptions and neurological therapies. *Cold Spring Harb Perspect Med*, **1(1)**: a008862.
- Goetz, C.G., B.C. Tilley, S.R. Shaftman, G.T. Stebbins, S. Fahn, P. Martinez-Martin, W. Poewe, C. Sampaio, M.B. Stern, R. Dodel, B. Dubois, R. Holloway, J. Jankovic, J. Kulisevsky, A.E. Lang, A. Lees, S. Leurgans, P.A. LeWitt, D. Nyenhuis, C.W. Olanow, O. Rascol, A. Schrag, J.A. Teresi, J.J. van Hilten, and N. LaPelle. (2008) Movement Disorder Society-sponsored revision of the United Parkinson's Disease Rating Scale (MDS-UPDRS): scale presentation and clinimetric testing results. *Mov Disord*, **23(15)**: 2129-2170.
- Goetz, C.G., J. Wu, M.P. McDermott, C.H. Adler, S. Fahn, C.R. Freed, R.A. Hauser, W.C. Olanow, I. Shoulson, P.K. Tandon, Parkinson Study Group, and S. Leurgans. (2008). Placebo response in Parkinson's disease: comparisons among 11 trials covering medical and surgical interventions. *Movement Disorders*, **23(5)**: 690-699.
- Goldman, J.E., S.H. Yen, F.C. Chiu, and N.S. Peress. (1983). Lewy bodies of Parkinson's disease contain neurofilament antigens. *Science*, **221(4615)**: 1082-1084.

- Grondin, R., Z. Zhang, A. Yi, W.A. Cass, N. Maswood, A.H Andersen, D.D. Elsberry, M.C. Klein, G.A. Gerhardt, and D.M. Gash. (2002). Chronic, controlled GDNF infusion promotes structural and functional recovery in advanced parkinsonian monkeys. *Brain*, **125(10)**: 2191-2201.
- Grondin, R., Z. Zhang, Y. Ai, F. Ding, A.A. Walton, S.P. Surgener, G.A. Gerhardt, and D.M. Gash. (2008). Intraputamenal infusion of exogenous neurturin protein restores motor and dopaminergic function in the globus pallidus of MPTP-lesioned rhesus monkeys. *Cell Transplant*, **17(4)**: 373-381.
- Hamani, C., J.A. Saint-Cyr, J. Fraser, M. Kaplitt, and A.M. Lozano. (2004). The subthalamic nucleus in the context of movement disorders. *Brain*, **127**: 4-20.
- Herrington, T.M., J.J. Cheng, and E.N. Eskandar. (2016). Mechanisms of deep brain stimulation. *J Neurophysiol*, **115(1)**: 19-38.
- Herzog, C.D., B. Dass, J.E. Holden, J. Stansell III, M. Gasmi, M.H. Tuszynski, R.T. Bartus, and J.H. Kordower. (2007). Striatal delivery of CER-120, an AAV2 vector encoding human neurturin, enhances activity of the dopaminergic nigrostriatal system in aged monkeys. *Mov Disord*, **22(8)**: 1124-1132.
- Herzog, C.D., L. Brown, B.R. Kruegel, A. Wilson, M.G. Tansey, F.H. Gage, E.M. Johnson Jr, and R.T. Bartus. (2013). Enhanced neurotrophic distribution, cell signaling and neuroprotection following substantia nigral versus striatal delivery of AAV2-NRTN (CER-120). *Neurobiol Dis*, **58**: 38-48.
- Hirosue, S., K. Senn, N. Clement, M. Nonnenmacher, L. Gigout, R.M. Linden, and T. Weber. (2007). Effect of inhibition of dynein function and microtubule-altering drugs on AAV2 transduction. *Virology*, **367(1)**: 10-18.
- Hoffer, B.J., A. Hoffman, K. Bowenkamp, P. Huettl, J. Hudson, D. Martin, L.F. Lin, and G.A. Gerhardt. (1994). Glial cell line-derived neurotrophic factor reverses toxin-induced injury to midbrain dopaminergic neurons in vivo. *Neurosci Lett*, **182(1)**: 107-111.
- Huack, B., W. Zhou, K. High, and W. Xiao. (2004). Intracellular viral processing, not single-stranded DNA accumulation, is crucial for recombinant adeno-associated virus transduction. *J Virol*, **78**: 13678-13686.
- Hughes, A.J., S.E. Daniel, and A.J. Lee. (1993). The clinical features of Parkinson's disease in 100 histologically proven cases. *Adv Neurol*, **60**: 595-599.
- Jankovic, J., and L.G. Aguilar. (2008). Current approaches to the treatment of Parkinson's disease. *Neuropsychiatr Dis Treat*, **4(4)**: 743-757.
- Jarraya, B., S. Boulet, G.S. Ralph, C. Jan, G. Bonvento, M. Azzouz, J.E. Miskin, M. Shin, T. Delzescaux, X. Drouot, A. Herard, D.M. Day, E. Brouillet, S.M. Kingsman, P. Hantraye, K.A. Mitrophanous, N.D. Mazarakis, and S. Palfi. (2009). Dopamine gene therapy for Parkinson's disease in a nonhuman primate without associated dyskinesia. *Science Trans Med*, **1(2)**: 2ra4.
- Jellinger, K.A. (1999). Post mortem studies in Parkinson's disease—Is it possible to detect brain areas for specific symptoms? *J Neural Transm Suppl*, **56**: 1-29.

- Johnson, J.S., and R.J. Samulski. (2009). Enhancement of adeno-associated virus infection by mobilizing capsids into and out of the nucleolus. *J Virol*, **83(6)**: 2632-2644.
- Kaludov, N., K.E. Brown, R.W. Walters, J. Zabner, and J.A. Chiorini. (2001). Adeno-associated virus serotype 4 (AAV4) and AAV5 both require sialic acid binding for hemagglutination and efficient transduction but differ in sialic acid linkage specificity. *J Virol*, **75**: 6884-6893.
- Kanaan, N.M. and F.P. Manfredsson. (2012). Loss of functional alpha-synuclein: a toxic event in Parkinson's disease? *J Parkinsons Dis*, **2(4)**: 249-267.
- Kang, H., and J.W. Lichtman. (2013). Motor axon regeneration and muscle reinnervation in young adult and aged animals. *J Neurosci*, **33(50)**: 19480-19491.
- Kapeller, R., and L.C. Cantley. (1994). Phosphatidylinositol 3-kinase. *Bioessays*, **16**: 565-576.
- Kaplitt, M.G., A. Feigin, C. Tang, H.L. Fitzsimons, P. Mattis, P.A. Lawlor, R.J. Bland, D. Young, K. Strybing, D. Eidelberg, and M.J. Doring. (2007). Safety and tolerability of gene therapy with an adeno-associated virus (AAV) borne GAD gene for Parkinson's disease: an open label, phase I trial. *Lancet*, **369(9579)**: 2097-2105.
- Kashiwakura, Y., K. Tamayose, K. Iwabuchi, Y. Hirai, T. Shimada, K. Matsumoto, T. Nakamura, M. Watanabe, K. Oshimi, and H. Daida. (2005). Hepatocyte growth factor receptor is a coreceptor for adeno-associated virus type 2 infection. *J Virol*, **79(1)**: 609-614.
- Kearns, C.M., and D.M. Gash. (1995). GDNF protects nigral dopamine neurons against 6-hydroxydopamine in vivo. *Brain Res*, **672(1-2)**: 104-111.
- Kells, A.P., J. Eberling, X. Su, P. Pivrotto, J. Bringas, P. Hadaczek, W.C. Narrow, W.J. Bowers, H.J. Federoff, J. Forsayeth, and K.S. Bankiewicz. (2010). Regeneration of the MPTP-lesioned dopaminergic system after convection-enhanced delivery of AAV2-GDNF. *J Neurosci*, **30(28)**: 9567-9577.
- Kelly, M.J., G.W. O'Keefe, and A.M. Sullivan. (2015). Viral vector delivery of neurotrophic factors for Parkinson's disease therapy. *Expert Rev Mol Med*, **17(e8)**: 1-14.
- Kirik, D., C. Rosenblad, A. Bjorklund, and R.J. Mandel. (2000). Long-term rAAV-mediated gene transfer of GDNF in the rat Parkinson's model: intrastriatal but not intranigral transduction promotes functional regeneration in the lesioned nigrostriatal system. *J Neurosci*, **20(12)**: 4686-4700.
- Klein, C., and A. Westenberger. (2012). Genetics of Parkinson's disease. *Cold Spring Harb Perspect Med*, **2(1)**: a008888.
- Klein, R.L., R.D. Datron, C.G. Diaczynsky, and D.B Wang. (2010). Pronounced microgliosis and neurodegeneration in aged rats after tau gene transfer. *Neurobiol Aging*, **31(12)**: 2091-2102.
- Kordower, J.H., S. Palfi, E.Y. Chen, S.Y. Ma, T. Sendera, E.J. Cochran, E.J. Mufson, R. Penn, C.G. Goetz, and C.D. Comella. (1999). Clinicopathological findings following intraventricular glial-derived neurotrophic factor treatment in a patient with Parkinson's disease. *Ann Neurol*, **46(3)**: 419-424.

- Kordower, J.H., M.E. Emborg, J. Bloch, S.Y. Ma, Y. Chu, L. Leventhal, J. McBride, E. Chen, S. Palfi, B.Z. Roitberg, W.D. Brown, J.E. Holden, R. Pyzalski, M.D. Taylor, P. Carvey, Z. Ling, D. Torno, P. Hantraye, N. Deglon, and P. Aebischer. (2000). Neurodegeneration prevented by lentiviral vector delivery of GDNF in primate models of Parkinson's disease. *Science*, **290(27)**: 767-773.
- Kordwer, J.H., C.D. Herzog, B. Dass, R.A.E. Bakay, J. Stansell III, M. Gasmi, and R.T. Bartus. (2006). Delivery of neurturin by AAV2 (CERE-120)-mediated gene transfer provides structural and functional neuroprotection and neurorestoration in MPTP-treated monkeys. *Ann Neurol*, **60(6)**: 706-715.
- Kotzbauer, P.T., P.A. Lampe, R.O. Heuckeroth, J.P. Golden, D.J. Creedon, E.M. Johnson Jr, and J. Milbrandt. (1996). Neurturin, a relative of glial-cell-line-derived neurotrophic factor. *Nature*, **384**: 467-470.
- Kramer, E.R., and B. Liss. (2015). GDNF-Ret signaling in midbrain dopaminergic neurons and its implication for Parkinson disease. *FEBS Letters*, **589(24A)**: 3760-3772.
- Kraytsberg, Y., E. Kudryavtseva, A.C. McKee, C. Geula, N.W. Kowall, and K. Khrapko. (2006). Mitochondrial DNA deletions are abundant and cause functional impairment in aged human substantia nigra neurons. *Nat Gen*, **38(5)**: 318-320.
- Kronenberg, S., B. Bottcher, C.W. von der Lieth, S. Bleker, and J.A. Kleinschmidt. (2005). A conformational change in the adeno-associated virus type 2 capsid leads to the exposure of hidden VP1 N termini. *J Virol*, **79**: 5296-5303.
- LaFemina, R.L., P.L. Callahan, and M.G. Cordingley. (1991). Substrate specificity of recombinant human immunodeficiency virus integrase protein. *J Virol*, **65(10)**: 5624-5630.
- Lang, A.E., S. Gill, N.K. Patel, A. Lozano, J.G. Nutt, R. Penn, D.J. Brooks, G. Hotton, E. Moro, P. Heywood, M.A. Brodsky, K. Burchiel, P. Kelly, A. Dalvi, B. Scott, M. Stacy, D. Turner, V.G.F. Wooten, W.J. Elias, E.R. Laws, V. Dhawan, A.J. Stoessl, J. Matcham, R.J. Coffey, and M. Traub. (2006). Randomized controlled trial of intraputamenal glial cell line-derived neurotrophic factor infusion in Parkinson disease. *Ann Neurol*, **59(3)**: 459-466.
- Lee, B., H. Lee, Y.R. Nam, J.H. Oh, Y.H. Cho, and J.W. Chang. (2005). Enhanced expression of glutamate decarboxylase 65 improves symptoms of rat parkinsonian models. *Gene Ther*, **12**: 1215-1222.
- Lee, C., R. Weindruch, and T.A. Prolla. (2000). Gene-expression profile of the ageing brain in mice. *Nat Gen*, **25**: 294-297.
- Lee, H.M., and S.B. Koh. (2015). Many faces of Parkinson's disease: non-motor symptoms of Parkinson's disease. *J Mov Disord*, **8(2)**: 92-97.
- Lees, A.J., E. Tolosa, and C.W. Olanow. (2015). Four pioneers of L-dopa treatment: Arvid Carlsson, Oleh Hornykiewicz, George Cotzias, and Melvin Yahr. *Mov Disord*, **30(1)**: 19-36.
- Lew, M.F. (2011). The evidence for disease modification in Parkinson's disease. *Int J Neurosci*, **121(Suppl 2)**: 18-26.

- LeWitt, P.A., A.R. Rezai, M.A. Leehey, S.G. Ojemann, A.W. Flaherty, E.N. Eskandar, S.K. Kostyk, K. Thomas, A. Sarkar, M.S. Siddiqui, S.B. Tatter, J.M. Schwalb, K.L. Poston, J.M. Henderson, R.M. Kurlan, I.H. Richard, L. Van Meter, C.V. Sapan, M.J. Doring, and M.G. Kaplitt. (2011). AAV2-GAD gene therapy for advanced Parkinson's disease: a double-blind, sham-surgery controlled, randomized trial. *Lancet Neurol*, **10(4)**: 309-319.
- Lidstone, S.C., M. Schulzer, K. Dinelle, E. Mak, V. Sossi, T.J. Ruth, R. Fuente-Fernandez, A.G. Phillips, and A.J. Stoessl. (2010). Effects of expectation on placebo-induced dopamine release in Parkinson's disease. *Arch Gen Psychiatry*, **67(8)**: 857-865.
- Lidstone, S.C. (2014). Great expectations: the placebo effect in Parkinson's disease. *Placebo*, **225**: 139-147.
- Lin, L.F., D.H. Doherty, J.D. Lile, S. Bektesh, and F. Collins. (1993). GDNF: a glial cell line-derived neurotrophic factor for midbrain dopaminergic neurons. *Science*, **260(5111)**: 1130-1132.
- Ling, C., Y. Lu, J.K. Kalsi, G.R. Jayandharan, B. Li, W. Ma, B. Cheng, S.W.Y. Gee, K.E. McGoogan, L. Govindasamy, L. Zong, M. Agbandje-McKenna, and A. Srivastava. (2010). Human hepatocyte growth factor receptor is a cellular coreceptor for adeno-associated virus serotype 3. *Hum Gene Ther*, **21(12)**: 1741-1747.
- Lombard, D.B., K.F. Chua, R. Mostoslavsky, S. Franco, M. Gostissa, and F.W. Alt. (2005). DNA repair, genome stability, and aging. *Cell*, **120(4)**: 497-512.
- Lowe, J., A. Blanchard, K. Morrell, G. Lennox, L. Reynolds, M. Billett, M. Landon, and R.J. Mayer. (1988). Ubiquitin is a common factor in intermediate filament inclusion bodies of diverse type in man, including those of Parkinson's disease, Pick's disease, and Alzheimer's disease, as well as Rosenthal fibres in cerebellar astrocytomas, cytoplasmic bodies in muscle, and Mallory bodies in alcoholic liver disease. *J Pathol*, **155(1)**: 9-15.
- Luo, J., M.G. Kaplitt, H.L. Fitzsimons, D.S. Zuzga, Y. Liu, M.L. Oshinsky, and M.J. Doring. (2002). Subthalamic GAD gene therapy in a Parkinson's disease rat model. *Science*, **298(5592)**: 425-429.
- Manfredsson, F.P., M.S. Okun, and R.J. Mandel. (2009). Gene therapy for neurological disorders: challenges and future prospects for the use of growth factors for the treatment of Parkinson's disease. *Curr Gene Ther*, **9(5)**: 375-388.
- Markakis, E.A., K.P. Vives, J. Bober, S. Leichtle, C. Leranath, J. Beecham, J.D. Elsworth, R.H. Roth, R.J. Samulski, and D.E. Redmond Jr. (2010). Comparative transduction efficiency of AAV vector serotypes 1-6 in the substantia nigra and striatum of the primate brain. *Mol Ther*, **18(3)**: 588-593.
- Marks Jr, W.J., J.L. Ostrem, L. Verhagen, P.A. Starr, P.S. Larson, R.A. Bakay, R. Taylor, D.A. Cahn-Weiner, A.J. Stoessl, C.W. Olanow, and R.T. Bartus. (2008). Safety and tolerability of intraputamenal delivery of CERE-120 (adeno-associated virus serotype 2-neurturin) to patients with idiopathic Parkinson's disease: an open-label, phase I trial. *Lancet Neurol*, **7(5)**: 400-408.
- Marks Jr, W.J., R.T. Bartus, J. Siffert, C.S. Davis, A. Lozano, N. Boulis, J. Vitek, M. Stacy, D. Turner, L. Verhagen, R. Bakay, R. Watts, B. Guthrie, J. Jankovic, R. Simpson, M. Tagliati, R. Alterman, M.

- Stern, G. Baltuch, P.A. Starr, P.S. Larson, J.L. Ostrem, J. Nutt, K. Kieburtz, J.H. Kordower, and C.W. Olanow. (2010). Gene delivery of AAV2-neurturin for Parkinson's disease: a double-blind, randomized, controlled trial. *Lancet Neurol*, **9(12)**: 1164-1172.
- McFarland, N.R., J. Lee, B.T. Hyman, and P.J. McLean. (2009). Comparison of transduction efficiency of recombinant AAV serotypes 1, 2, 5, and 8 in the rat nigrostriatal system. *J Neurochem*, **109**: 838-845.
- Mimuro, J., H. Mizukami, M. Shima, T. Matsushita, M. Taki, S. Muto, S. Higasa, M. Sakai, T. Ohmori, S. Madoiwa, K. Ozawa, and Y. Sakata. (2014). The prevalence in neutralizing antibodies against adeno-associated virus capsids is reduced in young Japanese individuals. *J Med Virol*, **86(11)**: 1990-1997.
- Mittermeyer, G., C.W. Christine, K.H. Rosenbluth, S.L. Baker, P. Starr, P. Larson, P.L. Kaplan, J. Forsayeth, M.J. Aminoff, and K.S. Bankiewicz. (2012). Long-term evaluation of a Phase I study of AADC gene therapy for Parkinson's disease. *Hum Gene Ther*, **23(4)**: 377-381.
- Mizukami, H. N.S. Young, and K.E. Brown. (1996). Adeno-associated virus 2 binds to a 150-kilodalton cell membrane glycoprotein. *Virology*, **217**: 124-130.
- Moldovan, A., S.J. Groiss, S. Elben, M. Sudmeyer, A. Schnitzler, and L. Wojtecki. (2015). The treatment of Parkinson's disease with deep brain stimulation: current issues. *Neural Regen Res*, **10(7)**: 1018-1022.
- Morawski, M., M. Filippov, A. Tzinia, E. Tsilibary, and L. Vargova. (2014). ECM in brain aging and dementia. *Prog Brain Res*, **214**: 207-227.
- Movement Disorder Society Task Force on Rating Scales for Parkinson's Disease. (2003). The Unified Parkinson's Disease Rating Scale (UPDRS): status and recommendations. *Mov Disord*, **18(7)**: 738-750.
- Muramatsu, S., K. Fujimoto, S. Kato, H. Mizukami, S. Asari, K. Ikeguchi, T. Kawakami, M. Urabe, A. Kume, T. Sato, E. Watanabe, K. Ozawa, and I. Nakano. (2010). A Phase I study of aromatic-amino acid decarboxylase gene therapy for Parkinson's disease. *Mol Ther*, **18(9)**: 1731-1735.
- Nakai, H. T.A. Storm, and M.A. Kay. (2000). Recruitment of single-stranded recombinant adeno-associated virus vector genomes and intermolecular recombination are responsible for stable transduction of liver in vivo. *J Virol*, **74**: 9451-9463.
- Ng, R., L. Govindasamy, B.L. Gurda, R. McKenna, O.G. Kozyreva, R.J. Samulski, K.N. Parent, T.S. Baker, and M. Agbandje-McKenna. (2010). Structural characterization of the dual glycan binding adeno-associated virus serotype 6. *J Virol*, **84**: 12945-12957.
- Nicolson, S.C., and R.J. Samulski. (2014). Recombinant adeno-associated virus utilizes host cell nuclear import machinery to enter the nucleus. *J Virol*, **88(8)**: 4132-4144.
- NINDS NET-PD Investigators. (2007). A randomized clinical trial of coenzyme Q10 and GPI-1485 in early Parkinson disease. *Neurology*, **68(1)**: 20-28.

- Nonnenmacher, M., and T. Weber. (2012). Intracellular transport of recombinant adeno-associated virus vectors. *Gene Ther*, **19(6)**: 649-658.
- Nutt, J.G., K.J. Burchiel, C.L. Comella, J. Jankovic, A.E. Lang, E.R. Laws Jr, A.M. Lozano, R.D. Penn, R.K. Simpson Jr, M. Stacy, and G.F. Wooten. (2003). Randomized, double-blind trial of glial cell line-derived neurotrophic factor (GDNF) in PD. *Neurology*, **60(1)**: 69-73.
- O'Connor, D.M., and N.M. Boulis. (2015). Gene therapy for neurodegenerative diseases. *Trends Mol Med*, **21(8)**: 504-512.
- Oiwa, Y., R. Yoshimura, K. Nakai, and T. Itakura. (2002). Dopaminergic neuroprotection and regeneration by neurturin assessed by using behavioral, biochemical and histochemical measurements in a model of progressive Parkinson's disease. *Brain Res*, **947(2)**: 271-283.
- Okun, M.S., B.V. Gallo, G. Mandybur, J. Jagid, K.D. Foote, F.J. Revilla, R. Alterman, J. Jankovic, R. Simpson, F. Junn, L. Verhagen, J.E. Arle, B. Ford, R.R. Goodman, R.M. Stewart, S. Horn, G.H. Baltuch, B.H. Kopell, F. Marshall, D. Peichel, R. Pahwa, K.E. Lyons, A.L. Troster, J.L. Vitek, and M. Tagliati. (2012). Subthalamic deep brain stimulation with a constant-current device in Parkinson's disease. *Lancet Neurol*, **11(2)**: 140-149.
- Olanow, C.W. (2009). Can we achieve neuroprotection with currently available anti-parkinsonian interventions? *Neurology*, **72(Suppl 2)**: S59-S64.
- Olanow, C.W., M.B. Stern, and K. Sethi. (2009). The scientific and clinical basis for the treatment of Parkinson disease. *Neurology*, **72**: S1-S136.
- Olanow, C.W., O. Rascol, R. Hauser, P.D. Feigin, J. Jankovic, A. Lang, W. Langston, E. Melamed, W. Poewe, F. Stocchi, and E. Tolosa. ADAGIO Study Investigators. (2009). A double-blind, delayed-start trial of rasagiline in Parkinson's disease. *N Engl J Med*, **361(13)**: 1268-1278.
- Olanow, C.W., R.T. Bartus, T.L. Baumann, S. Factor, N. Boulis, M. Stacy, D.A. Turner, W. Marks, P. Larson, P.A. Starr, J. Jankovic, R. Simpson, R. Watts, B. Guthrie, K. Poston, J.M. Henderson, M. Stern, G. Baltuch, C.G. Goetz, C. Herzog, J.H. Kordower, R. Alterman, A.M. Lozano, and A.E. Lang. (2015). Gene delivery of neurturin to putamen and substantia nigra in Parkinson disease: a double-blind, randomized, controlled trial. *Ann Neurol*, **78(2)**: 248-257.
- Palfi, S., J.M. Gurruchaga, G.S. Ralph, H. Lepetit, S. Lavisse, P.C. Buttery, C. Watts, J. Miskin, M. Kellher, S. Deeley, H. Iwamuro, J.P. Lefaucheur, C. Thiriez, G. Fenelon, C. Lucas, P. Brugieres, I. Gabriel, K. Abhay, X. Drouot, N. Tani, A. Kas, B. Ghaleh, P. Le Corvoisier, P. Dolphin, D.P. Breen, S. Mason, N. Valle Guzman, N.D. Mazarakis, P.A. Radcliffe, R. Harrop, S.M. Kingsman, O. Rascol, S. Naylor, R.A. Barker, P. Hantraye, P. Remy, P. Cesaro, and K.A. Mitrophanous. (2014). Long-term safety and tolerability of ProSavin, a lentiviral vector-based gene therapy for Parkinson's disease: a dose escalation, open-label, phase 1/2 trial. *Lancet*, **383**: 1138-1146.
- Pandey, A., H. Duan, P.P. Di Fiore, and V.M. Dixit. (1995). The Ret receptor protein kinase associates with the SH2-containing adapter protein Grb10. *J Biol Chem*, **270(37)**: 21461-21463.

- Pandey, A., X. Liu, J.E. Dixon, P.P. Di Fiore, and V.M. Dixit. (1996). Direct association between the Ret receptor tyrosine kinase and the Src homology 2-containing adapter protein Grb7. *J Biol Chem*, **271(18)**: 10607-10610.
- Park, J., W. Park, K. Cho, D. Kim, B. Jhun, S. Kim, and S.C. Park. (2001). Down-regulation of amphiphysin-1 is responsible for reduced receptor-mediated endocytosis in the senescent cells. *FASEB J*, **15**: 1625-1627.
- Parkinson Study Group QE3 Investigators. (2014). A randomized clinical trial of high-dosage coenzyme Q10 in early Parkinson disease: no evidence of benefit. *JAMA Neurol*, **71(5)**: 543-552.
- Parkinson Study Group SURE-PD Investigators. (2014). Inosine to increase serum and cerebrospinal fluid urate in Parkinson disease: a randomized clinical trial. *JAMA Neurol*, **71(2)**: 141-150.
- Parkinson Study Group. (2002). Dopamine transporter brain imaging to assess the effects of pramipexole vs levodopa on Parkinson disease progression. *JAMA*, **287(13)**: 1653-1661.
- Parkinson, J. (2002). An essay on the shaking palsy, 1817. *J Neuropsychiatry Clin Neurosci*, **14(2)**: 223-236.
- Parkinson's Disease Foundation. Understanding Parkinson's Disease. (2016). Web. 25 May 2016.
- Patel, N.K., M. Bunnage, P. Plaha, C.N. Svendsen, P. Heywood, and S.S. Gill. (2005). Intraputamenal infusion of glial cell line-derived neurotrophic factor in PD: a two-year outcome study. *Ann Neurol*, **57(2)**: 298-302.
- Paterna, J., J. Feldon, and H. Bueler. (2004). Transduction profiles of recombinant adeno-associated virus vectors derived from serotypes 2 and 5 in the nigrostriatal system of rats. *J Virol*, **78(13)**: 6808-6817.
- Paumier, K.L., K.C. Luk, F.P. Manfredsson, N.M. Kanaan, J.W. Lipton, T.J. Collier, K. Steece-Collier, C.J. Kemp, S. Celano, E. Schultz, I.M. Sandoval, S. Fleming, E. Dirr, N.K. Polinski, J.Q. Trojanowski, V.M. Lee, and C.E. Sortwell. (2015). Intra-striatal injection of pre-formed mouse alpha-synuclein fibrils into rats triggers alpha-synuclein pathology and bilateral nigrostriatal degeneration. *Neurobiol Dis*, **82**: 185-199.
- Pfeffer, S.R. (2001). Rab GTPase: specifying and deciphering organelle identity and function. *Trends Cell Biol*, **11**: 487-491.
- Pillay, S., N.L. Meyer, A.S. Puschnik, O. Davulcu, J. Diep, Y. Ishikawa, L.T. Jae, J.E. Wosen, C.M. Nagamine, M.S. Chapman, and J.E. Carette. (2016). An essential receptor for adeno-associated virus infection. *Nature*, **530(7588)**: 108-112.
- Pollanen, M.S., D.W. Dickson, and C. Bergeron. (1993). Pathology and biology of the Lewy body. *J Neuropathol Exp Neurol*, **52(3)**: 183-191.
- Polymeropoulos, M.H., C. Lavedan, E. Leroy, S.E. Ide, A. Dehejia, A. Dutra, B. Pike, H. Root, J. Rubenstein, R. Boyer, and E.S. Stenroos. (1997). Mutation in the α -synuclein gene identified in families with Parkinson's disease. *Science*, **276(5321)**: 2045-2047.

- Powell, S.K., R. Rivera-Soto, and S.J. Gray. (2015). Viral expression cassette elements to enhance transgene target specificity and expression in gene therapy. *Discov Med*, **19(102)**: 49-57.
- Qing, K., C. Mah, J. Hansen, S. Zhou, V. Dwarki, and A. Srivastava. (1999). Human fibroblast growth factor receptor 1 is a co-receptor for infection by adeno-associated virus 2. *Nat Med*, **5(1)**: 71-77.
- Qui, J., and K.E. Brown. (1999). A 110-kDa nuclear shuttle protein, nucleolin, specifically binds to adeno-associated virus type 2 (AAV-2) capsid. *Virology*, **257**: 373-383.
- Rabinowitz, J.E., F. Rolling, C. Li, H. Conrath, W. Xiao, X. Xiao, and R.J. Samulski. (2002). Cross-packaging of a single adeno-associated virus (AAV) type 2 vector genome into multiple AAV serotypes enables transduction with broad specificity. *J Virol*, **76**: 791-801.
- Rafii, M.S., T.L. Baumann, R.A. Bakay, J.M. Ostrove, J. Siffert, A.S. Fleisher, C.D. Herzog, D. Barba, M. Pay, D.P. Salmon, Y. Chu, J.H. Kordower, K. Bishop, D. Keator, S. Potkin, and R.T. Bartus. (2014). A phase 1 study of stereotactic gene delivery of AAV2-NGF for Alzheimer's disease. *Alzheimer's Dement*, **10(5)**: 571-581.
- Ramezani, A., and R.G. Hawley. (2002). Overview of the HIV-1 lentiviral vector system. *Curr Protoc Mol Biol*, **Chapt. 16**: Unit 16.21.
- Reeve, A., E. Simcox, and D. Turnbull. (2014). Ageing and Parkinson's disease: Why is advancing age the biggest risk factor? *Ageing Res Rev*, **14(100)**: 19-30.
- Rizzo, G., M. Copetti, S. Arcuti, D. Martino, A. Fontana, and G. Logroscino. (2016). Accuracy of clinical diagnosis of Parkinson disease: a systematic review and meta-analysis. *Neurology*, **86(6)**: 566-576.
- Rosenblad, C., A. Martinez-Serrano, and A. Bjorklund. (1998). Intrastratial glial cell line-derived neurotrophic factor promotes sprouting of spared nigrostriatal dopaminergic afferents and induces recovery of function in a rat model of Parkinson's disease. *Neuroscience*, **82(1)**: 129-137.
- Rosenblad, C., D. Kirik, B. Devaux, B. Moffat, H.S. Phillips, and A. Bjorklund. (1999). Protection and regeneration of nigral dopaminergic neurons by neurturin or GDNF in a partial lesion model of Parkinson's disease after administration into the striatum or the lateral ventricle. *Euro J Neurosci*, **11(5)**: 1554-1566.
- Ryazanov, A.G., and B.S. Nefsky. (2002). Protein turnover plays a key role in aging. *Mech Age Dev*, **123**: 207-213.
- Saarma, M., and H. Sariola. (1999). Other neurotrophic factors: glial cell line-derived neurotrophic factor (GDNF). *Microsc Res Tech*, **45(4-5)**: 292-302.
- Sakuma, T., M.A. Barry, and Y. Ikeda. (2012). Lentiviral vectors: basic to translational. *Biochem J*, **443**: 603-618.
- Sanchez-Pernaute, R., J. Harvey-White, J. Cunningham, and K.S. Bankiewicz. (2001). Functional effect of adeno-associated virus mediated gene transfer of aromatic L-amino acid decarboxylase into the striatum of 6-OHDA-lesioned rats. *Mol Ther*, **4(4)**: 324-330.

- Sanlioglu, S., M.M. Monick, G. Luleci, G.W. Hunninghake, and J.F. Engelhardt. (2001). Rate limiting steps of AAV transduction and implications for human gene therapy. *Curr Gene Ther*, **1**: 137-147.
- Sanlioglu, S., P.K. Benson, J. Yang, E.M. Atkinson, T. Reynolds, and J.F. Engelhardt. (2000). Endocytosis and nuclear trafficking of adeno-associated virus type 2 are controlled by Rac1 and phosphatidylinositol-3 kinase activation. *J Virol*, **74(19)**: 9184-9496.
- Sasaki, T., Y. Akimoto, Y. Sato, H. Kawakami, H. Hirano, and T. Endo. (2002). Distribution of sialoglycoconjugates in the rat cerebellum and its change with aging. *J Histo Cyto*, **50(9)**: 1179-1186.
- Sato, Y., and T. Endo. (1999). Differential expression of sialoglycoproteins in the rat hippocampus and its changes during aging. *Neurosci Lett*, **262**: 49-52.
- Sato, Y., Y. Akimoto, H. Kawakami, H. Hirano, and T. Endo. (2001). Location of sialoglycoconjugates containing the sialyl-2-3Gal and sialyl-2-6Gal groups in the rat hippocampus and the effect of aging on their expression. *J Histo Cyto*, **49(10)**: 1311-1319.
- Schapira, A.H.V. and J. Obeso. (2006). Timing of treatment initiation in Parkinson's disease: a need for reappraisal? *Annal Neurol*, **59(3)**: 559-562.
- Schultz, B.R., and J.S. Chamberlain. (2008). Recombinant adeno-associated virus transduction and integration. *Mol Ther*, **16(7)**: 1189-1199.
- Schuringa, J.J., K. Wojtachnio, W. Hagens, E. Vellenga, C.H. Buys, R. Hofstra, and W. Kruijer. (2001). MEN2A-RET-induced cellular transformation by activation of STAT3. *Oncogene*, **20(38)**: 5350-5358.
- Seisenberger, G., M.U. Ried, T. Endress, H. Buning, M. Hallek, and C. Brauchle. (2001). Real-time single-molecule imaging of the infection pathway of an adeno-associated virus. *Science*, **294**: 1929-1932.
- Shen, S., K.D. Bryant, S.M. Brown, S.H. Randell, and A. Asokan. (2011). Terminal N-linked galactose is the primary receptor for adeno-associated virus 9. *J Biol Chem*, **286**: 13532-13540.
- Shin, S., H.M. Tuinstra, D.M. Salvay, and L.D. Shea. (2010). Phosphatidylserine immobilization of lentivirus for localized gene transfer. *Biomaterials*, **31**: 4353-4359.
- Shoulson, I. (1989). Deprenyl and tocopherol antioxidative therapy of parkinsonism (DATATOP). Parkinson Study Group. *Acta Neurol Scand Suppl*, **126**: 171-175.
- Shulman, L.M., M. Armstrong, T. Ellis, A. Gruber-Baldini, F. Horak, A. Nieuwboer, S. Parashos, B. Post, M. Rogers, A. Siderowf, C.G. Goetz, A. Schrag, G.T. Stebbins, and P. Martinez-Martin. (2016). Disability rating scales in Parkinson's disease: critique and recommendations. *Mov Disord*, doi: 10.1002/mds.26649.
- Singleton, A.B., M. Farrer, J. Johnson, A. Singleton, S. Hague, J. Kachergus, M. Hulihan, T. Peuralinna, A. Dutra, R. Nussbaum, and S. Lincoln. (2003). α -Synuclein locus triplication causes Parkinson's disease. *Science*, **302 (5646)**: 841.

- Smith, C.B., Y. Sun, and L. Sokoloff. (1995). Effects of aging on regional rates of cerebral protein synthesis in the Sprague-dawley rat: examination of the influence of recycling of amino acids derived from protein degradation into the precursor pool. *Neurochem Int*, **27(4/5)**: 407-416.
- Sonntag, F., S. Bleker, B. Leuchs, R. Fischer, and J.A. Kleinschmidt. (2006). Adeno-associated virus type 2 capsids with externalized VP1/VP2 trafficking domains are generated prior to passage through the cytoplasm and are maintained until uncoating occurs in the nucleus. *J Virol*, **80**: 11040-11054.
- Spillantini, M.G., M.L. Schmidt, V.M. Lee, J.Q. Trojanowski, R. Jakes, and M. Goedert. (1997). Alpha-synuclein in Lewy bodies. *Nature*, **388(6645)**: 839-840.
- Stahnke, S., K. Lux, S. Uhrig, F. Kreppel, M. Hosel, O. Coutelle, M. Ogris, M. Hallek, and H. Buning. (2011). Intrinsic phospholipase A2 activity of adeno-associated virus is involved in endosomal escape of incoming particles. *Virology*, **409(1)**: 77-83.
- Stocchi, F., and C.W. Olanow. (2013). Obstacles to the development of a neuroprotective therapy for Parkinson's disease. *Mov Disord*, **28(1)**: 3-7.
- Su, X., A.P. Kells, E.J. Huang, H.S. Lee, P. Hadaczek, J. Beyer, J. Bringas, P. Pivrotto, J. Penticuff, J. Eberling, H.J. Federoff, J. Forsayeth, and K.S. Bankiewicz. (2009). Safety evaluation of AAV2-GDNF gene transfer into the dopaminergic nigrostriatal pathway in aged and parkinsonian rhesus monkeys. *Hum Gene Ther*, **20(12)**: 1627-1640.
- Sullivan, A.M., J. Opacka-Juffry, and S.B. Blunt. (1998). Long-term protection of the rat nigrostriatal dopaminergic system by glial cell line-derived neurotrophic factor against 6-hydroxydopamine in vivo. *Eur J Neurosci*, **10(1)**: 57-63.
- Summerford, C., and R.J. Samulski. (1998). Membrane-associated heparan sulfate proteoglycan is a receptor for adeno-associated virus type 2 virions. *J Virol*, **72(2)**: 1438-1445.
- Summerford, C., J.S. Bartlett, and R.J. Samulski. (1999). $\alpha V\beta 5$ integrin: a co-receptor for adeno-associated virus type 2 infection. *Nat Med*, **5(1)**: 78-82.
- Sykova, E., T. Mazel, R.U. Hasenohrl, A.R. Harvey, Z. Simonova, W.H. Mulders, and J.P. Huston. (2002). Learning deficits in aged rats related to decrease in extracellular volume and loss of diffusion anisotropy in hippocampus. *Hippocampus*, **12(2)**: 269-279.
- Tereshchenko, J., A. Maddalena, M. Bahr, and S. Kugler. (2014). Pharmacologically controlled, discontinuous GDNF gene therapy restores motor function in a rat model of Parkinson's disease. *Neurobiol Dis*, **65**: 35-42.
- Treanor, J.J., L. Goodman, F. de Sauvage, D.M. Stone, K.T. Poulsen, C.D. Beck, C. Gray, M.P. Armanini, R.A. Pollock, F. Hefti, H.S. Phillips, A. Goddard, M.W. Moore, A. Buj-Bello, A.M. Davies, N. Asai, M. Takahashi, R. Vandlen, C.E. Henderson, and A. Rosenthal. (1996). Characterization of a multicomponent receptor for GDNF. *Nature*, **382(6586)**: 80-83.
- Trono, D. (1995). HIV accessory proteins: leading roles for the supporting cast. *Cell*, **82(2)**: 189-192.

- Tsai, S.T., S.H. Lin, Y.C. Chou, Y.H. Pan, H.Y. Hung, C.W. Li, S.Z. Lin, and S.Y. Chen. (2009). Prognostic factors of subthalamic stimulation in Parkinson's disease: a comparative study between short- and long-term effects. *Stereotact Funct Neurosurg*, **87(4)**: 241-248.
- Van der Perren, A., J. Toelen, M. Carlon, C. Van den Haute, F. Coun, B. Heeman, V. Reumers, L.H. Vandenberghe, J.M. Wilson, Z. Debyser, and V. Baekelandt. (2011). Efficient and stable transduction of dopaminergic neurons in rat substantia nigra by rAAV 2/1, 2/2, 2/5, 2/6.2, 2/7, 2/8, and 2/9. *Gene Ther*, **18**: 517-527.
- Venkataramana, N.K., S.K. Kumar, S. Balaraju, R.C. Radhakrishnan, A. Bansal, A. Dixit, D.K. Rao, M. Das, M. Jan, P.K. Gupta, and S.M. Totey. (2010). Open-labeled study of unilateral autologous bone-marrow-derived mesenchymal stem cell transplantation in Parkinson's disease. *Transl Res*, **155(2)**: 62-70.
- Visanji, N., and C. Marras. (2015). The relevance of pre-motor symptoms in Parkinson's disease. *Expert Rev Neurother*, **15(10)**: 1205-1217.
- Walters, R.W., S.M. Yi, S. Keshavjee, K.E. Brown, M.J. Welsh, J.A. Chiorini, and J. Zabner. (2001). Binding of adeno-associated virus type 5 to 2,3-linked sialic acid is required for gene transfer. *J Biol Chem*, **276**: 20610-20616.
- Weller, M.L., P. Amornphimoltham, M. Schmidt, P.A. Wilson, J.S. Gutkind, and J.A. Chiorini. (2010). Epidermal growth factor receptor is a co-receptor for adeno-associated virus serotype 6. *Nat Med*, **16(6)**: 662-664.
- Whone, A.L., R.L. Watts, A.J. Stoessl, M. Davis, S. Reske, C. Nahmias, A.E. Lang, O. Rascol, M.J. Ribeiro, P. Remy, W.H. Poewe, R.A. Hauser, and D.J. Brooks. REAL-PET Study Group. (2003). Slower progression of Parkinson's disease with ropinirole versus levodopa: the REAL-PET study. *Ann Neurol*, **54(1)**: 93-101.
- Williams, A., S. Gill, T. Varma, C. Jenkinson, N. Quinn, R. Mitchell, R. Scott, N. Ives, C. Rick, J. Daniels, S. Patel, and K. Wheatley. (2010). Deep brain stimulation plus best medical therapy versus best medical therapy alone for advanced Parkinson's disease (PD SURG trial): a randomized, open-label trial. *Lancet Neurol*, **9**: 581-591.
- Wirdefeldt, K., P. Odin, and D. Nyholm. (2016). Levodopa-carbidopa intestinal gel in patients with Parkinson's disease: a systematic review. *CNS Drugs*, **30(5)**: 381-404.
- Wu, K., C.A. Meyers, N.K. Guerra, M.A. King, and E.M. Meyer. (2004). The effects of rAAV2-mediated NGF gene delivery in adult and aged rats. *Mol Ther*, **9(2)**: 262-269.
- Wu, Z., E. Miller, M. Agbandje-McKenna, and R.J. Samulski. (2006). Alpha2,3 and alpha2,6 N-linked sialic acids facilitate efficient binding and transduction by adeno-associated virus types 1 and 6. *J Virol*, **80(18)**: 9093-9103.
- Xiao, P.J., and R.J. Samulski. (2012). Cytoplasmic trafficking, endosomal escape, and perinuclear accumulation of adeno-associated virus type 2 particles are facilitated by microtubule network. *J Virol*, **86**: 10462-10473.

- Yoritaka, A., S. Kawajiri, Y. Yamamoto, T. Nakahara, M. Ando, K. Hashimoto, M. Nagase, Y. Saito, and N. Hattori. (2015). Randomized, double-blind, placebo-controlled pilot trial of reduced coenzyme Q10 for Parkinson's disease. *Parkinsonism Relat Disord*, **21(8)**: 911-916.
- Yuan, H., Z. Zhen-Wen, L. Li-Wu, Q. Shen, X. Wang, S. Ren, H. Ma, S. Jiao, and P. Liu. (2010). Treatment strategies for Parkinson's disease. *Neurosci Bull*, **26(1)**: 66-76.
- Zerial, M., and H. McBride. (2001). Rab proteins as membrane organizers. *Nat Rev Mol Cell Biol*, **2**: 107-117.
- Zhou, X., X. Zeng, Z. Fan, C. Li, T. McCown, R.J. Samulski, and X. Xiao. (2008). Adeno-associated virus of a single-polarity DNA genome is capable of transduction in vivo. *Mol Ther*, **16(3)**: 494-499.

Chapter 2: Recombinant adeno-associated virus 2/5-mediated gene transfer is reduced in the aged rat midbrain

Abstract

Clinical trials are examining the efficacy of viral vector-mediated gene delivery for treating Parkinson's disease (PD). While viral vector strategies have been successful in preclinical studies, to date clinical trials have disappointed. This may be due to the fact that preclinical studies fail to account for aging. Aging is the single greatest risk factor for developing PD and age alters cellular processes utilized by viral vectors. We hypothesized that the aged brain would be relatively resistant to transduction when compared to the young adult. We examined recombinant adeno-associated virus 2/5 mediated green fluorescent protein (rAAV2/5 GFP) expression in the young adult and aged rat nigrostriatal system. GFP overexpression was produced in both age groups. However, following rAAV2/5 GFP injection to the substantia nigra (SN) aged rats displayed 40-60% less GFP protein in the striatum, regardless of rat strain or duration of expression. Further, aged rats exhibited 40% fewer cells expressing GFP and 4-fold less GFP mRNA. rAAV2/5-mediated gene transfer is compromised in the aged rat midbrain, with deficiencies in early steps of transduction leading to significantly less mRNA and protein expression.

Introduction

Parkinson's disease (PD) is the second most common neurodegenerative disease and currently impacts approximately 4.6 million individuals worldwide, with the prevalence expected to increase in the coming decades with longer life expectancies [Dorsey *et al*, 2007]. The cardinal symptoms of PD are motor deficits resulting from the degeneration of dopaminergic neurons in the substantia nigra pars compacta (SNpc) and the accompanying loss of dopamine neurotransmission within the striatum. While it is still unclear what causes PD, aging is known to be a primary risk factor for this disease, with the vast

majority of idiopathic cases occurring in patients over the age of 65 [Collier *et al*, 2011]. Currently, there are no therapies that halt, slow, or reverse the progression of neurodegeneration in PD [Gombash *et al*, 2014]. However, viral vector-mediated gene therapy is a promising therapeutic avenue due to its ability to continuously replenish diminished proteins or overexpress neuroprotective factors that alleviate symptoms or alter disease progression.

Preclinical studies using viral vector-mediated gene transfer have been successful in ameliorating symptoms and rescuing nigral dopamine neuron loss in PD models [Emborg *et al*, 2009; Gash *et al*, 1996; Gasmi *et al*, 2007; Gombash *et al*, 2012; Herzog *et al*, 2008; Kordower *et al*, 2000], yet human clinical trials have not experienced similar success [Bartus *et al*, 2011; ClinicalTrials.gov, 2013; Marks *et al*, 2010; Stocchi and Olanow, 2013; Olanow *et al*, 2015]. Although this discrepancy may be due to a variety of factors such as targeting late-stage patients, needed a larger volume of expression, or needing to target other structures, another factor that could have led to the disappointing results is the almost exclusive use of young adult animals in preclinical studies that fail to recapitulate the aged host brain environment typical of most PD patients. For example, previous studies demonstrated that fetal dopamine neuron grafts completely ameliorated motor impairments in young rats yet produced no improvement in aged rats due to dramatically decreased survival and neurite extension in the aged host [Collier *et al*, 1999; Sortwell *et al*, 2001]. Thus, experimental results derived using young adult animals may have contributed to the overly optimistic expectations of clinical efficacy.

Several groups have reported successful viral vector-mediated gene transfer to the aged brain of rodents and non-human primates [Bartus *et al*, 2011; Emborg *et al*, 2009; Klein *et al*, 2010; Kordower *et al*, 2000; Wu *et al*, 2004]. However, only two of these reports directly compared transduction efficiency between aged and young animals, with contradicting results [Klein *et al*, 2010; Wu *et al*, 2004]. Klein *et*

al. (2010) reported equally efficient gene transfer in aged and young adult rat brains utilizing recombinant adeno-associated virus serotype 2/9 (rAAV2/9), while the Wu *et al.* (2004) concluded that serotype 2/2 (rAAV2/2) was less efficient in the aged brain as compared to the young adult brain. These results were secondary to the primary findings of the study and, consequently, additional experiments comparing viral vector efficiency between young adult and aged brains were not conducted.

It is well established that certain cellular processes that are normally altered in the aged brain [D'Angelo *et al.*, 2009; Gao *et al.*, 2013; Lee *et al.*, 2000; Ryazanov and Nefsky, 2002; Smith *et al.*, 1995] are also utilized by viral vectors for transduction [Schultz and Chamberlain, 2008]. The present study sought to determine whether viral vector-mediated transgene expression was reduced in the aged rat nigrostriatal system as compared to the young adult. We utilized the rAAV2/5 serotype to examine this question because of its efficient transduction of nigral neurons [Burger *et al.*, 2004; Gombash *et al.*, 2013]. Intranigral injections of rAAV serotype 2/5 expressing green fluorescent protein (rAAV2/5 GFP) resulted in significantly reduced exogenous protein expression in the aged rat brain as compared to the young adult brain. Significantly fewer cells throughout the aged rat midbrain expressed the transgene delivered by rAAV2/5 GFP, in addition to producing significantly less GFP protein and GFP mRNA. Collectively, our results indicate that rAAV2/5-mediated gene transfer is compromised in the aged rat brain environment.

Methods

I. Experimental overview

A cohort of twenty-one male Sprague Dawley (SD) rats, eleven young adult (3 months old) and ten aged (20 months old) were unilaterally injected with rAAV2/5 expressing GFP into the substantia nigra (SN).

Six young and five aged SD rats were sacrificed eleven days post-injection and five young and five aged SD rats were sacrificed three months post-injection. Similarly, a cohort of twelve male Fischer344 (F344) rats, six young adult and six aged, were unilaterally injected with rAAV2/5 expressing GFP in the SN and sacrificed twelve days post-injection. The striatum was used for western blot analysis from SD rats sacrificed 11 days and three months post-injection and the SN tissue was used for immunohistochemical staining and *in situ* hybridization. The striatum from F344 rats sacrificed 12 days post-injection was used for western blot analyses and the SN tissue was used for qPCR. The overall experimental design is illustrated in Figure 1.

II. Animals

Male, Sprague Dawley rats (Harlan, Indianapolis, IN) 3 months of age (n = 11) and 20 months of age (n = 10) and male, Fischer344 rats (National Institute on Aging, Bethesda, MD) 3 months of age (n = 6) and 20 months of age (n = 6) were used in this study. All animals were given food and water *ad libitum* and housed in 12h reverse light-dark cycle conditions in the Van Andel Research Institute vivarium, which is fully AAALAC approved. All procedures were conducted in accordance with guidelines set by the Institutional Animal Care and Use Committee (IACUC) of Michigan State University.

III. Viral vectors

Plasmid and rAAV vector production were completed as previously described [Gombash *et al*, 2014]. In short, humanized green fluorescent protein (GFP) was inserted into an AAV plasmid backbone. Expression of the transgene was driven by the chicken beta actin/cytomegalovirus enhancer (C β A/CMV) promoter hybrid. The vector contained AAV2 inverted terminal repeats (ITRs) and was packaged into AAV5 capsids via co-transfection with a plasmid containing *rep* and *cap* genes and adenovirus helper functions. Particles were purified using iodixanol gradients and Q-sepharose chromatography, and

dotblot was used to determine vector titer [Zolotukhin *et al*, 1999]. The vector titer used in this study was 5.88×10^{13} genomes/mL [Gombash *et al*, 2013]. In order to preserve the viral stability and titer, viral preparations were stored at 4°C and never frozen. All surfaces (syringes, pipettes, and microcentrifuge tubes) were coated in SigmaCote (Sigma-Aldrich, St. Louis, MO SL2) prior to coming in contact with the virus to minimize binding of viral particles.

IV. rAAV2/5 GFP injections

All surgical procedures were performed under isoflurane anesthesia (5% in O₂ for induction and 2% in O₂ for maintenance). Rats were placed in a stereotaxic frame and two 2µL injections of rAAV2/5 were injected in the left SN at coordinates (from dura) AP -5.3mm, ML +2.0mm, DV -7.2mm, and AP -6.0mm, ML +2.0mm, and DV -7.2mm as previously described (Gombash *et al*, 2013). A Hamilton syringe fitted with a glass capillary needle (Hamilton Gas Tight syringe 80,000, 26s/2" needle; Hamilton, Reno, NV; coated in SigmaCote) was used for injection. The glass needle was lowered to the site and vector injection began immediately at a rate of 0.5 µl/minute and remained in place after the injection for an additional 5 minutes before retraction.

V. Sacrifice and tissue preparation

Six young and five aged SD rats were sacrificed 11 days post-injection, all F344 rats were sacrificed 12 days post-injection, and five young and five aged SD rats were sacrificed 3 months post-injection. All rats were deeply anesthetized (60mg/kg, pentobarbital, i.p.) and perfused intracardially with 0.9% saline containing 1ml/10,000 USP heparin, followed by ice cold 0.9% saline. SD rat brains were immediately removed and hemisected in the coronal plane at approximately AP -2.64mm. The caudal tissue from SD rats was processed for immunohistochemistry, whereas rostral tissue from SD and whole brains from F344 were processed for microdissections.

VI. Microdissections

After brain removal, whole brains and rostral brains were flash frozen in 2-methylbutane on dry ice.

i. SD Striatal Tissue for Protein Analyses.

The rostral section of the brain was frozen at -18°C for at least one hour before striatal dissections. 1-2mm coronal slabs were blocked from each brain utilizing an aluminum brain blocker (Zivic, Pittsburg, PA) and striatal tissue from both hemispheres was microdissected with a small tissue punch while being held at a constant -12°C on a modified cold plate (Teca, Chicago, IL). Frozen dissected structures were stored at -80°C until analysis.

ii. F344 Striatal Tissue for Protein Analyses and SN Tissue for RNA Analyses.

All surfaces and instruments were sprayed with RNase Away (Invitrogen, Carlsbad, CA). Brains were moved from -80°C to -20°C before use. Brains were kept on dry ice and mounted onto metal chucks with Tissue-Tek O.C.T. (VWR, Vatavia, IL) before being moved to a -20°C cryostat for sectioning. Tissue was sectioned until the structures of interest became visible. 2mm sections of the striatum were removed from both hemispheres of SD brains with a small tissue punch, and 2mm sections of striatum and SN were removed from both hemispheres of the F344 brains with a small tissue punch. Punches were taken from the middle of the brain structures to ensure precision. Striatal punches were placed in separate pre-frozen RNase free microcentrifuge tubes and immediately placed back on dry ice. SN punches were placed in separate pre-frozen RNase free microcentrifuge tubes containing TRIzol Reagent (Invitrogen, Grand Island, NY) and tissue was homogenized with a pestle before storage. Samples were stored at -80°C until time of assay.

VII. Immunohistochemistry

The caudal portion of the brains was post-fixed in 4% paraformaldehyde (Electron Microscopy Sciences, Hatfield, PA) in 0.1mol PO₄ buffer for seven days. After this period they were transferred to 30% sucrose in 0.1mol PO₄ buffer until sinking. Brains were frozen on dry ice and sectioned at a 40µm thickness using a sliding microtome. Every sixth section was processed for immunohistochemistry using the free-floating method.

i. Immunohistochemistry

Tissue sections were rinsed in Tris buffer and quenched in 0.3% H₂O₂ for 15 minutes, blocked in 10% normal goat serum for 1 hour, and incubated in primary antisera (TH: Millipore MAB318, mouse anti-TH, 1:4000; GFP: Abcam Ab290, rabbit anti-GFP, 1:100,000) overnight at 4°C. Following primary incubation, TH-labeled sections were incubated in secondary antisera against mouse IgG (Vector BA-2001, biotinylated horse anti-mouse IgG, rat absorbed, 1:1000) and GFP-labeled sections were incubated in secondary antisera against rabbit IgG (Millipore AP132b, goat anti-rabbit IgG, 1:500) for 2 hours at room temperature, followed by Vector ABC detection kit using horseradish peroxidase (Vector Laboratories, Burlingame, CA). Antibody labeling was visualized by exposure to 0.5mg/ml 3,3' diaminobenzidine and 0.03% H₂O₂ in Tris buffer. Sections were mounted on subbed slides and coverslipped with Cytoseal. Images were taken on a Nikon Eclipse 90i microscope with a QICAM camera (QImaging, Surrey, British Columbia, Canada). Figures were produced in Photoshop 7.0 (San Jose, CA), with brightness, saturation, and sharpness adjusted only as needed to best replicate the immunostaining as viewed directly under the microscope.

ii. TH and GFP Double Label Immunofluorescence

Sections of rat tissue were blocked in 10% normal donkey serum for 1 hour and subsequently transferred to the primary antisera (TH: Millipore Ab152, rabbit anti-TH, 1:4000) to incubate overnight at 4°C. Following primary incubation, tissue was incubated in the dark in secondary antisera against rabbit IgG (Invitrogen A10042, Alexa Fluor 568 donkey anti-rabbit, 1:500) for 1 hour at room temperature. Tissue was then blocked in 10% normal goat serum for 20 minutes at room temperature before being incubated in the primary antisera against GFP (Abcam Ab290, rabbit anti-GFP, 1:100,000) overnight at room temperature in the dark. Following primary incubation, tissue was incubated in secondary antisera against chicken IgG (Life Technologies A11039, Alex Fluor 488 goat anti-chicken IgG, 1:400) for 3 hours at room temperature. Sections were mounted on subbed slides and coverslipped with Vectashield Hardset Mounting Medium (Vector Laboratories H1400, Burlingame, CA). Images were taken on a Nikon 90i fluorescence microscope with a Nikon DS-Ri1 camera. Figures were produced in Photoshop 7.0 (San Jose, CA). Brightness, saturation, and sharpness were adjusted only as necessary to best replicate the immunostaining as viewed directly under the microscope.

VIII. Western blot

Striatal punch samples were homogenized on ice in 2% SDS. Total protein concentration was determined by the Bradford protein assay. Samples were prepared at 25ng total protein samples. Western blot protocol was completed as previously described [Piltonen *et al*, 2009]. Samples were run using SDS-PAGE and transferred to Immobilon-FL membranes (Millipore, Bedford, MA). Membranes were incubated in primary GFP antisera (AbCam, Cambridge, MA; rabbit polyclonal IgG, Ab290, 1:1,000) and β -tubulin antisera (Cell Signaling, Danvers, MA; mouse monoclonal IgG, 4466, 1:1,000) overnight. IRDye800 conjugated goat anti-rabbit (LI-COR Biosciences; 926-32211, 1:15,000) and IRDye680 conjugated goat anti-mouse (LI-COR Biosciences, 926-68020, 1:15,000) were used as secondary

antibodies. All antibody dilutions were made in LI-COR specific blocking buffer (LI-COR Biosciences, 927-40000). Multiplexed signal intensities were imaged with both 700 and 800 nm channels in a single scan with a resolution of 169 μ m using the Odyssey infrared image system (LI-COR Biosciences). Reported integrated intensity measurements of GFP expression were normalized according to the corresponding β -tubulin densitometry measurements. The representative image was produced in Photoshop 7.0 (San Jose, CA).

IX. RNA isolation and cDNA synthesis

RNA was isolated using the QIAshredder (Quiagen, Valencia, CA) and RNeasy Plus Mini kit (Quiagen, Valencia, CA). The Quiagen protocol for purification of total RNA from animal tissue was used. RNA from tissue was then converted into cDNA using SuperScript VILO Master Mix (Life Technologies, Grand Island, NY). The RNA was assumed to be converted 100% to cDNA.

X. GFP qPCR

The PCR reactions were carried out with 1x TaqMan Universal Mastermix (ABI, Carlsbad, CA), and a customized TaqMan gene expression assay kit for GFP (ABI, Carlsbad, CA). This kit includes 6,000 pmoles of the TaqMan MGB-fluorescent probe and 10,000 pmoles of each manufactured primer. Forward (R) and reverse (L) primers, as well as the probe (P) sequence were synthesized by ABI. The sequences were as follows: R: AGACCATATGAAGCAGCATGACTTTT, L: GTCTTGTAGTCCCGTCATCTTTGA, P: 5'6FAM CTCCTGCACATAGCCC MGBNFQ. A total of 20ng of cDNA was added to each 50 μ l reaction mixture which also contained 150nM forward and 150nM reverse primers, a 150nM probe sequence, and TaqMan master mix. qPCR reactions to control for cDNA quantities were run using GAPDH (Life Technologies 4352338E, Grand Island, NY) as an endogenous control. The qPCR reactions were run on an ABI 7500 real-time thermocycler using the following setup: Step1: Incubation at 50°C for 2 minutes. Step 2:

Incubation at 95°C for 10 minutes. Step 3: Denaturation at 95°C for 15 seconds followed by annealing-elongation at 60°C for 1 minute followed by data collection. Step 3 was cycled 40 times for the qPCR run. Cycle thresholds were chosen during the linear phase of amplification using the AutoC_T function. All samples were run on the same plate along with a no-template control. Analysis was first carried out using the 2^{-ΔCT} method and Relative Expression Software Tool (REST-XL) method [Pfaffl *et al*, 2002; Schmittgen and Livak, 2008].

XI. RNAscope *in situ* hybridization for GFP mRNA

Tissue sections at the level of the SN were incubated in Pretreat 1 from the RNAscope Pretreatment Kit (310020, Advanced Cell Diagnostics, Hayward, CA) for 1 hour. Tissue was then incubated for 10 minutes in Pretreat 2 at 99°C before being mounted on Histabond slides and incubated on a plate warmer set to 60°C overnight. After Pretreat 2, slides were dipped in 100% ethanol and incubated with Pretreat 3 in a hybridization oven at 40°C. Slides were dried and the VS Probe for GFP (409016, Advanced Cell Diagnostics, Hayward, CA) was added for a 2 hour incubation in the hybridization oven. Six amplification steps with the amplification buffers (320600, Advanced Cell Diagnostics, Hayward, CA) were then performed in alternating 30 and 15 minute incubation intervals in the hybridization oven. Tissue was developed using the supplied DAB reagent (320600, Advanced Cell Diagnostics, Hayward, CA). Slides were rinsed and coverslipped with Cytoseal. Images were taken on a Nikon Eclipse 90i microscope with a QICAM camera (QImaging, Surrey, British Columbia, Canada). Figures were produced in Photoshop 7.0 (San Jose, CA), with brightness, saturation, and sharpness adjusted only as needed to best replicate the mRNA labeling as viewed directly under the microscope.

XII. Stereology

Quantification of TH immunoreactive (THir) neurons in the SN pars compacta (SNpc) or total number of GFP immunoreactive (GFPir) cells was completed as previously described [Gombash *et al*, 2012]. Briefly, stereology was performed using a Nikon Eclipse 80i microscope (Nikon), StereoInvestigator software (Microbrightfield Bioscience, Williston, VT) and Retiga 4000R camera (Qimaging, Surrey, BC Canada). Using the optical fractionator probe, THir neurons in the vector injected and control hemisphere in every sixth section of the entire SN were counted at 60x magnification. Similarly, GFPir cells were counted at 60x magnification in the injected hemisphere in every sixth section of the brain where GFP staining was visible. A coefficient of error <0.10 was accepted. THir data are reported as total estimates of THir neurons in each hemisphere.

XIII. Counts of GFP and TH immunoreactive cells

Tiled images at 10x magnification were taken on three SD brain sections per animal that were stained for GFP and TH immunofluorescence. These sections contained the medial terminal nucleus of the accessory optic tract (MTN) and were approximately -5.04mm, -5.28mm, and -5.52mm relative to bregma [Gombash *et al.*, 2014]. Images were taken with a Nikon 90i fluorescence microscope with a Nikon DS-Ri1. All GFP immunoreactive (GFPir) cells that were in focus with a clear nucleus were manually counted to determine the total number of transduced cells. All TH immunoreactive (THir) neurons that were in focus with a visible nucleus and were also GFPir were manually counted to determine the number of THir cells expressing GFP. The percentage of THir neurons that were transduced was determined by dividing the total number of GFPir cells by the number of neurons that were immunoreactive for both TH and GFP. The remaining GFPir cells that did not stain for TH were designated as non-TH transduced cells. Data are reported as the average percent of GFPir/THir and GFPir/non-THir cells.

XIV. Volume of GFPir Mesencephalic Expression

Neurolucida v.7, Neurolucida Explorer (Microbrightfield), a Nikon Eclipse 80i microscope (Nikon), and a Retiga 4000R camera (Qimaging) were used to outline the area of GFPir expression and calculate the volume of this area. The entire mesencephalic section and area of transgene expression were manually traced approximately every sixth serial section along the anterior-posterior (coronally sectioned) axis. Tracings began at -3.18mm from bregma and were terminated at -6.78mm from bregma. The 40 μ m section thickness and distance between each section (~240 μ m) allowed Neurolucida to construct a 3D model of the mesencephalon and area of transgene expression from 2D tracings. Using the model, characteristic volumes of these outlined areas were calculated by Neurolucida Explorer. These tracings and calculations were performed on a representative young adult and aged Sprague Dawley rat at 11 days post-injection with rAAV2/5 GFP as depicted in Figure 3.

XV. Statistical analyses

All statistical tests were completed using IBM SPSS statistics software (version 22.0, IBM, Armonk, NY). Graphs were created using GraphPad Prism software (version 6, GraphPad, La Jolla, CA). All studies utilized independent samples t-tests to assess differences between the young adult and aged animals. The THir quantification results were analyzed with two-way repeated measures ANOVA with two treatment factors, age and hemisphere. The GFPir/THir and GFPir/non-THir quantification results were analyzed with two-way repeated measures ANOVA with a single treatment factor. Tukey *post hoc* analyses were used on all ANOVA tests to determine significance between individual groups using the harmonic mean of the group sizes to account for unequal sample sizes. For the qPCR gene expression study, fold changes for the GFP gene were normalized to the GAPDH gene expression and calculated before being subjected to t-test analysis using the REST-XL.

Results

I. Aging and rAAV2/5 GFP injection do not impact SN pars compacta (SNpc) tyrosine hydroxylase immunoreactive (THir) neuron number

Sprague Dawley (SD) rats are classified as young adult from the time of sexual maturity (P35) until 6 months, middle aged between 6 and 18 months, old (aged) after 18 months, and senile after 24 months with an average lifespan of 26-32 months [Alemán *et al*, 1998; Gao *et al*, 2011]. Importantly, after 22-24 months, SD rats exhibit a 13% reduction in SN dopamine neurons [Gao *et al*, 2011]. In the present study, we used 3-month-old young adult rats and 20-month-old aged rats (Figure 5). In order to verify that no differences existed in the quantity of SNpc THir neurons due to aging (at 20 months) or rAAV2/5 GFP injection, we used unbiased stereology to estimate the number of SNpc THir neurons in both the uninjected and rAAV2/5 GFP injected hemispheres at 11 days post-injection (Figure 6a). Aged rats possessed equivalent SNpc THir neurons compared to young adult rats in both hemispheres ($F_{(1,9)}=0.025$, $p>0.05$). In addition, there were no significant differences between THir neuron counts in the SNpc ipsilateral to the rAAV2/5 GFP injection as compared to the SNpc contralateral to the injection, indicating that at 11 days post-injection the viral vector was not toxic to the SNpc neurons ($F_{(1,9)}=2.546$, $p>0.05$).

II. Aged rats exhibit decreased numbers of transduced cells as compared to young adult rats

We examined the total number of transduced cells in the SD mesencephalon at 11 days post-injection with rAAV2/5 GFP. Both young adult and aged SD rats exhibited GFP immunoreactivity in the midbrain that included the SNpc and numerous cells in the neighboring mesencephalic parenchyma (Figure 6b, Figure 7). However, the young adult midbrain appeared to possess a greater number of GFP immunoreactive (GFPir) cells as compared to the aged midbrain. Stereological quantification of the

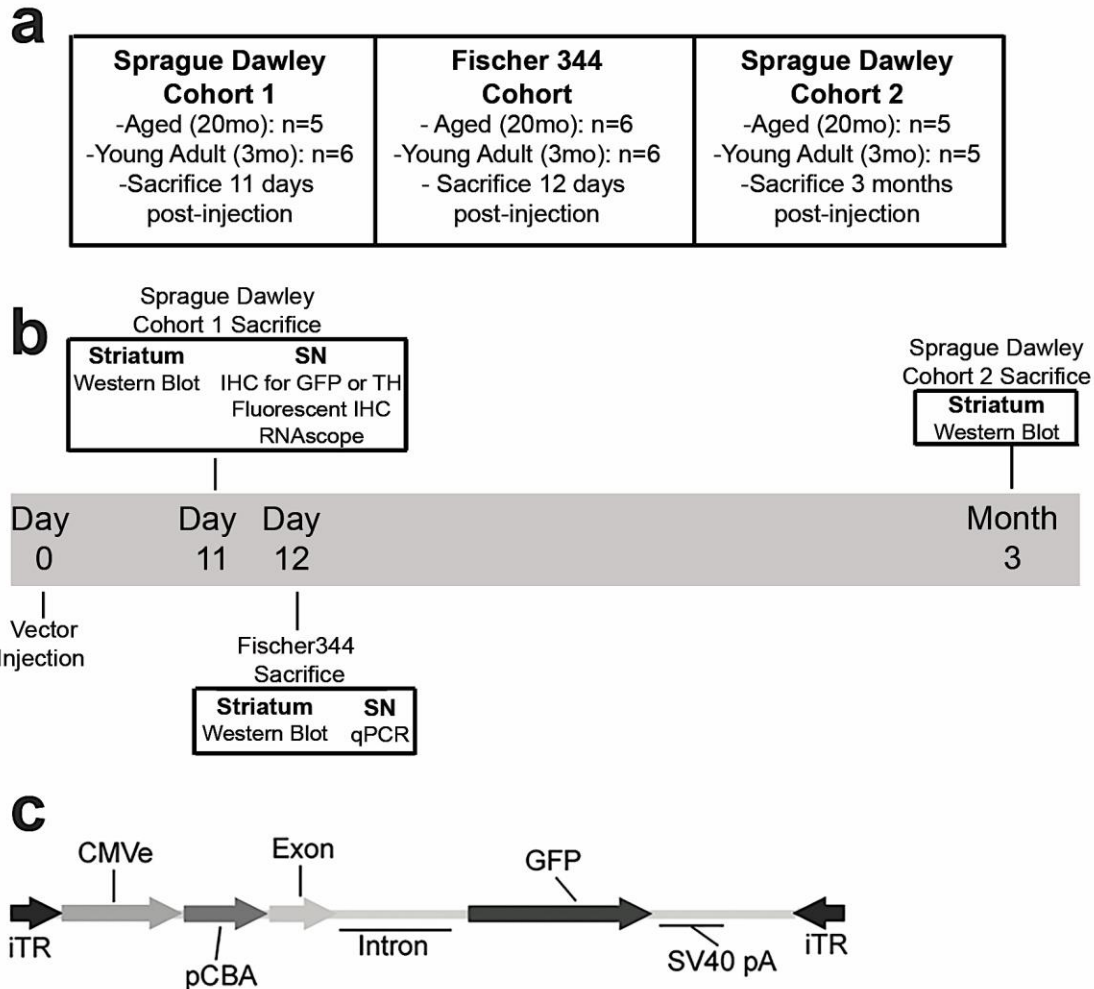


Figure 5. Schematic of experimental design and rAAV2/5 viral vector construct. (a-b) Overview and timeline of the three cohorts of rats used in these studies. Young adult (3 months) and aged (20 months) Sprague Dawley and Fischer344 rats were all injected in the substantia nigra (SN) with the rAAV2/5 GFP viral vector and were sacrificed at indicated time points to harvest tissue for various outcome measures. c) Recombinant adeno-associated virus (rAAV) genomic map of rAAV2/5 expressing GFP used in all experiments.

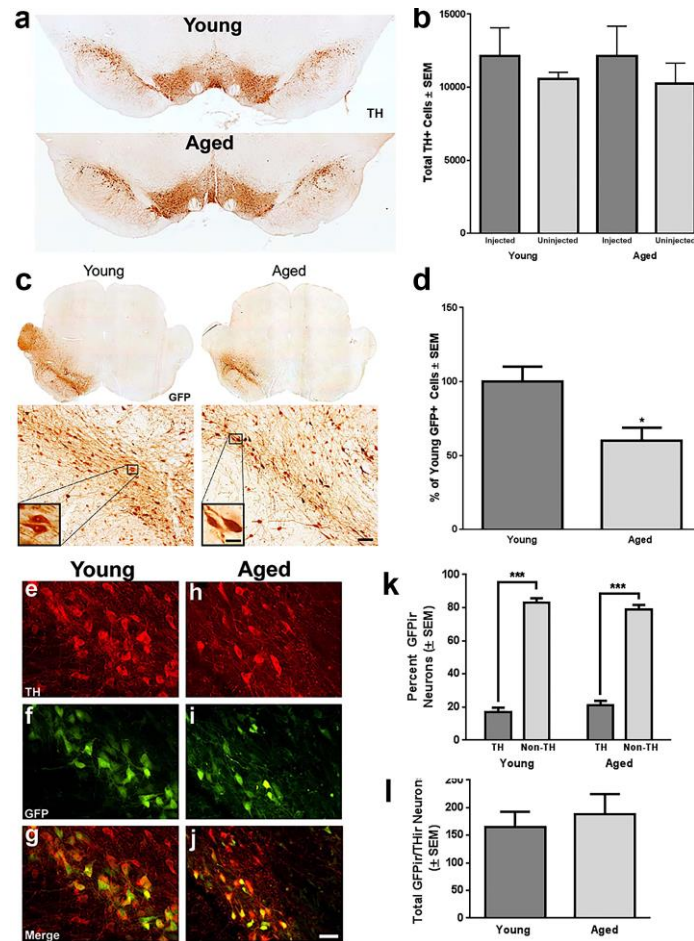


Figure 6. GFP immunoreactivity reveals fewer transduced cells in aged rats following rAAV2/5 GFP injection. a) Representative image of TH immunoreactive (THir) neurons in the substantia nigra pars compacta (SNpc) of young adult (Young) and aged (Aged) SD brains at 11 days post-injection. TH immunoreactivity appears equal between hemispheres and age groups. Scale bar = 1000 μ m. b) Stereological quantification of THir neurons in young adult and aged SD rats in the rAAV2/5 GFP injected and uninjected SNpc. No significant reductions in tyrosine hydroxylase immunoreactive (THir) neurons are observed in aged (n=5) as compared to young adult (n=6) rats or in the injected as compared to the uninjected hemisphere 11 days following rAAV2/5 GFP injection. c) Representative samples of GFP immunoreactivity in the Young and Aged SD rat brain 11 days post-injection. GFP immunoreactivity is observed throughout the midbrain ipsilateral to the injection site (left) with dense cellular staining observed at higher magnifications. GFP immunoreactivity in the midbrain of aged rats is visibly less abundant than that of young adult rats. Scale bars = 1000 μ m in top panels, 100 μ m in lower panels and 25 μ m in the high magnification inserts. d) Stereological quantification of the total number of GFP immunoreactive cells for young adult (n=6) and aged (n=5) rats revealed a statistically significant (*p<0.05) 40% decrease in GFP immunoreactive cells in the aged brain as compared to the young adult brain. (e-j) GFP co-expression within THir SN neurons in young adult (e-g) and aged (h-j). Numerous THir neurons and non-THir cells expressing GFP are apparent in both age groups. Scale bar = 50 μ m. k) Quantification of the number of THir neurons expressing GFP in three sections containing a readily identifiable SNpc in young adult and aged rats. No significant differences were observed in the number of GFPir/THir neurons at these levels of the mesencephalon. l) Quantification of the percentage THir and non-THir cells that colocalize with GFP expression. No significant differences were observed between young adult and aged rats in the percent of THir neurons or the percent of non-THir cells expressing GFP, although both age groups exhibited significantly more GFPir non-THir cells than GFPir/THir neurons (Aged, n=5; Young Adult, n=6). All values are expressed as the mean \pm SEM for each group (Aged, n=5; Young Adult, n=6).

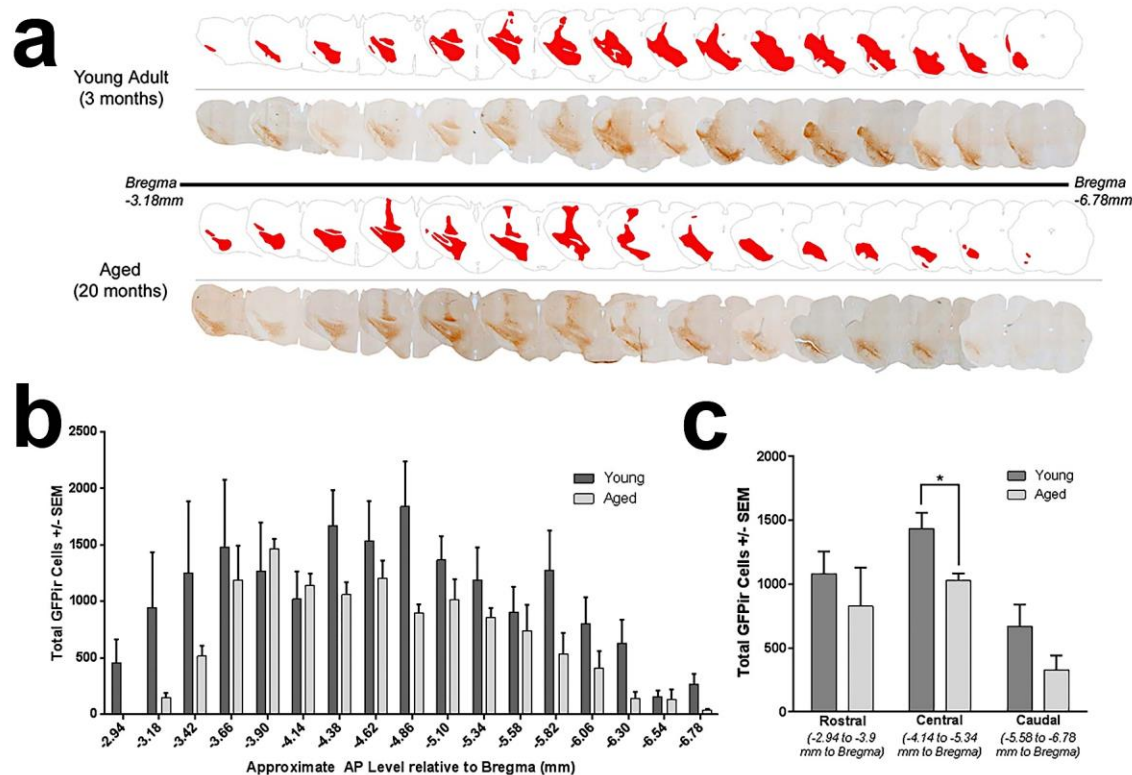


Figure 7. Decreases in exogenous transgene expression in the aged brain span the anterior-posterior (AP) mesencephalic axis. a) Representative montage of GFP immunoreactivity within individual midbrain sections 11 days following rAAV2/5 GFP injection to either young adult or aged rats. GFP immunoreactive cells are generally observed spanning the entire AP axis in both young adult and aged rats, with aged rats generally exhibiting smaller areas of transgene expression within individual coronal sections. The total volume of transgene expression in the young adult brain was 205,524,000 μm^3 , or 10.47% of the mesencephalon, whereas the total volume of transgene expression in the aged brain was 135,517,000 μm^3 , or 6.62% of the mesencephalon. b) Stereological estimates of the number of GFP immunoreactive cells per individual mesencephalic coronal section indicate a general trend of fewer GFP immunoreactive cells within each aged brain section as compared to the comparable section in the young adult. c) Stereological estimates of the number of GFP immunoreactive cells within the rostral, central, and caudal regions of the area displaying transgene expression. Aged rats possess a trend for fewer GFP immunoreactive cells in the rostral and caudal regions with significantly fewer GFP immunoreactive cells in the central region (* $p < 0.05$) than young adult rats. Values are expressed as the mean \pm SEM for each group (Young Adult, $n = 6$; Aged, $n = 5$).

number of cells displaying GFP immunoreactivity indicated that the aged rat had significantly fewer (approximately 40%) total transduced cells as compared to the young adult rat ($p=0.038$; Figure 6c). To determine whether THir neurons of the SNpc in aged rats specifically were resistant to gene transfer we determined the number of THir cells expressing GFP and the percentage of THir versus non-THir transduced cells in both age groups within sections in which the THir neurons of the SNpc could be definitively delineated from THir neurons of the ventral tegmental area. Dual immunofluorescence revealed successful transduction of THir and non-THir neurons with rAAV2/5 GFP in both young and aged rats (Figure 6e-j). Unlike total cell counts resulting from unbiased stereology, no age-related differences were observed in the number of GFPir cells within this subregion of the mesencephalon (Figure 6b) and, similarly, no difference in the number of GFPir/THir cells was observed between young and aged rats ($p>0.05$, Figure 6k). Further, there were no significant differences in the percentage of THir and non-THir cells expressing GFP between the young adult and aged SD rat at 11 days post-injection ($F_{(1,7)}=1.161$, $p>0.05$, Figure 6l), although there were significantly more (~80% more) non-THir cells than THir neurons expressing GFP in both age groups ($F_{(1,7)}=257.78$, $p<0.001$). Together, these results suggest that identical rAAV2/5 vector injections result in significantly fewer total cells expressing the rAAV2/5 transgene in the aged SN as compared to the young adult SN, and that age-related deficiencies in gene transfer are not specific to SNpc THir neurons.

III. Reduced exogenous transgene expression in the aged brain spans the entire rostral-caudal mesencephalic axis

We next investigated the pattern of transduction to determine whether reduced vector spread in the aged brain drives the observed age-related decrease in the number of cells expressing the GFP transgene. The number of GFPir cells per section was quantified within sixteen coronal sections spanning the extent of the visibly transduced area in the young adult and aged rat mesencephalon.

Qualitatively the anterior-posterior (AP) axis of transgene expression appeared to be approximately equal, with differences occasionally observed in both dorsal-ventral (DV) and medial-lateral (ML) spread (Figure 7a). Quantification of the number of GFPir cells per section indicated that the aged mesencephalon possessed fewer GFPir cells within the overwhelming majority of sections (13 of 16). Within individual mesencephalic sections, reductions in GFPir cells in the aged brain did not achieve significance ($p>0.05$, Figure 7b). However, when all sections were combined for stereological assessment of the total number of transgene-expressing cells, the aged brain exhibited significantly fewer GFPir cells (Figure 6c). Furthermore, when sections were grouped into rostral, central, and caudal regions of transgene expression, there is a trend for decreased GFPir neurons in the rostral and caudal regions with a significant decrease ($p=0.014$) in total GFPir neurons in the central region of transgene expression. The lack of significant differences at the level of the individual sections suggests that a difference in the diffusivity of the vector does not underlie the age-related decrease in transgene expression.

IV. Aged rats display decreased GFP protein expression in the striatum as compared to young adult rats

rAAV2/5-mediated protein expression in young adult rats is not maximal until 1 month after injection [Gombash *et al*, 2012], and it is possible that the aged brain may require more time to achieve maximal GFP expression. Therefore, we utilized protein immunoblotting to more accurately quantify GFP protein levels at varying time points after rAAV2/5 GFP injection. We examined the levels of striatal GFP protein expression induced by rAAV2/5 GFP in young adult and aged rats from two different rat strains at three different time points post-injection (SD at 11 days, F344 at 12 days, and SD at 3 months, Figure 8a-d). Aged rats consistently displayed lower levels of GFP protein (approximately 40-60% less) as compared to their young adult rat counterparts, regardless of the rat strain or the duration of gene expression (SD 11 days, $p=0.030$; F344 12 days, $p=0.008$; SD 3 months, $p=0.014$). These results indicate that although GFP

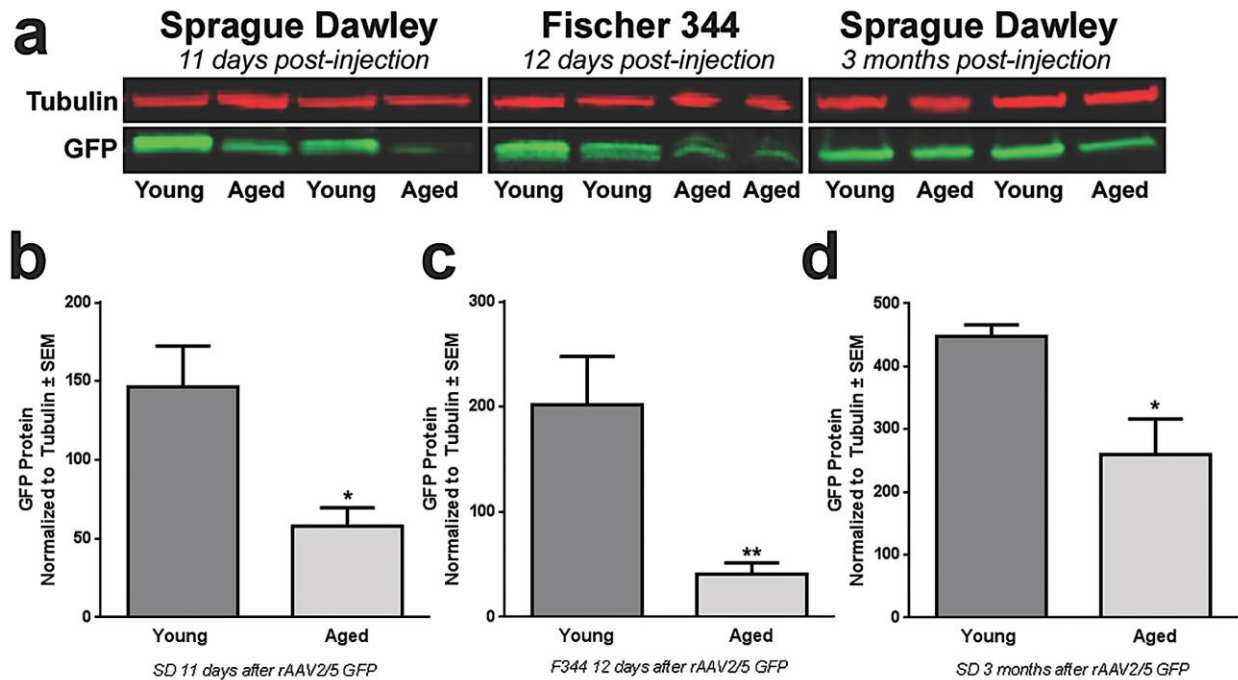


Figure 8. rAAV2/5-mediated GFP protein expression is diminished in the aged striatum. a) Representative western blot of GFP immunodetection in striatal samples of young adult and aged Sprague Dawley (SD) rats 11 days post-injection and Fischer344 (F344) rats 12 days post-injection. Young adult rats consistently express more GFP protein than aged rats. b) Quantification of striatal GFP protein levels in young adult (n=6) and aged (n=5) SD rats 11 days post-injection. Aged rats exhibited significantly lower levels of GFP protein (*p<0.05) than young adult rats. c) Quantification of striatal GFP protein levels in young adult (n=6) and aged (n=6) F344 rats at 12 days post-injection; aged rats display significantly less GFP protein (**p<0.01) than young adult rats. d) Quantification of GFP protein levels in the striatum of young adult (n=5) and aged (n=5) SD rats at 3 months post-injection. Aged rats exhibit significantly less GFP protein (*p<0.05) than young adult rats. Values are expressed as the mean optical density scores, normalized to tubulin controls ± SEM for each group. rAAV, recombinant adeno-associated virus.

protein increases with duration of rAAV2/5 GFP expression, aged rats consistently display deficiencies in GFP protein expression in the midbrain as compared to young adult rats, regardless of rat strain.

V. Aged rats exhibit decreased levels of GFP mRNA expression as compared to young adult rats

To determine whether reduced GFP protein expression in the aged brain was the result of aging-related decreases in protein synthesis [Ryazanov and Nefsky, 2002; Smith *et al*, 1995], GFP mRNA expression in the SN was examined using the complementary approaches of qPCR and RNAscope in situ hybridization [Wang *et al*, 2012]. qPCR analyses revealed significantly lower ($p < 0.001$) GFP mRNA levels in the aged SN as compared to the young adult SN, with approximately 4-fold lower levels of mRNA expression in the aged rat (Figure 9a). Furthermore, GFP mRNA expression visualized using RNAscope in situ hybridization confirmed our qPCR results. GFP mRNA expression in the mesencephalon of both young adult and aged rats was observed, with a large areas of expression containing dense staining in the midbrain ipsilateral to the injection site (Figure 9b). Qualitatively, when compared to GFP mRNA expression in the young adult, the aged rat midbrain displayed a smaller area of cells expressing GFP with less dense staining within this area. Collectively, these findings indicate that rAAV2/5 transduction of the aged rat midbrain as compared to the young adult rat midbrain results in significantly less GFP mRNA expression, further leading to significant deficiencies in GFP protein levels. This signifies that steps prior to translation are deficient in the process of viral transduction in the aged midbrain.

Discussion

In the present study, we investigated the ability of rAAV2/5 to transduce neurons of the aged rat brain as compared to the young adult rat brain. We first verified, as demonstrated previously, that our

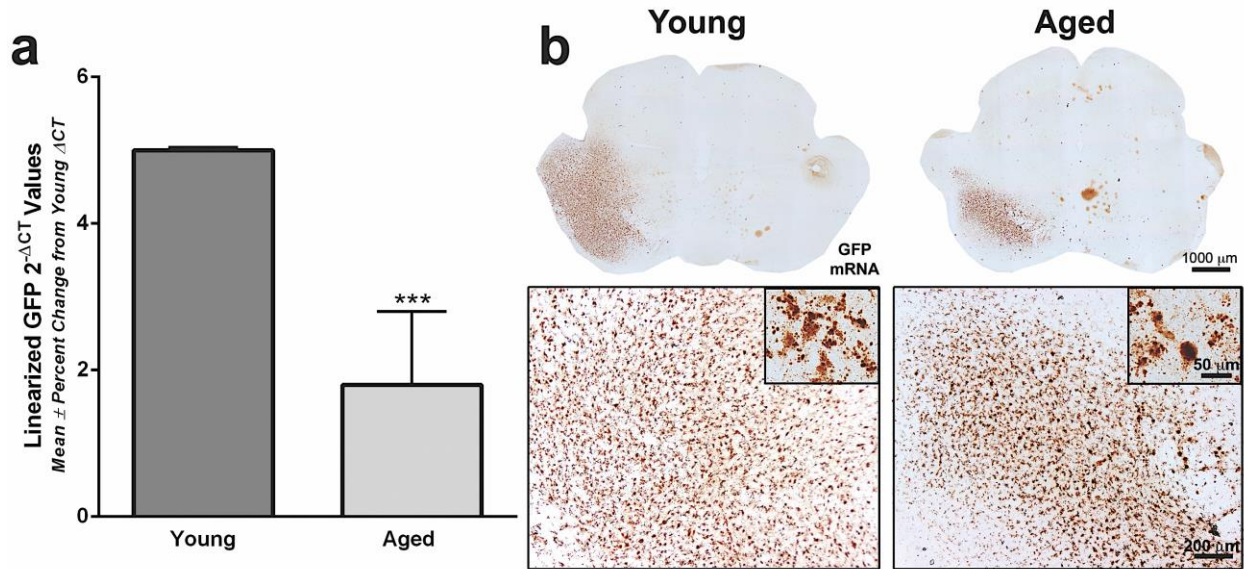


Figure 9. rAAV2/5-mediated GFP mRNA expression is diminished in the aged SN. a) GFP mRNA quantitation using qPCR of the Fischer344 (F344) substantia nigra (SN). GFP mRNA expression in the aged F344 SN was significantly lower (approximately 4-fold less) than expression levels in the young adult SN (** $p < 0.001$) 12 days following rAAV2/5 vector injection. Values are displayed as the mean linearized GFP $2^{-\Delta\text{CT}}$ values \pm percent change from young adult ΔCT values (Young Adult, $n=6$; Aged, $n=6$). b) Representative images using RNAscope in situ hybridization for GFP in the Sprague Dawley (SD) midbrain 11 days following rAAV2/5 vector injection. GFP mRNA expression in the young adult rat is observed throughout the midbrain ipsilateral to the injection site, with dense staining observed at higher magnifications. Scale bar = 1000 μm in top panel of lower magnification images, 200 μm in lower panel images and 50 μm in lower panel inserts. GFP mRNA expression in the midbrain of aged rats is visually less abundant than that of young adult rats with robust staining observed at higher magnifications.

rAAV2/5 expressing GFP is not toxic to nigral dopaminergic neurons of the SNpc [Gombash *et al*, 2013]. Age-related reductions in total nigral dopaminergic neurons are not a factor in our present results as equivalent numbers of nigral THir neurons are present in the SD rat at 20 months as compared to 3 months of age. Although we achieved rAAV2/5-mediated GFP overexpression in the nigrostriatal system of both young adult and aged rats, aged rats consistently displayed lower levels of exogenous transgene expression than young adult rats. Aged rats exhibited approximately 40% fewer total GFPir cells throughout the midbrain. Our data suggests that both THir and non-THir neurons are transduced in the young adult and aged brain, and that a lack of transgene expression in dopaminergic cells is not the primary cause of the observed discrepancy as both age groups exhibit approximately equal percentages of THir neurons expressing GFP. Furthermore, the decrease in GFPir neurons in the aged brain does not appear to be related to differences in vector spread, because although the aged brain displayed fewer total numbers of GFPir neurons, the spread of transgene expression was observed in approximately the same number of sections through the rostral-caudal axis of the midbrain in both age groups and the rostral and caudal regions of transgene expression in the aged brain did not display significantly fewer GFPir neurons than the young adult brain. We observed decreases in GFP protein (western blot) in the aged rat striatum as well as the aged SN (immunohistochemistry), suggesting that the reduction in transgene expression in the aged striatum is a result of the deficient transgene expression in aged SN. These decreases in GFP protein expression were generalizable across different rat strains (SD and F344) and different expression durations (11 days to 3 months). Furthermore, we observed the most pronounced deficits in levels of GFP mRNA in the aged SN, demonstrating that the transduction deficiencies occur prior to translation and are not primarily the result of decreased protein synthesis with age [Ryazanov and Nefsky, 2002; Smith *et al*, 1995].

Although previous studies have shown successful gene transfer in the aged brain [Bartus *et al*, 2011; Emborg *et al*, 2009; Klein *et al*, 2010; Kordower *et al*, 2000; Wu *et al*, 2004], to our knowledge only two studies have previously conducted a direct comparison between the transduction efficiencies in young adult and aged animals [Klein *et al*, 2010; Wu *et al*, 2004]. Wu *et al*. (2004) found transduction deficiencies in the aged rat when using rAAV2/2 to overexpress either GFP or nerve growth factor (NGF) in septal neurons in aged F344/Brown Norway rats. A modest and non-significant decrease in the total number of transduced cells in the aged septum was reported as compared to young adult rats. Due to the lighter immunostaining and decreased NGF protein levels in the aged as compared to the young adult rat, this group concluded that age-related deficits in protein expression within individual cells drove the observed transduction deficits. Klein *et al*. (2010) compared transduction efficiency of rAAV2/9 GFP or human wild-type tau in the SN of young adult and aged SD rats and reported no deficiencies in the aged rat brain. However, the sole comparative measure of transduction efficiency in this study was a western blot to quantify GFP and normalization to a loading control protein was not reported [Klein *et al*, 2010]. In contrast, our results examining viral vector-mediated gene transfer utilizing numerous methodologies to evaluate vector-driven GFP protein and mRNA levels demonstrate that robust deficits in transgene expression that are associated with aging in the midbrain, and that specifically, rAAV2/5-mediated gene transfer results in decreases in both transgene mRNA and protein in aged as compared to young adult rats.

Due to the overlap between the steps of rAAV transduction [Schultz and Chamberlain, 2008] and the cellular processes affected by age [Gao *et al*, 2013; Lee *et al*, 2000; Ryazanov and Nefsky, 2002; Smith *et al*, 1995], it is reasonable to suggest that the aging brain environment alters the ability of rAAV2/5 to transduce neurons (Summarized in Figure 10). Specifically, in order to transduce a cell, rAAV2/5 must first bind to the N-linked sialic acid glycan receptor [Walters *et al*, 2001], platelet derived growth factor

receptor (PDGFR) co-receptor [Di Pasquale *et al*, 2003], and possibly other receptors on the cell surface to initiate clathrin-mediated endocytosis of the rAAV5 capsid (Figure 10, Step 1) [Meier and Greber, 2004]. Previous work has shown that N-linked sialic acid receptors are present in large quantities in the SN [Takahashi *et al*, 1995], and that these receptors are necessary for rAAV5 transduction whereby blocking these receptors will prevent rAAV5 from entering and transducing cells [Walters *et al*, 2001]. Furthermore, age has been shown to impact levels of N-linked sialic acid receptors in various brain regions, with decreases reported in the aged rat hippocampus [Sato *et al*, 2001] and cerebellum [Sasaki *et al*, 2002] as compared to the young adult rats. Therefore, it is plausible that decreases in N-linked sialic acid receptors also exist in the aged rat SN, causing a decrease in the number of vector capsids that can bind the cells to initiate endocytosis and, consequently, a decrease in overall transduction in the aged brain.

Endocytosis of rAAV2/5 then occurs through clathrin-coated pits (Figure 10, Step 2) [Meier and Greber, 2004], a process which is thought to be less efficient in aged neurons [Blanpied *et al*, 2003; Park *et al*, 2001]. After endocytosis the viral particle is trafficked through the cytoskeleton by dynamin in early, late, and recycling endosomes where it undergoes acidification to initiate capsid breakdown and genome release (Figure 10, Step 3) [Ding *et al*, 2005]. Cytoskeletal trafficking is highly energy-dependent, and decreased mitochondrial functioning with age [Kraytsberg *et al*, 2006; Bender *et al*, 2006] could decrease energy levels available for use in trafficking, leading to a buildup of viral particles in the cytoplasm that are unable to continue through the transduction process. Viral particles that are successfully trafficked then undergo golgi-mediated capsid processing (Figure 10, Step 4) [Bantel-Schall *et al*, 2002] and enter the nucleus purportedly through the nuclear pore complex (NPC) (Figure 10, Step 5) [Hansen *et al*, 2001]. Aging neurons have demonstrated compromised NPC function [D'Angelo *et al*, 2009] which could decrease the ability of rAAV2/5 to enter the nucleus. However, once in the nucleus,

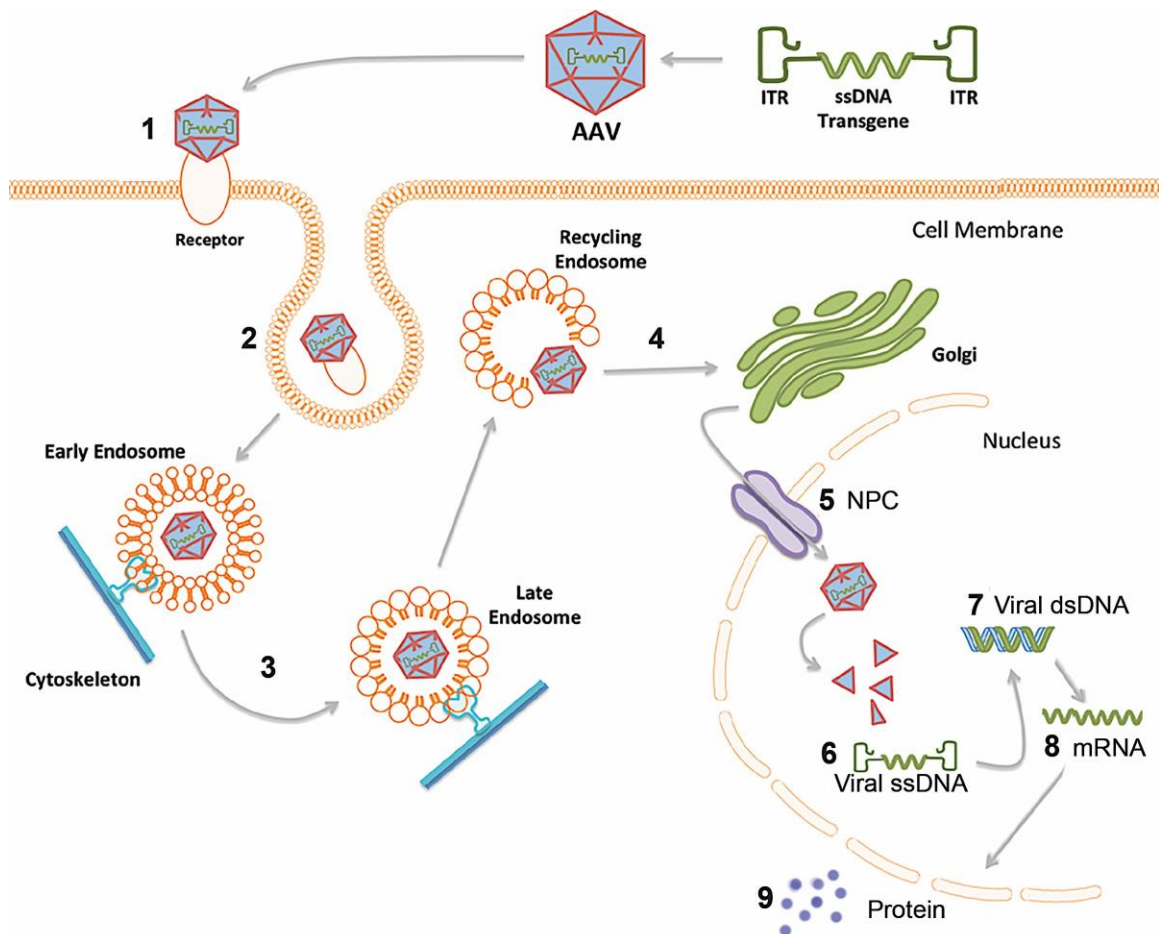


Figure 10. Steps of recombinant adeno-associated virus (rAAV) transduction and potential impact of the aged brain environment. In viral transduction a single stranded DNA (ssDNA) expression cassette of interest is flanked by inverted terminal repeats (ITRs) to make up the recombinant genome that is packaged into rAAV capsid. 1) Injected rAAV capsids bind to designated cell surface receptor and co-receptors; rAAV2/5 binds with high affinity to 2,3-linked sialic acid glycan receptor [Walters et al, 2001] and platelet derived growth factor receptor (PDGFR) co-receptor [Di Pasquale et al, 2003]. 2) Endocytosis of the viral particle occurs through clathrin coated pits or caveolar endocytosis; rAAV2/5 enters cell through clathrin-mediated endocytosis [Meier and Greber, 2004]. 3) The rAAV capsid is trafficked through the cytoskeleton by dynamin in early, late, and recycling endosomes where acidification processes within the endosomes initiate capsid breakdown and genome release [Ding et al, 2005]. 4) The viral particle is released from the endosome into the cytoplasm for golgi-mediated capsid processing [Bantel-Schall et al, 2002]. 5) The viral particle is internalized into the nucleus purportedly through the nuclear pore complex (NPC) [Hansen et al, 2001]. 6) The ssDNA genome is released from the viral capsid [Bartlett et al, 2000; Johnson and Samulski, 2009]. 7) Viral ssDNA is converted to double stranded DNA (dsDNA) either by strand annealing or by second strand synthesis. 8) Viral dsDNA is converted into mRNA encoded by the transgene. 9) Transgene mRNA is translated into the protein encoded by the transgene. Numbers represent steps where viral transduction could be impeded by age-related cellular deficiencies [Bender et al, 2006; Blanpied et al, 2003; D'Angelo et al, 2009; Gao et al, 2013; Kraytsberg et al, 2006; Park et al, 2001; Ryazanov and Nefsky, 2002; Sato et al, 2001; Sasaki et al, 2002; Smith et al, 1995]. In the present set of experiments we demonstrate that robust deficits in exogenous transgene expression are associated with aging and that deficiencies leading to 4-fold less mRNA encoded by the transgene are primarily responsible for the diminished protein expression observed in the aged rats.

the single stranded DNA (ssDNA) genome is released from the viral capsid (Figure 10, Step 6) [Bartlett *et al*, 2000; Johnson and Samulski, 2009] and is converted into double stranded DNA (dsDNA) by strand annealing or second strand synthesis (Figure 10, Step 7). As age increases the permeability of the NPC [D'Angelo *et al*, 2009], aged nuclei have an influx of large, obtrusive proteins that could interfere with virion uncoating or conversion of ssDNA to dsDNA.

Aging is also known to impact transcription levels in the rodent SN [Gao *et al*, 2013], which would lead to decreased levels of viral genome transcription into mRNA (Figure 10, Step 8). Thus, changes in transcription with age could potentially alter levels of other enzymes or proteins that are required for earlier stages of transduction, such as endocytosis or transport to the nucleus. This would hamper viral vector transduction before the level of transcription, reducing the levels of the viral transgene mRNA and, further downstream, the levels of viral protein produced (Figure 10, Step 9). Moreover, protein synthesis is known to be modestly decreased (17% lower) in the aged rat brain and the SN in particular [Ryazanov and Nefsky, 2002; Smith *et al*, 1995]. This could, in turn, affect viral vector transduction efficiency by decreasing the rate or amount of translation of the viral transgene into its protein products. We investigated this possibility by examining levels of protein expression of the viral transgene. While we did see a decrease in the viral protein product in the aged brain, the substantial (~50%) decrease that we observe cannot be completely accounted for by the previously reported modest decreases in SN protein synthesis with age [Smith *et al*, 1995]. Furthermore, examination of transgene mRNA levels support this conclusion by revealing a more marked, 4-fold, decrease in transgene mRNA expression in the aged as compared to the young adult rat brain. Future studies will be required to accurately pinpoint which step(s) of transduction are deficient in aged nigral neurons that result in reduced transgene mRNA.

Our results do not address whether the reduced transgene expression that we observe with rAAV2/5 in the aged rat midbrain can be generalized to other vector constructs, other brain regions, or other species. Additional experiments are required to make these determinations, determinations that will be critical to the success of clinical trials using gene therapy in neurodegenerative diseases of aging. In summary, there are no current therapies that can halt or alter disease progression in age-related neurodegenerative diseases, such as PD. If the promise of gene therapy to supply the nigrostriatal system with trophic factors is to be realized in a population of aged patients, characteristic of PD, clinical success will depend on adequate transgene transfer to the aged brain. It is possible that the diminished transgene expression in the aged midbrain will result in sufficient expression to provide the desired biological effect. Yet despite displaying remarkable efficacy in preclinical trials in young animal models of PD, clinical trials with rAAV2-neurturin have yielded disappointing results [Bartus *et al*, 2011; Marks *et al*, 2010]. Post-mortem analyses from human subjects that received rAAV2-neurturin indicated that transgene levels were remarkably low [Bartus *et al*, 2011]. Although a multitude of explanations have been put forth, we argue that age may contribute to this discrepancy between preclinical and clinical trials. Moreover, a gene therapy trial using rAAV to express glial cell line-derived neurotrophic factor (GDNF) is ongoing [ClinicalTrials.gov, 2013]. Aging-related deficits in exogenous transgene expression have the potential to impact these and other gene therapy trials in the future. Thus, future investigations examining transduction efficiency of various vector constructs and the mechanisms responsible for reductions in exogenous transgene expression in the aged brain are needed to identify approaches that will allow efficient transduction of the aged human brain.

LITERATURE CITED

LITERATURE CITED

- Alemán, C.L., R.M. Más, I. Rodeiro, M. Noa, C. Hernández, R. Menéndez, and R. Gámez. (1998). Reference database of the main physiological parameters in Sprague-Dawley rats from 6-32 months. *Lab Anim*, **32(4)**: 457-466.
- Bantel-Schall, U., B. Hub, and J. Kartenbeck. (2002). Endocytosis of adeno-associated virus type 5 leads to accumulation of virus particles in the Golgi compartment. *J Virol*, **76**: 2340-2349.
- Bartlett, J.S., R. Wilcher, and R.J. Samulski. (2000). Infectious entry pathway of adeno-associated virus and adeno-associated virus vectors. *J Virol*, **74**: 2777-2785.
- Bartus, R.T., C.D. Herzog, Y. Chu, A. Wilson, L. Brown, J. Siffert, E.M. Johnson Jr., C.W. Olanow, E.J. Mufson, and J.H. Kordower. (2011). Bioactivity of AAV2-neurturin gene therapy (CERE-120): differences between Parkinson's disease and nonhuman primate brains. *Mov Disord*, **28(1)**: 27-36.
- Bender, A., K.J. Krishnan, C.M. Morris, G.A. Taylor, A.K. Reeve, R.H. Perry, E. Jaros, J.S. Hersheson, J. Betts, T. Klopstock, R.W. Taylor, and D.M. Turnbull. (2006). High levels of mitochondrial DNA deletions in substantia nigra neurons in aging and Parkinson's disease. *Nat Genet*, **38(5)**: 515-517.
- Blanpied, T.A., D.B. Scott, and M.D. Ehlers. (2003). Age-related regulation of dendritic endocytosis associated with altered clathrin dynamics. *Neurobiol Aging*, **24(8)**: 1095-1104.
- Burger, C., O.S. Gorbatyuk, M.J. Velardo, C.S. Peden, P. Williams, S. Zolotukhin, P.J. Reier, R.J. Mandel, and M. Muzczka. (2004). Recombinant AAV viral vectors pseudotyped with viral capsids from serotypes 1,2, and 5 display differential efficacy and cell tropism after delivery to different regions of the central nervous system. *Mol Ther*, **10(2)**: 302-317.
- ClinicalTrials.gov. (2013). AAV2-GDNF for advanced Parkinson's disease. <http://www.clinicaltrials.gov/ct2/show/NCT01621581>
- Collier, T.J., C.E. Sortwell, and B.F. Daley. (1999). Diminished viability, growth, and behavioral efficacy of fetal dopamine neuron grafts in aging rats with long-term dopamine depletion: an argument for neurotrophic supplementation. *J Neurosci*, **19(13)**: 5563-5573.
- Collier, T.J., N.M. Kanaan, and J.H. Kordower. (2011). Ageing as a primary risk factor for Parkinson's disease: evidence from studies of non-human primates. *Nat Rev Neurosci*, **12(6)**: 359-366.
- D'Angelo, M.A., M. Raices, S.H. Panowski, and M.W. Hetzer. (2009). Age-dependent deterioration of nuclear pore complexes causes a loss of nuclear integrity in postmitotic cells. *Cell*, **136**: 284-295.
- Di Pasquale, G., B.L. Davidson, C.S. Stein, I. Martins, D. Scudiero, A. Monks, and J.A. Chiorini. (2003). Identification of PDGFR as a receptor for AAV-5 transduction. *Nat Med*, **9**: 1306-1312.

- Ding, W., L. Zhang, Z. Yan, and J.F. Engelhardt. (2005). Intracellular trafficking of adeno-associated viral vectors. *Gene Ther*, **12**: 873-880.
- Dorsey, E.R., R. Constantinescu, J.P. Thompson, K.M. Biglan, R.G. Holloway, K. Kieburtz, F.J. Marshall, B.M. Ravina, G. Schifitto, A. Siderowf, and C.M. Tanner. (2007). Projected number of people with Parkinson disease in the most populous nations, 2005 through 2030. *Neurology*, **68**: 384-386.
- Emborg, M.E., J. Miorano, J. Raschke, V. Bondarenko, R. Zufferey, S. Peng, A.D. Ebert, V. Joers, B. Roitberg, J.E. Holden, J. Koprach, J. Lipton, J.H. Kordower, and P. Aebischer. (2009). Response of aged parkinsonian monkeys to in vivo gene transfer of GDNF. *Neurobiol Dis*, **36(2)**: 303-311.
- Gao, J., H. Miao, C.H. Xiao, Y. Sun, X. Du, H.H. Yuan, H.L. Yu, and D.S. Gao. (2011). Influence of aging on the dopaminergic neurons in the substantia nigra pars compacta of rats. *Curr Aging Sci*, **4(1)**: 19-24.
- Gao, L., M. Hidalgo-Figueroa, L.M. Escudero, J. Diaz-Martin, J. Lopez-Barneo, and A. Pascual. (2013). Age-mediated transcriptomic changes in adult mouse substantia nigra. *PlosOne*, **8(4)**: e62456.
- Gash D.M., Z. Zhang, A. Ovadia, W.A. Cass, A. Yi, L. Simmerman, D. Russell, D. Martin, P.A. Lapchak, F. Collins, B.J. Hoffer, and G.A. Gerhardt. (1996). Functional recovery in parkinsonian monkeys treated with GDNF. *Nature*, **380**: 252-255.
- Gasmi M., E.P. Brandon, C.D. Herzog, A. Wilson, K.M. Bishop, E.K. Hofer, J.J. Cunningham, M.A. Printz, J.H. Kordower, and R.T. Bartus. (2007). AAV2-mediated delivery of human neurturin to the rat nigrostriatal system: Long-term efficacy and tolerability of CERE-120 for Parkinson's disease. *Neurobiol Dis*, **27**: 67-76.
- Gombash S.E., Manfredsson F.P., Mandel R.J., Collier T.J., Fischer D.L., Kemp C.J., N.M. Kuhn, S.L. Wohlgenant, S.M. Fleming, and C.E. Sortwell. (2014). Striatonigral pleiotrophin overexpression provides superior protection compared to overexpression in both striatonigral and nigrostriatal pathways. *Gene Ther*, **21(7)**: 682-693.
- Gombash, S.E., F.P. Manfredsson, C.J. Kemp, N.C. Kuhn, S.M. Fleming, A.E. Egan, L.M. Grant, M.R. Ciucci, J.P. MacKeigan, and C.E. Sortwell. (2013). Morphological and behavioral impact of AAV2/5-mediated overexpression of human wildtype alpha-synuclein in the rat nigrostriatal system. *PLoS One*, **8(11)**: e81426.
- Gombash, S.E., J.W. Lipton, T.J. Collier, L. Madhavan, K. Steece-Collier, A. Cole-Strauss, B.T. Terpstra, A.L. Spieles-Engemann, B.F. Daley, S.L. Wohlgenant, V.B. Thompson, F.P. Manfredsson, R.J. Mandel, and C.E. Sortwell. (2012). Striatal pleiotrophin overexpression provides functional and morphological neuroprotection in the 6-hydroxydopamine model. *Mol Ther*, **20(3)**: 544-554.
- Hansen, J., K. Qing, and A. Srivastava. (2001). Infection of purified nuclei by adeno-associated virus 2. *Mol Ther*, **4(4)**: 289-296.
- Herzog, C.D., L. Brown, D. Gammon, B. Kruegel, R. Lin, A. Wilson, A. Bolton, M. Printz, M. Gasmi, K.M. Bishop, K.H. Kordower, and R.T. Bartus. (2008). Expression, bioactivity, and safety 1 year after adeno-associated viral vector type 2-mediated delivery of neurturin to the monkey nigrostriatal system support CERE-120 for Parkinson's disease. *Neurosurgery*, **64(6)**: 602-613.

- Johnson, J., and R. Samulski. (2009). Enhancement of adeno-associated virus infection by mobilizing capsids into and out of the nucleolus. *J Virol*, **83**: 2632-2644.
- Klein, R.L., R.D. Dayton, C.G. Diaczynsky, and D.B. Wang. (2010). Pronounced microgliosis and neurodegeneration in aged rats after tau gene transfer. *Neurobiol Aging*, **31(12)**: 2091-2102.
- Kordower, J.H., M.E. Emborg, J. Bloch, S.Y. Ma, Y. Chu, L. Leventhal, J. McBride, E.Y. Chen, S. Palfi, B.Z. Roitberg, W.D. Brown, J.E. Holden, R. Pyzalski, M.D. Taylor, P. Carvey, Z. Ling, D. Trono, P. Hantraye, N. Déglon, and P. Aebischer. (2000). Neurodegeneration prevented by lentiviral vector delivery of GDNF in primate models of Parkinson's disease. *Science*, **290**: 767-773.
- Kraytsberg, Y., E. Kudryavtseva, A.C. McKee, C. Geula, N.W. Kowall, and N. Khrapko. (2006). Mitochondrial DNA deletions are abundant and cause functional impairment in aged human substantia nigra neurons. *Nat Genet*, **38(5)**: 518-520.
- Lee, C., R. Weindruch, and T.A. Prolla. (2000). Gene-expression profile of the ageing brain in mice. *Nat Genet*, **25**: 294-297.
- Marks Jr, W.J., R.T. Bartus, J. Siffert, C.S. Davis, A. Lozano, N. Boulis, J. Vitek, M. Stacy, D. Turner, L. Verhagen, R. Bakay, R. Watts, B. Guthrie, J. Jankovic, R. Sompson, M. Tagliati, R. Alterman, M. Stern, G. Baltuch, P.A. Starr, P.S. Larson, J.L. Ostrem, J. Nutt, K. Kieburtz, J.H. Kordower, and C.W. Olanow. (2010). Gene delivery of AAV2-neurturin for Parkinson's disease: a double-blind randomized, controlled trial. *Lancet*, **9**: 1164-1172.
- Meier, O., and U.F. Greber. (2004). Adenovirus endocytosis. *J Gene Med*, **6 (Suppl 1)**: S152-S163.
- Park, J., W. Park, K. Cho, D. Kim, B. Jhun, S. Kim, and S.C. Park. (2001). Down-regulation of amphiphysin-1 is responsible for reduced receptor-mediated endocytosis in the senescent cells. *FASEB J*, **15(9)**: 1625-1627.
- Pfaffl, M.W., G.W. Horgan, and L. Dempfle. (2002). Relative expression software tool (REST©) for group-wise comparison and statistical analysis of relative expression results in real-time PCR. *Nucleic Acids Research*, **30(9)**: e36.
- Piltonen, M., M.M. Beshpalov, D. Ervasti, T. Matilainen, Y.A. Sidorova, H. Rauvala, M. Saarma, and P.T. Mannisto. (2009). Heparin-binding determinants of GDNF reduce its tissue distribution but are beneficial for the protection of nigral dopaminergic neurons. *Exp Neurol*, **219(2)**: 499-506.
- Ryazanov, A.G., and B.S. Nefsky. (2002). Protein turnover plays a key role in aging. *Mec Ageing Dev*, **123**: 207-213.
- Sasaki, T., Y. Akimoto, Y. Sato, H. Kawakami, H. Hirano, and T. Endo. (2002). Distribution of sialoglycoconjugates in the rat cerebellum and its change with age. *J Histochem Cytochem*, **50(9)**: 1179-1186.
- Sato, Y., Y. Akimoto, H. Kawakami, H. Hirano, and T. Endo. (2001). Location of sialoglycoconjugates containing sia(alpha)2-3Gal and Sia(alpha)2-6Gal groups in the rat hippocampus and the effect of aging on their expression. *J Histochem Cytochem*, **49(10)**: 1311-1319.

- Schmittgen, T.D., and K.J. Livak. (2008). Analyzing real-time PCR data by the comparative C(T) method. *Nat Protoc*, **3**: 1101-1108.
- Schultz, B.R., and J.S. Chamberlain. (2008). Recombinant adeno-associated virus transduction and integration. *Mol Ther*, **16(7)**: 119-1199.
- Smith, C.B., Y. Sun, and L. Sokoloff. (1995). Effects of aging on regional rates of cerebral protein synthesis in the Sprague-Dawley rat: examination of the influence of recycling of amino acids derived from protein degradation into the precursor pool. *Neurochem*, **27(4/5)**: 407-416.
- Sortwell, C.E., M.D. Camargo, M.R. Pitzer, S. Gyawali, and T.J. Collier. (2001). Diminished survival of mesencephalic dopamine neurons grafted into aged hosts occurs during the immediate postgrafting interval. *Exp Neurol*, **169(1)**: 23-29.
- Stocchi, F., and C.W. Olanow. (2013). Obstacles to the development of a neuroprotective therapy for Parkinson's disease. *Mov Disord*, **28(1)**: 3-7.
- Takahashi, M., T. Yamada, S. Nakajima, T. Yamamoto, and H. Okada. (1995). The substantia nigra is a major target for neurovirulent influenza A virus. *J Exp Med*, **181(6)**: 2161-2169.
- Walters, R.W., S.M. Yi, S. Keshavjee, K.E. Brown, M.J. Welsh, J.A. Chiorini, and J. Zabner. (2001). Binding of adeno-associated virus type 5 to 2,3-linked sialic acid is required for gene transfer. *J Biol Chem*, **276**: 20610-20616.
- Wang, F., J. Flanagan, N. Su, L. Wang, S. Bui, A. Nielson, X. Wu, H.T. Vo, X.J. Ma, and Y. Luo. (2012). RNAscope: A novel in situ RNA platform for formalin-fixed, paraffin-embedded tissues. *J Mol Diagn*, **14(1)**: 22-29.
- Wu, K., C.A. Meyers, N.K. Guerra, M.A. King, and E.M. Meyer. (2004). The effects of rAAV2-mediated NGF gene delivery in adult and aged rats. *Mol Ther*, **9(2)**: 262-269.
- Zolotukhin, S., B.J. Byrne, E. Mason, E. Zolotukhin, M. Potter, K. Chesnut, C. Summerford, R.J. Samulski, and N. Muzyczka. (1999). Recombinant adeno-associated virus purification using novel methods improves infectious titer and yield. *Gene Ther*, **6**: 973-985.

Chapter 3: Impact of Age and Vector Construct on Striatal and Nigral Transduction Efficiency

Abstract

Therapeutic protein delivery using viral vectors has shown promise in preclinical models of Parkinson's disease (PD) but clinical trial success remains elusive. This may partially be due to a failure to include advanced age as a covariate despite aging being the primary risk factor for PD. We investigated the transduction efficiency of recombinant adeno-associated virus pseudotypes 2/2 (rAAV2/2), 2/5 (rAAV2/5), 2/9 (rAAV2/9), and lentivirus (LV) expressing green fluorescent protein (GFP) in aged versus young adult rats. Both rAAV2/2 and rAAV2/5 yielded lower GFP expression following injection to either the aged substantia nigra or striatum. However, for rAAV2/9 and LV, age-related transduction deficiencies were target structure-specific. rAAV2/9 was deficient in transducing the aged striatonigral system but displayed identical transduction efficiency in the aged vs. young nigrostriatal system. LV delivered GFP to the aged and young striatonigral system with equal efficiency; however, it was deficient in transducing the aged nigrostriatal system. Notably, age-related transduction deficiencies revealed by protein quantitation were poorly predicted by GFP-immunoreactive cell counts. Further, *in situ* hybridization for the viral C β A promoter revealed surprisingly limited tropism for astrocytes compared to neurons. Our results demonstrate that aging is a critical covariate to consider when designing gene therapy approaches for PD.

Introduction

Viral vectors are useful tools to deliver genes to the central nervous system (CNS), allowing stable expression of an exogenous protein, short hairpin RNA, or other genomic material. The benefits of viral vectors include site-specific expression, delivery of transgenes to dividing and non-dividing cells, stable transgene expression, and targeted tropism [O'Connor and Boulis, 2015; Choudhury *et al*, 2016]. These

benefits, along with an improved safety profile, have led to the use of viral vector-mediated gene therapy to treat diseases of the difficult-to-target CNS or to generate animal models of CNS disorders [Nobre and Almeida, 2011; Van der Perren *et al*, 2012; O'Connor and Boulis, 2015; Tuszynski *et al*, 2015; Choudhury *et al*, 2016; Combs *et al*, 2016; Fischer *et al*, 2016]. In particular, gene therapy is currently being explored in clinical trials for Alzheimer's disease (AD) [O'Connor and Boulis, 2015; Tuszynski *et al*, 2015] and Parkinson's disease (PD) [Marks *et al*, 2010; Bartus *et al*, 2011; O'Connor and Boulis, 2015; Olanow *et al*, 2015]—two diseases in which there are no disease-modifying treatments and symptomatic treatments only provide a moderate benefit [Cummings *et al*, 2013; Stochi and Olanow, 2013; Maguire *et al*, 2014]. Multiple clinical trials have completed Phase I safety testing for viral vector-mediated gene therapy in PD [Marks *et al*, 2010; Bartus *et al*, 2011; O'Connor and Boulis, 2015]. Unfortunately, the early Phase II efficacy trials have not shown improvement beyond the placebo effect or above levels currently achieved with symptomatic treatments [O'Connor and Boulis, 2015; Olanow *et al*, 2015]. While issues such as the enrollment of late-stage patients and limitations in the predictive validity of PD models likely impacted translation of gene therapy to the clinic, consideration should also be given to the fact that preclinical studies almost exclusively used young adult animals [Bjorklund *et al*, 2000; Kordower *et al*, 2000; Herzog *et al*, 2008; Emborg *et al*, 2009; Marks *et al*, 2010; Bartus *et al*, 2011; Palfi *et al*, 2014]. Age is the single greatest risk factor for developing PD and previous results demonstrate that age can dramatically influence therapeutic efficacy in PD models [Collier *et al*, 1999; Collier *et al*, 2015]. In the case of trophic factor gene therapy for PD, it is likely that transgene expression must reach a critical threshold in order to be therapeutically effective. Understanding the impact of age on viral vector transduction efficiency is required for the design of successful gene therapy for PD.

The two most common vector classes used for delivery of genes to the CNS are recombinant adeno-associated virus (rAAV) and lentivirus (LV) [O'Connor and Boulis, 2015; Nanou and Azzouz, 2009; Nobre

and Almeida, 2011; Combs *et al*, 2016; Fischer *et al*, 2016]. The transduction properties of these recombinant vector classes has been extensively characterized in the CNS of young adult animals, with both resulting in stable transduction that can last years after injection [Davidson *et al*, 2000; Reimsnider *et al*, 2007; Leone *et al*, 2012; O'Connor and Boulis, 2015; Choudhury *et al*, 2016]. Limited evidence suggests that the age of the transduced subject can negatively impact the efficiency of certain rAAV pseudotypes. For example, aged rat septal neurons have been shown to be relatively resistant to transduction mediated by rAAV2/2 [Wu *et al*, 2004]. Further, we have documented a robust deficiency in rAAV2/5-mediated transduction of the substantia nigra pars compacta (SNpc) in aged as compared to young adult rats [Fischer *et al*, 2016; Polinski *et al*, 2015]. Taken together, this limited evidence suggests certain vectors may not perform as efficiently in the aged brain.

To directly address this concern, the present study compared the transduction efficiency of three rAAV and one LV vector construct in the young adult (3 month) and aged (20 month) rat brain. The constructs chosen were rAAV2/2, rAAV2/5, rAAV2/9, and LV pseudotyped with vesicular stomatitis virus (VSV-G) due to previous reports of transduction changes [Wu *et al*, 2004; Polinski *et al*, 2015]—or lack thereof [Klein *et al*, 2010]—with age and relevance to PD preclinical and clinical trials [Bjorklund *et al*, 2000; Kordower *et al*, 2000; Wu *et al*, 2004; Herzog *et al*, 2008; Emborg *et al*, 2009; Klein *et al*, 2010; Marks *et al*, 2010; Bartus *et al*, 2011; Palfi *et al*, 2014; O'Connor and Boulis, 2015; Polinski *et al*, 2015]. The respective viral vectors, expressing a green fluorescent protein (GFP) transgene, were unilaterally injected into either the SNpc to transduce the nigrostriatal system or into the striatum to transduce the striatonigral system. The striatum is the structure most often targeted in PD gene therapy clinical trials [Marks *et al*, 2010; Bartus *et al*, 2011; Palfi *et al*, 2014; Clinicaltrials.gov, NCT01621581]. Transduction efficiency was determined by quantifying the number of GFP immunoreactive cells, GFP protein expression via Western blot of anterograde structures, as well as GFP mRNA expression via qPCR and *in*

situ hybridization. Since the ultimate goal of trophic factor gene therapy is protein delivery, we designated GFP expression levels obtained via Western blot of anterograde structures as the primary outcome measure. Using this criterion, our results show a significant deficiency in transduction of the aged *nigrostriatal* system using rAAV2/2, rAAV2/5, and LV, but not with rAAV2/9. In contrast, in the aged *striatonigral* system, rAAV2/2, rAAV2/5, and rAAV2/9 are deficient whereas LV is equally as efficient ages. Collectively, our results demonstrate that advanced age impacts the efficacy of viral vectors, with most—but not all—viral vectors impaired in the aged as compared to the young adult rat brain.

Methods

I. Experimental Overview

Cohorts of Fischer 344 (F344) rats, ten young adult (3 months old) and ten aged (20 months old) per cohort, were unilaterally injected with rAAV2/5, rAAV2/2, rAAV2/9, or VSV-G pseudotyped LV (LV) expressing GFP into the SNpc (nigrostriatal transduction) or into the striatum (striatonigral transduction) (Figure 11). All cohorts were sacrificed one month post-injection. In general, the anterograde structure of the system – striatum for nigrostriatal system and SN pars reticulata (SNpr) for striatonigral system – was used for Western blot analysis of GFP protein and the brain region containing the injected structure was used for immunohistochemical staining and *in situ* hybridization (or qPCR for rAAV2/2 and rAAV2/9 injections in the SNpc). Outliers were removed if they displayed a misplaced injection or met the criteria for exclusion through the ADAM outlier method [Leys *et al*, 2013] and were not included in any outcome measure in this study.

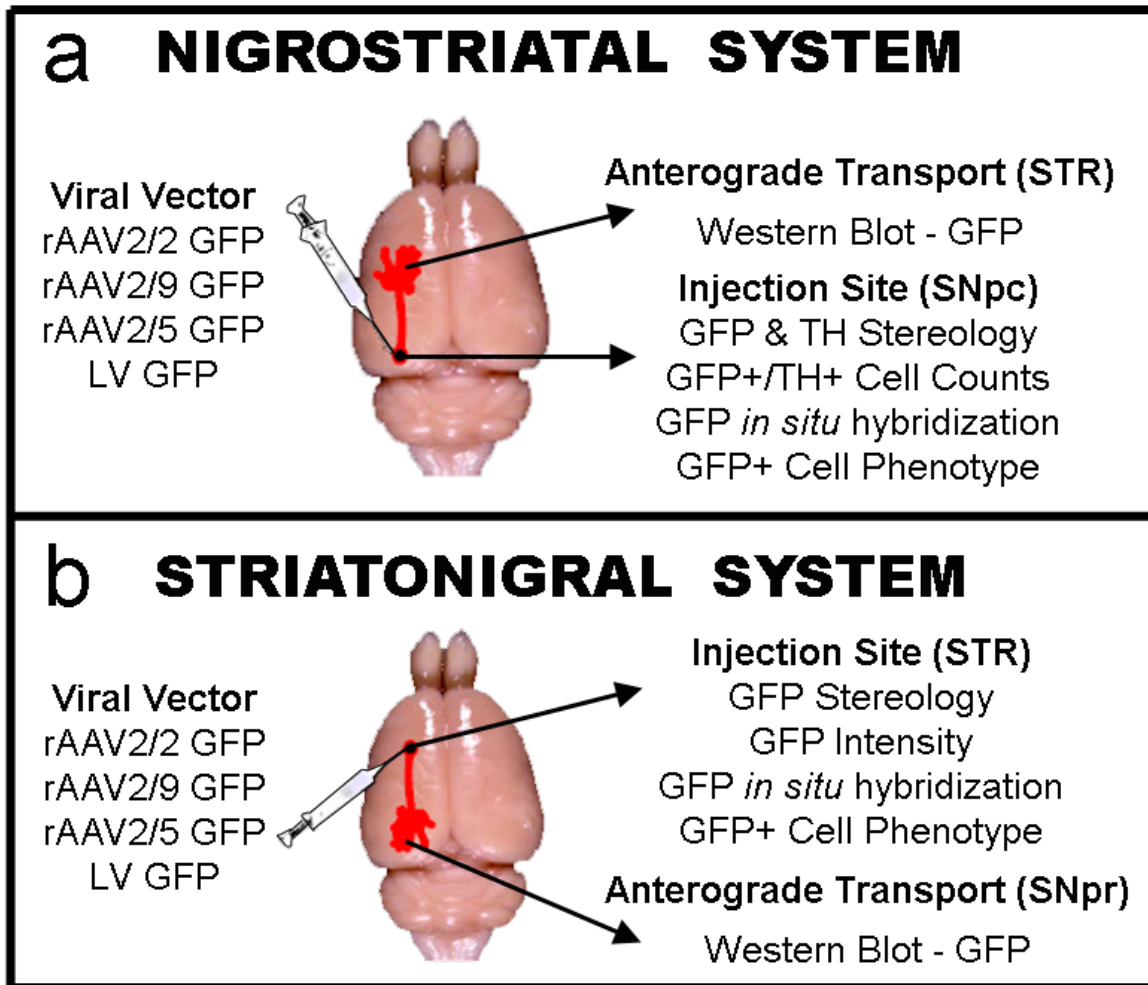


Figure 11. Schematic of experimental design for nigrostriatal and striatonigral rAAV2/2, rAAV2/5, rAAV2/9, or LV GFP transduction experiments. a) Overview of nigrostriatal system transduction analyses. Rats were injected in the substantia nigra pars compacta (SNpc) for transduction of the dopaminergic neurons projecting to the striatum. The anterograde striatal tissue was used for Western blot analyses of GFP, and the injection site tissue was used for histochemical or RNA analyses. b) Overview of striatonigral transduction analyses. Rats were injected in the striatum for transduction of the medium spiny neurons projecting to the SN pars reticulata (SNpr). The anterograde nigral tissue was used for Western blot analyses of GFP, and the injection site tissue was used for histochemical or RNA analyses. Abbreviations: GFP, green fluorescent protein; rAAV, recombinant adeno-associated virus; LV, lentivirus.

II. Animals

Male, Fischer344 rats (National Institute on Aging, Bethesda, MD) 3 months of age (n = 98) and 20 months of age (n = 102) were used in this study. All animals were given food and water *ad libitum* and housed in 12h reverse light-dark cycle conditions in the Van Andel Research Institute vivarium, which is fully AAALAC approved. All procedures were conducted in accordance with guidelines set by the Institutional Animal Care and Use Committee (IACUC) of Michigan State University.

III. Viral Vectors

All rAAV viral vector constructs were purchased from the University of Florida Powell Gene Therapy Center Vector Core (University of Florida, Gainesville, FL). Plasmid and vector production were completed as previously described [Zolotukhin *et al*, 1999; Benskey and Manfredsson, 2016a; Benskey and Manfredsson, 2016b]. For all vectors, expression of the transgene was driven by the chicken beta actin/cytomegalovirus enhancer (C β A/CMV) promoter hybrid. For rAAV production, humanized GFP was inserted into an AAV plasmid backbone containing AAV2 inverted terminal repeats and was packaged into AAV5, AAV2, or AAV9 capsids via co-transfection with a plasmid containing *rep* and *cap* genes and adenovirus helper functions. Particles were purified using iodixanol gradients followed by column chromatography, and dotblot was used to determine vector titer [Benskey *et al*, 2016]. For LV production, the same GFP expression cassette was inserted into an LV transfer vector and triple transfections were performed into HEK-293 cells with the LV transfer vector and LV helper plasmids and LV was purified from cellular media by ultracentrifugation [Benskey *et al*, 2016a]. The vector titers used in this study were the following: rAAV2/2 GFP at 1.9×10^{12} vector genomes (vg)/mL, rAAV2/5 GFP at either 1.2×10^{12} vg/mL or 2.0×10^{12} vg/mL, rAAV2/9 GFP at 2.0×10^{12} vg/mL, LV in the striatum at 2.0×10^7 vg/mL, and LV in the SNpc at 5.0×10^7 vg/mL. All surfaces (syringes, pipettes, and microcentrifuge

tubes) were coated in SigmaCote (Sigma-Aldrich, St. Louis, MO) prior to coming in contact with the virus to minimize binding of viral particles [Benskey and Manfredsson, 2016b].

IV. Viral Vector Injections

All surgical procedures were performed under isoflurane anesthesia (5% in O₂ for induction and 2% in O₂ for maintenance). Rats were placed in a stereotaxic frame and a Hamilton syringe fitted with a glass capillary needle (Hamilton Gas Tight syringe 80,000, 26s/2" needle; Hamilton, Reno, NV; coated in SigmaCote) was used for injections. For intranigral injections of GFP-expressing viruses, two 2 μ L injections were injected in the left SNpc at coordinates (from dura) AP -5.3mm, ML +2.0mm, DV -7.2mm, and AP -6.0mm, ML +2.0mm, and DV -7.2mm as previously described [Polinski *et al*, 2015]. For intrastriatal injections of GFP-expressing viruses, one 2 μ L injection was injected in the left striatum at coordinates (from dura) AP +0.0mm, ML +2.7mm, DV -4.0mm in the young adult and adjusted to AP +0.0mm, ML +3.0mm, DV -4.0mm in the aged rat [Gombash *et al*, 2012]. The glass needle was lowered to the site and vector injection began immediately at a rate of 0.5 μ l/minute and remained in place after the injection for an additional 5 minutes before retraction.

V. Euthanasia and Tissue Preparation

All rats were sacrificed one month post-injection. Rats were deeply anesthetized (60mg/kg, pentobarbital, i.p.) and perfused intracardially with 0.9% saline containing 1ml/10,000 USP heparin, followed by ice cold 0.9% saline. Rat brains were immediately removed and hemisected in the coronal plane at approximately AP -2.64mm. In rats that were injected in the SNpc, rostral tissue was processed for microdissections and caudal tissue was processed for immunohistochemistry. In rats that were injected in the striatum with GFP-expressing viral vectors, rostral tissue was processed for immunohistochemistry, and caudal tissue was processed for microdissections.

VI. Microdissections

After brain removal, portions of the brains designated for microdissection were chilled in ice-cold saline for 2 min and immediately microdissected (striatal tissue) or flash frozen in 2-methylbutane on dry ice and stored at -80°C (nigral tissue).

i. Striatal Tissue for Protein Analyses (SN-Injected GFP Vectors)

Following 2 min incubation in ice-cold saline to firm and chill the tissue, 2mm coronal slabs were blocked from each brain utilizing an aluminum brain blocker (Zivic, Pittsburg, PA). Striatal tissue from both hemispheres was microdissected with a 2mm tissue punch on a petri dish over ice. Frozen dissected structures were placed in pre-chilled microcentrifuge tubes and stored at -80°C.

ii. SNpc Tissue for RNA Analyses (SN-Injected rAAV2/2 GFP and rAAV2/9 GFP)

All surfaces and instruments were cleaned with RNase Away (Invitrogen, Carlsbad, CA) when collecting tissue for RNA analyses. Brains were warmed from -80°C to -15°C for 1 hour before use. Brains were mounted onto metal chucks with Tissue-Tek O.C.T. (VWR, Vatavia, IL) before being moved to a -20°C cryostat for sectioning. Tissue was sectioned until the SNpc became visible. Punches were taken from the rostral face of the brain structures once the structure was definitively apparent to ensure precision. A 2mm x 1mm oval punch of tissue was taken of the SNpc for GFP RNA analyses using a custom punch. Tissue punches were placed in separate pre-frozen RNase-free microcentrifuge tubes containing TRIzol Reagent (Invitrogen, Grand Island, NY) and tissue was homogenized with a pestle before storage. Samples were stored at -80°C until time of assay.

iii. SNpr Tissue for Protein Analyses (STR-Injected GFP Vectors)

Brains were transferred from -80°C to -20°C before microdissections. Brains were mounted on metal chucks with Tissue-Tek O.C.T. (VWR, Vatavia, IL) before being mounted in the cryostat at -15°C. Tissue was sectioned until the level of the SNpr and punches were taken from the rostral face of the brain structures once the structure was definitively apparent to ensure precision. A 2mm x 1mm oval punch was taken of the SNpr using a custom tissue punch. Tissue punches were placed in separate pre-frozen microcentrifuge tubes and stored at -80°C until time of analysis. Precision of the punch was verified by placement of the punch and subsequent sectioning and immunostaining for tyrosine hydroxylase (Figure 12).

VII. Western Blot

Striatal samples for western blot analyses were homogenized on ice in RIPA Lysis Buffer System (Santa Cruz, Dallas, TX) and SNpr samples for western blot analyses were homogenized on ice in 2% SDS. Total protein concentration was determined by the Bradford protein assay. Samples were prepared at 30ng total protein samples. Western blot protocol was completed as previously described [Polinski *et al*, 2015]. Samples were electrophoresed using SDS-PAGE gels and transferred to Immobilon-FL membranes (Millipore, Bedford, MA). Membranes were incubated in primary GFP antisera (Abcam, Cambridge, MA; rabbit polyclonal IgG, Ab290, 1:1,000) with β -tubulin antisera (Cell Signaling, Danvers, MA; mouse monoclonal IgG, 4466, 1:1,000) overnight. IRDye800 conjugated goat anti-rabbit (LI-COR Biosciences; 926-32211, 1:15,000) and IRDye680 conjugated goat anti-mouse (LI-COR Biosciences, 926-68020, 1:15,000) were used as secondary antibodies. All antibody dilutions were made in LI-COR compatible StartingBlock™ T20 (TBS) Blocking Buffer (Thermo Scientific, Waltham, MA). Multiplexed signal intensities were imaged with both 700 and 800 nm channels in a single scan with a resolution of 169 μ m using the Odyssey infrared image system (LI-COR Biosciences). Reported integrated intensity

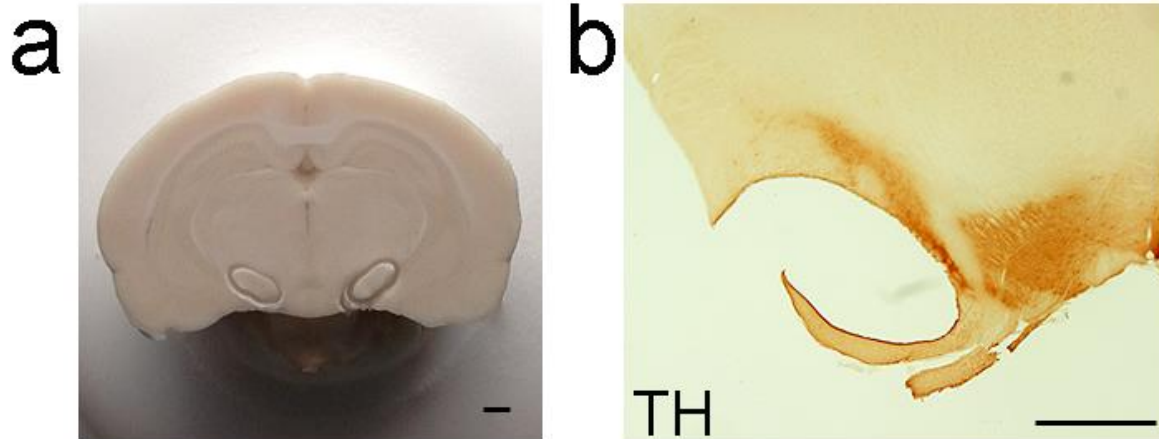


Figure 12. Validation of SNpr tissue punch for analysis of anterograde transport in the striatonigral system. a) Representative image of substantia nigra pars reticulata (SNpr) punch location in the intact midbrain. Scale bars = 1000 μ m. b) Representative image of the SNpr punch location in a section of midbrain stained for TH immunoreactivity to identify the SN pars compacta (SNpc). Scale bars = 1000 μ m. SNpr punches selectively collect the SNpr tissue, avoiding the adjacent SNpc that may express GFP through retrograde transport from the striatum through the nigrostriatal system. Abbreviations: GFP, green fluorescent protein; TH, tyrosine hydroxylase.

measurements of GFP expression were normalized according to the corresponding β -tubulin densitometry measurements as β -tubulin protein levels do not change with age [O'Callaghan and Miller, 1991]. The representative image was produced in Photoshop 7.0 (San Jose, CA).

VIII. Immunohistochemistry

The portion of the brains designated for immunohistochemistry were post-fixed in 4% paraformaldehyde (Electron Microscopy Sciences, Hatfield, PA) in 0.1M PO_4 buffer for seven days. After this period they were transferred to 30% sucrose in 0.1M PO_4 buffer until saturated. Brains were frozen on dry ice and tissue was collected as a 1 in 6 series in a 24 well plate. The first 5 sections were taken at a 40 μm thickness with the remaining well housing 2 sections taken at a 20 μm thickness using a sliding microtome. Every sixth section was processed for immunohistochemistry using the free-floating method (or every twelfth section in the case of glial immunohistochemistry).

i. Immunohistochemistry

Tissue sections were rinsed in Tris buffer and quenched in 0.3% H_2O_2 for 15 minutes, blocked in 10% normal goat serum for 1 hour, and incubated in primary antisera (TH: Millipore MAB318, mouse anti-TH, 1:4000; GFP: Abcam Ab290, rabbit anti-GFP, 1:100,000) overnight at 4°C. Following primary incubation, TH-labeled sections were incubated in biotinylated secondary antisera against mouse IgG (Vector BA-2001, biotinylated horse anti-mouse IgG, rat absorbed, 1:1000) and GFP-labeled sections were incubated in biotinylated secondary antisera against rabbit IgG (Millipore AP132b, goat anti-rabbit IgG, 1:500) for 2 hours at room temperature, followed by Vector ABC detection kit using horseradish peroxidase (Vector Laboratories, Burlingame, CA). Antibody labeling was visualized by exposure to 0.5mg/ml 3,3' diaminobenzidine and 0.03% H_2O_2 in Tris buffer. Sections were mounted on subbed slides, dehydrated via ascending ethanol washes, cleared with xylene, and coverslipped with Cytoseal.

Images were taken on a Nikon Eclipse 90i microscope with a QICAM camera (QImaging, Surrey, British Columbia, Canada). Figures were produced in Photoshop 7.0 (San Jose, CA), with brightness, saturation, and sharpness adjusted only as needed to best replicate the immunostaining as viewed directly under the microscope.

ii. TH and GFP Double Label Immunofluorescence

Sections were blocked in 10% normal donkey serum for 1 hour and subsequently transferred to the primary antisera (TH: Millipore Ab318, mouse anti-TH, 1:4000) to incubate overnight at 4°C. Following primary incubation, tissue was incubated in the dark in secondary antisera against mouse IgG (Invitrogen A10037, Alexa Fluor 568 donkey anti-mouse, 1:500) for 1 hour at room temperature. Tissue was then blocked in 10% normal goat serum for 1 hour at room temperature before being incubated in the primary antisera against GFP (Abcam Ab290, rabbit anti-GFP, 1:100,000) overnight at 4°C in the dark. Following primary incubation, tissue was incubated in secondary antisera against rabbit IgG (Life Technologies A21206, Alex Fluor 488 goat anti-rabbit IgG, 1:500) for 1 hour at room temperature. Sections were mounted on subbed slides and coverslipped with Vectashield Hardset Mounting Medium (Vector Laboratories, Burlingame, CA). Images were taken on a Nikon 90i fluorescence microscope with a Nikon DS-Ri1 camera. Figures were produced in Photoshop 7.0 (San Jose, CA). Brightness, saturation, and sharpness were adjusted only as necessary to best replicate the immunostaining as viewed directly under the microscope.

iii. TH and GFP Double Label Near-Infrared Staining

Sections were blocked in StartingBlock™ T20 (TBS) Blocking Buffer (Thermo Scientific, Waltham, MA) for 1 hour and subsequently transferred to the primary antisera (TH: Millipore Ab318, mouse anti-TH, 1:4000) to incubate overnight at 4°C. Following primary incubation, tissue was incubated in the dark in

secondary antisera against mouse IgG (LI-COR 926-32212, donkey anti-mouse IRDye® 800CW, 1:500) for 1 hour at room temperature. Tissue was then blocked in StartingBlock™ T20 (TBS) Blocking Buffer (Thermo Scientific) for 1 hour at room temperature before being incubated in the primary antisera against GFP (Abcam Ab290, rabbit anti-GFP, 1:100,000) overnight at 4°C in the dark. Following primary incubation, tissue was incubated in secondary antisera against rabbit IgG (LI-COR 925-68021, goat anti-rabbit IRDye® 680LT, 1:500) for 1 hour at room temperature. Sections were mounted on subbed slides, dehydrated via ascending ethanol washes, cleared with xylene, and coverslipped with Cytoseal. Multiplexed signal intensities were imaged with both 700 and 800 nm channels in a single scan with a resolution of 42µm and depth set to 1.0mm using the Odyssey infrared image system (LI-COR Biosciences, Lincoln, NE).

iv. GFP/NeuN/Glia Immunofluorescence

A one in twelve series of sections were blocked in 10% normal donkey serum for 1 hour and subsequently transferred to the primary antisera (NeuN: Millipore Ab377, mouse anti-NeuN 1:1000) to incubate overnight at 4°C. Following primary incubation, tissue was incubated in the dark in secondary antisera against mouse IgG (Invitrogen A10037, Alexa Fluor 568 donkey anti-mouse, 1:500) for 1 hour at room temperature. Tissue was then blocked in 10% normal goat serum for 1 hour at room temperature before being incubated in the primary antisera against GFAP (Abcam AB7260, rabbit anti-GFAP, 1:10,000) or Iba-1 (Wako 019-19741, rabbit anti-Iba-1, 1:1,000) overnight at 4°C in the dark. Following primary incubation, tissue was incubated in secondary antisera against rabbit IgG (LI-COR 925-68021, goat anti-rabbit IRDye® 680LT, 1:500) for 1 hour at room temperature. Sections were mounted on subbed slides and coverslipped with Vectashield Hardset Mounting Medium (Vector Laboratories, Burlingame, CA). Images were taken on a Nikon 90i fluorescence microscope with a Nikon DS-Ri1 camera. Figures were produced in Photoshop 7.0 (San Jose, CA). Brightness, saturation, and sharpness

were adjusted only as necessary to best replicate the immunostaining as viewed directly under the microscope.

IX. RNA Isolation and cDNA Synthesis

RNA was isolated using the QIAshredder (Qiagen, Valencia, CA) and RNeasy Plus Mini kit (Qiagen, Valencia, CA). The Quiagen protocol for purification of total RNA from animal tissue was used. RNA from tissue was then converted into cDNA using SuperScript VILO Master Mix (Life Technologies, Grand Island, NY). The RNA was assumed to be converted 100% to cDNA.

X. GFP qPCR

GFP qPCR reactions were carried out with 1x TaqMan Universal Mastermix (ABI, Carlsbad, CA), and a customized TaqMan gene expression assay kit for GFP (ABI, Carlsbad, CA). This kit includes 6,000 pmoles of the TaqMan MGB-fluorescent probe and 10,000 pmoles of each manufactured primer. Forward (R) and reverse (L) primers, as well as the probe (P) sequence were synthesized by ABI. The sequences were as follows: R: AGACCATATGAAGCAGCATGACTTTT, L: GTCTTG TAGTCCCGTCATCTTTGA, P: 5'6FAM CTCCTGCACATAGCCC MGBNFQ. A total of 20ng of cDNA was added to each 50 μ l reaction mixture which also contained 150nM forward and 150nM reverse primers, a 150nM probe sequence, and TaqMan master mix. qPCR reactions to control for cDNA quantities were run using GAPDH (Life Technologies 4352338E, Grand Island, NY) as an endogenous control that is not altered with advanced age in F344 rats. The qPCR reactions were run on an ABI 7500 real-time thermocycler using the following setup: Step1: Incubation at 50°C for 2 minutes. Step 2: Incubation at 95°C for 10 minutes. Step 3: Denaturation at 95°C for 15 seconds followed by annealing-elongation at 60°C for 1 minute followed by data collection. Step 3 was cycled 40 times for the qPCR run. Cycle thresholds were chosen during the linear phase of amplification using the AutoC_T function. All samples were run on the same plate along with a

no-template control. Analysis was first carried out using the $2^{-\Delta CT}$ method [Schmittengen and Livak, 2008] and Relative Expression Software Tool (REST-XL) method [Pfaffl *et al*, 2002].

XI. RNAscope *in situ* Hybridization for GFP or C β A mRNA

Young adult and aged rats from all eight vector cohorts (rAAV2/2, rAAV2/5, rAAV2/9, and LV injected in the SNpc or striatum) were used for RNAscope for GFP mRNA. Young adult and aged rats from all striatal injection cohorts (rAAV2/2, rAAV2/5, rAAV2/9, and LV injected in the striatum) were used for RNAscope for the viral particle C β A promoter. 20 μ m thick tissue sections at the level of the SNpc (nigral injections) or striatum (striatal injections) were incubated in Pretreat 1 from the RNAscope Pretreatment Kit (Advanced Cell Diagnostics, Hayward, CA; 310020) for 1 hour. Sections were washed in TBS and then mounted on Gold Seal Ultrastick slides (VWR, Randor, PA; 3039) and left at room temperature overnight. Slides were then incubated for 7 minutes in Pretreat 2 at 99°C and left to air dry 10 min. After Pretreat 2, slides were dipped in water, dried, dipped in 100% ethanol, dried, and then incubated with Pretreat 3 in a hybridization oven at 40°C for 15 min. Slides were dried and the VS Probe for GFP (Advanced Cell Diagnostics, Hayward, CA; 409016) or a custom VS Probe for C β A was added for a 2 hour incubation in the hybridization oven. Six amplification steps with the amplification buffers (Advanced Cell Diagnostics, Hayward, CA; 320600) were then performed in alternating 30 and 15 minute incubation intervals in the hybridization oven, as per kit instructions. Tissue was developed using the supplied DAB reagent (Advanced Cell Diagnostics, Hayward, CA; 320600). C β A RNAscope tissue was then counterstained for S100B (Abcam AB52642, rabbit anti-S100B, 1:1000) or NeuN (Millipore MAB377, mouse anti-NeuN, 1:500) following the same procedures as detailed for the other immunohistochemical stains with the exception that the Vector SG reagent (Vector Laboratories, Burlingame, CA) was used as the chromagen. Slides were rinsed and coverslipped with Cytoseal. Images were taken on a Nikon Eclipse 90i microscope with a QICAM camera (QImaging, Surrey, British Columbia, Canada). Figures were

produced in Photoshop 7.0 (San Jose, CA), with brightness, saturation, and sharpness adjusted only as needed to best replicate the mRNA labeling as viewed directly under the microscope.

XII. Stereology

Quantification of the number of GFP immunoreactive (GFPir) cells in the midbrain (nigral injected rats), GFPir cells in the striatum (striatal injected rats), and TH immunoreactive (THir) neurons in the SNpc (nigral injected rats) was completed as previously described [Polinski *et al*, 2015]. Briefly, stereology was performed using a Nikon Eclipse 80i microscope (Nikon), StereoInvestigator software (Microbrightfield Bioscience, Williston, VT) and Retiga 4000R camera (Qimaging, Surrey, BC Canada). Using the optical fractionator probe, THir neurons in the vector injected and control hemisphere in every sixth section of the entire SN were counted at 60x magnification. GFPir cells were counted at 60x magnification in the injected hemisphere in every sixth section of the brain where GFP staining was visible. All boundaries were drawn at 1x magnification and a 50x50 counting frame was used. A Gunderson coefficient of error <0.10 was accepted. THir data are reported as total estimates of THir neurons in each hemisphere. GFPir data are reported as percent of young estimates in the analyzed hemispheres.

XIII. Counts of GFP and TH Immunoreactive Cells

Tiled images at 10x magnification were taken on GFP and TH immunofluorescently stained midbrain sections containing the SNpc (average of 8 sections/rat) of four rats per age per cohort injected in the SNpc with GFP-expressing viral vectors. The rats chosen represented the median GFP+ cell counts at the injection site and GFP protein in the anterograde structure. Images were taken with a Nikon 90i fluorescence microscope with a Nikon DS-Ri1 with the exposure constant between images. All GFPir cells that were in focus with a clear nucleus and appeared to be counterstained with TH were manually counted to determine the total number of GFPir/THir cells in the SNpc. Total numbers of GFPir/THir cells

for rat were calculated. Data is represented as the percent of the young mean GFPir/THir cells in the SNpc.

XIV. Counts of GFP/NeuN, GFP/GFAP, and GFP/Iba-1 Immunoreactive Cells

Tiled images at 10x magnification were taken on the 1:12 series of GFP/NeuN/GFAP and GFP/NeuN/Iba-1 immunofluorescently stained midbrain or striatal sections of three rats per age per cohort injected in the SNpc with GFP-expressing viral vectors or injected in the striatum with GFP-expressing viral vectors, respectively. The rats chosen represented the median GFP+ cell counts at the injection site and GFP protein in the anterograde structure. Images were taken with a Nikon 90i fluorescence microscope with a Nikon DS-Ri1 with the exposure constant between images. All GFPir cells that were in focus with a clear nucleus and appeared to be counterstained with NeuN, GFAP, or Iba-1 were manually counted to determine the total number of GFPir/NeuNir, GFPir/GFAPir, and GFPir/Iba-1ir cells. Total numbers of these categories of cells were collected for each rat and then represented as the percent of GFPir cells that were NeuNir, GFAPir, or Iba-1ir.

XV. Near-Infrared Signal Intensity and Striatal Transduction Area Measurements

Scans were obtained of the 1:6 series of tissue stained with the LI-COR near-infrared secondary antibodies and used to determine GFP signal intensity and the area of GFP expression. For GFP signal intensity, boundaries were drawn around the entire striatum using the 800nm channel (TH) and outlined freehand using the LI-COR Image Studio 3.1 software to obtain an average signal strength. Reported integrated intensity measurements of GFP expression were collected using the 700nm channel and were normalized to background levels obtained in the right hemisphere striatum on the first section per brain. Data were represented as the mean striatal GFP integrated intensity measurement per brain. For GFP transduction area, boundaries were drawn directly around the area of GFP expression using the 700nm

channel (GFP) and outlined freehand using the LI-COR Image Studio 3.1 software. The individual drawing the boundaries around the transduction area was blinded to the age of the brains. The representative image was produced in Photoshop 7.0 (San Jose, CA).

XVI. Comparisons Between Vectors

For comparisons between vector cohorts in Figure 23 and Figure 24, Western blots were rerun to include striatal or SNpr samples on one blot to reduce variability. Due to space constraints, only the samples with median GFP protein amounts from the original western blots were run for each group. In addition, only rAAV2/5-injected rats at the 2.0×10^{12} genomes/mL were used to normalize titer between rAAV psueodtypes for all comparisons between vectors. All data are presented as the raw numbers that were reported as percent of young in earlier figures.

XVII. Statistical Analyses

All statistical tests were completed using IBM SPSS statistics software (version 22.0, IBM, Armonk, NY). Graphs were created using GraphPad Prism software (version 6, GraphPad, La Jolla, CA). To compare young adult vs. aged rats injected in the same structure with the identical vector construct independent samples t-tests were used. Due to variance in the dataset, Levene's Test for Equality of Variance was performed and *p*-values were reported based on the passing or failing of the homogeneity of variance test. Results of THir SNpc neuron quantification were analyzed with two-way repeated measures ANOVA with two treatment factors, age and hemisphere. When appropriate, Bonferroni *post hoc* analyses were used on ANOVA tests to determine significance between individual groups. For the qPCR gene expression study, fold changes for the GFP gene were normalized to the GAPDH gene expression and calculated before being subjected to t-test analysis using the REST-XL [Pfaffl *et al*, 2002]. For comparisons between vectors in Figures 6 and 7, a two-way ANOVA was run with Bonferroni *post hoc*

tests to determine significance between individual groups using the harmonic mean of the group sizes to account for unequal sample sizes.

Results

Previous reports have found transduction deficiencies in the aged rat following injection of rAAV2/2 in the septum, rAAV2/5 in the SN, but not with rAAV2/9 in the SN [Wu *et al*, 2004; Klein *et al*, 2010; Polinski *et al*, 2015]. However, systematic comparison of the impact of age and brain region on viral vector transduction efficiency is lacking. In order to validate and expand previous findings, we sought to investigate the generalizability of this age-related deficiency in various vector constructs and an additional brain structure by systematically characterizing the changes in transduction efficiency with age. To accomplish this, we injected rAAV2/2, rAAV2/5, rAAV2/9, or LV expressing GFP driven by the chicken beta actin/cytomegalovirus enhancer (C β A/CMV) promoter hybrid into the SNpc to target the nigrostriatal system, or into the striatum to target the striatonigral system (Figure 11). At one month post-injection, when transgene expression levels asymptote [Reimsnider *et al*, 2007], we assessed transduction efficiency at the injection site with immunohistochemical or RNA measures, as well as overall transduction efficiency in the anterograde structure (striatum following SNpc injection, or SN pars reticulata (SNpr) following striatal injection) using Western blotting for GFP to measure system-specific transduction. To preclude signal resulting from retrograde transport of the viral vectors, special care was taken with SNpr samples to avoid inclusion of SNpc tissue in the microdissection (Figure 12). In addition, to ensure any changes in GFP expression with age were not due to age-related neuronal loss or vector-related toxicity, we quantified the numbers of tyrosine hydroxylase immunoreactive (TH+) neurons in the SNpc of young adult and aged rats. No significant difference was found for either age or vector injection for rAAV2/2 GFP (age: $F_{(1,5)}=2.90$, $p=0.149$; injection: $F_{(1,5)}=0.421$, $p=0.545$; Figure 13a), rAAV2/9 GFP (age: $F_{(1,12)}=0.029$, $p=0.868$; injection: $F_{(1,12)}=1.98$, $p=0.185$; Figure 13b), rAAV2/5 GFP (age:

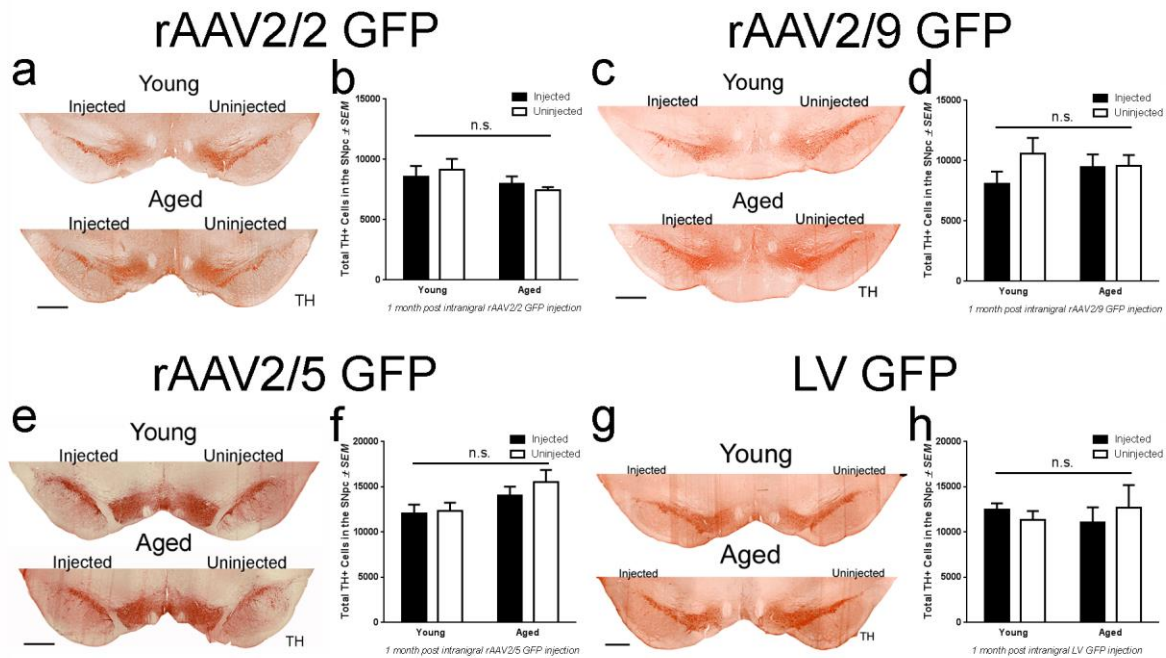


Figure 13. No age- or vector-related toxicity is observed in the SNpc following injection of rAAV2/2, rAAV2/5, rAAV2/9, or LV. (a,c,e,g) Representative images of tyrosine hydroxylase (TH) immunoreactivity in the substantia nigra pars compacta (SNpc) in the injected and uninjected hemispheres of young adult (Young) and aged (Aged) rats. Scale bars = 1000µm. (b,d,f,h) Quantitation of TH+ cells in the SNpc in the injected and uninjected hemispheres of young adult and aged rats following b) rAAV2/2, d) rAAV2/9, f) rAAV2/5, and h) LV GFP injection. No statistical differences ($p > 0.05$) were observed in the number of TH+ cells between hemispheres or ages. Values are expressed as the total number of TH+ cells in the SNpc \pm SEM for each group. Abbreviations: GFP, green fluorescent protein; rAAV, recombinant adeno-associated virus; LV, lentivirus; TH, tyrosine hydroxylase; SEM, standard error of the mean.

$F_{(1,11)}=4.63$, $p=0.054$; injection: $F_{(1,11)}=0.63$, $p=0.444$; Figure 13c), or LV GFP (age: $F_{(1,7)}=0.05$, $p=0.833$; injection: $F_{(1,7)}=0.81$, $p=0.398$; Figure 13d), as has been reported previously [Gao *et al*, 2011; Polinski *et al*, 2015].

I. Transduction efficiency in the nigrostriatal system and midbrain following intranigral injections to the young adult and aged rat

i. Age-related decreases in exogenous GFP protein in the nigrostriatal system are observed with rAAV2/2, rAAV2/5, and LV, but not rAAV2/9 intranigral injections

To specifically investigate transduction efficiency of the nigrostriatal system, we injected our viral constructs into the SNpc and performed Western blot analyses of the innervated striatal tissue at one month post-injection. This approach allowed us to measure levels of GFP within nigrostriatal circuitry specifically, thereby avoiding detection of non-dopaminergic neurons in the SN and ventral mesencephalon that also are transduced following SNpc vector injections [Burger *et al*, 2004; McFarland *et al*, 2009; Polinski *et al*, 2015]. Aged rats displayed significantly lower levels of GFP in the striatum as compared to young adult rats following injection with three of the four vector constructs (Figure 14). Aged rat striatal tissue contained 62% less GFP following rAAV2/2 GFP transduction ($p=0.005$; Figure 14a), 75% less GFP following rAAV2/5 GFP transduction ($p=0.043$; Figure 14c), and 57% less GFP following LV GFP transduction ($p=0.016$; Figure 14d) as compared to their young adult rat counterparts. The sole viral vector that did not decrease in transduction efficiency in the aged rats was rAAV2/9, which conversely, trended toward an increase in striatal GFP levels in the aged compared to young adult rat ($p=0.087$; Figure 14b). These results demonstrate that advanced age presents a barrier to efficient transduction with many, but not all, of the viral vector constructs tested in the rat nigrostriatal system.

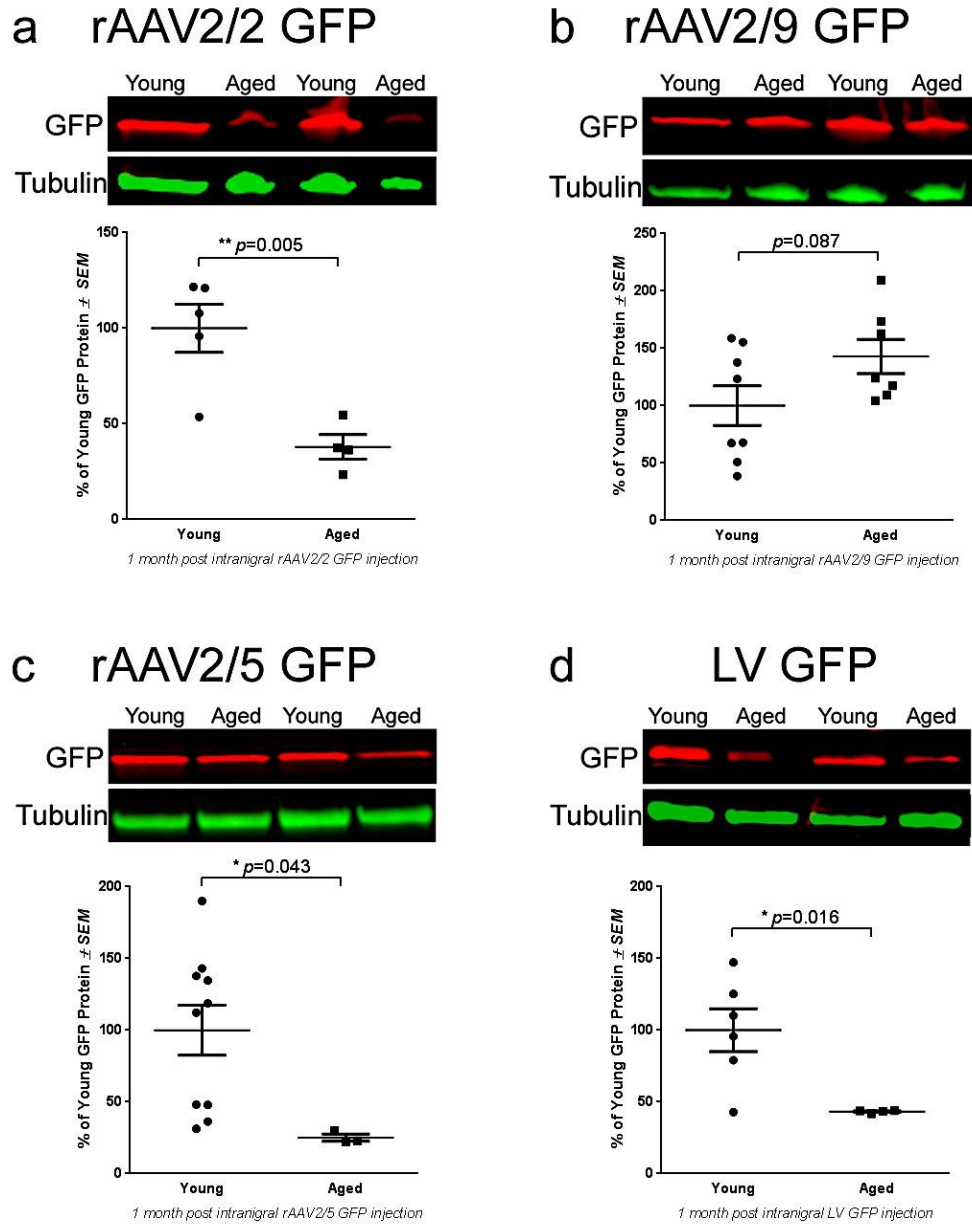


Figure 14. Viral vector-mediated expression of GFP is reduced in the aged nigrostriatal system with rAAV2/2, rAAV2/5, and LV, but not rAAV2/9. Representative Western blot and quantitation of GFP in striatal samples of young adult (Young) and aged (Aged) rats one month post-injection with a) rAAV2/2 GFP, b) rAAV2/9 GFP, c) rAAV2/5 GFP, or d) LV GFP. a) Aged (n=4) rats expressed significantly less striatal GFP than young adult (n=5) rats following rAAV2/2 GFP transduction (** $p \leq 0.01$). b) Young adult (n=8) and aged (n=7) rats expressed equivalent levels of GFP following rAAV2/9 GFP transduction ($p > 0.05$). c) Aged (n=3) rats expressed significantly less GFP than young adult (n=10) rats following rAAV2/5 GFP transduction (* $p \leq 0.05$). d) Aged (n=4) rats expressed significantly less striatal GFP than young adult (n=6) rats following LV GFP transduction (* $p \leq 0.05$). Values are expressed as the percent of the young mean optical density scores, with GFP signal normalized to tubulin controls \pm SEM for each group. Abbreviations: GFP, green fluorescent protein; rAAV, recombinant adeno-associated virus; LV, lentivirus; SEM, standard error of the mean.

i. Age-related nigrostriatal transduction deficiencies are not reflected by differences in total GFP-positive cells within the mesencephalon

To assess the relationship between the number of transduced cells in the mesencephalon and transduction efficiency in the nigrostriatal system, we first quantified the total number of GFP-positive (GFP+) cells throughout the midbrain with unbiased stereology. No significant differences were observed in total numbers of GFP+ cells in the midbrain following rAAV2/2 GFP ($p=0.135$; Figure 15a), rAAV2/5 GFP ($p=0.141$; Figure 15g), and LV GFP ($p=0.307$; Figure 15j) injection into the aged as compared to young adult rat SNpc. However, following rAAV2/9 GFP injection into the SNpc, aged rats exhibited greater numbers of GFP+ cells in the midbrain as compared to young adult rats ($p=0.037$; Figure 15d). To determine whether aging impacted the phenotype of cells expressing GFP, we quantified the ratio of GFP+ neurons to GFP+ glia (microglia and astrocytes). No differences were seen between ages in the percent of neurons, astrocytes, or microglia expressing GFP for any vector construct (Figure 16a). The overwhelming majority (>98% for rAAV pseudotypes and >85% for LV) of GFP+ cells were neuronal following injection in the SNpc (Figure 16, **Table 3**). These results demonstrate that age-related transduction deficiencies, as determined by transgene protein expression in the nigrostriatal system (Figure 14), are not readily detectable using total counts of GFP+ cells in the mesencephalon.

ii. Quantification of GFP+/TH+ SNpc neurons reveals fewer GFP+ nigrostriatal dopamine neurons in aged rats injected with rAAV2/2 GFP and LV GFP

To investigate the number of transduced SNpc neurons specifically, we performed dual immunofluorescent labeling for GFP and TH (Figure 15b,e,h,k). rAAV2/2 GFP and LV GFP displayed a 47% ($p=0.022$) and 35% ($p=0.025$) reduction, respectively, in the number of nigrostriatal SNpc dopaminergic neurons expressing GFP in the aged brain as compared to the young adult rat brain (Figure 15b-c,k-l). No

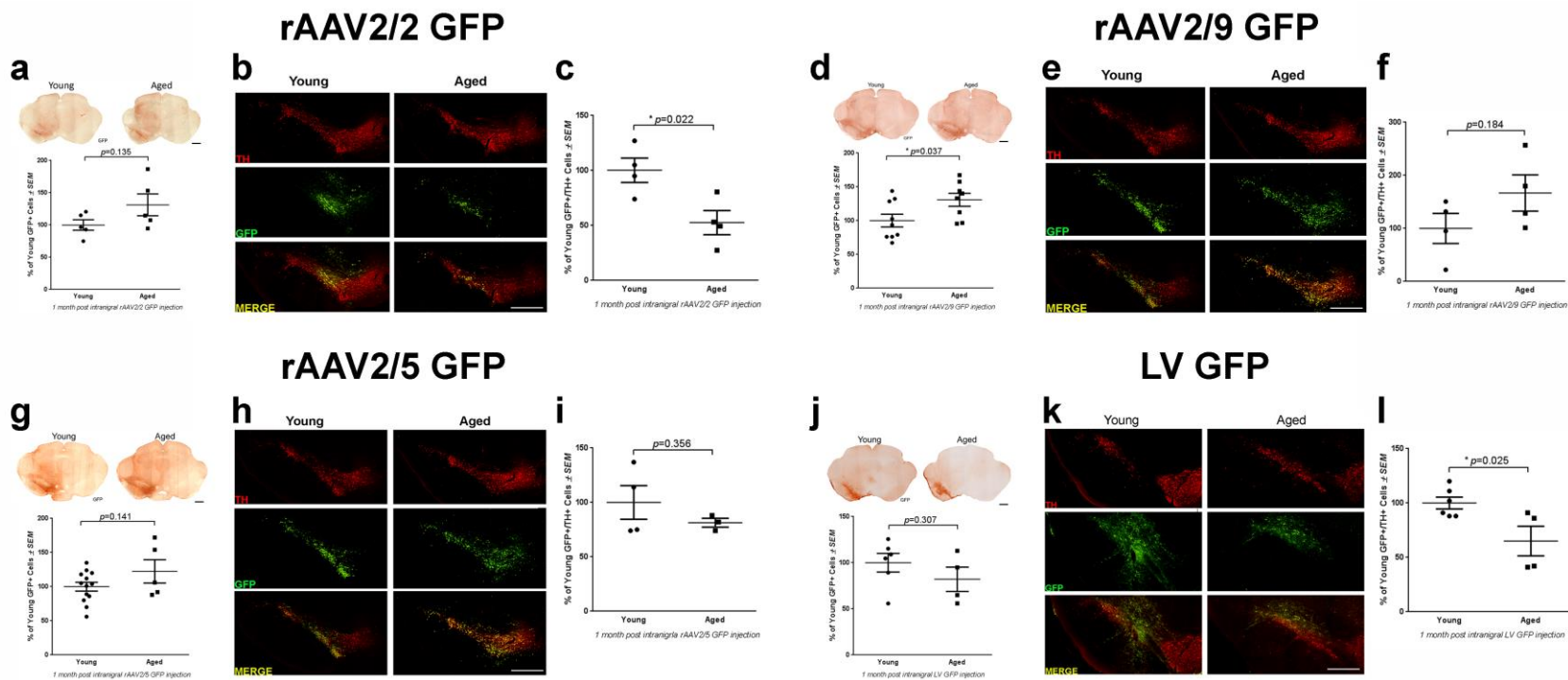


Figure 15. Quantitation of GFP-positive cells after intranigral injection does not consistently reveal age-related nigrostriatal transduction deficiencies. (a,d,g,j) Representative image and quantitation of total GFP+ cells in the midbrain of young adult (Young) and aged (Aged) rats following rAAV2/2, rAAV2/9, rAAV2/5, and LV GFP transduction, respectively. Scale bars = 1000 μ m. No significant differences ($p > 0.05$) were seen between young adult and aged rats in total GFP+ cells with a) rAAV2/2 ($n=5$ /age), g) rAAV2/5 ($n=13$ young, 5 aged), and j) LV ($n=6$ young, 4 aged), but aged ($n=9$) rats had significantly more GFP+ cells than young adult ($n=8$) rats following d) rAAV2/9 GFP transduction ($*p \leq 0.05$). (b,e,h,k) GFP expression within THir SNpc neurons in young adult and aged rats following rAAV2/2, rAAV2/9, rAAV2/5, and LV GFP transduction, respectively. Scale bars = 1000 μ m. (c,f,i,l) Quantitation of GFP+ cells co-localizing with TH+ cells in the SNpc following rAAV2/2, rAAV2/9, rAAV2/5, and LV GFP injection, respectively. Aged rats had significantly fewer ($*p \leq 0.05$) GFP+/TH+ cells than young adult rats following c) rAAV2/2 and l) LV injection ($n=4$ /age/vector). No significant differences ($p > 0.05$) were observed in the number of GFP+/TH+ cells in the SNpc between ages for f) rAAV2/9 ($n=4$ /age) and i) rAAV2/5 ($n=4$ young, 3 aged). Values are expressed as the percent of the young cell counts \pm SEM for each group. Abbreviations: GFP, green fluorescent protein; rAAV, recombinant adeno-associated virus; LV, lentivirus; GFP+, GFP immunoreactive; TH+, tyrosine hydroxylase immunoreactive; SEM, standard error of the mean.

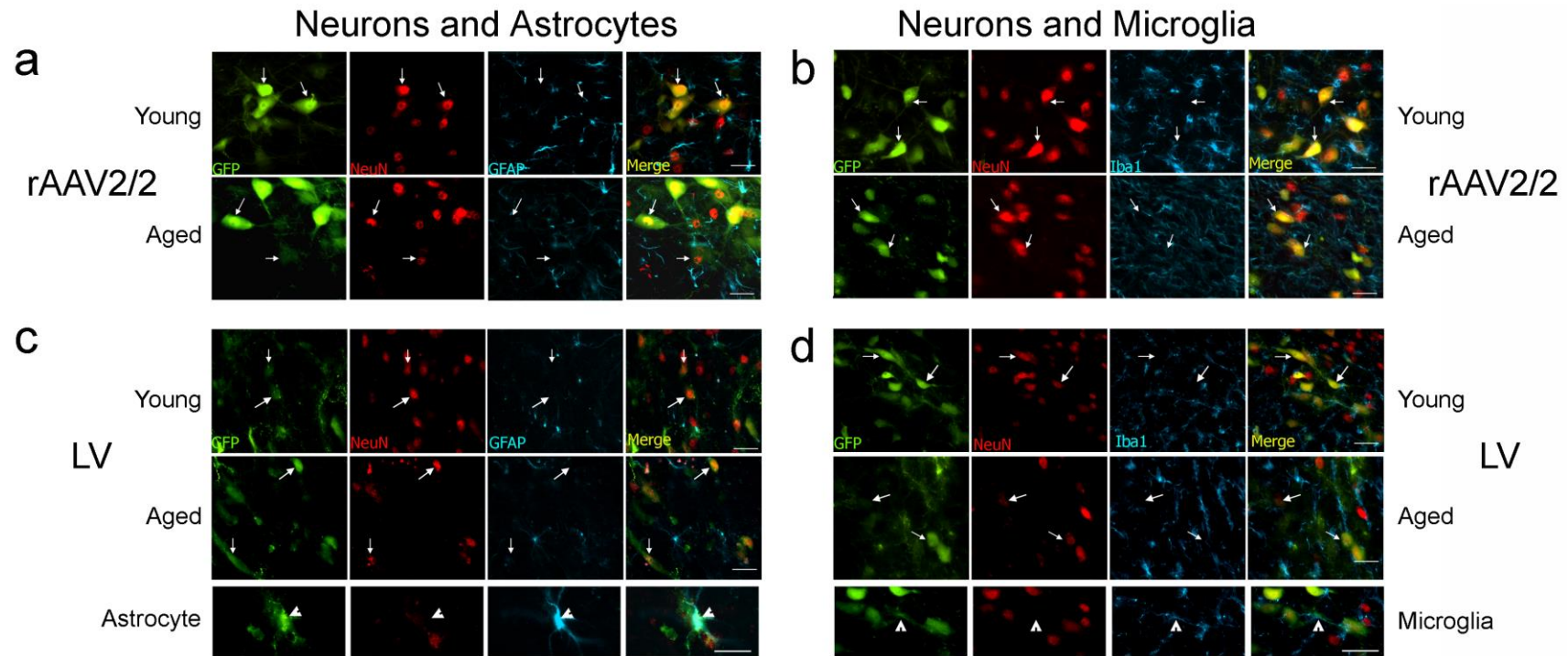


Figure 16. The ratio of neurons and glia expressing GFP does not change with age in the SNpc following intranigral injection. (a,c) Representative images of triple label immunofluorescence for GFP, neurons (NeuN), and astrocytes (GFAP) in the substantia nigra pars compacta (SNpc) following intranigral injection with a) rAAV2/2 GFP or c) LV GFP in young adult (Young) and aged (Aged) rats. (b,d) Representative images of triple label immunofluorescence for GFP, neurons (NeuN), and microglia (Iba-1) in the SNpc following intranigral injection with b) rAAV2/2 GFP or d) LV GFP. Following rAAV2/2 injection, GFP colocalizes with neurons, but not astrocytes (a) or microglia (b). Following LV GFP injection, GFP colocalizes with neurons, as well as c) astrocytes and d) microglia to a lesser extent. Arrows depict GFP+/NeuN+ cells. Arrowheads depict GFP+/GFAP+ or GFP+/Iba-1+ cells. Scale bars = 50µm. Abbreviations: GFP, green fluorescent protein; rAAV, recombinant adeno-associated virus; LV, lentivirus; NeuN, neuronal nuclei; GFAP, glial fibrillary acidic protein; Iba-1, ionized calcium-binding adapter molecule 1; GFP+, GFP immunoreactive; NeuN+, NeuN immunoreactive; GFAP+, GFAP immunoreactive, Iba-1+, Iba-1 immunoreactive.

Table 3. Percent of GFP+ Transduced Cells Classified by Phenotype following Intranigral or Intrastriatal Injection of rAAV2/2, rAAV2/5, rAAV2/9, or LV GFP.

Vector	Structure	Age	Mean Percent of GFP+ Cells by Phenotype ¹		
			Neurons	Astrocytes	Microglia
rAAV2/2 GFP	SNpc	Young	99.8 ± 0.2	0.0 ± 0.0	0.2 ± 0.2
		Aged	99.8 ± 0.1	0.1 ± 0.1	0.1 ± 0.1
rAAV2/5 GFP	SNpc	Young	100.0 ± 0.0	0.0 ± 0.0	0.0 ± 0.0
		Aged	99.7 ± 0.2	0.0 ± 0.0	0.3 ± 0.2
rAAV2/9 GFP	SNpc	Young	99.5 ± 0.0	0.2 ± 0.1	0.3 ± 0.1
		Aged	99.5 ± 0.2	0.2 ± 0.2	0.3 ± 0.1
LV GFP	SNpc	Young	84.4 ± 2.2	14.4 ± 2.2	1.2 ± 0.3
		Aged	85.8 ± 2.3	13.5 ± 2.1	0.7 ± 0.2
rAAV2/2 GFP	Striatum	Young	99.8 ± 0.2	0.0 ± 0.0	0.2 ± 0.2
		Aged	99.6 ± 0.2	0.2 ± 0.2	0.1 ± 0.1
rAAV2/5 GFP	Striatum	Young	98.9 ± 0.3	0.5 ± 0.3	0.7 ± 0.0
		Aged	99.6 ± 0.1	0.2 ± 0.2	0.2 ± 0.1
rAAV2/9 GFP	Striatum	Young	99.8 ± 0.1	0.1 ± 0.1	0.1 ± 0.0
		Aged	99.8 ± 0.1	0.1 ± 0.1	0.1 ± 0.1
LV GFP	Striatum	Young	96.6 ± 0.3	0.7 ± 0.4	2.7 ± 0.3
		Aged	98.2 ± 0.5	0.2 ± 0.1	1.6 ± 0.4

¹Percentages represented as Mean ± SEM.

significant differences in the number of SNpc dopaminergic neurons expressing GFP were observed between ages following rAAV2/5 GFP ($p=0.356$; Figure 15h-i) or rAAV2/9 GFP ($p=0.184$; Figure 15e-f). The fact that decreases in striatal GFP levels in aged rats following intranigral injections (Figure 14) are associated with decreased GFP+/TH+ SNpc neurons in some (rAAV2/2, LV) but not all (rAAV2/5) vector constructs suggests that the dual labeling GFP/TH approach can be somewhat predictive of the impact of aging on vector-mediated transgene expression in to the nigrostriatal system.

iii. Age-related decreases in GFP mRNA are observed following intranigral injection with rAAV2/2, rAAV2/5, and LV, but not with rAAV2/9

To determine whether age-related changes in GFP protein expression are due to deficiencies in steps of transduction upstream of protein synthesis, we used the complimentary approaches of qPCR and RNAscope *in situ* hybridization. qPCR was not conducted on the rAAV2/5 and LV SNpc due to lack of tissue availability. qPCR analyses of SNpc tissue from young adult and aged rats injected with rAAV2/2 GFP revealed a trend towards an age-related decrease in GFP mRNA, with the aged rat SNpc containing 5-fold lower levels of GFP mRNA than the young adult SNpc ($p=0.109$; Figure 17c). In contrast, the SNpc of rats injected with rAAV2/9 contained equal levels of GFP mRNA between young adult and aged rats ($p=0.723$; Figure 17d). RNAscope *in situ* hybridization for GFP mRNA in the midbrain revealed a similar pattern, with decreased GFP mRNA puncta in the aged as compared to young adult rat following intranigral rAAV2/2 GFP injection, but not rAAV2/9 GFP injection (Figure 17a-b). Decreased GFP mRNA in aged rats was also observed in RNAscope *in situ* hybridization with rAAV2/5 and LV (Figure 17e-f), following the trends observed with rAAV2/2 (Figure 17a,c) and a previous report demonstrating decreased GFP mRNA in the aged ventral mesencephalon following transduction with rAAV2/5 [Polinski *et al*, 2015]. Together, these results suggest that levels of GFP mRNA are also decreased in cases where viral vectors display an age-related decrease in nigrostriatal transduction as assessed by GFP protein.

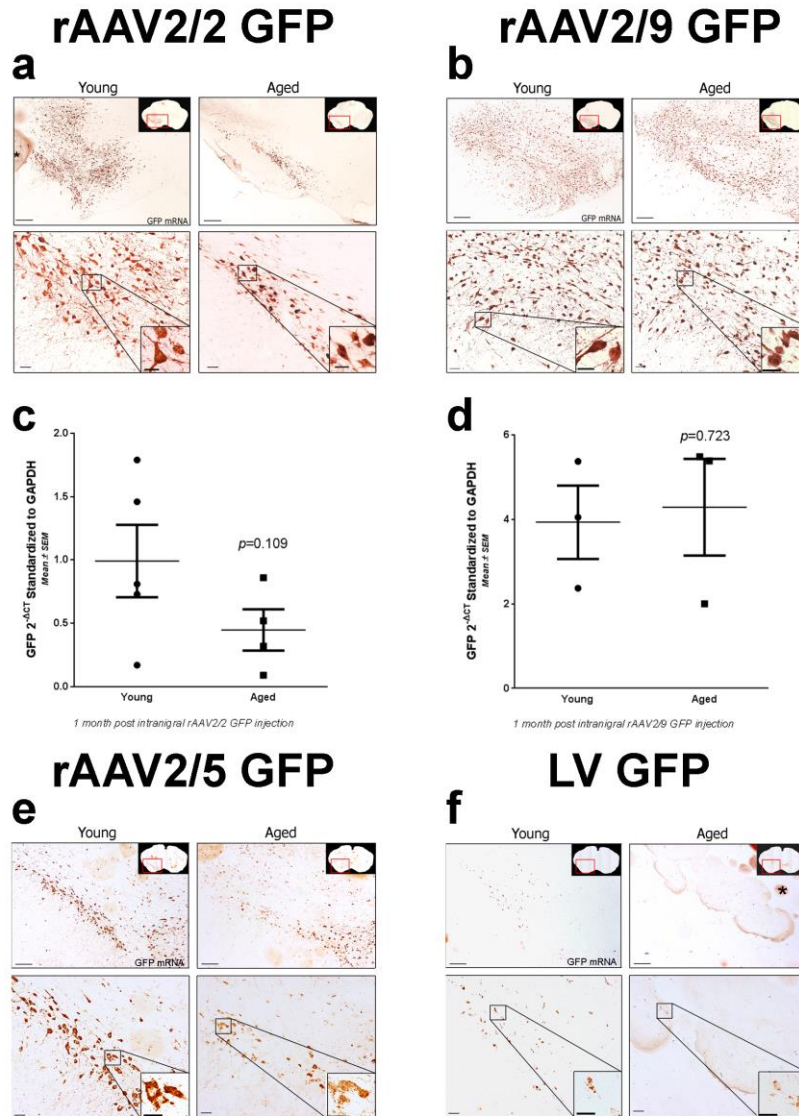


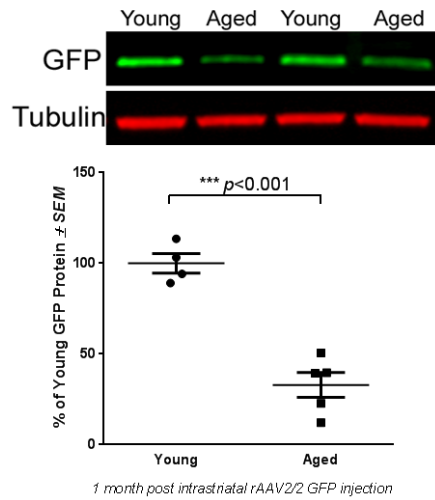
Figure 17. Evidence for decreased GFP mRNA expression in the aged as compared to the young adult rat midbrain and SNpc following rAAV2/2, rAAV2/5, and LV, but not rAAV2/9 GFP injection to the SNpc. (a,b,e,f) Representative images using RNAscope in situ hybridization for GFP mRNA in the young adult (Young) and aged (Aged) rat midbrain following rAAV2/2, rAAV2/9, rAAV2/5, and LV GFP transduction, respectively. Scale bars = 100 μ m in top panel images, 50 μ m in bottom panel images, and 25 μ m in bottom panel high magnification inserts. Qualitative analyses of GFP mRNA levels indicate an age-related decrease in the aged as compared to young adult rat following a) rAAV2/2, e) rAAV2/5, and f) LV GFP injection, but not b) rAAV2/9 GFP injection. (c,d) GFP mRNA quantitation using qPCR of the young adult and aged rat injected substantia nigra pars compacta (SNpc). Values are displayed as the mean GFP- Δ CT values standardized to GAPDH controls, \pm SEM for each group. GFP mRNA expression appears to be decreased in the aged (n=5/vector) as compared to young adult (n=5/vector) rat following c) rAAV2/2 GFP, but not d) rAAV2/9 GFP injection, although a statistical difference was not observed ($p > 0.05$). Asterisks (*) designate non-punctate background staining that is not indicative of GFP mRNA presence. Abbreviations: GFP, green fluorescent protein; rAAV, recombinant adeno-associated virus; LV, lentivirus; mRNA, messenger RNA; SEM, standard error of the mean.

II. Transduction efficiency in the striatonigral system following intrastriatal injections to the young adult and aged rat.

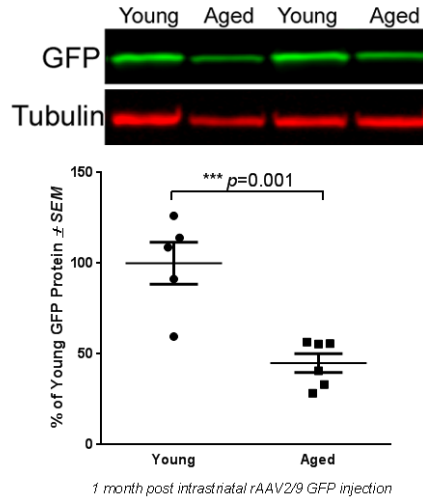
i. Age-related decreases in exogenous GFP protein in the striatonigral system are observed following intrastriatal rAAV2/2, rAAV2/5, and rAAV2/9, but not LV injections

Similar to our assessment of the nigrostriatal system, the ability of intrastriatal vector injections to deliver exogenous GFP to the anterograde SNpr was measured by protein analyses in SNpr tissue (Figure 11, Figure 12). Striatal injection of viral vectors expressing tropic factors are used to simultaneously provide exogenous protein to dopaminergic nigrostriatal terminals through local transgene expression and tropic factor secretion, and anterogradely deliver protein to the SNpc via the striatonigral pathway [Ciesielska *et al*, 2011; Kells *et al*, 2012]. Aged rats displayed significantly lower levels of GFP protein as compared to young adult rats following injection with three of the four vector constructs (Figure 18). Similar to results following intranigral injections, rAAV2/2 displayed a 67% reduction in GFP expression ($p=0.001$; Figure 18a) and rAAV2/5 displayed a 58% reduction in GFP expression ($p=0.023$; Figure 18c) in the aged as compared to the young adult SNpr. However, unlike results with rAAV2/9, which displayed no age-related deficits following intranigral injections, following intrastriatal injections rAAV2/9 GFP expression was reduced by 55% in the aged SNpr as compared to the young adult rat ($p=0.001$; Figure 18b). In contrast, LV GFP was the sole viral vector resistant to the age-related decrease in transduction of the striatonigral system ($p=0.402$; Figure 18d) despite displaying a deficiency in transducing the aged as compared to young adult nigrostriatal system (Figure 14d). These results indicate that the aged rat striatonigral system is, in general, also relatively resistant to viral vector transduction when compared to the young adult rat. However, age-related transduction deficiencies are unique to viral vectors and cannot be generalized across brain structures.

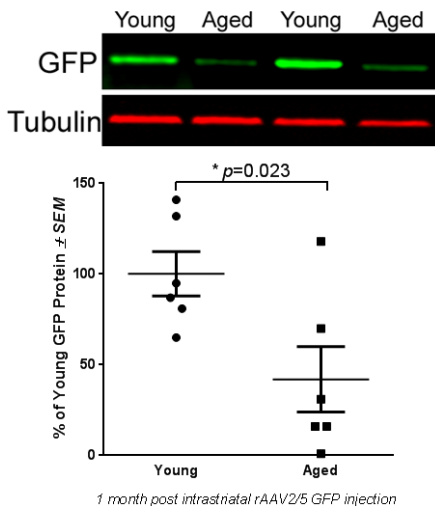
a rAAV2/2 GFP



b rAAV2/9 GFP



c rAAV2/5 GFP



d LV GFP

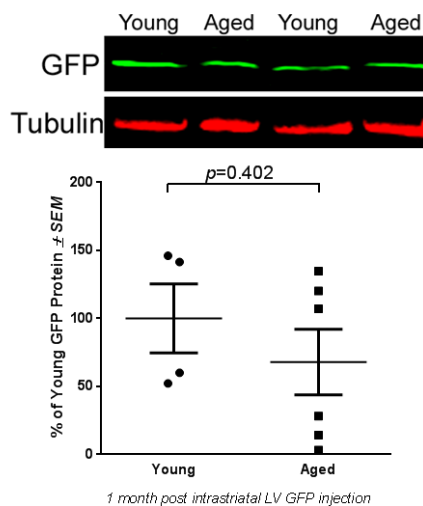


Figure 18. Viral vector-mediated expression of GFP is reduced in the aged striatonigral system with rAAV2/2, rAAV2/5, and rAAV2/9, but not LV. Representative Western blot and quantitation of GFP immunodetection in substantia nigra pars reticulata (SNpr) samples of young adult (Young) and aged (Aged) rats one month post-injection with a) rAAV2/2 GFP, b) rAAV2/9 GFP, c) rAAV2/5 GFP, or d) LV GFP. a) Aged (n=5) rats displayed significantly less GFP than young adult (n=4) rats following rAAV2/2 GFP transduction ($***p < 0.001$). b) Aged (n=6) rats display decreased GFP levels in the SNpr as compared to young adult (n=5) rats following rAAV2/9 GFP transduction ($***p \leq 0.001$). c) Aged (n=6) rats expressed significantly less GFP than young adult (n=6) rats following rAAV2/5 GFP transduction ($*p < 0.05$). d) Aged (n=4) and young adult (n=6) rats equivalent GFP in the SNpr following LV GFP transduction ($p > 0.05$). Values are expressed as the percent of the young mean optical density scores, with GFP signal normalized to tubulin controls \pm SEM for each group. Abbreviations: GFP, green fluorescent protein; rAAV, recombinant adeno-associated virus; LV, lentivirus; SEM, standard error of the mean.

ii. Age-related changes in striatonigral transduction efficiency are not detectable by quantitation of GFP+ cells in the striatum.

To assess the relationship between the number of transduced cells in the striatum and transduction efficiency of the striatonigral pathway, we quantified the total number of GFP+ cells within the striatum using unbiased stereology. No significant differences were observed in total numbers of striatal GFP+ cells following rAAV2/2 GFP ($p=0.448$; Figure 19a), rAAV2/9 GFP ($p=0.506$; Figure 19d), rAAV2/5 GFP ($p=0.096$; Figure 19g), or LV GFP ($p=0.762$; Figure 19j) injection into the aged versus young adult rat. As observed when we quantified total numbers of mesencephalic GFP+ cells, quantification of the total number of striatal GFP+ cells does not accurately reflect differences in transduction efficiency. Again, we quantified the ratio of GFP+ neurons to glia and did not see any differences with age as the vast majority (>98% for all vectors) of GFP+ cells displayed a neuronal phenotype (Figure 20, **Table 3**). Due to tissue processing requirements for striatal GFP+ cell quantitation, we were unable to perform direct protein quantification in the striatum. Therefore, to capture potential differences in levels of GFP expression within cells of the striatum, we quantified GFP immunoreactivity using near-infrared densitometry in the striatum (Figure 19b,e,h,k). Again, no significant differences were observed between ages with rAAV2/2 GFP ($p=0.332$; Figure 19c), rAAV2/9 GFP ($p=0.147$; Figure 19f), or LV GFP ($p=0.758$; Figure 19i). However, advanced age resulted in a significant decrease in GFP immunoreactivity following intrastriatal rAAV2/5 GFP injection ($p=0.021$; Figure 19i). Taken together, these results suggest that an age-related difference in striatonigral transduction efficiency is difficult to detect at the level of the striatum following intrastriatal injection.

i. Evaluation of GFP mRNA expression following intrastriatal injection

RNAscope *in situ* hybridization was used to detect levels of GFP mRNA in striatal tissue one month after intrastriatal viral vector injection. Qualitative analyses failed to reveal any striking differences between

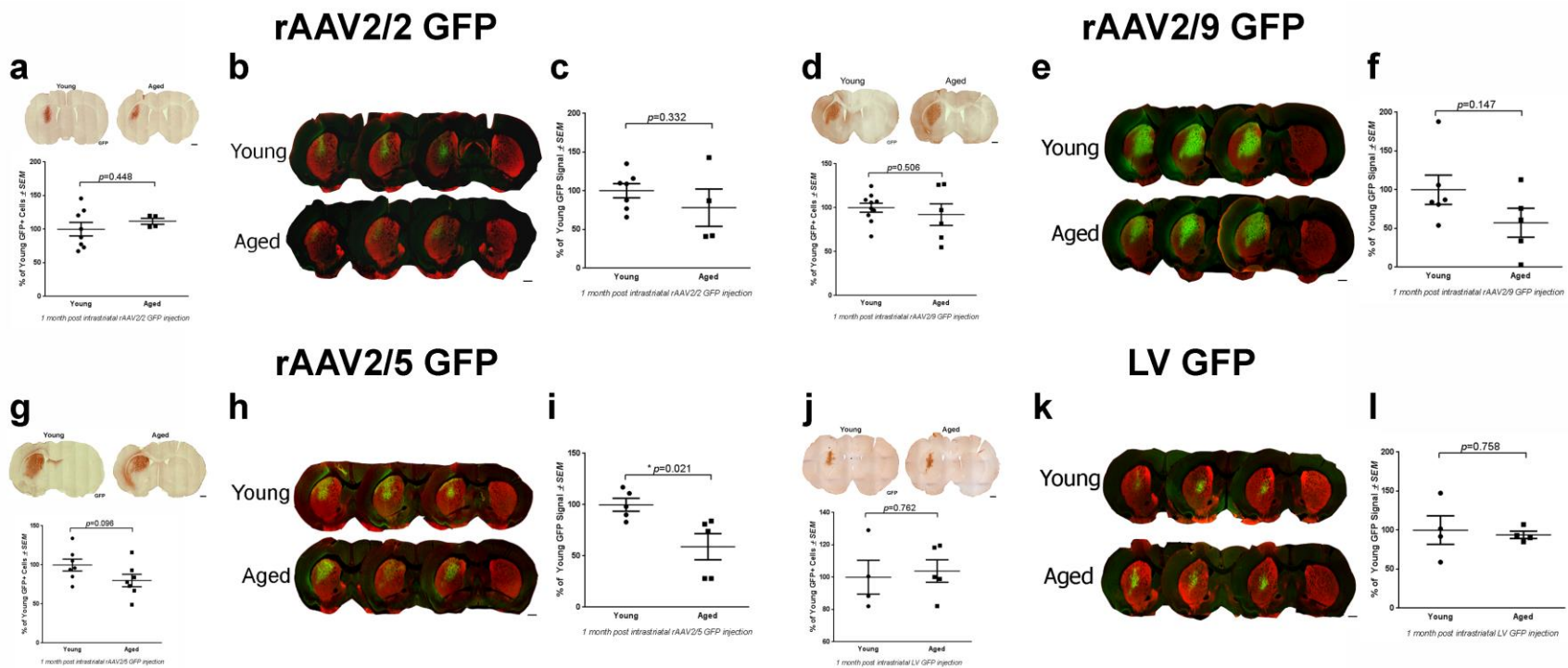


Figure 19. Quantitation of GFP-positive cells after intrastriatal injection does not reveal an age-related decrease in striatonigral transduction efficiency. (a,d,g,j) Representative image and quantitation of total GFP+ cells in the striatum of young adult (Young) and aged (Aged) rats following rAAV2/2, rAAV2/9, rAAV2/5, and LV GFP transduction, respectively. Scale bars = 1000 μ m. No significant differences ($p>0.05$) were seen between young adult and aged rats in total GFP+ cells with a) rAAV2/2 (n=8 young, 4 aged), d) rAAV2/5 (n=10 young, 6 aged), g) rAAV2/5 (n=10 young, 6 aged), and j) LV (n=4 young, 5 aged). (b,e,h,k) GFP (green) and TH (red) expression detected using near-infrared imaging within the striatum of young adult and aged rats following rAAV2/2, rAAV2/9, rAAV2/5, and LV GFP transduction, respectively. Scale bars = 1000 μ m. (c,f,i,l) Quantitation of near-infrared GFP signal within the striatum following rAAV2/2, rAAV2/9, rAAV2/5, and LV GFP injection, respectively. Aged rats only displayed significantly decreased ($*p\leq 0.05$) GFP signal following i) rAAV2/5 GFP injection (n=5/age), with no significant differences ($p>0.05$) between ages following c) rAAV2/2 (n=7 young, 4 aged), f) rAAV2/9 (n=6 young, 5 aged), or l) LV injection (n=4/age). Values are expressed as the percent of the young GFP signal, normalized to background levels of staining in the cortex, \pm SEM for each group. Abbreviations: GFP, green fluorescent protein; rAAV, recombinant adeno-associated virus; LV, lentivirus; TH, tyrosine hydroxylase; SEM, standard error of the mean.

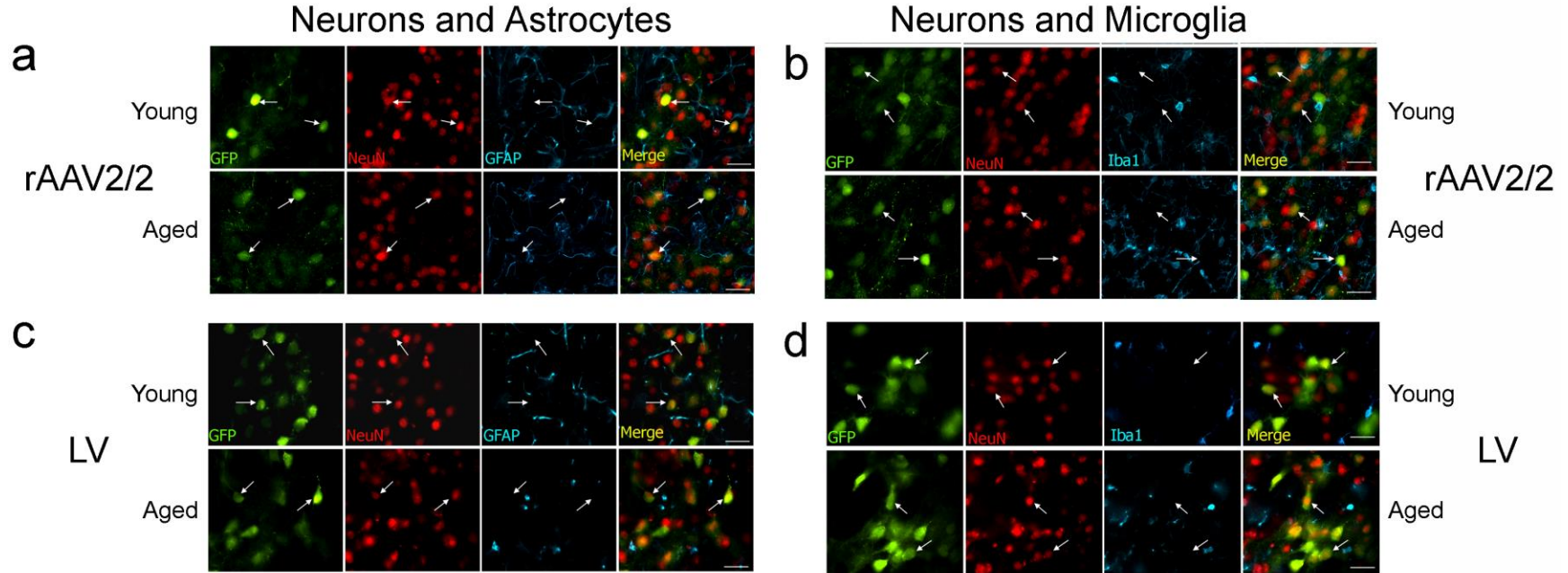


Figure 20. The ratio of neurons and glia expressing GFP does not change with age in the striatum following intrastriatal injection. (a,c) Representative images of triple label immunofluorescence for GFP, neurons (NeuN), and astrocytes (GFAP) in the striatum following intrastriatal injection with a) rAAV2/2 GFP or c) LV GFP in young adult (Young) and aged (Aged) rats. (b,d) Representative images of triple label immunofluorescence for GFP, neurons (NeuN), and microglia (Iba-1) in the striatum following intrastriatal injection with b) rAAV2/2 GFP or d) LV GFP. Following either injection, GFP colocalizes primarily with neurons, but not astrocytes (a,c) or microglia (b,d). Arrows depict GFP+/NeuN+ cells. Scale bars = 50µm. Abbreviations: GFP, green fluorescent protein; rAAV, recombinant adeno-associated virus; LV, lentivirus; NeuN, neuronal nuclei; GFAP, glial fibrillary acidic protein; Iba-1, ionized calcium-binding adapter molecule 1; GFP+, GFP immunoreactive; NeuN+, NeuN immunoreactive.

young adult and aged rats in levels of GFP mRNA following intrastriatal injection with rAAV2/5, rAAV2/9 or LV (Figure 21). However, striatal sections transduced using rAAV2/2 displayed an appreciable decrease in GFP mRNA in the aged as compared to young adult rat striatum (Figure 21a). These results suggest, at least for rAAV2/2, that age-related deficiencies in GFP protein expression are related to an age-related decreased in GFP mRNA levels [Ryazanov and Nefsky, 2002; Polinski *et al*, 2015].

ii. Astrocytes display limited tropism for viral particles in the young adult and aged rat striatum

Previous studies report a doubling of astrocytes in the striatum in aged as compared to young adult rats [Yurek *et al*, 2015]. We investigated the possibility that an increased astrocyte to neuron ratio impacted striatal neuronal transduction efficiency in the aged brain due to astrocytes sequestering viral particles; a phenomenon that would not have been detected simply by looking at GFP expression since the activity of the C β A promoter is highly limited in astrocytes. We used a novel combination of RNAscope *in situ* hybridization for the viral C β A promoter [Grabinski *et al*, 2015] and immunohistochemistry for astrocytes (S100 calcium-binding protein B, S100B) or neurons (Neuronal Nuclei, NeuN) to visualize the cellular location of viral particles in the transduced zone in the striatum. Despite previous evidence suggesting an increase in the population of astrocytes in the striatum with aging [Yurek *et al*, 2015], no qualitative increase in S100B astrocytes was observed in the aged compared to the young striatum. Further, in both the young adult and aged brain, for all vector constructs, viral genomes overwhelmingly colocalized with NeuN immunoreactive neurons (Figure 22a-c, g-i), indicating their presence within appeared as numerous, dense C β A puncta. In contrast, viral genomes were rarely observed in astrocytes (Figure 22d-f, j-l) and if observed, most often appeared as puncta representative of single viral genomes (Figure 22f,l). These results indicate that astrocytes in aged striatum do not impact transduction efficiency via sequestration of viral particles. Further, although use of astrocyte-specific promoters such

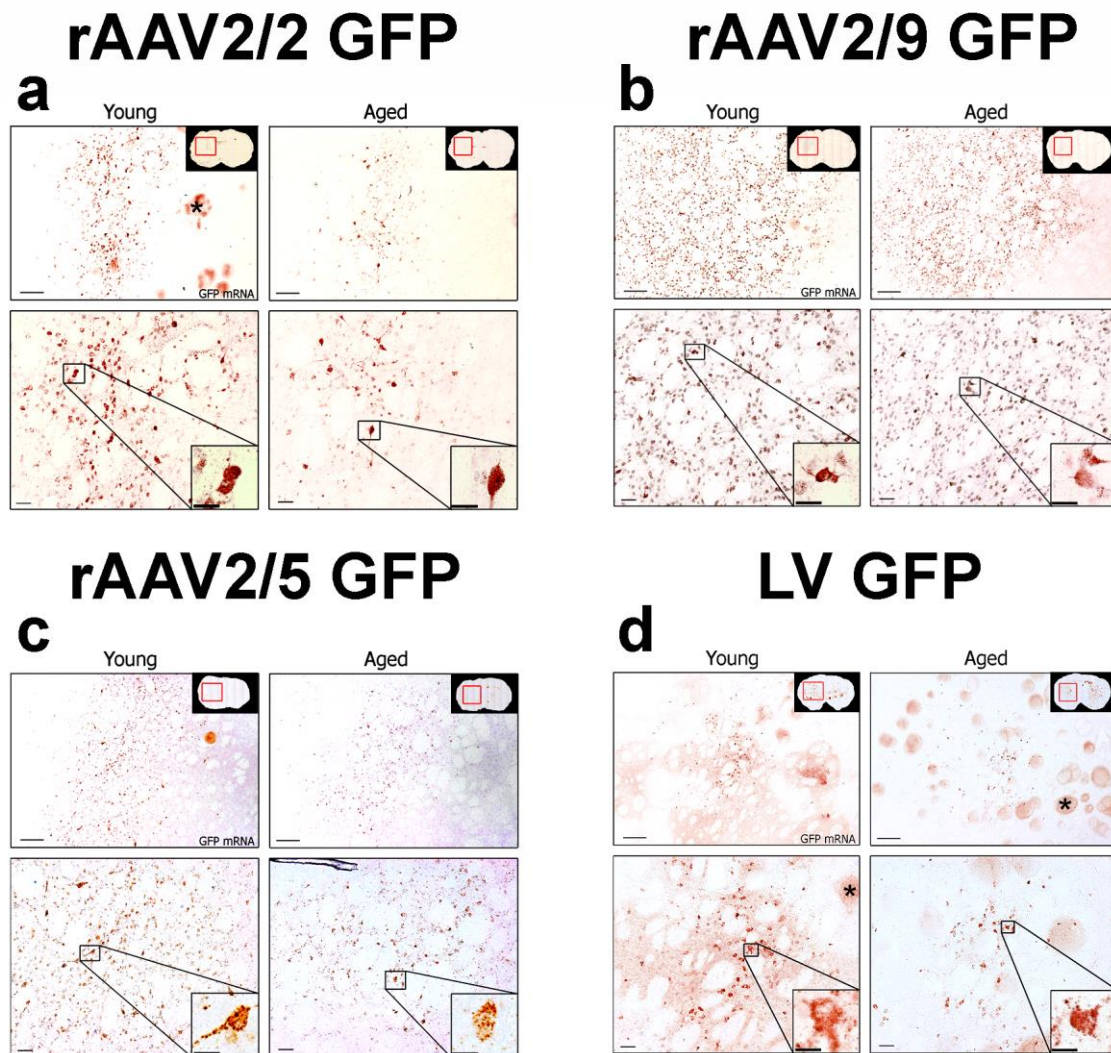


Figure 21. GFP mRNA expression in the aged as compared to the young adult rat striatum following rAAV2/2, rAAV2/9, rAAV2/5, and LV GFP injection to the striatum. (a-d) Representative images using RNAscope in situ hybridization for GFP mRNA in the young adult (Young) and aged (Aged) rat midbrain following rAAV2/2, rAAV2/9, rAAV2/5, and LV GFP transduction, respectively. Scale bars = 100 μ m in top panel images, 50 μ m in bottom panel images, and 25 μ m in bottom panel high magnification inserts. Asterisks (*) designate non-punctate background staining that is not indicative of GFP mRNA presence. Abbreviations: GFP, green fluorescent protein; rAAV, recombinant adeno-associated virus; LV, lentivirus; mRNA, messenger RNA; SEM, standard error of the mean.

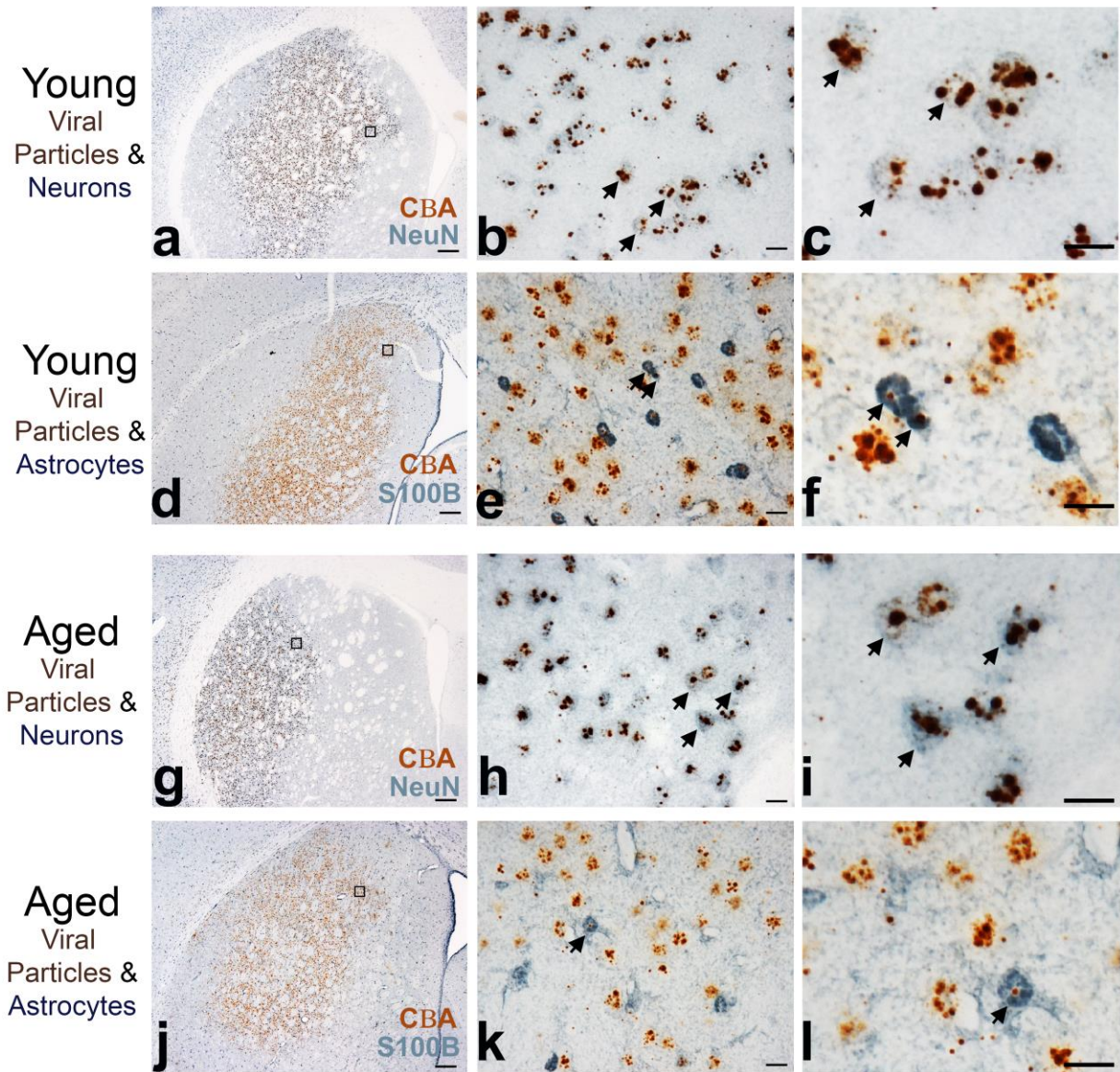


Figure 22. *In situ* hybridization combined with immunohistochemistry reveals viral particles located within neurons and largely absent within astrocytes in the striatum. (a-c, g-i) Representative image of RNAscope in situ hybridization of the C β A promoter of viral genomes (brown) and NeuN for neurons (blue) in young adult (a-c) or aged (g-i) rats one month post-injection of rAAV2/9 GFP in the striatum. (d-f, j-l) Representative image of RNAscope in situ hybridization for the C β A promoter of viral particles (brown) and S100B for astrocytes (blue) in young adult (d-f) or aged (j-l) rats one month post-injection of rAAV2/9 GFP in the striatum. Scale bars = 500 μ m in lowest magnification panel, 25 μ m in the intermediate and highest magnification panels. Box insets in a, d, g, j identify location of higher magnification images. Arrows indicate areas of AAV genome co-localization within neurons or astrocytes.

as the GFAP promoter (rather than the C β A promoter) can limit gene expression to astrocytes [Weller *et al*, 2008], our results suggest that rAAV2/2, rAAV2/5, rAAV2/9 and LV have limited tropism for astrocytes in the brain compared to neurons.

III. Comparisons between rAAV pseudotype transduction efficiency in young adult and aged rats

i. rAAV2/9 delivers the most exogenous GFP protein to the nigrostriatal system of both young adult and aged rats

Nigrostriatal transduction levels following injection into the SNpc were assessed by quantifying GFP protein levels in the ipsilateral striatum (Figure 11). Comparisons were made between all three rAAV pseudotypes. LV was excluded from between vector comparisons due to marked titer and transduction process differences. The titers for all three rAAV pseudotypes injected into the SNpc were relatively identical (rAAV2/2 = 1.9×10^{12} genomes/mL, rAAV2/5 = 2.0×10^{12} genomes/mL and rAAV2/9 GFP at 2.0×10^{12} genomes/mL). Injection of rAAV2/9 GFP into the SNpc resulted in significantly higher levels of GFP protein in the striatum of young adult ($F_{(2,5)}=1232.34$, $p<0.001$; rAAV2/2 vs rAAV2/9, $p<0.001$; rAAV2/5 vs rAAV2/9, $p<0.001$) and aged brains ($F_{(2,3)}=74.79$, $p=0.003$; rAAV2/2 vs rAAV2/9, $p=0.005$; rAAV2/5 vs rAAV2/9, $p=0.005$) (Figure 23a). rAAV2/5 nigrostriatal transduction efficiency was comparable with rAAV2/2 in aged rats, and although higher than rAAV2/2 in young rats, this did not reach statistical significance ($p>0.05$). These results demonstrate that rAAV2/9 injections into both the young and aged SNpc result in the most efficient delivery of exogenous protein to nigrostriatal circuitry.

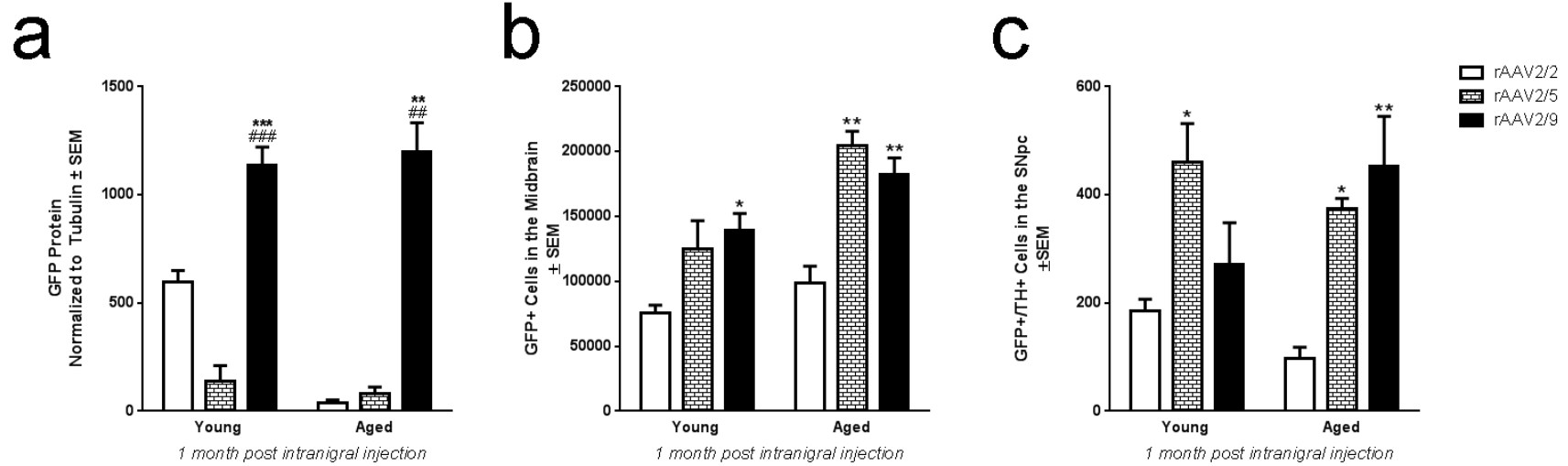


Figure 23. Comparisons between rAAV2/2, rAAV2/5, and rAAV2/9 in the young adult or aged rat nigrostriatal system. a) Quantitation of Western blot GFP immunodetection in striatal tissue after intranigral injection of rAAV pseudotypes in the young adult and aged rat. b) Quantitation of total numbers of GFP+ cells in the young adult (Young) and aged (Aged) rat midbrain following injection of rAAV2/2 GFP, rAAV2/5 GFP, or rAAV2/9 GFP into the substantia nigra pars compacta (SNpc). c) Quantitation of the number of cells co-expressing GFP and tyrosine hydroxylase (TH) in the young adult and aged rat SNpc following SNpc injection. Data is expressed as mean values \pm SEM for each group. Statistical differences between vectors in each age group are depicted as follows—comparisons against rAAV2/2: * $p \leq 0.05$, ** $p \leq 0.01$, *** $p \leq 0.001$; comparisons against rAAV2/5: # $p \leq 0.05$, ## $p \leq 0.01$, ### $p \leq 0.001$. Abbreviations: GFP, green fluorescent protein; rAAV, recombinant adeno-associated virus; GFP+, GFP immunoreactive; TH+, tyrosine hydroxylase immunoreactive; SEM, standard error of the mean.

ii. rAAV2/5 and rAAV2/9 transduce the greatest numbers of mesencephalic neurons in both young adult and aged rats

Following injection into the SNpc, comparisons were made between vectors in the number of total GFP+ cells throughout the midbrain (Figure 23b). Statistical differences were observed between vectors in both the young adult ($F_{(2,15)}=5.23$, $p=0.019$) and the aged ($F_{(2,12)}=11.80$, $p=0.001$) rats. Specifically, in the young adult midbrain, rAAV2/2 injection into the SNpc resulted in the lowest number of midbrain GFP+ cells with significantly fewer than rAAV2/9 ($p=0.018$) but not rAAV2/5 ($p=0.165$) (Figure 23b). In aged rats a similar pattern was observed in which rAAV2/2 injections into the SNpc resulted in the fewest number of GFP+ cells in the mesencephalon, with significantly fewer than rAAV2/5 ($p=0.008$) and rAAV2/9 ($p=0.003$). These results indicate that rAAV2/9 and rAAV2/5 yield the greatest number of transduced cells in the mesencephalon following SNpc injection, regardless of age.

iii. rAAV2/5 and rAAV2/9 transduce the greatest numbers of TH+ SNpc neurons in young adult and aged rats

Statistical differences between vector constructs were also observed when SNpc neurons co-expressing TH and GFP were quantified (young adult, $F_{(2,9)}=5.21$, $p=0.031$; aged, $F_{(2,8)}=9.88$, $p=0.007$) (Figure 23c). In young adult rats, injection of rAAV2/5 into the SNpc resulted in the highest number of GFP+/TH+ SNpc neurons, with rAAV2/5 displaying significantly more GFP+/TH+ cells than rAAV2/2 ($p=0.035$), but not rAAV2/9 ($p=0.172$) (Figure 23c). In aged rats, the pattern was similar in that both rAAV2/5 and rAAV2/9 injected rats possessed significantly more GFP+/TH+ SNpc neurons than rAAV2/2 (rAAV2/5 vs rAAV2/2, $p=0.045$; rAAV2/9 vs rAAV2/2, $p=0.008$) (Figure 23c). rAAV2/5 (both young adult and aged) and rAAV2/9 (aged) yield the greatest number of transduced SNpc neurons following intranigral injection.

Collectively, our results demonstrate that injections of both rAAV2/5 and rAAV2/9 result in the greatest numbers of transduced nigrostriatal dopamine neurons in young adult and aged rats compared to

rAAV2/2. However, rAAV2/9 demonstrates the greatest transduction efficiency of the young adult and aged nigrostriatal system by delivering the highest levels of GFP transgene ($\approx 35\text{-}63\times$ greater) (Figure 23a).

iv. rAAV2/9 delivers the most exogenous GFP protein to the striatonigral system of both young adult and aged rats

Comparisons in striatonigral transduction efficiency were made following intrastriatal injection of rAAV2/2 and rAAV2/9 in young adult and aged rats. As previously described, transduction efficiency in the striatonigral system was assessed by quantifying GFP levels in the SNpr following injection into the striatum (Figure 11, Figure 12). rAAV2/5 was excluded from the GFP SNpr protein analyses due to lack of sample. The titers for the two rAAV pseudotypes injected into the striatum were relatively identical (rAAV2/2 = 1.9×10^{12} genomes/mL and rAAV2/9 GFP = 2.0×10^{12} genomes/mL). Similar to overall transduction efficiency measures in the nigrostriatal system, GFP levels in the SNpr resulting from intrastriatal rAAV2/9 injection were significantly greater than SNpr GFP levels following intrastriatal rAAV2/2 injection in both the young adult ($p=0.003$) and aged ($p<0.001$) rat (Figure 24a). These results demonstrate that although advanced age negatively impacts the striatonigral transduction efficiency of rAAV2/9, it is still the vector construct most capable of delivery of high levels of exogenous protein to the striatonigral circuitry of both young adult and aged rats.

i. rAAV2/9 transduces the greatest number of striatal cells in both young adult and aged rats

Total numbers of GFP+ cells in the striatum were quantified after intrastriatal vector injection into young adult and aged rats and compared between vectors within each age group. Multiple significant differences were observed in the young adult striatum using this outcome measure ($F_{(2,18)}=69.89$,

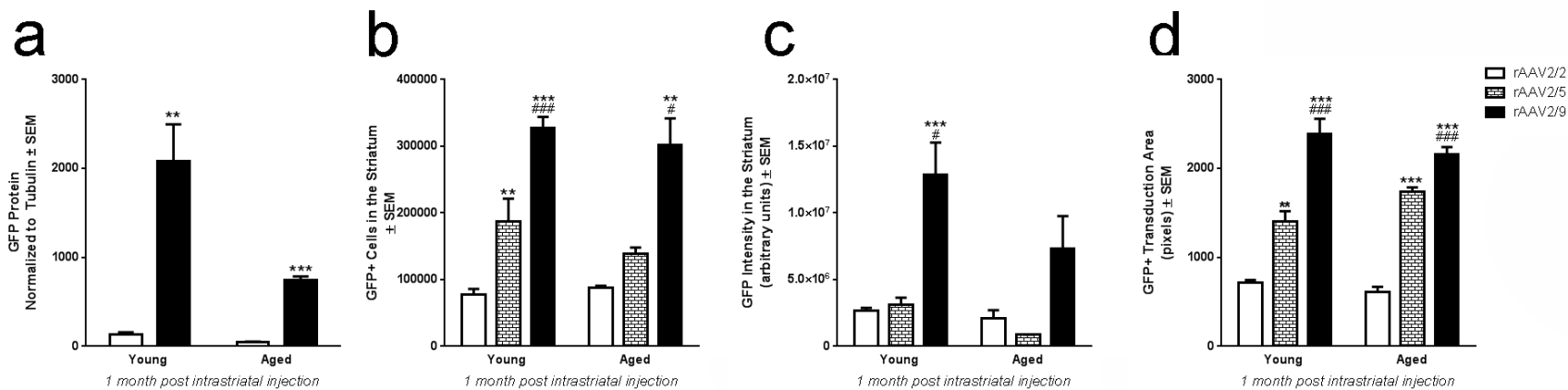


Figure 24. Comparisons between rAAV2/2, rAAV2/5, and rAAV2/9 in the young adult or aged rat striatonigral system. a) Quantitation of Western blot GFP immunodetection in SN pars reticulata (SNpr) tissue after intrastratial injection of rAAV2/2 and rAAV2/9 in the young adult and aged rat. rAAV2/5 was excluded in this Western blot due to lack of tissue. b) Quantitation of total numbers of GFP+ cells in the striatum of young adult (Young) and aged (Aged) rats following injection of rAAV2/2, rAAV2/5, and rAAV2/9. c) Quantitation of GFP signal following rAAV2/2, rAAV2/5, or rAAV2/9 injection in the striatum, as detected by near-infrared immunostaining. d) Quantitation of the area of GFP expression (GFP+ Transduction Area) in the striatum as calculated by the LI-COR Image Studio 3.1 software. Data is expressed as mean values ± SEM for each group. Statistical differences between vectors in each age group are depicted as follows—comparisons against rAAV2/2: * $p \leq 0.05$, ** $p \leq 0.01$, *** $p \leq 0.001$; comparisons against rAAV2/5: # $p \leq 0.05$, ### $p \leq 0.01$, ### $p \leq 0.001$. Abbreviations: GFP, green fluorescent protein; rAAV, recombinant adeno-associated virus; GFP+, GFP immunoreactive; SEM, standard error of the mean.

$p < 0.001$) (Figure 24b). rAAV2/9 resulted in more GFP+ cells than rAAV2/2 ($p < 0.001$) and rAAV2/5 ($p < 0.001$). In addition, rAAV2/5 resulted in more GFP+ cells than rAAV2/2 ($p = 0.006$). A similar pattern was observed in the aged brain ($F_{(2,10)} = 12.54$, $p = 0.002$) (Figure 24b) with rAAV2/9 injection resulting in significantly more GFP+ cells in the striatum compared to all other vectors (rAAV2/9 vs rAAV2/5, $p = 0.025$; rAAV2/9 vs rAAV2/2, $p = 0.002$). However, unlike results in young adults rats where intrastriatal injection of rAAV2/5 yielded more GFP+ neurons compared to rAAV2/2, in the aged brain intrastriatal rAAV2/5 resulted in statistically equivalent numbers as rAAV2/2 ($p > 0.05$). These results indicate that intrastriatal injection of rAAV2/9 yields the highest number of transduced cells in the striatum, regardless of age.

ii. Following intrastriatal vector injections, GFP intensity in the striatum parallels GFP levels in the SNpr

Due to tissue processing requirements for striatal GFP+ cell quantification, we were unable to perform direct protein quantification in the striatum. To approximate striatal GFP protein delivery we analyzed near-infrared labeled GFP immunoreactive signal intensity in the striatum and made comparisons between vectors within age groups. Significant differences were observed in GFP signal intensity in the young adult ($F_{(2,12)} = 12.20$, $p = 0.001$), but not the aged ($F_{(2,8)} = 2.97$, $p = 0.109$) rat striatum (Figure 24c). As with SNpr GFP protein levels following intrastriatal injection, rAAV2/9 in the young adult brain resulted in the highest striatal GFP signal intensity compared to rAAV2/5 ($p = 0.029$) or rAAV2/2 ($p = 0.001$). GFP signal intensity also appeared highest following intrastriatal rAAV2/9 injection to aged rats, however this intensity was not significantly higher than those observed in aged rats with intrastriatal rAAV2/5 or rAAV2/2 injection. These results suggest that comparisons in striatonigral protein delivery quantified using direct protein measurements in the SNpr can generally be predicted using quantification of near-infrared signal intensity within the injected striatum. These results also suggest that in the young adult

striatum, and to a lesser extent the aged striatum, rAAV2/9 results in the highest level of exogenous protein delivery.

iii. rAAV2/9 results in the largest area of striatal transduction in both young adult and aged rats.

The degree of vector spread away from the injection site can be a critical characteristic informing vector construct selection, particularly when targeting large structures like the striatum. To compare the area of striatal transduction between vectors we measured the area of the GFP immunoreactivity in the striatum for each vector at both ages (Figure 24d). Significant differences were observed in the size of the GFP+ transduction area in both the young adult ($F_{(2,16)}=44.56, p<0.001$) and aged ($F_{(2,13)}=37.67, p<0.001$) rats. Similar patterns were observed for both young adult and aged rats, with the transduction area of rAAV2/9 being significantly greater than all other vectors ($p<0.001$ for all comparisons in young adult and rAAV2/2 in aged, $p=0.002$ for rAAV2/5 in aged). Similarly, in rats of both ages the transduction area following rAAV2/5 injection was significantly greater than that achieved using intrastriatal rAAV2/2 (young adult, $p=0.005$; aged, $p=0.001$) (Figure 24d). Furthermore, no significant differences ($p>0.05$) were observed in the transduction area of any viral construct for aged as compared to young adult rats (Figure 24d), supporting previous reports that an age-dependent diffusivity barrier is not the mechanism of the decreased transduction efficiency [Polinski *et al*, 2015]. Collectively, our results using different vector constructs injected to the striatum indicate that despite reductions in transductions efficiency with advanced age, rAAV2/9 provides the greatest exogenous protein delivery and transduces the most striatal neurons compared to rAAV2/5 and rAAV2/2.

Discussion

In the present study, we systematically investigated the generalizability of previous findings that advanced age appears to present a barrier to efficient viral vector transduction in the rat brain [Wu *et al*, 2004; Polinski *et al*, 2015]. To this end, we injected rAAV2/2, rAAV2/5, rAAV2/9, and LV expressing GFP into the SNpc to transduce the nigrostriatal system or into the striatum to transduce the striatonigral system. We designated GFP expression in the anterograde structure as the primary determinant of transduction efficiency based on the ability of this outcome measure to provide a simultaneous readout of protein delivery and pathway specificity. We also used multiple additional outcome measures to quantify transduced neurons, measure GFP mRNA, and evaluate vector spread. In general, we observe a deficiency in transduction following injection of most of the viral vectors tested in the nigrostriatal and striatonigral systems. Importantly, age-related transduction deficiencies are not identical when targeting nigrostriatal versus striatonigral pathways. Specifically, following injections into the aged SNpc, transduction efficiency mediated by rAAV2/2, rAAV2/5, and LV is significantly compromised whereas rAAV2/9-mediated transduction is not negatively impacted by advanced age (Figure 14). Transduction in the aged striatonigral system is similarly compromised for all the rAAV pseudotypes; however, transduction mediated by LV is not deficient with age (Figure 18). For both neural pathways, however, rAAV2/9 emerged as the viral construct capable of delivering the most exogenous GFP protein to both young adult and aged rats, despite the age-related deficiency observed in transduction of the striatonigral system (Figure 23 and Figure 24). For transduction of the greatest number of nigrostriatal dopamine neurons, both rAAV2/5 and rAAV2/9 were superior to the other vector constructs, regardless of age. These results provide evidence that age-related transduction deficiencies are specific to viral construct and cannot be generalized across brain structures.

Another important finding of our study is that age-related transduction deficiencies (reduced GFP expression) in both neural pathways were not appreciable using quantitation of GFP+ cells. Unbiased stereological counts of GFP+ cells at the injection site did not reveal significant deficits in aged rats following SNpc or striatal injections, and differences in GFP protein delivery between vector constructs were not always detectable using GFP+ cell counts. This could be the result of multiple factors. For instance, the binary nature of cell counts (GFP+ “yes” or “no”) could conceal differences in per-cell multiplicity of infection (MOI) that could account for the observed decrease in GFP protein expression with advanced age. This possibility is corroborated by a previous report describing decreased immunoreactivity in individually transduced aged neurons following rAAV2/2 transduction of the aged and young adult rat septum [Wu *et al*, 2004]. Further, injections into the SNpc result in the transduction of both nigral dopamine neurons as well as other non-dopaminergic neurons in the SN and surrounding ventral mesencephalon. As a result, counts of GFP+ cells in the mesencephalon could provide an inaccurate picture of the relative numbers of GFP+/TH+ SNpc neurons.

Quantitation of GFP+ cells is the most common outcome measure used to report transduction efficiency [Davidson *et al*, 2000; Burger *et al*, 2004; Reimsnider *et al*, 2007; McFarland *et al*, 2009; Dodiya *et al*, 2010; Cannon *et al*, 2011; Van der Perren *et al*, 2012]. Our findings confirm previous reports in which rAAV2/9 generally results in the greatest number of GFP+ cells, followed by rAAV2/5 and lastly rAAV2/2 [Van der Perren *et al*, 2012]. Further, our results mirror those in which counts of GFP+/TH+ nigral neurons are greater following injection of rAAV2/5 into the SNpc compared to rAAV2/2 [McFarland *et al*, 2009]. However, despite the fact that both rAAV2/9 and rAAV2/5 resulted in similar numbers of transduced SNpc neurons, this only partially predicted GFP protein expression. These results indicate that caution should be exercised when using counts of GFP+ cells or GFP+/TH+ neurons to assess transduction efficiency.

The mechanism dictating vector-mediated transduction deficiencies in the aged brain is unclear. Previous studies have reported a doubling of astrocytes in the striatum of aged as compared to young adult rats [Yurek *et al*, 2015]. To investigate the possibility that the age-related transduction deficiencies in the striatum are due to increased numbers of astrocytes sequestering viral genomes from neurons, we analyzed the number of viral particles within neurons vs. astrocytes. We did not observe any appreciable qualitative differences in the number of astrocytes in the young adult versus aged rat striatum. Regardless of vector construct, viral genomes were overwhelmingly observed within neurons and rarely observed within astrocytes. Taken together, these results indicate that the mechanism of the age-related decrease in striatal AAV transduction is not due to astrocyte sequestration of viral particles.

The fact that age-related transduction deficiencies in the brain are not universal eliminates potential ubiquitous age-related impairments such as axonal transport deficits as a possible mechanism. Our present and past data demonstrating that vector spread appeared unaffected by aging [Polinski *et al*, 2015] also suggest that reduced diffusivity in the aged brain is not a factor. Instead, we suggest that capsid-mediated differences are implicated in the observed transduction deficiencies. We point to the fact that rAAV2/2 and rAAV2/5 transduction is deficient in the aged nigrostriatal system whereas rAAV2/9 is not. The viral genome of these three rAAV pseudotypes is identical, and the sole difference between them is the capsid used—implicating capsid-related steps of transduction in the age-related deficiencies for rAAV [Nonnenmacher and Weber, 2012]. One capsid-related step of transduction that could be deficient with age is receptor-mediated endocytosis. Each vector pseudotype uses a distinct set of receptors for endocytosis (main receptors: rAAV2, heparin sulfate proteoglycan [Summerford and Samulski, 1998; Qui *et al*, 2000]; rAAV5, 2,3-linked sialic acid [Walters *et al*, 2001]; rAAV9, N-linked galactose [Shen *et al*, 2011; Shen *et al*, 2012]; VSV-G LV, phosphatidylserine [Shin *et al*, 2010; Hwang and Schaffer, 2013]) and a precedence exists for a decrease in some receptors in the aged as compared to

young adult brain [Sato *et al*, 2001; Sasaki *et al*, 2002]. Furthermore, the qualitative and quantitative deficits in GFP mRNA we observed parallel protein deficits, further implicating steps of transduction prior to protein synthesis in our observed transduction deficiencies [Ryazanov and Nefsky, 2002; Nonnenmacher and Weber, 2012; Polinski *et al*, 2015]. Additional experiments will be required to determine the cause of the age-related transduction deficiencies in an effort to circumvent deficiencies and improve transduction in the aged brain.

Characterizing the efficiency of transduction between young adult and aged rats is important when using viral vectors as research tools in studies of aging or age-related disease. For instance, previous studies in our lab attempted to overexpress human wildtype alpha-synuclein (α -syn) using rAAV2/5 injected into the young adult and aged rat SNpc in order to investigate mechanisms of α -syn-related toxicity in the aged brain environment [Fischer *et al*, 2016]. Unbiased stereological estimates in the SNpc revealed equivalent neuronal loss between young adult and aged rats. Without the additional examination of α -syn protein expression, these results could have been misinterpreted to suggest that aging does not impact α -syn-mediated toxicity. However, measurements of exogenous human wildtype α -syn in the striatum revealed substantially less rAAV2/5-delivered α -syn protein in the aged as compared to young adult rat striatum [Fischer *et al*, 2016]. With this information, our results suggest the opposite conclusion—that aging exacerbates α -syn toxicity. Importantly, any paradigm utilizing viral vector-delivered protein to make comparisons between the aged and young adult brain should verify equivalent expression levels in their neural system of interest.

The striatum is the structure most often targeted in PD gene therapy clinical trials [Marks *et al*, 2010; Bartus *et al*, 2011; Palfi *et al*, 2014; Clinicaltrials.gov, NCT01621581] as this approach can be used to simultaneously provide exogenous protein to dopaminergic nigrostriatal terminals and anterogradely

deliver protein to the SN via the striatonigral pathway [Ciesielska *et al*, 2011; Kells *et al*, 2012]. In our laboratory we have successfully used intrastriatal transduction of the young adult rat striatum with a trophic factor (pleiotrophin) to protect the nigrostriatal dopamine system from 6-hydroxydopamine toxicity [Gombash *et al*, 2012]. Our present results suggest that despite the age-related deficiency in transduction observed, intrastriatal rAAV2/9 may be optimally suited to deliver the greatest amount of trophic factor to the aged striatonigral system (as well as the aged nigrostriatal system). However, it is important to note that multiple concerns underlie the use of rAAV9, such as an elicitation of an adaptive immune response and subsequent neuronal loss that has been associated with this vector [Ciesielska *et al*, 2013; Samaranch *et al*, 2014]. Furthermore, the ability of rAAV9 to cross the blood-brain-barrier and possibly escape the brain after intraparenchymal injection may also be an important consideration [Lowenstein *et al*, 2014]. It is possible that altering the promoter, transgene, vector backbone, or titer may combat some of these issues and improve the safety profile of the rAAV9 for use in gene therapy for neurodegenerative diseases [Lowenstein *et al*, 2014; Samaranch *et al*, 2014].

Gene therapy clinical trials for PD use rAAV2/2 or LV for transduction of the aged striatum [Marks *et al*, 2010; Bartus *et al*, 2011; Palfi *et al*, 2014; Clinicaltrials.gov, NCT01621581]. Our results demonstrate that striatonigral rAAV2/2 transduction is markedly reduced with aging and is less efficient compared to rAAV2/5 and rAAV2/9. Additional studies should be conducted to identify the optimal vector construct for safe and efficient transduction of the aged parkinsonian brain. Ideally, studies should be extended to also address whether expression of other transgenes is impacted by aging, especially those encoding biologically-relevant or secretable proteins such as glial cell line-derived neurotrophic factor (GDNF). The impact of age on viral vector transduction efficiency is an extremely important consideration as efficient transduction will be required for functionally-meaningful gene therapy for age-related neurodegenerative diseases.

LITERATURE CITED

LITERATURE CITED

- Bartus, R.T., C.D. Herzog, Y. Chu, A. Wilson, L. Brown, J. Siffert, E.M. Johnson Jr, C.W. Olanow, E.J. Mufson, and J.H. Kordower. (2011). Bioactivity of AAV2-neurturin gene therapy (CERE-120): differences between Parkinson's disease and nonhuman primate brains. *Mov Disord*, **26(1)**: 27-36.
- Benskey, M.J., and F.P. Manfredsson. (2016a). Lentivirus Production and Purification. *Methods Mol Biol*, **1382**: 107-114.
- Benskey, M.J., and F.P. Manfredsson. (2016b). Intraparenchymal stereotaxic delivery of rAAV and special consideration in vector handling. *Methods Mol Biol*, **1382**: 199-215.
- Benskey, M.J., I.M. Sandoval, and F.P. Manfredsson. (2016). Continuous collection of adeno-associated virus from producer cell medium significantly increases total viral yield. *Hum Gene Ther Methods*, **27(1)**: 32-45.
- Bjorklund, A., D. Kirik, C. Rosenblad, B. Georgievask, C. Lundberg, and R.J. Mandel. (2000). Towards a neuroprotective gene therapy for Parkinson's disease: use of adenovirus, AAV and lentivirus vectors for gene transfer of GDNF to the nigrostriatal system in the rat Parkinson model. *Brain Res*, **886(1-2)**: 82-98.
- Burger, C., O.S. Gorbatyuk, M.J. Velardo, C.S. Peden, P. Williams, S. Zolotukhin, P.J. Reier, R.J. Mandel, and N. Muzyczka. (2004). Recombinant AAV viral vectors pseudotyped with viral capsids from serotypes 1, 2, and 5 display differential efficiency and cell tropism after delivery to different regions of the central nervous system. *Mol Ther*, **10(2)**: 302-317.
- Cannon, J.R., T. Sew, L. Montero, E.A. Burton, and J.T. Greenamyre. (2011). Pseudotype-dependent lentiviral transduction of astrocytes or neurons in the rat substantia nigra. *Exp Neurol*, **228(1)**: 41-52.
- Choudhury, S.R., E. Hudry, C.A. Maguire, M. Sena-Esteves, X.O. Breakefield, and P. Grandi. (2016). Viral vectors for therapy of neurologic diseases. *Neuropharmacology*, doi: 10.1016/j.neuropharm.2015.02.013.
- Ciesielska, A., P. Hadaczek, G. Mittermeyer, S. Zhou, J.F. Wright, K.S. Bankiewicz, and J. Forsayeth. (2013). Cerebral infusion of AAV9 vector-encoding non-self proteins can elicit cell-mediated immune responses. *Mol Ther*, **21**: 158-166.
- Ciesielska, A., G. Mittermeyer, P. Hadaczek, A.P. Kells, J. Forsayeth and K.S. Bankiewicz. (2011). Anterograde axonal transport of AAV2-GDNF in rat basal ganglia. *Mol Ther*, **19(5)**: 922-927.
- ClinicalTrials.gov. (2015). AAV2-GDNF for Advanced Parkinson s Disease (NCT01621581). <https://http://www.clinicaltrials.gov/ct2/show/NCT01621581?term=gdnf&rank=1>.
- Collier, T.J., J. O'Malley, D.J. Rademacher, J.A. Stancati, K.A. Sisson, C.E. Sortwell, K.L. Paumier, K.G. Gebremedhin, and K. Steece-Collier. (2015). Interrogating the aged striatum: robust survival of

- grafted dopamine neurons in aging rats produces inferior behavioral recovery and evidence of impaired integration. *Neurobiol Dis*, **77**: 191-203.
- Collier, T.J., C.E. Sortwell, and B.F. Daley. (1999). Diminished viability, growth, and behavioral efficacy of fetal dopamine neuron grafts in aging rats with long-term dopamine depletion: an argument for neurotrophic supplementation. *J Neurosci*, **19(13)**: 5563-5573.
- Combs, B., A. Kneynsberg, and N.M. Kanaan. (2016). Gene therapy models of Alzheimer's and other dementias. *Methods Mol Biol*, **1382**: 339-366.
- Cummings, J.L., S.J. Banks, R.K. Gary, J.W. Kinney, J.M. Lombardo, R.R. Walsh, and K. Zhong. (2013). Alzheimer's disease drug development: translational neuroscience strategies. *CNS Spectrums* **18(3)**: 128-138.
- Davidson, B.L., C.S. Stein, J.A. Heth, I. Martins, R.M. Kotin, T.A. Derksen, J. Zabner, A. Ghodsi, and J.A. Chiorini. (2000). Recombinant adeno-associated virus type 2, 4, and 5 vectors: transduction of variant cell types and regions in the mammalian central nervous system. *PNAS*, **97(7)**: 3428-3432.
- Dodiya, H.B., T. Bjorklund, J. Stansell III, R.J. Mandel, D. Kirik, and J.H. Kordower. (2010). Differential transduction following basal ganglia administration of distinct pseudotyped AAV capsid serotypes in nonhuman primates. *Mol Ther*, **18(3)**: 579-587.
- Emborg, M.E., J. Moirano, J. Raschke, V. Bondarenko, R. Zufferey, S. Peng, A.D. Ebert, V. Joers, B. Roitberg, J.E. Holden, J. Koprach, J. Lipton, J.H. Kordower, and P. Aebischer. (2009). Response of aged parkinsonian monkeys to in vivo gene transfer of GDNF. *Neurobiol Dis*, **36(2)**: 303-311.
- Fischer, D.L., S.E. Gombash, C.J. Kemp, F.P. Manfredsson, N.K. Polinski, M.F. Duffy, and C.E. Sortwell. (2016). Viral vector-based modeling of neurodegenerative disorders: Parkinson's disease. *Methods Mol Biol*, **1382**: 367-382.
- Gao, L., M. Hidalgo-Figueroa, L.M. Escudero, J. Diaz-Martin, J. Lopez-Barneo, and A. Pascual. (2013). Age-mediated transcriptomic changes in adult mouse substantia nigra. *PLoSone*, **9(4)**: e62456.
- Gombash, S.E., J.W. Lipton, T.J. Collier, L. Madhavan, K. Steece-Collier, A. Cole-Strauss, B.T. Terpstra, A.L. Spieles-Engemann, B.F. Daley, S.L. Wohlgenant, V.B. Thompson, F.P. Manfredsson, R.J. Mandel, and F.P. Manfredsson. (2012). Striatal pleiotrophin overexpression provides functional and morphological neuroprotection in the 6-hydroxydopamine model. *Mol Ther*, **20(3)**: 544-554.
- Grabinski, T.M., A. Kneynsberg, F.P. Manfredsson, and N.M. Kanaan. (2015). A method of combining RNAscope in situ hybridization with immunohistochemistry in thick free-floating brain sections and primary neuronal cultures. *PLoS One*, **10(3)**: e0120120.
- Herzog, C.D., L. Brown, D. Gammon, B. Kruegel, R. Lin, A. Wilson, A. Bolton, M. Printz, M. Gasmi, K.M. Bishop, J.H. Kordower, and R.T. Bartus (2008). Expression, bioactivity, and safety 1 year after adeno-associated viral vector type 2-mediated delivery of neuritin to the monkey nigrostriatal system support CERE-120 for Parkinson's disease. *Neurosurgery*, **64(6)**: 602-613.

- Hwang, B.Y., and D.V. Schaffer. (2013). Engineering a serum-resistant and thermostable vesicular stomatitis virus G glycoprotein for pseudotyping retroviral and lentiviral vectors. *Gene Ther*, **20**: 807-815.
- Kells, A.P., J. Forsayeth, and K.S. Bankiewicz. (2012). Glial-derived neurotrophic factor gene transfer for Parkinson's disease: anterograde distribution of AAV2 vectors in the primate brain. *Neurobiol Dis*, **48(2)**: 228-235.
- Klein, R.L., R.D. Dayton, C.G. Diaczynsky, and D.B. Wang. (2010). Pronounced microgliosis and neurodegeneration in aged rats after tau gene transfer. *Neurobiol Aging*, **31(12)**: 2091-2102.
- Kordower J.H., M.E. Emborg, J. Bloch, S.Y. Ma, Y. Chu, L. Leventhal, J. McBride, E.Y. Chen, S. Palfi, B.Z. Roitberg, W.D. Brown, J.E. Holden, R. Pyzalski, M.D. Taylor, P. Carvey, Z. Ling, D. Trono, P. Hantraye, N. Deglon, and P. Aebischer. (2000). Neurodegeneration prevented by lentiviral vector delivery of GDNF in primate models of Parkinson's disease. *Science*, **290**:767–773.
- Leone, P., D. Shera, S.W. McPhee, J.S. Francis, E.H. Kolodny, L.T. Bilaniuk, D.J. Wang, M. Assadi, O. Goldfarb, H.W. Goldman, A. Freese, D. Young, M.J. During, R.J. Samulski, and C.G. Janson. (2012). Long-term follow-up after gene therapy for canavan disease. *Sci Transl Med*, **19(4)**: 165ra163.
- Leys, C., C. Ley, O. Klein, P. Bernard, and L. Licata. (2013). Detecting outliers: Do not use standard deviation around the mean, use absolute deviation around the median. *J Exp Soc Psychol*, **49**: 764-766.
- Lowenstein, P.R., V.N. Yadav, P. Chockley, and M. Castro. (2014). There must be a way out of here: Identifying a safe and efficient combination of promoter, transgene, and vector backbone for gene therapy of neurological disease. *Mol Ther*, **22(2)**: 246-247.
- Maguire, C., S.H. Ramirez, S.F. Merkel, M. Sena-Esteves, and X.O. Breakefield. (2014). Gene therapy for the nervous system: challenges and new strategies. *Neurotherapeutics*, **11(4)**: 817-839.
- Marks Jr., W.J., R.T. Bartus, J. Siffert, C.S. Davis, A. Lozano, N. Boulis, J. Vitek, M. Stacy, D. Turner, L. Verhagen, R. Bakay, R. Watts, B. Guthrie, J. Jankovic, R. Simpson, M. Tagliati, R. Alterman, M. Stern, G. Baltuch, P.A. Starr, P.S. Larson, J.L. Ostrem, J. Nutt, K. Kiebertz, J.H. Kordower, and C.W. Olanow. (2010). Gene delivery of AAV2-neurturin for Parkinson's disease: a double-blind randomized, controlled trial. *Lancet*, **9**: 1164-1172.
- McFarland, N.R., J. Lee, B.T. Hyman, and P.J. McLean. (2009). Comparison of transduction efficiency of recombinant AAV serotypes 1, 2, 5, and 8 in the rat nigrostriatal system. *J Neurochem*, **109**: 838-845.
- Nanou, A., and M. Azzouz. (2009). Gene therapy for neurodegenerative diseases based on lentiviral vectors. *Prog Brain Res*, **175**: 187-200.
- Nobre, R.J., and L.P. Almeida. (2011). Gene therapy for Parkinson's and Alzheimer's disease: from the bench to clinical trials. *Curr Pharm Des*, **17(31)**: 3434-3445.

- Nonnenmacher, M., and T. Weber. (2012). Intracellular transport of recombinant adeno-associated virus vectors. *Gene Ther*, **19(6)**: 649-658.
- O'Callaghan, J.P., and D.B. Miller. (1991). The concentration of glial fibrillary acidic protein increases with age in the mouse and rat brain. *Neurobiol Aging*, **12**: 171-174.
- O'Connor, D.M. and N.M. Boulis. (2015). Gene therapy for neurodegenerative diseases. *Trends Mol Med*, **21(8)**: 504-512.
- Olanow, C.W., R.T. Bartus, T.L. Baumann, S. Factor, N. Boulis, M. Stacy, D.A. Turner, W. Marks, P. Larson, P.A. Starr, J. Jankovic, R. Simpson, R. Watts, B. Guthrie, K. Poston, J.M. Henderson, M. Stern, G. Baltuch, C.G. Goetz, C. Herzog, J.H. Kordower, R. Alterman, A.M. Lozano, and A.E. Lang. (2015). Gene delivery of neurturin to putamen and substantia nigra in Parkinson's disease: a double-blind, randomized, controlled trial. *Ann Neurol*, **78(2)**: 248-257.
- Palfi, S., J.M. Gurruchaga, G.S. Ralph, H. Lepetit, S. Lavis, P.C. Buttery, C. Watts, J. Miskin, M. Kellher, S. Deeley, H. Iwamuro, J.P. Lefaucheur, C. Thiriez, G. Fenelon, C. Lucas, P. Brugieres, I. Gabriel, K. Abhay, X. Drouot, N. Tani, A. Kas, B. Ghaleh, P. Le Corvoisier, P. Dolphin, D.P. Breen, S. Mason, N. Valle Guzman, N.D. Mazarakis, P.A. Radcliffe, R. Harrop, S.M. Kingsman, O. Rascol, S. Naylor, R.A. Barker, P. Hantraye, P. Remy, P. Cesaro, and K.A. Mitrophanous. (2014). Long-term safety and tolerability of ProSavin, a lentiviral vector-based gene therapy for Parkinson's disease: a dose escalation, open-label, phase 1/2 trial. *Lancet*, **383**: 1138-1146.
- Pfaffl, M.W., G.W. Horgan, and L. Dempfle. (2002). Relative expression software tool (REST©) for group-wise comparison and statistical analysis of relative expression results in real-time PCR. *Nucleic Acids Res*, **30(9)**: e36.
- Polinski, N.K., S.E. Gombash, F.P. Manfredsson, J.W. Lipton, C.J. Kemp, A. Cole-Strauss, N.M. Kanaan, K. Steece-Collier, N.C. Kuhn, S.L. Wohlgenant, and C.E. Sortwell (2015). Recombinant adeno-associated virus 2/5-mediated gene transfer is reduced in the aged rat midbrain. *Neurobiol Aging*, **36(2)**: 1110-1120.
- Qiu, J., A. Handa, M. Kirby, and K.E. Brown. (2000). The interaction of heparin sulfate and adeno-associated virus 2. *Virology*, **269**: 137-147.
- Reimsnider, S., F.P. Manfredsson, N. Muzyczka, and R.J. Mandel. (2007). Time course of transgene expression after intrastriatal pseudotyped rAAV2/1, rAAV2/2, rAAV2/5, and rAAV2/8 transduction in the rat. *Mol Ther*, **15(8)**: 1504-1511.
- Ryazanov, A.G., and B.S. Nefsky. (2002). Protein turnover plays a key role in aging. *Mech Age Dev*, **123**: 207-213.
- Samaranch, L., W. San Sebastian, A.P. Kells, E.A. Salegio, G. Heller, J.R. Bringas, P. Pivrotto, S. DeArmond, J. Forsayeth, and K.S. Bankiewicz. (2014). AAV9-mediated expression of a non-self protein in nonhuman primate central nervous system triggers widespread neuroinflammation driven by antigen-presenting cell transduction. *Mol Ther*, **22(2)**: 329-337.

- Sasaki, T., Y. Akimoto, Y. Sato, H. Kawakami, H. Hirano, and T. Endo. (2002). Distribution of sialoglycoconjugates in the rat cerebellum and its change with aging. *J Histo Cyto*, **50(9)**: 1179-1186.
- Sato, Y., Y. Akimoto, H. Kawakami, H. Hirano, and T. Endo. (2001). Location of sialoglycoconjugates containing the sialyl-2-3Gal and sialyl-2-6Gal groups in the rat hippocampus and the effect of aging on their expression. *J Histo Cyto*, **49(10)**: 1311-1319.
- Schmittgen, T.D., and K.J. Livak. (2008). Analyzing real-time PCR data by the comparative C(T) method. *Nat Protoc*, **3**: 1101-1108.
- Shen, S., K.D. Bryant, S.M. Brown, S.H. Randell, and A. Asokan. (2011). Terminal N-linked galactose is the primary receptor for adeno-associated virus 9. *J Biol Chem*, **286**: 13532-13540.
- Shen, S., Bryant, KD, Sun, J, Brown, SM, Troupes, A, Pulicherla, N, and A. Asokan. (2012). Glycan binding avidity determines the systemic fate of adeno-associated virus type 9. *J Virol*, **86(19)**: 10408-10417.
- Shin, S., H.M. Tuinstra, D.M. Salvay, and L.D. Shea. (2010). Phosphatidylserine immobilization of lentivirus for localized gene transfer. *Biomaterials*, **31(15)**: 4353-4359.
- Stocchi, F., and C.W. Olanow. (2013). Obstacles to the development of a neuroprotective therapy for Parkinson's disease. *Mov Disord*, **28(1)**: 3-7.
- Summerford, C., and R.J. Samulski. (1998). Membrane-associated heparin sulfate proteoglycan is a receptor for adeno-associated virus type 2 virions. *J Virology*, **72(2)**: 1438-1445.
- Tuszynski, M.H., J.H. Yang, D. Barba, U. HS, R.A. Bakay, M.M. Pay, E. Masliah, J.M. Conner, P. Robalka, S. Roy, and A.H. Nagahara. (2015). Nerve growth factor gene therapy: activation of neuronal responses in Alzheimer's disease. *JAMA Neurol*, **72(10)**: 1139-1147.
- Van der Perren, A., J. Toelen, J.M. Taymans, and V. Baekelandt. (2012). Using recombinant adeno-associated viral vectors for gene expression in the brain. *Neuromethods*, **65**: 47-68.
- Walters, R.W., S.M. Yi, S. Keshavjee, K.E. Brown, M.J. Welsh, J.A. Chiorini, and J. Zabner. (2001). Binding of adeno-associated virus type 5 to 2,3-linked sialic acid is required for gene transfer. *J Biol Chem*, **276**: 20610-20616.
- Weller, M.L., I.M. Stone, A. Goss, T. Rau, C. Rova, and D.J. Poulsen. (2008). Selective overexpression of excitatory amino acid transporter 2 (EAAT2) in astrocytes enhances neuroprotection from moderate but not severe hypoxia-ischemia. *Neuroscience*, **155(4)**: 1204-1211.
- Wu, K., C.A. Meyers, N.K. Guerra, M.A. King, and E.M. Meyer. (2004). The effects of rAAV2-mediated NGF gene delivery in adult and aged rats. *Mol Ther*, **9(2)**: 262-269.
- Yurek, D.M., U. Hasselrot, W.A. Cass, O. Sesenoglu-Laird, L. Padegimas, and M.J. Cooper. (2015). Age and lesion-induced increases of GDNF transgene expression in brain following intracerebral injections of DNA nanoparticles. *Neuroscience*, **284**: 500-512.

Zolotukhin, S., B.J. Byrne, E. Mason, E. Zolotukhin, M. Potter, K. Chesnut, C. Summerford, R.J. Samulski, and N. Muzyczka. (1999). Recombinant adeno-associated virus purification using novel methods improves infectious titer and yield. *Gene Ther*, **6**: 973-985.

Chapter 4. Age-related deficiencies exist in rAAV2/2 GDNF transduction of the basal ganglia following intrastriatal injection in rats.

Abstract

In an effort to slow or halt the progression of Parkinson's disease (PD)—the second most common neurodegenerative disease—clinical trials are currently investigating the possibility of using viral vectors to overexpress neurotrophic factors in brain regions involved in PD motor deficits. One clinical trial that is currently recruiting patients is using recombinant adeno-associated virus serotype 2/2 to deliver human glial cell line-derived neurotrophic factor (rAAV2/2 GDNF). Unfortunately, a recent clinical trial that used rAAV2/2 to deliver a GDNF-homolog did not result in functional benefits for PD patients. This could partially be due to the fact that rAAV2/2 has been shown to be less efficient in the aged as compared to young adult brain and the preclinical work that led to the clinical trials for PD almost exclusively used young adult animals. To test whether age impacts rAAV2/2 GDNF transduction, we used intrastriatal injections of rAAV2/2 GDNF in young adult (3 month) and aged (20 month) rats to measure transduction efficiency and downstream GDNF-mediated neuroprotective signaling. At one month post-injection, robust age-related deficiencies were observed at the level of GDNF protein in the injected striatum and anterograde structures of the direct and indirect pathways. These deficiencies were not observed at the level of GDNF mRNA in the striatum. Furthermore, phosphorylation of ribosomal protein S6 (pS6) was used as a marker of GDNF prosurvival signaling cascades involving Akt and ERK. Aged rats displayed significantly greater baseline levels of pS6 in nigral dopaminergic neurons as compared to young adult rats that did not change following rAAV2/2 GDNF injection for either age. These results indicate a robust age-related deficiency in rAAV2/2 GDNF transduction of the rat basal ganglia. In addition, this study is the first to find significant increases in pS6 levels in the rat SNpc with

age. Taken together, age is an important factor in transduction efficiency and downstream signaling for rAAV2/2 GDNF.

Introduction

Parkinson's disease (PD) is classified as a motor disease that arises from degeneration of the nigrostriatal system which sends dopaminergic projections from cell bodies in the substantia nigra pars compacta (SNpc) to the striatum. This disease is the second most common neurodegenerative disease, after Alzheimer's disease, and currently affects approximately 1 million Americans over the age of 65 [Parkinson's Disease Foundation, 2016]. Although this disease was first classified almost 200 years ago [Parkinson, 2002], no treatment is available that can slow or alter the progression of PD [Olanow, 2009; de la Fuente-Fernandez et al, 2010]. Furthermore, the increase in life expectancy and aging of the Baby Boomer generation in the United States is expected to increase the prevalence of PD in the coming decades, leading to an ever-pressing need to develop a disease-modifying treatment for PD [Dorsey *et al*, 2007].

Viral vector-mediated gene therapy is currently being investigated for its potential to deliver transgenes of interest to affected brain regions in PD and thereby slow or halt disease progression. The potential for viral vectors to deliver neurotrophic factors to the striatum or SNpc in PD patients is an especially promising strategy as proteins such as glial cell line-derived neurotrophic factor (GDNF) and neurturin, a GDNF-homolog, have been shown to have neuroprotective and neurorestorative effects in various animal models of PD after direct infusion of the protein [Hoffer *et al*, 1994; Gash *et al*, 1996].

Unfortunately, translation of direct GDNF infusion into the PD brain in patients led to dangerous side effects and a lack of functional efficacy [Nutt *et al*, 2003; Lang *et al*, 2006]. It is believed that the delivery

avenue of GDNF must be perfected in order to achieve clinical efficacy without damaging adverse effects [d'Anglemont de Tassigny *et al*, 2015].

Viral vectors allow for spatially- and physiologically-controlled transgene expression by using the host cell machinery to produce the protein of interest. This improved control led to the development of viral vectors expressing GDNF and other related neurotrophic factors for the treatment of PD. Preclinical trials using recombinant adeno-associated virus (rAAV) or lentivirus (LV) to deliver GDNF or neurturin have shown neuroprotective and neurorestorative effects in multiple PD animal models [Bjorklund *et al*, 2000; Kirik *et al*, 2000; Kordower *et al*, 2000; Herzog *et al*, 2008]. This promise led to the testing of rAAV serotype 2/2 expressing neurturin (CERE-120) in Phase I and Phase II clinical trials for PD [Marks *et al*, 2010; Bartus *et al*, 2011]. Unfortunately, the clinical trials with CERE-120 were not successful, with no functional recovery over the placebo effect or benefits above those offered by conventional dopaminergic therapies [Bartus *et al*, 2011].

Following the death of two patients who received CERE-120, authors noted lower-than-expected levels of neurturin expression in the SNpc [Bartus *et al*, 2011]. Authors concluded that this low expression of neurturin in the SNpc could have contributed to the lack of functional benefit after CERE-120 treatment in patients [Bartus *et al*, 2011]. This conclusion is further supported by studies in non-human primates that found a strong correlation between GDNF overexpression, neuroanatomical markers of recovery, and behavioral measures of recovery, with a threshold of expression existing that must be surpassed in order to receive benefit from the treatment [Emborg *et al*, 2009]. Although this low expression could be due to a variety of reasons such as recruitment of late-stage patients and improper targeting, it should be noted that the vast majority of preclinical trials testing the efficacy of viral vectors delivering neurturin or GDNF were performed in young adult animals modeling PD, therefore failing to account for

aging in an age-related disease [Bjorklund *et al*, 2000; Kirik *et al*, 2000; Kordower *et al*, 2000; Herzog *et al*, 2008].

Importantly, a few previous studies have investigated the impact of age on viral vector-mediated gene transfer to the brain. In one such study, rAAV2/2 expressing nerve growth factor (rAAV2/2 NGF) was injected into the septum to transduce neurons of young adult and aged rats [Wu *et al*, 2004]. Age presented a significant barrier to rAAV2/2 NGF transduction in the rat septum, with aged rats exhibiting significantly lower levels of transgene expression as compared to young adult rats [Wu *et al*, 2004]. Furthermore, age-related transduction deficiencies with rAAV2/2 were also observed in the nigrostriatal and striatonigral systems of the rat brain—the two systems commonly targeted in viral vector-mediated gene therapy for PD. In this study, rAAV2/2 was used to overexpress green fluorescent protein (rAAV2/2 GFP) to transduce the nigrostriatal system following injection to the SNpc or striatonigral system following intrastriatal injection in young adult (3 month) and aged (20 month) rats [Dissertation Chapter 3]. rAAV2/2 GFP in both systems resulted in significantly less GFP protein expression in the aged versus young adult rat [Dissertation Chapter 3]. Taken together, these results highlight the importance of investigating the impact of age on viral vector-mediated gene transfer when using viral vectors in aged animal models or patients with age-related neurodegenerative diseases such as PD.

In this study, we directly investigate the transduction efficiency of rAAV2/2 expressing GDNF (rAAV2/2 GDNF) as this construct will be used in a clinical trial currently recruiting PD patients [Clinicaltrials.gov, NCT01621581]. It is important to directly test this construct for age-related transduction deficiencies as the only other transgene tested for viral vector-mediated overexpression in the striatonigral and nigrostriatal system was GFP—a protein that is not endogenously expressed or secreted like GDNF. As a result, we are mirroring the proposed clinical trial by using rAAV2/2 GDNF injections to the striatum to

overexpress GDNF in the striatum and anterograde structures like the SN pars reticulata (SNpr), globus pallidus (GP), and entopeduncular nucleus (EP) where GDNF overexpression would aid recovery from PD symptoms [Ciesielska *et al*, 2011]. One month following rAAV2/2 GDNF injection to the striatum of young adult (3 month) and aged (20 month) Fischer344 rats, GDNF protein expression was significantly lower in the aged as compared to young adult rat striatum, GP, EP, and trending towards a decrease in the SNpr. Interestingly, GDNF mRNA levels in the injected striatum were equivalent between young adult and aged rats at this time-point. Furthermore, we measured downstream GDNF neuroprotective signal activation in the ipsilateral SNpc to determine whether the age-related transduction deficiency was biologically-relevant. Results from this study highlight the importance of accounting for age when designing therapeutic strategies for age-related diseases.

Methods

I. Experimental Overview

For GDNF-expression studies, cohorts of Fischer344 (F344) rats, 8 young adult (3 months old) and 12 aged (20 months old) were bilaterally injected into the striatum with rAAV2/2 overexpressing human wildtype GDNF (rAAV2/2 GDNF) for striatonigral transduction. Rats were sacrificed at one month post-injection and tissue was processed appropriately for the designated outcome measures. The left striatum, GP, EP and SNpr were used for GDNF ELISA. The left SNpc was used for Western blot for pS6 levels. The right striatum was used for GDNF qPCR. The right midbrain tissue was used for immunohistochemical staining for pS6 intensity measures. Outlier removal was only performed on the ELISA-designated tissue as this was the only tissue in which injection accuracy could be verified. To assess injection success, we compared the striatal GDNF protein level of rAAV2/2 GDNF-injected rats to GDNF levels in the naïve young adult striatum. The average level of overexpression after injection was

73x that of naïve GDNF levels. If expression after injection was not greater than 30x that of naïve GDNF protein levels, injections were labeled as a failure due to clogged needles or inaccurate targeting. In addition, outliers were confirmed using a second method in which levels of SNpr GDNF were compared to levels of striatal GDNF. The two outliers indicated by the first method displayed an impossibly high ratio of SNpr:striatal GDNF with over 120% striatal GDNF undergoing axonal transport to the SNpr whereas all other rats displayed approximately 20% of striatal GDNF transported. These illogical numbers confirmed exclusion of these two rats as outliers. An overview of the experimental design can be seen in Figure 25.

II. Animals

Male, F344 rats (National Institute on Aging, Bethesda, MD) 3 months of age (n = 8) and 20 months of age (n = 12) were used in this study. All animals were given food and water *ad libitum* and housed in 12h reverse light-dark cycle conditions in the Van Andel Research Institute vivarium, which is fully AAALAC approved. All procedures were conducted in accordance with guidelines set by the Institutional Animal Care and Use Committee (IACUC) of Michigan State University.

III. Viral Vectors

The rAAV2/2 GDNF viral vector construct was purchased from the University of Florida Powell Gene Therapy Center Vector Core (University of Florida, Gainesville, FL). Plasmid and vector production were completed as previously described [Zolotukhin *et al*, 1999; Benskey and Manfredsson, 2016a; Benskey and Manfredsson, 2016b]. For all vectors, expression of the transgene was driven by the chicken beta actin/cytomegalovirus enhancer (C β A/CMV) promoter hybrid. In short, human wildtype GDNF (GDNF)

rAAV2/2 GDNF

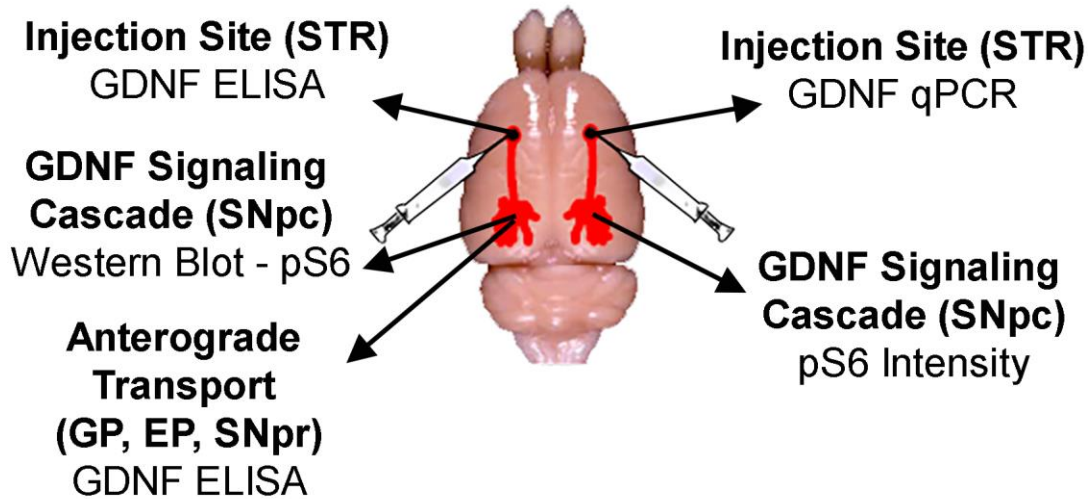


Figure 25. Schematic of experimental design of rAAV2/2 GDNF striatonigral transduction experiments. Rats were injected bilaterally into the striatum with rAAV2/2 overexpressing human wildtype GDNF. One month after injection, rats were sacrificed and tissue was processed for the designated outcome measures. The left striatum was used for GDNF ELISA to measure GDNF protein at the injection site. The left GP, EP, and SNpr were used for GDNF ELISA to measure GDNF protein in anterograde structures. The left SNpc was used for pS6 Western blot to quantify downstream GDNF pro-survival signaling in the SNpc. The right striatum was used for GDNF qPCR to measure GDNF mRNA expression at the injection site. The right midbrain was used for immunofluorescent staining to measure pS6 intensity as a readout of downstream GDNF pro-survival signaling at a cellular level. Abbreviations: rAAV2/2, recombinant adeno-associated virus pseudotype 2/2; GDNF, human wildtype glial cell line-derived neurotrophic factor; STR, striatum; ELISA, enzyme-linked immunosorbent assay; SNpc, substantia nigra pars compacta; pS6, phosphorylated ribosomal protein S6; GP, globus pallidus; EP, entopeduncular nucleus; SNpr, substantia nigra pars reticulata; qPCR, quantitative polymerase chain reaction.

was inserted into an AAV plasmid backbone. The vector contained AAV2 inverted terminal repeats (ITRs) and was packaged into AAV2 capsids via co-transfection with a plasmid containing *rep* and *cap* genes and adenovirus helper functions. Particles were purified using iodixanol gradients followed by column chromatography, and dotblot was used to determine vector titer [Benskey *et al*, 2016]. The vector titer used in this study was 1.26×10^{12} genomes/mL. All surfaces (syringes, pipettes, and microcentrifuge tubes) were coated in SigmaCote (Sigma-Aldrich, St. Louis, MO) prior to coming in contact with the virus to minimize binding of viral particles [Benskey and Manfredsson, 2016b].

IV. Viral Vector Injections

All surgical procedures were performed under isoflurane anesthesia (5% in O₂ for induction and 2% in O₂ for maintenance). Rats were placed in a stereotaxic frame and a Hamilton syringe fitted with a glass capillary needle (Hamilton Gas Tight syringe 80,000, 26s/2" needle; Hamilton, Reno, NV; coated in SigmaCote) was used for injections. For intrastriatal injections of GDNF-expressing viruses, one 2 μ L injection was injected in the each striatum at coordinates (from dura) AP +0.0mm, ML \pm 2.7mm, DV -4.0mm in the young adult and adjusted to AP +0.0mm, ML \pm 3.0mm, DV -4.0mm in the aged rat [Gombash *et al*, 2012]. The glass needle was lowered to the site and vector injection began immediately at a rate of 0.5 μ l/minute and remained in place after the injection for an additional 5 minutes before retraction.

V. Sacrifice and Tissue Preparation

All rats were sacrificed one month post-injection. Rats were deeply anesthetized (60mg/kg, pentobarbital, i.p.) and perfused intracardially with 0.9% saline containing 1ml/10,000 USP heparin, followed by ice cold 0.9% saline. Rat brains were immediately removed and hemisected in the coronal plane at approximately AP -2.64mm. The rostral portion of the brain containing the striatum was flash

frozen and processed for microdissections. The caudal portion of the brain was further hemisected using an aluminum brain blocker (Zivic, Pittsburg, PA) in the sagittal plane at the midline. The left portion was flash frozen and processed for microdissections whereas the right portion was post-fixed and processed for immunohistochemistry.

VI. Microdissections

After brain removal, brains were chilled in ice-cold saline for 2 min and immediately hemisected in the coronal and sagittal planes. Tissue designated for microdissection was flash frozen in 2-methylbutane on dry ice and stored at -80°C. For all microdissections, brains were transferred from -80°C to -20°C before microdissections. Brains were mounted on metal chucks with Tissue-Tek O.C.T. (VWR, Vavaria, IL) before being mounted in the cryostat at -15°C.

i. Tissue for GDNF ELISA (Left Striatum, GP, EP, and SNpr)

Tissue was sectioned to the level of the structure of interest and punches were taken from the rostral face of the brain structures once the structure was definitively apparent to ensure precision. The striatum was punched with a 2mm x 2mm circular punch, whereas the GP, EP, and SNpr were punched with a 2mm x 1mm oval punch using a custom tissue punch. Tissue punches were placed in separate pre-frozen microcentrifuge tubes and stored at -80°C until time of analysis.

ii. Tissue for GDNF RNA Analyses (Right Striatum)

All surfaces and instruments were sprayed with RNase Away (Invitrogen, Carlsbad, CA) when collecting tissue for RNA analyses. Tissue was sectioned until the striatum became visible. Punches were taken from the rostral face of the striatum once the structure was definitively apparent to ensure precision. A 2mm x 2mm circular punch of tissue was taken of the striatum for GDNF RNA analyses. Tissue punches

were placed in separate pre-frozen RNase-free microcentrifuge tubes containing TRIzol Reagent (Invitrogen, Grand Island, NY) and tissue was homogenized with a pestle before storage. Samples were stored at -80°C until time of assay.

iii. Tissue for pS6 Protein Analyses (Left SNpc)

Tissue was sectioned until the level of the SNpc. Punches were taken from the rostral face of the SNpc once the structure was definitively apparent to ensure precision. A 2mm x 1mm oval punch was taken of the SNpc using a custom tissue punch. Tissue punches were placed in separate pre-frozen microcentrifuge tubes and stored at -80°C until time of analysis.

VII. GDNF ELISA

GDNF ELISAs were completed using the Promega GDNF E_{max}[®] ImmunoAssay System kit (Promega G7621, Madison, WI) following all kit instructions. The protein concentrations for the different structures analyzed were determined using naïve striatal and SN tissue samples to measure endogenous levels of GDNF, as well as with dilution curves on a few samples per age and tissue structure. Briefly, the tissue punches collected for GDNF ELISAs were homogenated in a solution of T-PER (Pierce, Rockford, IL) and protease inhibitors (Thermo Scientific, Waltham, MA) using a 300 V/T Ultrasonic Homogenizer (BioLogics, Manassas, VA). Total protein concentration was determined by the Bradford protein assay. Plates were coated with the provided anti-GDNF monoclonal antibody in carbonate coating buffer through an overnight incubation. Blocking with performed using the provided Block and Sample Buffer followed by addition of the GDNF standards and samples. Samples were diluted to the following concentrations in this study: striatum (1:200), GP (1:40), EP (1:20), and SNpr (1:40). After incubation of the samples for 6hrs shaking at room temp, the provided anti-GDNF polyclonal antibody was added for an overnight incubation at 4°C. Anti-chicken IgY HRP conjugate (provided by the kit) was then added to

the plates for a 2 hour incubation at room temperature, followed by addition of TMB OneSolution (provided by the kit) for 15 minutes at room temp. To stop development, 1N HCl was added and the absorbance was read at 450nm on a spectrophotometer (Thermo Scientific, Waltham, MA). GDNF concentrations determined by the ELISA were divided by the protein concentrations determined by the Bradford assay and multiplied by 1000 to get the pg/mg GDNF to total protein ratio.

VIII. RNA Isolation and cDNA Synthesis

RNA was isolated using the QIAshredder (Qiagen, Valencia, CA) and RNeasy Plus Mini kit (Qiagen, Valencia, CA). The Qiagen protocol for purification of total RNA from animal tissue was used. RNA from tissue was then converted into cDNA using SuperScript VILO Master Mix (Life Technologies, Grand Island, NY). The RNA was assumed to be converted 100% to cDNA.

IX. GDNF qPCR

GDNF qPCR reactions were carried out with 1x TaqMan Universal Mastermix (ABI, Carlsbad, CA), and a ThermoFischer Human GDNF qPCR set (ThermoFischer Hs01931883_s1, Waltham, MA). A total of 20ng of cDNA was added to each 50µl reaction mixture, which also contained the primer-probe mixture from the qPCR set and TaqMan master mix. qPCR reactions to control for cDNA quantities were run using GAPDH (Life Technologies 4352338E, Grand Island, NY) as an endogenous control that is not altered with advanced age in F344 rats [Slagboon *et al*, 1990]. The qPCR reactions were run on an ABI 7500 real-time thermocycler using the following setup: Step1: Incubation at 50°C for 2 minutes. Step 2: Incubation at 95°C for 10 minutes. Step 3: Denaturation at 95°C for 15 seconds followed by annealing-elongation at 60°C for 1 minute followed by data collection. Step 3 was cycled 40 times for the qPCR run. Cycle thresholds were chosen during the linear phase of amplification using the AutoC_T function. All samples were run on the same plate along with a no-template control. Analysis was first carried out using the 2⁻

ΔCT method [Schmittengen and Livak, 2008] and Relative Expression Software Tool (REST-XL) method [Pfaffl *et al*, 2002].

X. pS6 Western Blot

SNpc samples for pS6 western blot analyses were homogenized on ice in 2% SDS. Total protein concentration was determined by the Bradford protein assay. Samples were prepared at 30ng total protein samples. Western blot protocol was completed as previously described [Polinski *et al*, 2015; Dissertation Chapter 3]. Samples were run using SDS-PAGE and transferred to Immobilon-FL membranes (Millipore, Bedford, MA). Membranes were incubated in pS6 antisera (Cell Signaling, Danvers, MA; rabbit anti-pS6, 2211S, 1:400) with β -tubulin antisera (Cell Signaling, Danvers, MA; mouse monoclonal IgG, 4466, 1:1,000) overnight. IRDye800 conjugated goat anti-rabbit (LI-COR Biosciences; 926-32211, 1:15,000) and IRDye680 conjugated goat anti-mouse (LI-COR Biosciences, 926-68020, 1:15,000) were used as secondary antibodies. All antibody dilutions were made in LI-COR compatible StartingBlock™ T20 (TBS) Blocking Buffer (Thermo Scientific, Waltham, MA). Multiplexed signal intensities were imaged with both 700 and 800 nm channels in a single scan with a resolution of 169 μm using the Odyssey infrared image system (LI-COR Biosciences). Reported integrated intensity measurements of pS6 expression were normalized according to the corresponding β -tubulin densitometry measurements. The representative image was produced in Photoshop 7.0 (San Jose, CA).

XI. Immunofluorescence

The portion of the brains designated for immunohistochemistry were post-fixed in 4% paraformaldehyde (Electron Microscopy Sciences, Hatfield, PA) in 0.1M PO_4 buffer for seven days. After this period they were transferred to 30% sucrose in 0.1M PO_4 buffer until saturated. Brains were frozen on dry ice and tissue was collected as a 1 in 6 series in a 24 well plate. All sections were taken at a 40 μm

thickness using a sliding microtome. Every sixth section was processed for immunohistochemistry using the free-floating method.

i. VMAT2 and pS6 Double Label Immunofluorescence

To label dopaminergic neurons of the SNpc and counterstain for pS6 in rats injected with rAAV2/2 GDNF, VMAT2 was chosen as the label for dopaminergic neurons as GDNF overexpression has been shown to downregulate TH expression [Georgievska *et al*, 2004]. In the VMAT2/pS6 double label immunofluorescent stain, sections were blocked in 10% normal donkey serum for 1 hour and subsequently transferred to the primary antisera for VMAT2 (My BioSource MBS421308, Goat anti-VMAT2, 1:400) and pS6 (Cell Signaling 2211S, rabbit anti-pS6, 1:400) to incubate overnight at 4°C. Following primary incubation, tissue was incubated in the dark in secondary antisera against goat IgG (Invitrogen A11055, Alexa Fluor 488 donkey anti-goat, 1:500) and rabbit IgG (Invitrogen A10042, Alexa Fluor 568 donkey anti-rabbit, 1:500) for 1 hour at room temperature. Sections were mounted on subbed slides and coverslipped with Vectashield Hardset Mounting Medium (Vector Laboratories, Burlingame, CA). Images were taken on a Nikon 90i fluorescence microscope with a Nikon DS-Ri1 camera. Figures were produced in Photoshop 7.0 (San Jose, CA). Brightness, saturation, and sharpness were adjusted only as necessary to best replicate the immunostaining as viewed directly under the microscope.

ii. TH/Total S6/pS6 Triple Label Immunofluorescence

A triple label immunofluorescent stain for TH, Total S6, and pS6 was performed on spare naïve SNpc tissue from naïve rats sacrificed, processed, and sectioned the same as the rAAV2/2 GDNF rats. This stain was performed in order to determine if any changes occur in total S6 protein or pS6 protein in the aged as compared to young adult naïve SNpc. For this stain, sections were blocked in 10% normal donkey serum for 1 hour and subsequently transferred to the primary antisera for TH (Millipore Ab1542,

sheep anti-TH, 1:4000), Total S6 (Cell Signaling 2317, mouse anti-ribosomal protein S6, 1:400), and pS6 (Cell Signaling 2211S, rabbit anti-pS6, 1:400) to incubate overnight at 4°C. Following primary incubation, tissue was incubated in the dark in secondary antisera against sheep IgG (Invitrogen A11015, Alexa Fluor 488 donkey anti-sheep, 1:500), rabbit IgG (Invitrogen A10042, Alexa Fluor 568 donkey anti-rabbit, 1:500), and mouse IgG (LiCOR 925-68072, LiCOR 680, donkey anti-mouse, 1:500) for 1 hour at room temperature. Sections were mounted on subbed slides and coverslipped with Vectashield Hardset Mounting Medium (Vector Laboratories, Burlingame, CA). Images were taken on a Nikon 90i fluorescence microscope with a Nikon DS-Ri1 camera. Figures were produced in Photoshop 7.0 (San Jose, CA). Brightness, saturation, and sharpness were adjusted only as necessary to best replicate the immunostaining as viewed directly under the microscope.

XII. Intensity Measures for Immunofluorescent Staining

Immunofluorescence intensity levels were quantified on a per-cell basis with each cell serving as a technical replicate. For each brain, the first three SNpc sections with visible fibers of the medial terminal nucleus of the accessory optic tract were photographed at 20X at a single focal plane using a Nikon Eclipse microscope, with images stitched using Nikon Elements software to create a single image view of the entire SNpc. Identical exposure times and settings within each channel were used across all sections to enable comparisons between animals. Using the same analysis software, regions of interest (ROIs) were drawn around every VMAT2+ SNpc neuron in the VMAT2/pS6 tissue or every TH+ SNpc neuron in the TH/Total S6/pS6 tissue. Only cells with clear cell boundaries and evidence of a nucleus were outlined. During outlines, the only visible channel was TH or VMAT to ensure that the experimenter was not biasing sample collection based on pS6 or Total S6 levels. ROI mean intensity data were exported for all channels. All ROIs/neuron across the three tissue sections were averaged to create a single intensity value per animal.

XIII. Statistical Analyses

All statistical tests were completed using IBM SPSS statistics software (version 22.0, IBM, Armonk, NY). Graphs were created using GraphPad Prism software (version 6, GraphPad, La Jolla, CA). To compare young adult vs. aged rats, we used independent samples t-tests. For the qPCR gene expression study, fold changes for the GDNF gene were normalized to the GAPDH gene expression and calculated before being subjected to t-test analysis using the REST-XL [Pfaffl *et al*, 2002]. All data are reported as the percent of the young adult values.

Results

Numerous clinical trials in the United States have investigated the possibility of using rAAV2/2 in viral vector-mediated gene therapy strategies to treat neurodegenerative diseases such as PD. However, previous reports have suggested age may present a barrier to efficient rAAV2/2 transduction in the brain [Wu *et al*, 2004; Dissertation Chapter 3]. To test whether advanced age may impact the outcome of a currently-recruiting clinical trial, we examined the transduction efficiency and downstream neuroprotective signaling of the viral vector, rAAV2/2 overexpressing GDNF, in the young adult and aged rat basal ganglia.

To this end, we injected rAAV2 GDNF bilaterally into the young adult and aged rat striatum. This injection site and gene of interest were chosen due to the upcoming clinical trial testing the safety and efficacy of rAAV2/2 GDNF in the human putamen for treatment of PD [Clinicaltrials.gov, NCT01621581]. Transduction efficiency of the striatum was examined at the protein and mRNA level, and GDNF protein overexpression was measured in multiple structures of the basal ganglia that receive axonal projections

from the striatum. Furthermore, activation of downstream GDNF signaling cascades was assessed as a measure of GDNF pro-survival signals and biological relevance of GDNF overexpression. An overview of tissue use and experimental design can be found in Figure 25.

I. GDNF protein overexpression is lower in the aged vs young adult basal ganglia following intrastriatal rAAV2/2 GDNF injection

To measure levels of GDNF protein in the injected striatum and anterograde structures, GDNF ELISAs were performed as a sensitive, quantitative outcome measure. ELISAs on tissue punches from the injected striatum revealed robust overexpression of GDNF at one month post-injection. When comparing GDNF overexpression between the young adult and aged rat striatum, aged rats exhibited significantly less (43% lower) GDNF protein when compared to young adult rats ($p=0.04$; Figure 26a). Decreased transduction efficiency was also observed in the aged as compared to young adult rat striatonigral system as assessed through measures of GDNF protein in the SNpr. Aged rats displayed approximately 32% less GDNF protein in the SNpr as compared to young adult rats (Figure 26b). Although trending, these differences did not reach statistical significance ($p=0.087$). These decreases in GDNF protein in the SNpr were not the result of impaired axonal transport of GDNF protein through the striatonigral system in aged animals, as young adult rats displayed 17% of the striatal protein levels in the SNpr and aged rats displayed 22% of striatal protein levels in the SNpr ($p=0.494$; Figure 26c).

Transduction deficiencies were also observed in GDNF protein levels in other anterograde structures that receive axonal input from the striatum. Specifically, aged rats displayed approximately 59% less GDNF in the aged versus young adult rat GP of the indirect pathway ($p=0.003$; Figure 26d) and approximately 46% less GDNF in the aged versus young adult rat EP in the direct pathway ($p=0.036$; Figure 26e) one month after intrastriatal injection with rAAV2/2 GDNF. Taken together, these results

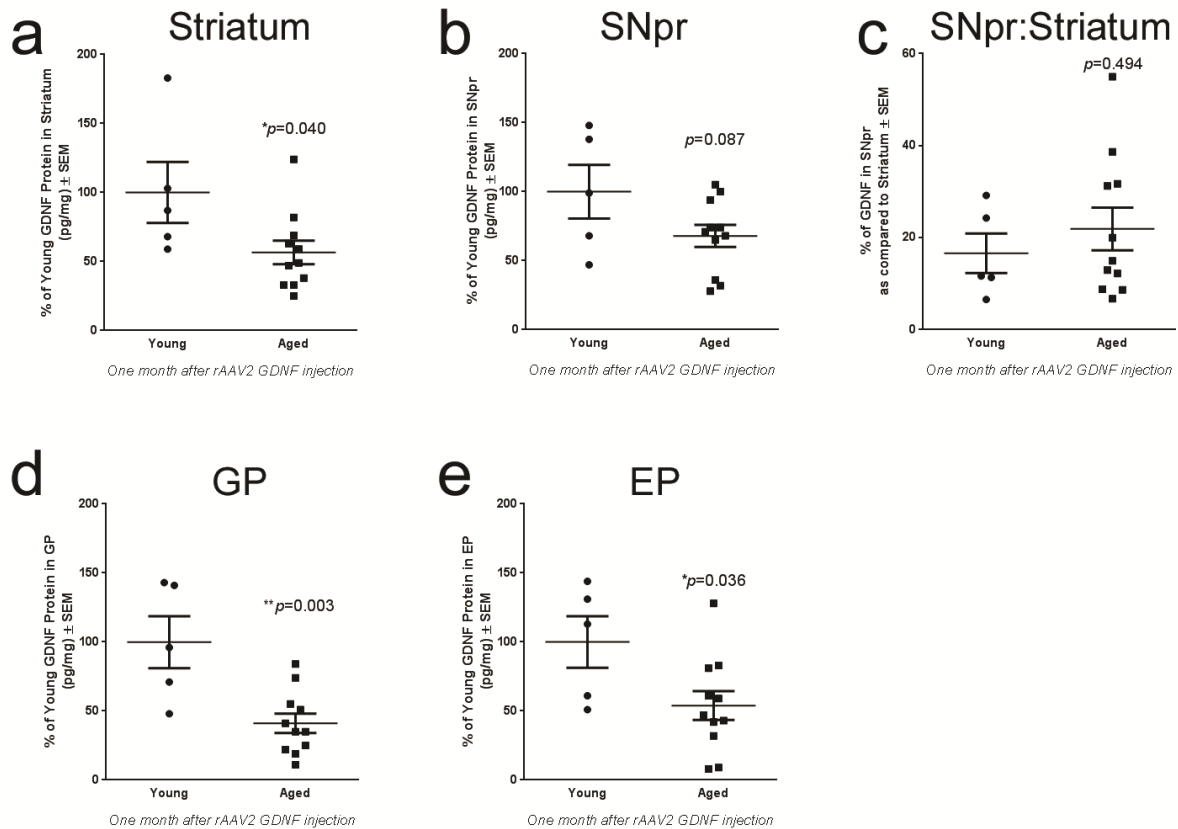


Figure 26. GDNF protein overexpression is lower in the aged versus young adult rat basal ganglia. GDNF protein levels as assessed by GDNF ELISA in the (a) injected striatum, (b) ipsilateral SNpr, (d) ipsilateral GP, and (e) ipsilateral EP one month after rAAV2/2 GDNF injection to the young adult (Young, n=5) and aged (Aged, n=11) rat striatum. a) Aged rats displayed 43% less GDNF protein in the striatum as compared to young adult rats. b) Aged rats trended toward a decrease in GDNF protein in the SNpr as compared to young adult rats, with 32% less GDNF protein in the SNpr of the striatonigral, direct pathway. c) Decreases in GDNF protein in the aged SNpr were not due to age-related decreases in anterograde transport of GDNF as no significant differences were observed in the percent of GDNF in the SNpr as compared to striatum. d) Aged rats displayed 59% less GDNF as compared to young adult rats in the GP of the basal ganglia direct pathway. e) Aged rats displayed 46% less GDNF as compared to young adult rats in the EP of the basal ganglia indirect pathway. * $p \leq 0.05$, ** $p \leq 0.01$. Abbreviations: GDNF, glial cell line-derived neurotrophic factor; SEM, standard error of the mean; rAAV2, recombinant adeno-associated virus serotype 2; SNpr, substantia nigra pars reticulata; GP, globus pallidus; EP, entopeduncular nucleus.

suggest a robust deficiency in rAAV2/2 GDNF transduction of the aged basal ganglia. Specifically, aged rats that received intrastriatal injections of rAAV2/2 GDNF displayed significantly less GDNF protein overexpression in the injected structure (striatum), as well as structures that receive afferents from the striatum in the direct and indirect pathways of the basal ganglia. Furthermore, evidence suggests these decreases in GDNF protein in anterograde structures are not merely the result of decreased anterograde transport of GDNF protein along axons.

II. GDNF mRNA overexpression is equivalent between ages

To determine whether decreased levels of GDNF protein in the striatum were due to decreased levels in protein synthesis in the aged brain [Ryazanov and Nefsky, 2002], we next performed qPCR to quantify GDNF mRNA levels in the injected striatum. GDNF mRNA levels were equivalent between ages in the injected striatum (Figure 27). These results indicate a possibility that decreases in rAAV2/2-mediated GDNF overexpression is due to deficiencies are processes after transcription, such as translation or protein degradation.

III. Measures of GDNF downstream signaling activation are greater in the aged versus young adult brain regardless of rAAV2/2 GDNF injection

As the purpose of overexpressing GDNF in gene therapy preclinical and clinical trials is to initiate downstream neuroprotective signaling cascades in the dopaminergic neurons of the SNpc, we investigated the biological relevance of age-related changes in rAAV2/2-mediated GDNF overexpression by measuring activation of pro-survival signaling in the SNpc of the young adult and aged rats. To this end, we quantified levels of pS6, a downstream indicator of GDNF receptor activation [Decressac *et al*, 2012; Chtarto *et al*, 2016].

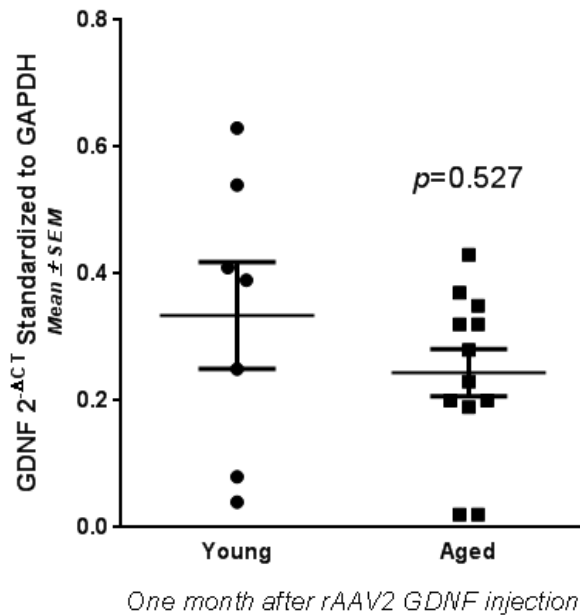


Figure 27. GDNF mRNA levels do not differ between ages one month after rAAV2/2 GDNF injection. GDNF mRNA levels were assessed in the striatum one month following rAAV2/2 GDNF intrastriatal injection using qPCR. At one month post-injection, no significant differences were observed in the level of GDNF mRNA in the aged (Aged, n=12) versus young adult (Young, n=7) rat striatum. GDNF mRNA levels were standardized to levels of GAPDH within the same samples. Values are displayed as the mean linearized GDNF 2-ΔCT values ± SEM for each group. Abbreviations: GDNF, glial cell line-derived neurotrophic factor; SEM, standard error of the mean; rAAV2, recombinant adeno-associated virus serotype 2; GAPDH, glyceraldehyde 3-phosphate dehydrogenase.

Western blots for pS6 were performed on tissue punches of the SNpc in young adult and aged rats that received intrastriatal rAAV2/2 GDNF injection one month prior. No significant differences were observed in the levels of pS6 between the young adult and aged rat SNpc (Figure 28a). As this outcome measure does not allow specificity in the cell population analyzed, we chose to investigate pS6 levels within individual dopaminergic neurons of the SNpc. To accomplish this, we performed a double immunofluorescent stain for pS6 and VMAT2—a marker of the dopaminergic cells of the SNpc that is not affected by age [Cruz-Muros *et al*, 2008] or GDNF overexpression [Georgievska *et al*, 2004]—in midbrain tissue of young adult and aged rats. Using only the VMAT2 channel, individual cells of the SNpc were outlined to identify the region of interest (ROI) and intensity measures of VMAT2 and pS6 staining were obtained for each individual cell. This was performed for the three sections of the SNpc that displayed a clear medial terminal nucleus of the optic chiasm, with intensity measures for ROIs averaged to determine an overall intensity value per rat. Surprisingly, aged rats exhibited significantly greater ($p=0.013$) levels of pS6 staining intensity than young adult rats following rAAV2/2 GDNF intrastriatal injection (Figure 28j).

To determine whether these increased levels of pS6 in the aged versus young adult brain following rAAV2/2 GDNF intrastriatal injection were the result of age-related changes in pS6 or total ribosomal protein S6 levels, we performed a similar immunofluorescent stain investigating pS6 and total S6 levels in naïve tissue of the young adult and aged rat midbrain (Figure 28b-i). No significant differences were seen in total levels of S6 between naïve young adult and aged rats (Figure 28k). However, an age-related increase was observed in naïve levels of pS6 in the rat dopaminergic neurons of the SNpc. Furthermore, the levels of pS6 measured in naïve tissue were equivalent to levels observed in rats following rAAV2/2 GDNF injection. Taken together, these results suggest levels of pS6 are increased with aging in the rat

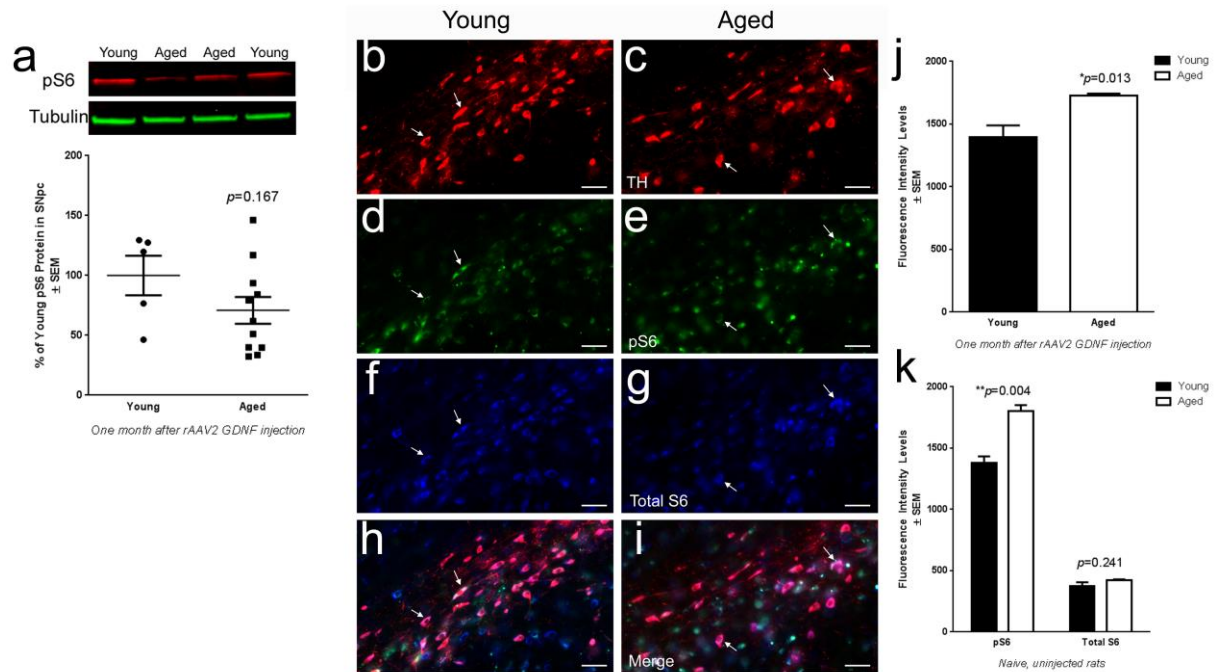


Figure 28. pS6 levels are greater in aged versus young adult rat SNpc dopaminergic neurons regardless of rAAV2/2 GDNF injection. a) Tissue punches of the young adult (Young, n=5) and aged (Aged, n=11) rat SNpc one month after intrastriatal rAAV2/2 GDNF injection were used for western blot for pS6 levels. No significant differences were observed in pS6 levels between ages using this technique. Values are represented as the percent of young adult pS6 protein levels \pm SEM. b-i) Immunofluorescent staining for TH, pS6, and total S6 protein levels in the naïve SNpc of young adult and aged rats. Scale bars = 50 μ m. b-c) TH was used as a marker of the dopaminergic neurons of the SNpc and was the only channel visible during all tracings of ROIs. In rats that received rAAV2/2 GDNF intrastriatal injections, VMAT2 was substituted for TH as TH is down-regulated following GDNF overexpression [Georgievska et al, 2004]. Arrows depict areas of colocalization. d-e) pS6 staining for measurements of downstream GDNF neuroprotective signal activation. This stain was performed for both rAAV2/2 GDNF-injected and naïve rats. f-g) Total S6 protein staining for measurements of total levels of the S6 protein available for phosphorylation into pS6. This stain was only performed in naïve rats. h-i) Merged images depicting colocalization of TH, pS6, and total S6 staining in the naïve young adult and aged rat SNpc. j) Fluorescent intensity signal levels of pS6 staining in young adult and aged rat SNpc dopaminergic neurons following rAAV2/2 GDNF intrastriatal injection. Aged rats exhibit significantly greater pS6 staining intensity as compared to young adult rats. k) Fluorescent intensity levels of pS6 and total S6 protein in the dopaminergic neurons of the SNpc of naïve rats. Aged rats display significantly greater levels of pS6 staining intensity than young adult rats. No age-related differences were observed in total S6 staining intensity in naïve rats. j-k) Values are represented as mean fluorescent intensity levels for each age \pm SEM. Abbreviations: GDNF, glial cell line-derived neurotrophic factor; SEM, standard error of the mean; rAAV2, recombinant adeno-associated virus serotype 2; S6, ribosomal protein S6; pS6, phosphorylated ribosomal protein S6; SNpc, substantia nigra pars compacta; TH, tyrosine hydroxylase.

dopaminergic neurons of the SNpc and our rAAV2/2 GDNF injection to the striatum did not trigger detectable phosphorylation of S6 above endogenous levels.

Discussion

Currently, multiple clinical trials are exploring or have explored the possibility of using viral vector-mediated gene therapy to treat PD. Unfortunately, the clinical trials using this approach that have been completed have failed to report any disease-modifying effects or benefits over conventional dopaminergic therapies [O'Connor and Boulis, 2015; Choudhury *et al*, 2016]. One factor that could explain the discrepancy between successful preclinical trials using this technology and the failed clinical trials could be the fact that the preclinical trials were almost exclusively performed in young adult animals modeling PD [Bjorklund *et al*, 2000; Kordower *et al*, 2000; Herzog *et al*, 2008; Emborg *et al*, 2009; Marks *et al*, 2010; Bartus *et al*, 2011]. However, advanced age is the primary risk factor for developing PD, indicating the covariate of age is most likely an important factor to consider when designing therapies for PD. We hypothesized that the construct used in all viral vector-mediated gene therapy clinical trials for PD in the United States, rAAV2/2, is less effective in the aged as compared to young adult brain. This was based on previous reports that rAAV2/2 is less effective in the aged as compared to young adult rat septum when expressing NGF [Wu *et al*, 2004] and nigrostriatal and striatonigral systems when expressing GFP [Dissertation Chapter 3].

Although clinical trials have already used rAAV2/2 to overexpress the GDNF-homolog neurturin to no avail [Olanow *et al*, 2015], a new clinical trial is recruiting patients to test the safety and efficacy of rAAV2/2-mediated GDNF delivery to the basal ganglia through intrastriatal injection [Clinicaltrials.gov, NCT01621581]. To test the impact of age on rAAV2/2 GDNF delivery to the basal ganglia, we injected

rAAV2/2 GDNF into the striatum of young adult and aged rats and examined transduction efficiency one month post-injection. Although we have previously reported transduction deficiencies in the striatonigral system following rAAV2/2 GFP injection, we chose to overexpress GDNF in the present series of experiments to test the impact of age on this biologically- and clinically-relevant protein. GDNF protein levels were quantified in the injected striatum and anterograde structures that receive striatal input to assess transduction efficiency in clinically-relevant structures [Ciesielska *et al*, 2011] of aged as compared to young adult rats.

Overall, lower levels of GDNF overexpression are observed in the aged rat basal ganglia as compared to the young adult rat one month after rAAV2/2 GDNF injection in the striatum. Aged rats displayed significantly less GDNF protein as compared to young adult rats at the site of injection (Figure 26a), indicating a transduction deficiency in the striatum with rAAV2/2 GDNF. In addition, the aged rat SNpr trended towards less GDNF expression as compared to their young adult rat counterparts (Figure 26b), indicating a potential transduction deficiency in the aged rat striatonigral system. Transduction deficiencies were also observed in other structures of the direct and indirect pathways of the basal ganglia as significantly less GDNF protein was observed in the aged versus young adult rat GP and EP (Figure 26d-e). Comparisons between young adult and aged rats in levels of anterograde transport in the striatonigral system indicated that age-related impairments occur prior to GDNF protein transport along striatal axons, at least in the case of the striatonigral system (Figure 26c). These results indicate the importance of accounting for age in the design of clinical trials for rAAV2/2 GDNF gene therapy for PD, especially when high levels of protein overexpression are necessary for any functional or neuroanatomical benefit of viral vector-mediated gene therapy neurotrophic factor treatment [Emborg *et al*, 2009].

We next sought to determine whether the lower levels of GDNF protein overexpression in the striatum were the result of age-related decreases in protein synthesis [Ingvar *et al*, 1985; Ryazanov and Nefsky, 2002] or steps of transduction prior to protein synthesis [Nonnenmacher and Weber, 2012]. No significant differences were observed between young adult and aged rats in levels of GDNF mRNA in the striatum (Figure 27). These results could implicate age-related decreases in protein synthesis in the decreased expression of GDNF protein in the aged versus young adult rat following rAAV2/2 GDNF injection. Although general rates of protein synthesis are decreased in the aged rat brain as a whole, the rate of striatal protein synthesis does not appear to decrease with age [Ingvar *et al*, 1985]. In addition, the lack of significant differences in GDNF mRNA in the young adult versus aged striatum could be explained by the collection of the entire striatum for GDNF mRNA analyses. As, rAAV2/2 only transduces about 15% of the striatum (data not shown from rAAV2/2 GFP intrastriatal injections), any differences in GDNF mRNA could have been masked by the collection of the entire striatum diluting out any difference in GDNF mRNA overexpression with age. As a result, we suggest interpreting these results with caution as this lack of a difference between young adult and aged rats in GDNF mRNA could be the result of an issue in experimental design rather than a decrease in protein synthesis.

In addition, quality control for injection success was only performed in the left hemisphere as we were able to compare levels of GDNF overexpression in the striatum of injected versus naïve rats and the proportion of GDNF protein in the striatum as compared to the ipsilateral SNpr (Figure 25, see Experimental Overview in Methods). Quality control could not be performed in the right hemisphere as naïve striatal tissue was not available for GDNF qPCR to compare overexpression at the level of mRNA and exclude outliers. To attempt to identify failed injections, we stained the ipsilateral midbrain tissue for GDNF to visually verify GDNF overexpression in the axonal terminals of the SNpr. Unfortunately, the limited spread of rAAV2/2 coupled with the single injection paradigm and moderate titer used did not

result in robust GDNF overexpression in the SNpr that could be readily detected and used for quality control. Therefore, we were unable to perform the necessary quality control steps to exclude rats based on injection failure, which would most likely have included the two rats per age with GDNF $2^{-\Delta CT}$ values below 0.1 (Figure 27).

To determine the biological relevance of age-related differences in rAAV2/2-mediated GDNF overexpression, we investigated activation of the downstream neuroprotective signaling that results from GDNF-receptor activation in the dopaminergic neurons of the SNpc. To this end, we measured levels of pS6 as an indicator of activation of the neuroprotective pathways resulting from GDNF receptor activation, namely the Akt/mTOR and ERK pathways [Decressac *et al*, 2012; Biever *et al*, 2015; Chtarto *et al*, 2016; Dissertation Chapter 1]. Unexpectedly, we saw a greater intensity of pS6 staining in aged as compared to young adult rat dopaminergic neurons of the SNpc (Figure 28). The intensity measures of pS6 in rats injected with rAAV2/2 GDNF mirrored the levels of pS6 in naïve, uninjected rats, potentially indicating a lack of pS6 activation and detectable GDNF neuroprotective signaling in both young adult and aged rats. This is most likely due to a floor effect of the pS6 measurement and the need to increase the titer or amount of rAAV2/2 GDNF injected in the striatum, as mentioned when discussing the lack of visible GDNF overexpression in the SNpr one month after intrastriatal rAAV2/2 GDNF injection.

Measurements of S6 and pS6 in naïve tissue provide insight into basal age-related changes in pS6. Total S6 levels were equivalent between young adult and aged rats in the dopaminergic neurons of the SNpc whereas levels of pS6 were significantly greater in the aged as compared to young adult rats (Figure 28k). These results suggest an increase in phosphorylation or decrease in dephosphorylation of ribosomal protein S6 in the naïve aged SNpc. Much is still unknown about the regulation and function of pS6 in the brain [Biever *et al*, 2015]. Phosphorylation of S6 can occur through a variety of mechanisms

and levels of pS6 are used as a marker of various conflicting cellular states such as: activation, oxidative stress, synaptic plasticity, neuroprotection, injury, and others [for review see Biever *et al*, 2015]. The use of pS6 as a marker of oxidative stress [Castellani *et al*, 2011], the high levels of oxidative stress in the aged nigrostriatal dopaminergic neurons of the SNpc [Kraytsberg *et al*, 2006; Bender *et al*, 2006; Collier *et al*, 2011], and the shift from a uniform pS6 stain in young adult neurons to a granular pS6 appearance in aged SNpc neurons (Figure 28b-i) lend credence to the idea that the increased pS6 intensity in the aged rat SNpc is the result of oxidative stress triggering neuroprotective mechanisms involving ERK activation and subsequent S6 phosphorylation [Castellani *et al*, 2011; Biever *et al*, 2015]. Future studies investigating GDNF neuroprotective signaling should use a marker of neuroprotection that does not change with age in order to allow comparisons of GDNF-signaling between young adult and aged rats.

In sum, this study is the first of its kind to investigate the impact of age on transduction of a biologically- and clinically-relevant viral vector construct for PD treatment. Following intrastriatal injection of rAAV2/2 GDNF, we find robust and significant deficiencies in transduction efficiency in the aged brain at the site of injection (striatum), anterograde structures of the direct pathway (SNpr and GP), and anterograde structures of the indirect pathway (EP). Furthermore, this study was the first to report an age-related increase in pS6 in the dopaminergic neurons of the SNpc. Future studies should continue investigating age-related changes in viral vector-mediated gene therapy transduction efficiency to better understand the potential impact of age-related transduction deficiencies on clinical trial outcomes for neurodegenerative diseases like PD and Alzheimer's disease.

LITERATURE CITED

LITERATURE CITED

- Bartus, R.T., C.D. Herzog, Y. Chu, A. Wilson, L. Brown, J. Siffert, E.M. Johnson Jr, C.W. Olanow, E.J. Mufson, J.H. Kordower. (2011). Bioactivity of AAV2-neurturin gene therapy (CERE-120): differences between Parkinson's disease and nonhuman primate brains. *Mov Disord*, **26(1)**: 27-36.
- Bender, A., K.J. Krishnan, C.M. Morris, G.A. Taylor, A.K. Reeve, R.H. Perry, E. Jaros, J.S. Hersheson, J. Betts, T. Klopstock, R.W. Taylor, and D.M. Turnbull. (2006). High levels of mitochondrial DNA deletions in substantia nigra neurons in aging and Parkinson's disease. *Nat Gen*, **38(5)**: 515-517.
- Benskey, M.J., and F.P. Manfredsson. (2016a). Lentivirus Production and Purification. *Methods Mol Biol*, **1382**: 107-114.
- Benskey, M.J., and F.P. Manfredsson. (2016b). Intraparenchymal stereotaxic delivery of rAAV and special consideration in vector handling. *Methods Mol Biol*, **1382**: 199-215.
- Benskey, M.J., I.M. Sandoval, and F.P. Manfredsson. (2016). Continuous collection of adeno-associated virus from producer cell medium significantly increases total viral yield. *Hum Gene Ther Methods*, **27(1)**: 32-45.
- Biever, A., E. Valjent, and E. Puighermanal. (2015). Ribosomal protein S6 phosphorylation in the nervous system: from regulation to function. *Front Mol Neurosci*, **8(75)**: doi: 10.3389/fnmol.2015.00075.
- Bjorklund, A., D. Kirik, C. Rosenblad, B. Georgievask, C. Lundberg, and R.J. Mandel. (2000). Towards a neuroprotective gene therapy for Parkinson's disease: use of adenovirus, AAV and lentivirus vectors for gene transfer of GDNF to the nigrostriatal system in the rat Parkinson model. *Brain Res*, **886(1-2)**: 82-98.
- Choudhury, S.R., E. Hudry, C.A. Maguire, M. Sena-Esteves, X.O. Breakefield, and P. Grandi. (2016). Viral vectors for therapy of neurologic diseases. *Neuropharmacology*, doi:10.1016/j.neuropharm.2016.02.013.
- Ch tarto, A., M. Humbert-Claude, O. Bockstael, A.T. Das, S. Boutry, L.S. Breger, B. Klaver, C. Melas, P. Barroso-Chinea, T. Gonzalez-Hernandez, R.N. Muller, O. DeWitte, M. Levivier, C. Lundberg, B. Berkhout, and L. Tenenbaum. (2016). A regulatable AAV vector mediated GDNF biological effects at clinically-approved sub-antimicrobial doxycycline doses. *Mol Ther Methods Clin Dev*, **5**: 16027.
- ClinicalTrials.gov. (2016). AAV2-GDNF for Advanced Parkinson s Disease (NCT01621581). <https://http://www.clinicaltrials.gov/ct2/show/NCT01621581?term=gdnf&rank=1>.
- Collier, T.J., N.M. Kanaan, and J.H. Kordower. (2011). Ageing as a primary risk factor for Parkinson's disease: evidence from studies of non-human primates. *Nat Rev Neurosci*, **12(6)**: 359-366.

- Cruz-Muros, I., D. Afonso-Oramas, P. Abreu, M. Rodriguez, M.C. Gonzalez, and T. Gonzalez-Hernandez. (2008). Deglycosylation and subcellular redistribution of VMAT2 in the mesostriatal system during normal aging. *Neurobiol Aging*, **29(11)**: 1702-1711.
- Cuanalo-Contreras, K., A. Mukherjee, and C. Soto. (2013). Role of protein misfolding and proteostasis deficiency in protein misfolding diseases and aging. *Int J Cell Biol*, 638083.
- D'Anglemont de Tassigny, X., A. Pascual, and J. Lopez-Barneo. (2015). GDNF-based therapies, GDNF-producing interneurons, and trophic support of the dopaminergic nigrostriatal pathway. Implications for Parkinson's disease. *Front Neuroanat*, **9**: 10.
- De la Fuente-Fernandez, R., M. Schulzer, E. Mak, and V. Sossi. (2010). Trials of neuroprotective therapies for Parkinson's disease: problems and limitations. *Parkinsonism Relat Disord*, **16(6)**: 356-369.
- Decressac, M., B. Kadkhodaei, B. Mattsson, A. Laguna, T. Perlmann, and A. Bjorklund. (2012). Alpha-synuclein-induced down-regulation of Nurr1 disrupts GDNF signaling in nigral dopamine neurons. *Science Trans Med*, **4(163)**: 163ra156.
- Dorsey, E.R., R. Constantinescu, J.P. Thompson, K.M. Biglan, R.G. Holloway, K. Kieburtz, F.J. Marshall, B.M. Ravina, G. Schifitto, A. Siderowf, and C.M. Tanner. 2007. Projected number of people with Parkinson disease in the most populous nations, 2005 through 2030. *Neurology* **68**: 384-386.
- Emborg, M.E., J. Moirano, J. Raschke, V. Bondarenko, R. Zufferey, S. Peng, A.D. Ebert, V. Joers, B. Roitberg, J.E. Holden, J. Koprach, J. Lipton, J.H. Kordower, and P. Aebischer. (2009). Response of aged parkinsonian monkeys to in vivo gene transfer of GDNF. *Neurobiol Dis*, **36(2)**: 303-311.
- Gash, D.M., Z. Zhang, A. Ovadia, W.A. Cass, A. Yi, L. Simmerman, D. Russell, D. Martin, P.A. Lapchak, F. Collins, B.J. Hoffer, and G.A. Gerhardt. (1996). Functional recovery in parkinsonian monkeys treated with GDNF. *Nature*, **380(6571)**: 252-255.
- Georgievska, B., D. Kirik, and A. Bjorklund. (2004). Overexpression of glial cell line-derived neurotrophic factor using a lentiviral vector induces time- and dose-dependent downregulation of tyrosine hydroxylase in the intact nigrostriatal dopamine system. *J Neurosci*, **24(29)**: 6437-6445.
- Gombash, S.E., J.W. Lipton, T.J. Collier, L. Madhavan, K. Steece-Collier, A. Cole-Strauss, B.T. Terpstra, A.L. Spieles-Engemann, B.F. Daley, S.L. Wohlgenant, V.B. Thompson, F.P. Manfredsson, R.J. Mandel, and C.E. Sortwell. (2012). Striatal pleiotrophin overexpression provides functional and morphological neuroprotection in the 6-hydroxydopamine model. *Mol Ther*, **20(3)**: 544-554.
- Herzog, C.D., L. Brown, D. Gammon, B. Kruegel, R. Lin, A. Wilson, A. Bolton, M. Printz, M. Gasmi, K.M. Bishop, J.H. Kordower, and R.T. Bartus. (2008). Expression, bioactivity, and safety 1 year after adeno-associated viral vector type 2-mediated delivery of neuritin to the monkey nigrostriatal system support CERE-120 for Parkinson's disease. *Neurosurgery*, **64(6)**: 602-613.
- Hoffer, B.J., A. Hoffman, K. Bowenkamp, P. Huettl, J. Hudson, D. Martin, L.F. Lin, and G.A. Gerhardt. (1994). Glial cell line-derived neurotrophic factor reverses toxin-induced injury to midbrain dopaminergic neurons in vivo. *Neurosci Lett*, **182**: 107-111.

- Ingvar, M.C., P. Maeder, L. Sokoloff, and C.B. Smith. (1985). Effects of ageing on local rates of cerebral protein synthesis in sprague-dawley rats. *Brain*, 108: 155-170.
- Kirik, D., C. Rosenblad, A. Bjorklund, and R.J. Mandel. (2000). Long-term rAAV-mediated gene transfer of GDNF in the rat Parkinson's model: intrastriatal but not intranigral transduction promotes functional regeneration in the lesioned nigrostriatal system. *J Neurosci*, **20(12)**: 4686-4700.
- Kordower, J.H., M.E. Emborg, J. Bloch, S.Y. Ma, Y. Chu, L. Leventhal, J. McBride, E. Chen, S. Palfi, B.Z. Roitberg, W.D. Brown, J.E. Holden, R. Pyzalski, M.D. Taylor, P. Carvey, Z. Ling, D. Torno, P. Hantraye, N. Deglon, and P. Aebischer. (2000). Neurodegeneration prevented by lentiviral vector delivery of GDNF in primate models of Parkinson's disease. *Science*, **290(27)**: 767-773.
- Kraytsberg, Y., E. Kudryavtseva, A.C. McKee, C. Geula, N.W. Kowall, and K. Khrapko. (2006). Mitochondrial DNA deletions are abundant and cause functional impairment in aged human substantia nigra neurons. *Nat Gen*, **38(5)**: 318-320.
- Lang, A.E., S. Gill, N.K. Patel, A. Lozano, J.G. Nutt, R. Penn, D.J. Brooks, G. Hotton, E. Moro, P. Heywood, M.A. Brodsky, K. Burchiel, P. Kelly, A. Dalvi, B. Scott, M. Stacy, D. Turner, V.G.F. Wooten, W.J. Elias, E.R. Laws, V. Dhawan, A.J. Stoessl, J. Matcham, R.J. Coffey, and M. Traub. (2006). Randomized controlled trial of intraputamenal glial cell line-derived neurotrophic factor infusion in Parkinson disease. *Ann Neurol*, **59(3)**: 459-466.
- Marks Jr., W.J., R.T. Bartus, J. Siffert, C.S. Davis, A. Lozano, N. Boulis, J. Vitek, M. Stacy, D. Turner, L. Verhagen, R. Bakay, R. Watts, B. Guthrie, J. Jankovic, R. Simpson, M. Tagliati, R. Alterman, M. Stern, G. Baltuch, P.A. Starr, P.S. Larson, J.L. Ostrem, J. Nutt, K. Kiebertz, J.H. Kordower, and C.W. Olanow. (2010). Gene delivery of AAV2-neurturin for Parkinson's disease: a double-blind randomized, controlled trial. *Lancet*, **9**: 1164-1172.
- Nonnenmacher, M., and T. Weber. (2012). Intracellular transport of recombinant adeno-associated virus vectors. *Gene Ther*, **19(6)**: 649-658.
- Nutt, J.G., K.J. Burchiel, C.L. Comella, J. Jankovic, A.E. Lang, E.R. Laws Jr, A.M. Lozano, R.D. Penn, R.K. Simpson Jr, M. Stacy, and G.F. Wooten. (2003). Randomized, double-blind trial of glial cell line-derived neurotrophic factor (GDNF) in PD. *Neurology*, **60(1)**: 69-73.
- O'Connor, D.M. and N.M. Boulis. (2015). Gene therapy for neurodegenerative diseases. *Trends Mol Med*, **21(8)**: 504-512.
- Olanow, C.W. (2009). Can we achieve neuroprotection with currently available anti-parkinsonian interventions? *Neurology*, **72(Suppl 2)**: S59-S64.
- Olanow, C.W., R.T. Bartus, T.L. Baumann, S. Factor, N. Boulis, M. Stacy, D.A. Turner, W. Marks, P. Larson, P.A. Starr, J. Jankovic, R. Simpson, R. Watts, B. Guthrie, K. Poston, J.M. Henderson, M. Stern, G. Baltuch, C.G. Goetz, C. Herzog, J.H. Kordower, R. Alterman, A.M. Lozano, and A.E. Lang. (2015). Gene delivery of neurturin to putamen and substantia nigra in Parkinson disease: a double-blind, randomized, controlled trial. *Ann Neurol*, **78(2)**: 248-257.
- Parkinson, J. (2002). An essay on the shaking palsy, 1817. *J Neuropsychiatry Clin Neurosci*, **14(2)**: 223-236.

- Parkinson's Disease Foundation. Understanding Parkinson's Disease. (2016). Web. 25 May 2016.
- Pfaffl, M.W., G.W. Horgan, and L. Dempfle. (2002). Relative expression software tool (REST©) for group-wise comparison and statistical analysis of relative expression results in real-time PCR. *Nucleic Acids Res*, **30(9)**: e36.
- Polinski, N.K., S.E. Gombash, F.P. Manfredsson, J.W. Lipton, C.J. Kemp, A. Cole-Strauss, N.M. Kanaan, K. Steece-Collier, N.C. Kuhn, S.L. Wohlgenant, and C.E. Sortwell (2015). Recombinant adeno-associated virus 2/5-mediated gene transfer is reduced in the aged rat midbrain. *Neurobio Aging*, **36(2)**: 1110-1120.
- Richardson, R.M., A.P. Kells, K.H. Rosenbluth, E.A. Salegio, M.S. Fiandaca, P.S. Larson, P.A. Starr, A.J. Martin, R.R. Lonser, H.J. Federoff, J.F. Forsayeth, and K.S. Bankiewicz. (2011). Interventional MRI-guided putaminal delivery of AAV2-GDNF for a planned clinical trial in Parkinson's disease. *Mol Ther*, **19(6)**: 1048-1057.
- Ryazanov, A.G., and B.S. Nefsky. (2002). Protein turnover plays a key role in aging. *Mech Ageing Dev*, **123**: 207-213.
- Schmittgen, T.D. and K.J. Livak. (2008). Analyzing real-time PCR data by the comparative C(T) method. *Nat Protoc*, **3**: 1101-1108.
- Slagboom, P.E., W.J.F. de Leeuw, and J. Vijg. (1990). Messenger RNA levels and methylation patterns of GAPDH and beta-actin genes in rat liver, spleen, and brain in relation to aging. *Mech Age Devel*, **53**: 243-257.
- Wu, Z., E. Miller, M. Agbandje-McKenna, and R.J. Samulski. (2006). Alpha2,3 and alpha2,6 N-linked sialic acids facilitate efficient binding and transduction by adeno-associated virus types 1 and 6. *J Virol*, **80(18)**: 9093-9103.
- Zolotukhin, S., B.J. Byrne, E. Mason, E. Zolotukhin, M. Potter, K. Chesnut, C. Summerford, R.J. Samulski, and N. Muzyczka. (1999). Recombinant adeno-associated virus purification using novel methods improves infectious titer and yield. *Gene Ther*, **6**: 973-985.

Chapter 5: Age-Related Transduction Deficiencies are Rescued by Altered Receptor Binding in the Rat Nigrostriatal System

Abstract

Recently, a deficiency in the ability of many viral vectors to transduce the aged rat brain has been uncovered. Recombinant adeno-associated virus pseudotype 2/2 (rAAV2/2)—the viral vector used in clinical trials for age-related neurodegenerative diseases—was deficient in transducing the aged nigrostriatal system. Conversely, rAAV2/9 was not deficient in the aged nigrostriatal system. This discrepancy implicates AAV capsid-mediated steps of transduction in the age-related deficiency, as this is the only difference between these vectors. As AAV initiates transduction by binding to specific cell surface receptors that differ between vector capsid serotypes and can be decreased with age, we hypothesized that the previously observed deficiencies are caused by age-related changes in receptor-mediated steps of transduction. To test this hypothesis, we used a chimeric virus composed of AAV2 with the receptor binding motifs of AAV9 grafted onto the capsid (rAAV2G9). The addition of the AAV9 receptor binding motifs abolished the age-related transduction deficiency of rAAV2/2 in the rat nigrostriatal system. These results indicate a role for cell surface receptors in the age-related transduction deficiency. Understanding the mechanism behind the transduction deficiency in the aged brain can help inform future preclinical and clinical trials for age-related neurodegenerative diseases.

Introduction

Viral vector-mediated gene therapy is currently being tested as a strategy to halt or slow the progression of age-related neurodegenerative diseases like Alzheimer's disease and Parkinson's disease (PD). This therapy holds promise in that it is a localized treatment with the ability to replenish diminished proteins

or overexpress neurotrophic factors that may prove neuroprotective or neurorestorative [O'Connor and Boulis, 2015; Choudhury *et al*, 2016]. To date, many clinical trials have been conducted to evaluate the safety and efficacy of viral vector-mediated gene therapy for PD—the second most common neurodegenerative disease. Although Phase I trials demonstrated favorable safety profiles and hints of clinical efficacy, placebo-controlled, double-blinded Phase II trials have all failed to meet primary endpoints or show benefits over conventional, less invasive therapies [O'Connor and Boulis, 2015; Choudhury *et al*, 2016]. Furthermore, analyses of transgene expression levels in patients have found lower expression in the substantia nigra than predicted from preclinical trials [Bartus *et al*, 2011]. These results are extremely important as preclinical trials have shown that the level of transgene expression highly correlates with the degree of functional and anatomical benefits provided by the therapy [Emborg *et al*, 2009]. As a result, the unimpressive levels of transgene expression could be one factor contributing to the lack of therapeutic efficacy in the clinical trials.

Recently, reports have indicated that age may present a barrier to efficient gene transfer in viral vector-mediated gene therapy. Recombinant adeno-associated virus (rAAV) displays age-related transduction deficiencies that are vector pseudotype-specific and target structure-specific. rAAV pseudotype 2/2 (rAAV2/2) is less efficient in transducing the aged as compared to young adult rat septum [Wu *et al*, 2004], nigrostriatal system [Dissertation Chapter 3], and striatonigral system [Dissertation Chapter 3]. Similarly, rAAV2/5 displays age-related transduction deficiencies in the rat substantia nigra pars compacta (SNpc) [Polinski *et al*, 2015; Fischer *et al*, 2016], nigrostriatal system [Polinski *et al*, 2015; Dissertation Chapter 3], and striatonigral system [Dissertation Chapter 3]. rAAV2/9, however, is deficient in the aged striatonigral system but does not display an age-related transduction deficiency in the nigrostriatal system [Dissertation Chapter 3]. As the sole difference between these rAAV constructs is

the capsid in which the viral genome is packaged, this implicates capsid-mediated steps of transduction in the age-related transduction deficiencies.

We hypothesize that the step of transduction causing the age-related transduction deficiency is receptor binding and internalization. This hypothesis stems from four observations. First, receptor binding and internalization is a capsid-mediated step of transduction [Schultz and Chamberlain, 2008; Nonnenmacher and Weber, 2012]. Therefore, this fits with our previous observations of deficiencies that depend on the vector capsid [Dissertation Chapter 3]. Second, each AAV serotype uses specific receptors and co-receptors that differ between rAAV2 (primary receptor: heparan sulfate proteoglycan, HSPG) [Summerford and Samulski, 1998], rAAV5 (primary receptor: 2,3-linked sialic acid) [Walters *et al*, 2001], and rAAV9 (primary receptor: N-linked galactose, N-Gal) [Shen *et al*, 2011]. Third, AAV transduction efficiency is dependent on expression levels of the cognate receptors, with fewer receptors resulting in lower levels of transduction [Summerford and Samulski, 1998; Walters *et al*, 2001; Shen *et al*, 2011]. Finally, some receptors involved in AAV transduction have been shown to be downregulated with advanced age. In particular, 2,3-linked sialic acid levels are decreased in the aged as compared to young adult rat cerebellum [Sasaki *et al*, 2002] and hippocampus [Sato *et al*, 2001].

To test this hypothesis, we sought to determine whether enabling rAAV2/2 (deficient in the nigrostriatal system) to use the receptors of AAV9 (not deficient in the nigrostriatal system) would diminish the age-related transduction deficiency observed with rAAV2/2 in the aged versus young adult rat nigrostriatal system. To do this, we compared the transduction efficiency in the nigrostriatal system one month after SNpc-injection with rAAV2/2 expressing GFP (rAAV2 GFP) or an AAV2 chimeric virus that includes the receptor binding motifs of rAAV9 (rAAV2G9). rAAV2G9 is the result of numerous rounds of site-directed mutagenesis to imprint the galactose-binding residues of AAV9 on the capsid of AAV2 [Shen *et al*, 2013].

In this way, rAAV2G9 is able to exploit the AAV2 HSPG receptor as well as the AAV9 N-Gal receptor without altering downstream processes of transduction [Shen *et al*, 2013]. rAAV2G9 displays the tropism of AAV2 with the transduction kinetics of AAV9, and affinity-binding experiments demonstrate this chimera binds equally with HSPG and N-Gal [Shen *et al*, 2013].

rAAV2 GFP and rAAV2G9 GFP were injected unilaterally into the SNpc of young adult (3 months) and aged (20 months) rats. One month post-injection, we investigated the efficiency of each vector in transducing the young adult versus aged nigrostriatal system. Although no age-related differences were observed in total GFP-immunoreactive (GFP+) cells of the midbrain for either vector, aged rats injected with rAAV2/2 GFP displayed significantly fewer GFP+ dopaminergic neurons of the SNpc and significantly less GFP protein in the anterograde structure of the nigrostriatal system—the striatum—as compared to their young adult rat counterparts. rAAV2G9 GFP, however, did not display any age-related differences in the number of GFP+ dopaminergic neurons of the SNpc or total levels of GFP protein in the ipsilateral striatum. These results indicate that capsid-receptor interactions are integral to the transduction deficiencies observed with rAAV in the aged rat nigrostriatal system. In addition, these age-related deficiencies can be overcome by circumventing the impairments through vector-modifications. This information will be important for designing clinical trials for age-related neurodegenerative diseases or when using viral vectors as an experimental tool in aged animals.

Methods

I. Experimental Overview

Twenty-one young adult (3 months old) and 27 aged (20 months old) Fischer344 (F344) rats were split into two injection groups—one group of young adult (n=13) and aged rats (n=15) receiving rAAV2

injections and the other group of young adult (n=8) and aged (n=12) rats receiving rAAV2G9 injections into the left SNpc. All rats were sacrificed one month post-injection and brains were hemisected in the coronal plane. The rostral portion of the brain underwent striatal microdissections for Western blot analysis of GFP protein in the striatum. The caudal portion of the brain was used for immunohistochemical staining. Outliers were removed if they displayed a misplaced injection or met the criteria for exclusion through the ADAM outlier method [Leys *et al*, 2013] and were not included in any outcome measure in this study.

II. Animals

Male, F344 rats (National Institute on Aging, Bethesda, MD) 3 months of age (n = 21) and 20 months of age (n = 27) were used in this study. All animals were given food and water *ad libitum* and housed in 12h reverse light-dark cycle conditions in the Van Andel Research Institute vivarium, which is fully AAALAC approved. All procedures were conducted in accordance with guidelines set by the Institutional Animal Care and Use Committee (IACUC) of Michigan State University.

III. Viral Vectors

Both rAAV viral vector constructs were purchased from the University of North Carolina Vector Core (University of North Carolina, Chapel Hill, NC). Plasmid and vector production were completed as previously described [Zolotukhin *et al*, 1999; Benskey and Manfredsson, 2016a; Benskey and Manfredsson, 2016b]. For all vectors, expression of the transgene was driven by the chicken beta actin/cytomegalovirus enhancer (C β A/CMV) promoter hybrid. Details on the mutagenesis involved in the production of the chimeric virus can be found in Shen *et al*, 2013. Briefly, humanized GFP was inserted into an AAV plasmid backbone containing AAV2 inverted terminal repeats and was packaged into AAV2 or the chimeric AAV2G9 capsids via co-transfection with a plasmid containing *rep* and *cap*

genes and adenovirus helper functions. Particles were purified using iodixanol gradients followed by column chromatography, and dotblot was used to determine vector titer [Benskey *et al*, 2016a]. The vector titers used in this 1.6×10^{12} vector genomes/mL. All surfaces (syringes, pipettes, and microcentrifuge tubes) were coated in SigmaCote (Sigma-Aldrich, St. Louis, MO) prior to coming in contact with the virus to minimize binding of viral particles [Benskey and Manfredsson, 2016b].

IV. Viral Vector Injections

All surgical procedures were performed under isoflurane anesthesia (5% in O₂ for induction and 2% in O₂ for maintenance). Rats were placed in a stereotaxic frame and a Hamilton syringe fitted with a glass capillary needle (Hamilton Gas Tight syringe 80,000, 26s/2" needle; Hamilton, Reno, NV; coated in SigmaCote) was used for injections. Two 2µL injections were injected in the left SNpc at coordinates (from dura) AP -5.3mm, ML +2.0mm, DV -7.2mm, and AP -6.0mm, ML +2.0mm, and DV -7.2mm as previously described [Polinski *et al*, 2015]. The glass needle was lowered to the site and vector injection began immediately at a rate of 0.5 µl/minute and remained in place after the injection for an additional 5 minutes before retraction.

V. Euthanasia and Tissue Preparation

All rats were sacrificed one month post-injection. Rats were deeply anesthetized (60mg/kg, pentobarbital, i.p.) and perfused intracardially with 0.9% saline containing 1ml/10,000 USP heparin, followed by ice cold 0.9% saline. Rat brains were immediately removed and hemisected in the coronal plane at approximately AP -2.64mm. Rostral tissue was processed for microdissections and caudal tissue was processed for immunohistochemistry.

VI. Microdissections

Microdissections were performed immediately after brain removal. Following 2 min incubation in ice-cold saline to firm and chill the tissue, 2mm coronal slabs were blocked from each brain using an aluminum brain blocker (Zivic, Pittsburg, PA). Striatal tissue from both hemispheres was microdissected with a 2mm tissue punch on a petri dish over ice. Frozen dissected structures were placed in pre-chilled microcentrifuge tubes and stored at -80°C.

VII. Western Blot

Striatal samples for western blot analyses were homogenized on ice in RIPA Lysis Buffer System (Santa Cruz, Dallas, TX). Total protein concentration was determined by the Bradford protein assay. Samples were prepared at 30ng total protein samples. Western blot protocol was completed as previously described [Polinski *et al*, 2015]. Briefly, samples were electrophoresed using SDS-PAGE gels and transferred to Immobilon-FL membranes (Millipore, Bedford, MA). Membranes were incubated in primary GFP antisera (Abcam, Cambridge, MA; rabbit polyclonal IgG, Ab290, 1:1,000) with β -tubulin antisera (Cell Signaling, Danvers, MA; mouse monoclonal IgG, 4466, 1:1,000) overnight. IRDye800 conjugated goat anti-rabbit (LI-COR Biosciences; 926-32211, 1:15,000) and IRDye680 conjugated goat anti-mouse (LI-COR Biosciences, 926-68020, 1:15,000) were used as secondary antibodies. All antibody dilutions were made in LI-COR compatible StartingBlock™ T20 (TBS) Blocking Buffer (Thermo Scientific, Waltham, MA). Multiplexed signal intensities were imaged with both 700 and 800 nm channels in a single scan with a resolution of 169 μ m using the Odyssey infrared image system (LI-COR Biosciences). Reported integrated intensity measurements of GFP expression were normalized according to the corresponding β -tubulin densitometry measurements as β -tubulin protein levels do not change with age [O'Callaghan and Miller, 1991]. The representative image was produced in Photoshop 7.0 (San Jose, CA).

VIII. Immunohistochemistry

The caudal portion of the brains designated for immunohistochemistry were post-fixed in 4% paraformaldehyde (Electron Microscopy Sciences, Hatfield, PA) in 0.1M PO₄ buffer for seven days. After this period they were transferred to 30% sucrose in 0.1M PO₄ buffer until saturated. Brains were frozen on dry ice and tissue was collected at a 40µm thickness as a 1 in 6 series in a 24 well plate. Every sixth section was processed for immunohistochemistry using the free-floating method.

i. Immunohistochemistry

Tissue sections were rinsed in Tris buffer and quenched in 0.3% H₂O₂ for 15 minutes, blocked in 10% normal goat serum for 1 hour, and incubated in primary antisera (TH: Millipore MAB318, mouse anti-TH, 1:4000; GFP: Abcam Ab290, rabbit anti-GFP, 1:100,000) overnight at 4°C. Following primary incubation, TH-labeled sections were incubated in biotinylated secondary antisera against mouse IgG (Vector BA-2001, biotinylated horse anti-mouse IgG, rat absorbed, 1:1000) and GFP-labeled sections were incubated in biotinylated secondary antisera against rabbit IgG (Millipore AP132b, goat anti-rabbit IgG, 1:500) for 2 hours at room temperature, followed by Vector ABC detection kit using horseradish peroxidase (Vector Laboratories, Burlingame, CA). Antibody labeling was visualized by exposure to 0.5mg/ml 3,3' diaminobenzidine and 0.03% H₂O₂ in Tris buffer. Sections were mounted on subbed slides, dehydrated via ascending ethanol washes, cleared with xylene, and coverslipped with Cytoseal. Images were taken on a Nikon Eclipse 90i microscope with a QICAM camera (QImaging, Surrey, British Columbia, Canada). Figures were produced in Photoshop 7.0 (San Jose, CA), with brightness, saturation, and sharpness adjusted only as needed to best replicate the immunostaining as viewed directly under the microscope.

ii. TH and GFP Double Label Immunofluorescence

Sections were blocked in 10% normal donkey serum for 1 hour and subsequently transferred to the primary antisera (TH: Millipore Ab318, mouse anti-TH, 1:4000) to incubate overnight at 4°C. Following primary incubation, tissue was incubated in the dark in secondary antisera against mouse IgG (Invitrogen A10037, Alexa Fluor 568 donkey anti-mouse, 1:500) for 1 hour at room temperature. Tissue was then blocked in 10% normal goat serum for 1 hour at room temperature before being incubated in the primary antisera against GFP (Abcam Ab290, rabbit anti-GFP, 1:100,000) overnight at 4°C in the dark. Following primary incubation, tissue was incubated in secondary antisera against rabbit IgG (Life Technologies A21206, Alex Fluor 488 goat anti-rabbit IgG, 1:500) for 1 hour at room temperature. Sections were mounted on subbed slides and coverslipped with Vectashield Hardset Mounting Medium (Vector Laboratories, Burlingame, CA). Images were taken on a Nikon 90i fluorescence microscope with a Nikon DS-Ri1 camera. Figures were produced in Photoshop 7.0 (San Jose, CA). Brightness, saturation, and sharpness were adjusted only as necessary to best replicate the immunostaining as viewed directly under the microscope.

IX. Stereology

Quantification of the number of GFP-immunoreactive (GFP+) cells in the midbrain and TH-immunoreactive (TH+) neurons in the SNpc was completed as previously described [Polinski *et al*, 2015]. Briefly, stereology was performed using a Nikon Eclipse 80i microscope (Nikon), StereoInvestigator software (Microbrightfield Bioscience, Williston, VT) and Retiga 4000R camera (Qimaging, Surrey, BC Canada). Using the optical fractionator probe, TH+ neurons in the vector injected and control hemisphere in every sixth section of the entire SN were counted at 60x magnification. GFP+ cells were counted at 60x magnification in the injected hemisphere in every sixth section of the brain where GFP staining was visible. All boundaries were drawn at 1x magnification and a 50x50 counting frame was

used. A Gundersen coefficient of error <0.10 was accepted. TH+ data are reported as total estimates of TH+ neurons in each hemisphere. GFP+ data are reported as percent of young estimates in the analyzed hemispheres.

X. Counts of GFP and TH Immunoreactive Cells

Tiled images at 10x magnification were taken on GFP and TH immunofluorescently stained midbrain sections containing the SNpc (average of 8 sections/rat). Images were taken with a Nikon 90i fluorescence microscope with a Nikon DS-Ri1 with the exposure constant between images. All GFP+ cells that were in focus with a clear nucleus and appeared to be counterstained with TH were manually counted to determine the total number of GFP+/TH+ cells in the SNpc. Total numbers of GFP+/TH+ cells for each rat were calculated. Data is represented as the percent of the young mean GFP+/TH+ cells in the SNpc.

XI. Statistical Analyses

All statistical tests were completed using IBM SPSS statistics software (version 22.0, IBM, Armonk, NY). Graphs were created using GraphPad Prism software (version 6, GraphPad, La Jolla, CA). To compare young adult vs. aged rat GFP+ stereology counts, GFP+/TH+ cell counts, and GFP western blot values, independent samples t-tests were used. Results of TH+ SNpc neuron quantification were analyzed with two-way repeated measures ANOVA with two treatment factors, age and hemisphere. When appropriate, Bonferroni *post hoc* analyses were used on ANOVA tests to determine significance between individual groups using the harmonic mean of the group sizes to account for unequal sample sizes.

Results

Previous reports have noted an age-related transduction deficiency following rAAV2/2 GFP, but not rAAV2/9 GFP injection to the SNpc [Wu *et al*, 2004; Klein *et al*, 2010; Dissertation Chapter 3]. The difference in AAV pseudotype indicates that the transduction deficiency must be the result of age-related changes in capsid-mediated steps of transduction as both vector pseudotypes use the AAV2 genome and differ only in AAV capsid. As receptor binding and endocytosis is an important step of transduction that relies heavily on the quantity of specific cell-surface receptors used by these viruses [Summerford and Samulski, 1998; Walters *et al*, 2001; Shen *et al*, 2011], and some of the implicated receptors have been shown to be down-regulated with age [Sato *et al*, 2001; Sasaki *et al*, 2002], we hypothesized that the age-related transduction deficiency of rAAV2/2 is receptor-mediated.

To test this hypothesis, we used a chimeric viral vector that consists of the AAV2 genome and an AAV2 capsid onto which the AAV9 receptor-binding motifs are grafted [Shen *et al*, 2013]. In this way, the chimeric viral vector, rAAV2G9, is able to use the cell surface receptors of both AAV2 and AAV9 for cell entry without altering downstream AAV2 transduction processes [Shen *et al*, 2013]. rAAV2G9 or the control rAAV2 expressing GFP driven by the chicken beta actin/cytomegalovirus enhancer (C β A/CMV) promoter hybrid were injected unilaterally into the SNpc to target the nigrostriatal system. Rats were sacrificed at one month post-injection when transgene expression levels are known to asymptote [Reimsnider *et al*, 2007]. To verify that neither rAAV2G9 nor rAAV2 were toxic and confirm that no age-related decreases in nigral dopaminergic neuron numbers exist, we quantified TH+ neurons in the injected and uninjected SNpc. To assess overall transduction efficiency as measured by GFP+ cell counts, we quantified total number of GFP+ cells with stereology. To assess nigrostriatal transduction efficiency, we measured GFP protein levels in the anterograde structure (striatum) and the number of GFP+/TH+ cells in the SNpc.

I. No age-related differences occur in total numbers of GFP+ midbrain cells

We first sought to determine whether age- or vector-related toxicity existed and altered the number of SNpc dopaminergic neurons, as this could confound interpretation of our results. No significant differences were detected in the number of TH+ cells in the SNpc of young adult versus aged rats, or the injected vs uninjected hemisphere for rAAV2 GFP (injection: $F_{(1,10)}=0.001$, $p=0.976$; age: $F_{(1,10)}=0.797$, $p=0.393$; Figure 29a-b) or rAAV2G9 GFP (injection: $F_{(1,13)}=0.378$, $p=0.549$; age: $F_{(1,13)}=1.998$, $p=0.181$; Figure 29c-d). As a result, measures of transduction efficiency should not be confounded by age or injection.

To determine if age-related differences occur in the total number of GFP+ cells, we performed blinded, unbiased stereology for GFP+ cells in the midbrain of the injected hemisphere. No significant differences were observed in total numbers of GFP+ cells in the midbrain following rAAV2 GFP ($p=0.205$; Figure 29e-f) or rAAV2G9 GFP ($p=0.531$; Figure 29g-h) injection into the aged as compared to young adult rat SNpc. These results are consistent with previous observations that age does not significantly alter the number of transgene-expressing cells at one month post-injection [Wu *et al*, 2004; Dissertation Chapter 3].

II. rAAV2 GFP transduction is deficient in the aged nigrostriatal system

In order to directly assess transduction of the nigrostriatal system, we first quantified the number of GFP+/TH+ cells in the SNpc. As our viral vectors will infect the dopaminergic neurons of the SNpc as well as non-dopaminergic neurons and regions adjacent to the SNpc, quantifying the number of GFP+/TH+ cells provides us with the ability to investigate transduction of the nigrostriatal system at the injection site. One month after rAAV2 GFP injection to the SNpc aged rats had significantly fewer GFP+ dopaminergic neurons than young adult rats ($p=0.024$; Figure 30a-c). Furthermore, we analyzed GFP

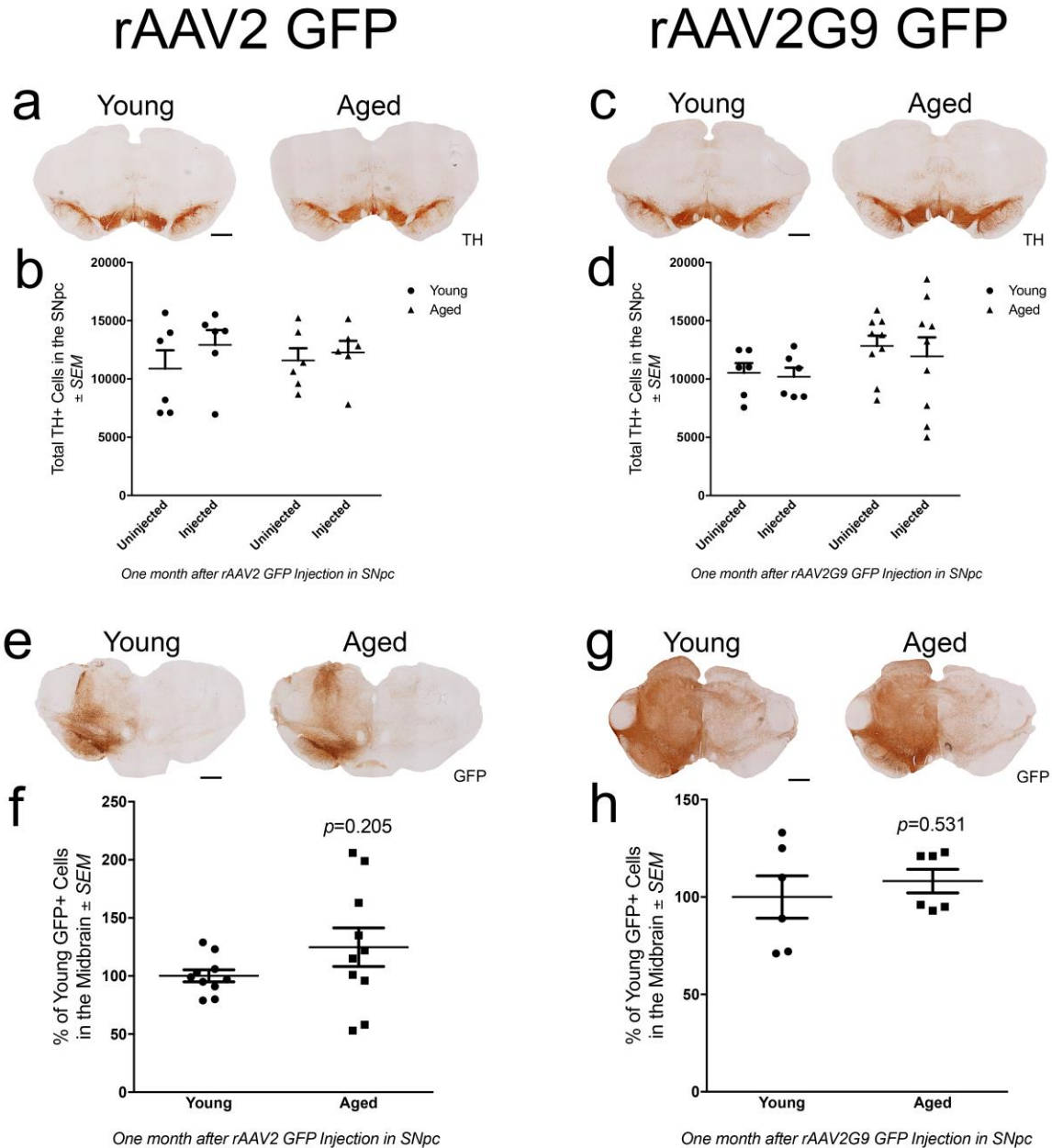


Figure 29. No age-related differences are observed in total number of GFP+ cells following rAAV2 or rAAV2G9 injection. a, c) Representative image of TH immunoreactivity in the SNpc of young adult (Young) and aged (Aged) rats following rAAV2 or rAAV2G9 GFP transduction. Scale bars = 1000 μ m. b, d) Quantitation of total TH+ cells in the young adult and aged injected and uninjected SNpc. No significant differences were seen between hemisphere or age (n=6/age in rAAV2; n=6 young and 9 aged in rAAV2G9). e, g) Representative image of GFP immunoreactivity in the midbrain of young adult and aged rats one month after rAAV2 or rAAV2G9 GFP injection. Scale bars = 1000 μ m. f, h) Quantitation of total GFP+ cells in the young adult and aged rat midbrain. No significant differences were seen between age in either group (n=10/age in rAAV2; n=6/age in rAAV2G9). Values in b and d are expressed as total cell counts \pm SEM for each group. Values in f and h are expressed as the percent of the young cell counts \pm SEM for each group. Abbreviations: TH, tyrosine hydroxylase; GFP, green fluorescent protein; rAAV, recombinant adeno-associated virus; SNpc, substantia nigra pars compacta; SEM, standard error of the mean.

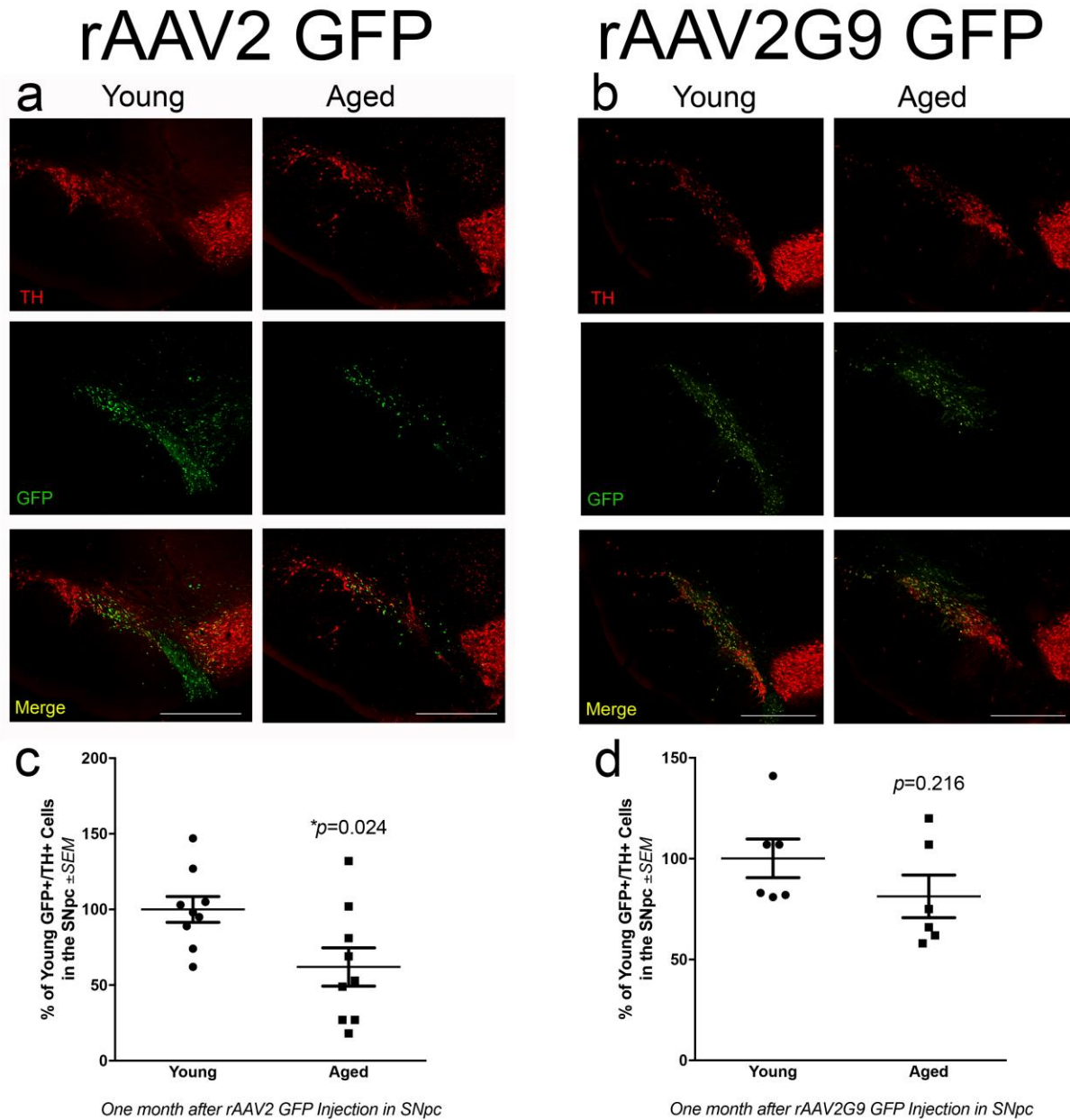


Figure 30. rAAV2 is deficient in transducing the aged nigrostriatal system at the injection site, whereas rAAV2G9 is equally as efficient between ages. a-b). Representative images of GFP expression within TH⁺ SNpc neurons in young adult (Young) and aged (Aged) rats following rAAV2 and rAAV2G9 GFP transduction, respectively. Scale bars = 1000 μ m. c-d) Quantitation of GFP⁺ cells co-localizing with TH⁺ cells in the SNpc following rAAV2 GFP injection and rAAV2G9 GFP injection, respectively. Aged rats had significantly fewer ($*p \leq 0.05$) GFP⁺/TH⁺ cells than young adult rats following rAAV2 injection ($n=9$ /age/vector), but not rAAV2G9 injection ($n=6$ /age/vector; $p > 0.05$). Values in c and d are expressed as the percent of the young GFP⁺/TH⁺ cell counts \pm SEM for each group. Abbreviations: TH, tyrosine hydroxylase; GFP, green fluorescent protein; TH⁺, TH-immunoreactive; GFP⁺, GFP-immunoreactive; rAAV, recombinant adeno-associated virus; SNpc, substantia nigra pars compacta; SEM, standard error of the mean.

protein levels in the nigrostriatal system with Western blots and near-infrared quantitation in the anterograde structure. Aged rats had approximately 60% less GFP in the ipsilateral striatum than young adult rats one month after rAAV2 GFP injection to the SNpc ($p=0.001$; Figure 31a). Taken together, these results indicate a robust deficiency in nigrostriatal transduction by rAAV2 GFP.

III. rAAV2G9 GFP transduction is not deficient in the aged nigrostriatal system

Similarly, we analyzed GFP expression in the nigrostriatal system one month following rAAV2G9 GFP injection to the SNpc. Unlike the age-related deficiencies observed with rAAV2, rAAV2G9 injection resulted in equal numbers of GFP+/TH+ neurons in the SNpc in young adult and aged rats ($p=0.216$; Figure 30b,d). In addition, striatal GFP levels were equivalent between young adult and aged rats with rAAV2G9 GFP ($p=0.934$; Figure 31b). These results indicate that the addition of AAV9 receptor-binding motifs on the capsid of AAV2 restores transduction in the aged rat nigrostriatal system.

Discussion

In the present study, we sought to identify the mechanism behind the previously observed age-related transduction deficiencies with rAAV2/2 [Wu *et al*, 2004; Dissertation Chapter 3], but not rAAV2/9 [Klein *et al*, 2010; Dissertation Chapter 3] in the nigrostriatal system. As the only difference between these two vector constructs is the viral capsid, the step of transduction that is less efficient with advanced age must be a capsid-related step of transduction. Such steps include receptor binding, endocytosis, intracellular trafficking, Golgi-mediated processing, release of the viral construct from the endosome, nuclear import, and release of the viral vector genome from the capsid [Ding *et al*, 2005; Schultz and Chamberlain, 2008; Nonnenmacher and Weber, 2012]. We hypothesized that viral binding to cell surface receptors was the step of transduction contributing to the lower transgene expression levels in

rAAV2 GFP

rAAV2Gal9 GFP

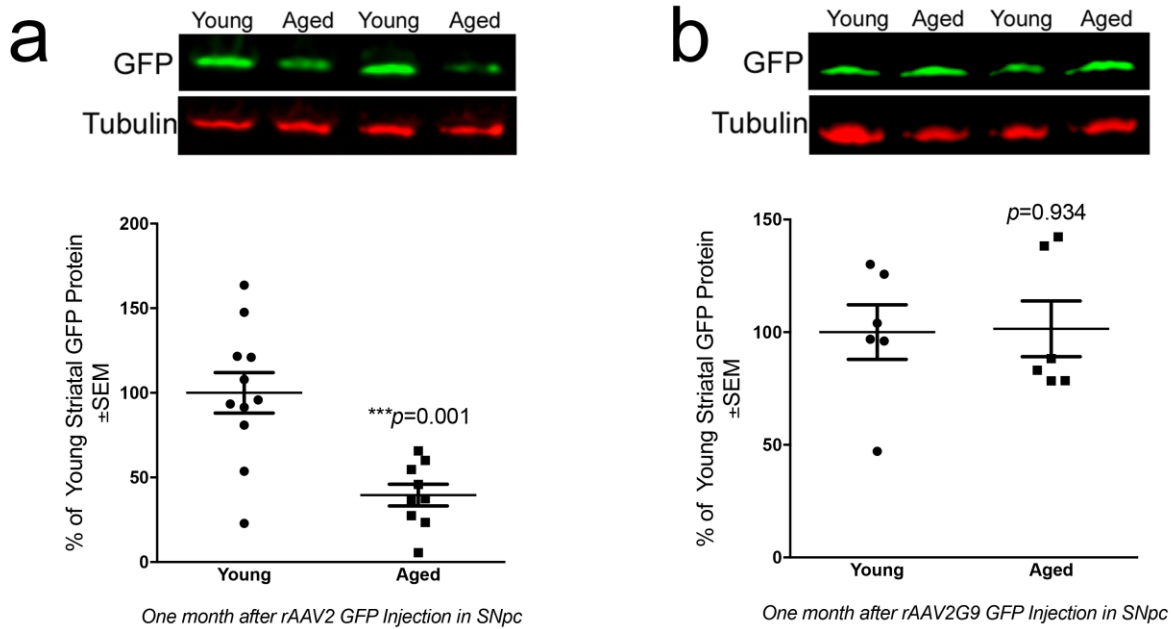


Figure 31. Viral vector-mediated expression of GFP is reduced in the aged nigrostriatal system with rAAV2, but not rAAV2G9, in the anterograde structure. Representative Western blot and quantitation of GFP in striatal samples of young adult (Young) and aged (Aged) rats one month post-injection with a) rAAV2 GFP and b) rAAV2G9 GFP. a) Aged (n=10) rats expressed significantly less striatal GFP than young adult (n=11) rats following rAAV2 GFP transduction (** $p \leq 0.001$). b) Young adult (n=6) and aged (n=6) rats expressed equivalent levels of GFP following rAAV2G9 GFP transduction ($p > 0.05$). Values are expressed as the percent of the young mean optical density scores, with GFP signal normalized to tubulin controls \pm SEM for each group. Abbreviations: GFP, green fluorescent protein; rAAV, recombinant adeno-associated virus; SNpc, substantia nigra pars compacta; SEM, standard error of the mean.

the aged as compared to young adult rat for the following reasons: (1) each viral pseudotype has a capsid that binds to specific cell surface receptors to initiate viral attachment and endocytosis into the cell [Schultz and Chamberlain, 2008; Nonnenmacher and Weber, 2012], (2) the number of cell surface receptors is a critical determinant of transduction efficiency [Summerford and Samulski, 1998; Walters *et al*, 2001; Ding *et al*, 2005; Shen *et al*, 2011], and (3) previous work has shown an age-related decrease in the receptors used for binding and endocytosis of some rAAV constructs [Sato *et al*, 2001; Sasaki *et al*, 2002]. Therefore, we examined the role of cell surface receptor binding/endocytosis in viral vector transduction deficiencies in the aged brain.

Using rAAV2 and the chimera rAAV2G9 that uses the AAV2 capsid with the addition of AAV9 receptor binding sites, we injected the young adult and aged rat SNpc and analyzed transduction efficiency one month later. This chimera was chosen as rAAV2 was previously shown to be deficient in the aged nigrostriatal system [Wu *et al*, 2004; Dissertation Chapter 3] whereas rAAV2/9 was equally as efficient in young adult and aged nigrostriatal system [Klein *et al*, 2010; Dissertation Chapter 3]. Using multiple outcome measures to assess nigrostriatal transduction at the level of the injection and the anterograde structure, we see a robust transduction deficiency following injection of rAAV2 GFP, but not rAAV2G9 GFP. In the SNpc, we used total counts of GFP+ cells to assess overall transduction and see no differences in the number of GFP-expressing cells in young adult versus aged rats with either viral vector (Figure 29). These results were consistent with previous findings that age does not change the total quantity of transgene-expressing cells [Wu *et al*, 2004; Dissertation Chapter 3]. However, when examining the number of GFP+ dopaminergic neurons of the SNpc in particular, age-related decreases can be seen in rAAV2 but not rAAV2G9 transduction (Figure 30). Similarly, less GFP protein in the anterograde striatum of the nigrostriatal system was observed following rAAV2, but not rAAV2G9, transduction (Figure 31). Taken together, these results indicate that a robust deficiency exists in rAAV2

transduction of the aged versus young adult rat nigrostriatal system that can be extinguished by enabling rAAV2 to also use the rAAV9 cell surface receptors.

Currently, rAAV2 is the only viral vector used in clinical trials for Alzheimer's or Parkinson's disease in the United States [O'Connor and Boulis, 2015; Choudhury *et al*, 2016]. This is most likely due to the fact that AAV2 was the first discovered rAAV serotype, rAAV2 is highly neurotropic, more is known about the transduction of rAAV2 than any other serotype, and rAAV2 has already undergone numerous preclinical and clinical safety evaluations. As a result, it is likely that rAAV2 will continue to be developed for use in clinical trials for age-related neurodegenerative diseases like Alzheimer's and Parkinson's disease.

Considering this fact, understanding which steps of rAAV2 transduction are less efficient with age and cause the age-related transduction deficiency will be important for future use of this technology in aged brains.

Furthermore, understanding the mechanism of the age-related transduction deficiency is important for a variety of additional reasons. First, understanding which step of transduction is impaired in the aged brain may enable us to predict which viral vectors will be less efficient in which structures. As not all viral vectors are deficient in the aged brain and the deficiencies vary based on the structure injected and pathway analyzed [Klein *et al*, 2010; Dissertation Chapter 3], developing a method for predicting which viral vectors will be deficient in which structures will be an important step for preclinical and clinical trials. For instance, rAAV2/5 has been shown to have a robust transduction deficiency in the aged versus young adult rat nigrostriatal system following injection into the SNpc [Polinski *et al*, 2015; Fischer *et al*, 2016; Dissertation Chapter 3]. If this deficiency can be definitively linked to decreases in levels of its primary receptor, 2,3-linked sialic acid [Walters *et al*, 2001], the use of rAAV2/5 can be avoided in structures like the hippocampus and cerebellum that display decreases in this receptor with age [Sato *et*

al, 2001; Sasaki *et al*, 2002]. In this way, transduction deficiencies can be avoided by using the appropriate viral vector for the structure of interest in the aged brain.

Understanding the mechanism of age-related transduction deficiencies will also be important in the interpretation of previous PD viral vector-mediated gene therapy clinical trials. Numerous clinical trials, almost all using rAAV2, have demonstrated promising results in Phase I safety and early efficacy trials for PD. However, upon moving to placebo-controlled, double-blinded Phase II efficacy trials, all viral vector-mediated gene therapy strategies have failed to meet primary endpoints or show benefits over those observed with conventional treatment [O'Connor and Boulis, 2015; Choudhury *et al*, 2016]. Assessments of human brains that underwent viral vector-mediated gene therapy to deliver a neurotrophic factor to the striatum indicated levels of expression in the SNpc much lower than anticipated from preclinical studies [Bartus *et al*, 2011]. This lack of expression is of critical significance as previous work has shown a strong correlation between the level of transgene expression, neuroanatomical benefits, and functional recovery [Emborg *et al*, 2009]. Although possibly due to other factors such as the method of delivery or the patients needing to be in an earlier stage of PD, this could also be due to age-related transduction deficiencies in viral vectors such as rAAV2. With this in mind, it is possible that the transgene expressed would have resulted in neuroprotection or functional gains if expressed more efficiently.

Should age-related transduction deficiencies exist in humans to a similar extent as those demonstrated in rats, dosage of the viral vector would have to increase by at least 60% to compensate for the decreased protein expression resulting from inefficient transduction of the aged versus young adult brain by rAAV2/2 (Figure 30, Figure 31) [Wu *et al*, 2004; Dissertation Chapter 3]. As a result, scaling would not only need to be performed to account for species differences, additional scaling would also

need to take place to account for age differences when translating work from young adult animals to aged humans. Although increasing the titer or amount of the vector administered may increase transgene expression to counter age-related transduction deficiencies, this strategy has the potential for increased negative side effects due to higher numbers of viral particles activating the immune system and causing toxicity [Howard *et al*, 2008; Choudhury *et al*, 2016]. As a result, understanding the mechanism(s) behind the transduction deficiency will be an important step in increasing transgene expression and overcoming the age-related deficiency.

Our study is the first of its kind to investigate the mechanism behind the previously observed age-related transduction deficiency of rAAV2 [Wu *et al*, 2004; Dissertation Chapter 3]. By employing the rAAV2G9 chimeric viral vector that uses the normal AAV2 vector with the addition of rAAV9 receptor-binding motifs [Shen *et al*, 2013], we were able to test our hypothesis that the age-related transduction deficiencies are due to capsid-mediated steps of transduction [Dissertation Chapter 3]. By abolishing the age-related transduction deficiencies of rAAV2 with the addition of AAV9 receptor-binding motifs and not other areas of the AAV9 capsid, we further narrowed the mechanism to involve deficiencies in capsid-receptor interactions. Presumably, this limits the mechanism of the age-related deficiency to cell surface receptor binding and initiation of endocytosis [Schultz and Chamberlain, 2008; Nonnenmacher and Weber, 2012].

However, one limitation of this study is that it does not definitively link the viral vector transduction deficiencies to age-related decreases in cell surface receptors. It is possible that the rAAV2G9 vector uses endocytosis and intracellular pathways distinct from those of rAAV2 [Shen *et al*, 2013], and the ameliorated transduction deficiency is due to improved endocytosis and intracellular trafficking rather than receptor binding and initiation of endocytosis. However, due to the importance of receptor

abundance in rAAV transduction efficiency and transgene expression [Summerford and Samulski, 1998; Walters *et al*, 2001; Ding *et al*, 2005; Schultz and Chamberlain, 2008; Nonnenmacher and Weber, 2012], previous reports of age-related decreases in cell surface receptors involved in rAAV binding and endocytosis [Sato *et al*, 2001; Sasaki *et al*, 2002], and the rescue of rAAV2 transduction in the aged SNpc with the addition of receptor binding motifs from an rAAV construct that displayed no SNpc age-related transduction deficiencies (Figure 30, Figure 31) [Shen *et al*, 2013; Dissertation Chapter 3], it is likely that the mechanism behind the age-related transduction deficiency of rAAV2 is due to impairments in receptor-mediated steps of transduction. Future experiments examining differences between young adult and aged animals in the number or functionality of different receptors and co-receptors involved in rAAV transduction will be important for determining whether changes in specific receptors can be correlated with altered transduction efficiency in the aged brain.

Characterizing changes in the transduction efficiency of different viral vector constructs with advanced age is an important, and often overlooked, step in designing viral vector-mediated gene therapy clinical trials for age-related neurodegenerative diseases. Understanding the mechanism behind any observed age-related transduction deficiencies is important for determining how to overcome the steps of transduction that are impaired in the aged brain to successfully deliver a transgene to the affected area. Taken together, our study highlights the likelihood that changes in receptor expression or functioning are causing the previously observed transduction deficiency of rAAV2/2, but not rAAV2/9, in the aged SNpc [Dissertation Chapter 3]. This information will be vital for interpreting the results of previous viral vector-mediated gene therapy clinical trials for age-related neurodegenerative diseases, designing new clinical trials using this therapy in aged patients, and developing predictive models for determining which viral vector will experience transduction deficiencies in different structures or cell populations within the aged brain.

LITERATURE CITED

LITERATURE CITED

- Bartus, R.T., C.D. Herzog, Y. Chu, A. Wilson, L. Brown, J. Siffert, E.M. Johnson Jr, C.W. Olanow, E.J. Mufson, and J.H. Kordower. (2011). Bioactivity of AAV2-neurturin gene therapy (CERE-120): differences between Parkinson's disease and nonhuman primate brains. *Mov Disord*, 26(1): 27-36.
- Benskey, M.J., and F.P. Manfredsson. (2016a). Lentivirus Production and Purification. *Methods Mol Biol*, 1382: 107-114.
- Benskey, M.J., and F.P. Manfredsson. (2016b). Intraparenchymal stereotaxic delivery of rAAV and special consideration in vector handling. *Methods Mol Biol*, 1382: 199-215.
- Choudhury, S.R., E. Hudry, C.A. Maguire, M. Sena-Esteves, X.O. Breakefield, and P. Grandi. (2016). Viral vectors for therapy of neurologic diseases. *Neuropharmacology*, doi:10.1016/j.neuropharm.2016.02.013.
- Ding, W., L. Zhang, Z. Yan, and J.F. Engelhardt. (2005). Intracellular trafficking of adeno-associated viral vectors. *Gene Ther*, 12: 873-880.
- Emborg, M.E., J. Moirano, J. Raschke, V. Bondarenko, R. Zufferey, S. Peng, A.D. Ebert, V. Joers, B. Roitberg, J.E. Holden, J. Koprach, J. Lipton, J.H. Kordower, and P. Aebischer. (2009). Response of aged parkinsonian monkeys to in vivo gene transfer of GDNF. *Neurobiol Dis*, 36(2): 303-311.
- Fischer, D.L., S.E. Gombash, C.J. Kemp, F.P. Manfredsson, N.K. Polinski, M.F. Duffy, and C.E. Sortwell. (2016). Viral vector-based modeling of neurodegenerative disorders: Parkinson's disease. *Methods Mol Biol*, 1382: 367-382.
- Howard, D.B., K. Powers, Y. Wang, and B.K. Harvey. (2008). Tropism and toxicity of adeno-associated viral vector serotypes 1, 2, 5, 6, 7, 8, and 9 in rat neurons and glia in vitro. *Virology*, 372(1): 24-34.
- Klein, R.L., R.D. Dayton, C.G. Diaczynsky, and D.B. Wang. (2010). Pronounced microgliosis and neurodegeneration in aged rats after tau gene transfer. *Neurobiol Aging*, 31(12): 2091-2102.
- Leys, C., C. Ley, O. Klein, P. Bernard, and L. Licata. (2013). Detecting outliers: Do not use standard deviation around the mean, use absolute deviation around the median. *J Exp Soc Psychol*, 49: 764-766.
- Nonnenmacher, M., and T. Weber. (2012). Intracellular transport of recombinant adeno-associated virus vectors. *Gene Ther*, 19(6): 649-658.
- O'Callaghan, J.P., and D.B. Miller. (1991). The concentration of glial fibrillary acidic protein increases with age in the mouse and rat brain. *Neurobiol Aging*, 12: 171-174.
- O'Connor, D.M. and N.M. Boulis. (2015). Gene therapy for neurodegenerative diseases. *Trends Mol Med*, 21(8): 504-512.

- Polinski, N.K., S.E. Gombash, F.P. Manfredsson, J.W. Lipton, C.J. Kemp, A. Cole-Strauss, N.M. Kanaan, K. Steece-Collier, N.C. Kuhn, S.L. Wohlgenant, and C.E. Sortwell (2015). Recombinant adeno-associated virus 2/5-mediated gene transfer is reduced in the aged rat midbrain. *Neurobio Aging*, **36(2)**: 1110-1120.
- Reimsnider, S., F.P. Manfredsson, N. Muzyczka, and R.J. Mandel. (2007). Time course of transgene expression after intrastriatal pseudotyped rAAV2/1, rAAV2/2, rAAV2/5, and rAAV2/8 transduction in the rat. *Mol Ther*, **15(8)**: 1504-1511.
- Sasaki, T., Y. Akimoto, Y. Sato, H. Kawakami, H. Hirano, and T. Endo. (2002). Distribution of sialoglycoconjugates in the rat cerebellum and its change with age. *J Histo Cyto*, **50(9)**: 1179-1186.
- Sato, Y., Y. Akimoto, H. Kawakami, H. Hirano, and T. Endo. (2001). Location of aialoglycoconjugates containing the sial α 2-3Gal and sial α 2-6Gal groups in the rat hippocampus and the effect of aging on their expression. *J Histo Cyto*, **49(10)**: 1311-1319.
- Schultz, B.R., and J.S. Chamberlain. (2008). Recombinant adeno-associated virus transduction and integration. *Mol Ther*, **16(7)**: 1189-1199.
- Shen, S., K.D. Bryant, S.M. Brown, S.H. Randell, and A. Asokan. (2011). Terminal N-linked galactose is the primary receptor for adeno-associated virus 9. *J Biol Chem*, **286**: 13532-13540.
- Shin, S., H.M. Tuinstra, D.M. Salvay, and L.D. Shea. (2010). Phosphatidylserine immobilization of lentivirus for localized gene transfer. *Biomaterials*, **31**: 4353-4359.
- Summerford, C., and R.J. Samulski. (1998). Membrane-associated heparan sulfate proteoglycan is a receptor for adeno-associated virus type 2 virions. *J Virol*, **72(2)**: 1438-1445.
- Walters, R.W., S.M. Yi, S. Keshavjee, K.E. Brown, M.J. Welsh, J.A. Chiorini, and J. Zabner. (2001). Binding of adeno-associated virus type 5 to 2,3-linked sialic acid is required for gene transfer. *J Biol Chem*, **276**: 20610-20616.
- Wu, Z., E. Miller, M. Agbandje-McKenna, and R.J. Samulski. (2006). Alpha2,3 and alpha2,6 N-linked sialic acids facilitate efficient binding and transduction by adeno-associated virus types 1 and 6. *J Virol*, **80(18)**: 9093-9103.
- Zolotukhin, S., B.J. Byrne, E. Mason, E. Zolotukhin, M. Potter, K. Chesnut, C. Summerford, R.J. Samulski, and N. Muzyczka. (1999). Recombinant adeno-associated virus purification using novel methods improves infectious titer and yield. *Gene Ther*, **6**: 973-985.

Chapter 6. Discussion

Conclusions, In Brief

In the present dissertation, we tested the hypothesis that advanced age would impact the efficiency of viral vector-mediated gene therapy and focused on structures relevant to PD. We found robust age-related transduction deficiencies that occur across multiple viral vector constructs, target structures, transgenes expressed, rat strains, and durations of expression. In summary, advanced age negatively impacts the ability of rAAV2/2, rAAV2/5, and LV to express GFP in the nigrostriatal system. In addition, age-related transduction deficiencies also exist in the striatonigral system following intrastriatal injection of rAAV2/2, rAAV2/5, and rAAV2/9 expressing GFP. We extended these findings to reveal that rAAV2/2-mediated delivery of GDNF was similarly deficient in the aged striatum. To understand the mechanism of the transduction deficiency, we capitalized on the finding that rAAV2/2, but not rAAV2/9, is deficient in the nigrostriatal system. This finding implicates capsid-mediated steps of transduction in the deficiency as the capsid differs between these pseudotypes while the genome remains constant. Using a chimeric rAAV2/2 that contains the receptor binding motifs of rAAV9, we were able to abolish the age-related rAAV2/2 transduction deficiency and thereby link capsid-receptor interactions to the mechanism of the deficiency. In total, these results indicate the presence of a robust inability of viral vectors to transduce the aged as compared to young adult nigrostriatal and striatonigral system that has the potential to be mitigated by selection of a viral vector appropriate for the aged target structure. Direct knowledge of age-related changes in specific cell surface receptors in particular structures would inform this selection.

Future Directions and Implications for Use of Viral Vectors in Aged Brains

I. Characterization of Age-Related Transduction Deficiencies

i. Defining Transduction Efficiency

In this study I characterized the nigrostriatal and striatonigral transduction efficiency of four viral vectors commonly used in preclinical and clinical trials for PD. In doing so, we needed to define what outcome measure would be used to determine overall “transduction efficiency”. Historically, transduction efficiency has been defined by the total number of cells expressing the transgene [Davidson *et al*, 2000; Burger *et al*, 2004; Reimsnider *et al*, 2007; McFarland *et al*, 2009; Dodiya *et al*, 2010; Cannon *et al*, 2011; Van der Perren *et al*, 2012]. While we did include counts of GFP+ cells in all experiments characterizing GFP-expressing viral vector transduction efficiency, we did not designate this as our primary outcome measure of efficiency. Rather, our primary outcome measure for transduction efficiency was the amount of GFP protein overexpressed in the circuitry of interest. We chose this method due to the fact that it is the total quantity of exogenous protein expressed, particularly the expression of trophic factors, that dictates functional and neuroanatomical recovery in viral vector-mediated gene therapy [Emborg *et al*, 2009]. Furthermore, we measured the GFP protein levels at the anterograde structure as this allowed us to increase specificity for our system and exclude other cell types and adjacent structures that have also been transduced. This emphasis on protein delivery in our working definition of transduction efficiency aligns with the ultimate therapeutic intent of this approach.

Importantly, in this study age-related decreases in transduction efficiency were oftentimes not detected when using bimodal methods (quantifying total numbers of GFP+ cells) versus linear methods (Western

blot and qPCR). This highlights the need to use linear methods of quantifying transduction when levels of total protein expression are relevant as these transduction deficiencies would have been overlooked if cell counts were the primary outcome measure, as is most-often done. This discrepancy between bimodal and linear measures could be due to the fact that counts of total GFP+ cells do not account for differences in GFP protein on a per-cell basis and do not provide the specificity of observing only the cell type of interest. To assess transduction efficiency of the nigrostriatal system at the injection site, counts of immunofluorescent cells in the SNpc that co-expressed GFP and TH were better predictors of nigrostriatal transduction efficiency, but discrepancies still existed in the ability to reliably identify the presence and magnitude of an age-related decrease in protein.

In the studies characterizing the transduction efficiency of GFP-expressing viral vectors in young adult versus aged rats, tissue from the injection site was not processed to allow definitive, sensitive quantitation of protein or mRNA overexpression. Rather, all injection-site tissue was processed for histochemical analyses that included GFP+ cell counts and other secondary measures of transduction efficiency, thereby limiting our ability to measure total protein overexpression levels at the injection site with techniques like Western blotting, qPCR, or ELISA. The decision was made to process injection site tissue for histochemistry as it allows excellent quality control through visual verification of injection placement and infusion success that is not possible with biochemical approaches. To gather additional data from the injection site, we measured GFP protein by quantifying the intensity of near-infrared GFP immunoreactivity and qualitatively examined GFP mRNA using *in situ* hybridization. While these measures are less direct and sensitive than performing Western blot or qPCR at the injection site, they were compatible with the existing tissue and did not require additional rats, aligning well with the three R's of animal work (reduce, refine, replace). In addition to these methods, we attempted to conduct laser capture microdissection (LCM) of the striatum for GFP qPCR.

Of the three approaches (near infrared immunoreactivity, *in situ* hybridization, and LCM combined with qPCR), quantitation of near-infrared immunoreactivity provided the most information but still may have lacked the sensitivity to detect transduction deficiencies when the injection volume was small or the age-related differences were not extremely pronounced [Dissertation Chapter 3]. RNAscope for GFP mRNA was qualitative and not quantified with optical density measures due to the common presence of non-specific background staining in the tissue. Lastly, we attempted LCM on the tissue sections to isolate the striatum for GFP qPCR. Unfortunately, this technique did not lend itself well to cutting such a large area and we were not able to extract the striatum from our tissue sections using this method. Another option with LCM would be to extract the individual GFP+ cells of the striatum so the GFP mRNA signal is not diluted by uninfected areas and to avoid the problems experienced when attempting to collect a large structure. However, this leads to a bias in measuring GFP mRNA only in cells with high levels of GFP transduction. Collecting all striatal cells would eliminate this bias but would be very time-consuming. LCM and subsequent qPCR for GFP mRNA may be feasible if capturing individual cells while blinded to GFP staining, but would again prove time-consuming and GFP mRNA signal could be diluted with nontransduced cells and decrease the chances of detecting age-related differences of a low magnitude.

With this in mind, future experiments studying transduction efficiency should incorporate analyses on exogenous protein level and the number of transgene-expressing cells. With age- and vector-related toxicity levels now established from previous experiments comparing the injected and uninjected hemispheres [Dissertation Chapters 2 and 3], future studies could use bilateral injections with one hemisphere processed for histology and the other for biochemistry. For instance, one hemisphere could be designated solely for histology. The injected structure could be analyzed for the number of

transgene-expressing cells, the volume of transduction, and the phenotype of transgene-expressing cells. In addition, tissue from the other structures in this hemisphere could be analyzed for retrograde and anterograde transport efficiency using cell counts and near-infrared immunoreactivity, respectively. In the contralateral hemisphere, tissue could be designated for biochemistry with the injected and anterograde/retrograde structures used to accurately quantify transduction efficiency and transport at the total-protein and total-mRNA level.

ii. Expanding Investigation to other Viral Vector Constructs

Although our experiments characterized the transduction efficiency of three rAAV pseudotypes and one LV pseudotype, a natural extension of this project would be to investigate the impact of age on other viral vectors relevant to age-related disease treatment or disease modeling. This line of research would not only provide a better catalog of which viral vectors are deficient in various aged brain structures, it would also provide more insight into the role of receptors in the age-related transduction deficiency. For instance, each rAAV serotype binds to specific cell surface receptor and co-receptors. HSPG is the primary receptor for rAAV2, as well as rAAV3 and rAAV6 [Dissertation Chapter 1, Table 1]. If HSPG is shown to be downregulated in the aged as compared to young adult brain, and these decreases correlate with transduction deficiencies in rAAV2, rAAV3, and rAAV6, this could provide stronger evidence for the role of virion-receptor interactions in the age-related transduction deficiencies. Furthermore, investigating the impact of age on rAAV2/8 and rAAV2/10 would be interesting due to their distinct capsid receptors [Dissertation Chapter 1, Table 1], phylogenic differences, and possible use in gene therapy of the CNS [Gao *et al*, 2002; Mori *et al*, 2004; Gurda *et al*, 2012; Raupp *et al*, 2012; Mietzsch *et al*, 2014; Halder *et al*, 2015].

Furthermore, it would be a worthwhile pursuit to test different rAAV2 mutants in the aged as compared to young adult brain. rAAV2 is the gold standard for viral vector-mediated gene therapy clinical trials in the CNS due to the fact that it was the first AAV serotype discovered, this AAV serotype was the first approved by the FDA, and more is known about the transduction mechanism of AAV2 than the other AAV serotypes [Nonnenmacher and Weber, 2012; Choudhury *et al*, 2016]. As a result, it is likely that rAAV2 will continue to be pursued for clinical trials in the future. Investigating AAV2 mutants that efficiently transduce the aged brain and express robust levels of the exogenous transgene will be necessary as increasing the titer of AAV2 is not a feasible method of overcoming age-related transduction deficiencies due to concerns over toxicity and safety of surpassing currently approved vector doses [Howard *et al*, 2008; Marks *et al*, 2010; Rafii *et al*, 2014; clinicaltrials.gov, NCT01621581]. Furthermore, identifying which rAAV2 mutant best transduces the aged brain would be beneficial for understanding the mechanism behind the age-related transduction deficiency. A list of four mutants that would be particularly interesting to test in the aged versus young adult brain are listed in **Table 4**. As each of these mutants alters different steps of transduction, comparing their efficiency in the young adult versus aged brain would provide insight into the impact of age on multiple cellular processes.

iii. Expanding Investigation to other Brain Systems and Structures

Although PD is the age-related brain disease with the most viral vector-mediated gene therapy clinical trials, clinical trials using this technology are also being developed and tested for Alzheimer's disease (AD). A Phase I clinical trial tested the effects of rAAV2 expressing NGF in the nucleus basalis of Meynert in the basal forebrain of AD patients [Rafii *et al*, 2014]. Similar to the PD clinical trials, treatment with the viral vector construct did not result in substantial functional benefits in patients during Phase II testing [O'Connor and Boulis, 2015]. Systematic testing of the efficiency of various AAV constructs, especially AAV2, in transducing the aged versus young adult basal forebrain would provide insight into

Table 4. AAV2 Mutant Viral Constructs and Implications of Efficient Transduction in the Aged Brain.

Mutant	Mutation and Implication	Citation
Endosomal Processing	Mutation: Tyrosine residues on the capsid are mutated into phenylalanine residues. This prevents phosphorylation of the tyrosine residues that would normally trigger endosomal escape, ubiquitination of the virion, and virion degradation and results in increased transgene expression.	Zhong <i>et al</i> , 2008.
	Implication: Efficient transduction of this mutant in the aged brain would indicate that processes involving endosomal escape or virion degradation are altered in the aged brain and circumventing these steps improves transduction.	
Nuclear Translocation	Mutation: Threonine residues on the capsid are mutated to valine residues. This prevents the phosphorylation of the threonine residues that would normally inhibit nuclear import of the virion and increases transgene expression.	Aslanidi <i>et al</i> , 2013
	Implication: Efficient transduction of this mutant in the aged brain would indicate that processes involving nuclear import are altered in the aged brain and circumventing these issues improves transduction.	
HSPG Binding	Mutation: Receptor binding motifs on the capsid are mutated to prevent binding to HSPG. This completely abolishes binding to HSPG and results in increased transgene expression.	Xu <i>et al</i> , 2005; Boyle <i>et al</i> , 2006
	Implication: Efficient transduction of this mutant in the aged brain would indicate virion binding to HSPG is altered in the aged brain. This could be due to prevention of virion sequestration by increased levels of HSPG in the aged extracellular matrix or circumventing impairments in HSPG-mediated steps of transduction.	
Conversion of ssDNA to dsDNA	Mutation: The conventional single stranded DNA genome is replaced by a self-complementary AAV genome. This circumvents the rate-limiting step of converting ssDNA to dsDNA through strand-annealing or second-strand synthesis and increases transgene expression.	McCarty <i>et al</i> , 2001; McCarty <i>et al</i> , 2003; Chan <i>et al</i> , 2011
	Implication: Efficient transduction of this mutant in the aged brain would indicate that processes involving the conversion of ssDNA to dsDNA are altered in the aged brain and circumventing these issues improves transduction.	

Abbreviations: HSPG, heparan sulfate proteoglycan; ssDNA, single stranded DNA; dsDNA, double stranded DNA.

whether the preclinical trials using young adult animals resulted in overly optimistic results which led to clinical testing.

iv. Expanding Investigation to other Species, Ages, and Sexes

Although the age-related transduction deficiencies in the rat are robust in that they occur regardless of duration of expression, rat strain, and transgene expressed, it is unclear whether this is a rat-specific phenomenon. An important step in determining whether these age-related transduction deficiencies in the rat occur in the human clinical trials will be directly comparing the transduction deficiency of viral vectors like rAAV2 in the young adult versus aged NHP. Although a previous study did compare rAAV2 transduction efficiency between young adult and aged NHPs, the titer used in the aged monkeys was significantly greater than that used in young adult monkeys [Bartus *et al*, 2011]. In this study, a higher vector titer and volume used in the aged NHPs resulted in similar transduction and transgene expression profiles as a lower titer and volume used in young adult NHPs, indicating a possible deficiency in transduction in the aged NHP [Bartus *et al*, 2011]. Systematically comparing the transduction efficiency between young adult and aged NHPs will provide valuable information regarding whether the age-related transduction deficiencies we observed in rats occur in higher-order species like NHPs and humans.

In addition, investigating when these transduction deficiencies begin will be an important extension of this research. Comparing the efficiency of these viruses in young adult, middle aged, and aged animals will allow greater insight into these deficiencies and a better guide for which viral constructs are best suited during the lifespan of animals. Finally, every study investigating transduction efficiency in the young adult versus aged brain to date has been performed in male animals [Wu *et al*, 2004; Klein *et al*, 2010; Fischer *et al*, 2016]. Future studies need to also factor sex into investigations of transduction in

the aged brain. This is especially important as estrogen has the potential to impact levels of the receptors used for viral binding and endocytosis [Damian-Matsumura *et al*, 1999]. In future studies of young adult and aged female rats, caution must be taken in monitoring the estrous cycle stage of the young adult rats for vector injections and interpretation of results.

v. Investigating the Impact of Age and Parkinson's Disease Pathology on Transduction

It is important to note that the age-related transduction deficiencies characterized in this dissertation occurred in the naïve, unlesioned brain. Additional cellular impairments that result from PD or AD pathogenesis could further impair viral vector transduction efficiency. As one example of this, denervation of the striatum can impact the level of retrograde transport of GDNF from the striatum to the SN following rAAV2 GDNF injections into the striatum of young adult rats [Ciesielska *et al*, 2011]. It is quite possible that age-related impairments in cellular processes are further exacerbated by neurodegenerative disease-mimicking lesions (e.g. viral vector-mediated α -syn overexpression or 6-OHDA induced axonal degeneration). This would be important to investigate for the design of clinical trials for age-related neurodegenerative diseases and designs of experiments using viral vectors in aged animal models of neurodegenerative diseases.

An ideal way to test this would be to examine the transduction efficiency of various viral vector constructs in animals that received a unilateral disease-modeling lesion. For example, animals could receive a unilateral lesion such as the 6-OHDA injection to the SNpc to mimic robust degeneration of the nigrostriatal system in PD. After the lesion has resulted in near-complete loss of the SNpc dopaminergic neurons (about four weeks post-lesion), animals could receive bilateral injections of GFP-expressing viral vectors to the striatum or SNpc to determine how parkinsonian lesions impact age-related differences in transduction. Furthermore, a bicistronic viral vector that expresses both GFP and GDNF could be used

for more clinical relevance. Similar to characterizing transduction efficiency in the naïve brain, it would be important to further investigate the role of disease-state in females and higher-order species like the NHP.

II. rAAV2/2 GDNF Transduction after Intrastratial Injection

In order to expand our knowledge of the clinical- and biological-relevance of the age-related transduction deficiencies observed in rat brain, we chose to test the impact of age on transduction using the design of an ongoing clinical trial for PD. In doing so, we tested the transduction efficiency and downstream neuroprotective signaling one month following rAAV2 GDNF injection in the striatum. Although transduction deficiencies were observed at the level of GDNF protein in numerous structures of the basal ganglia, additional experiments could answer some remaining questions. Although some studies have reportedly found no differences in GDNF expression in the aged versus young adult rat and NHP striatum [Collier *et al*, 2004; Yurek *et al*, 2015], at least one study has reported an age-related decrease in GDNF expression in the rat striatum [Yurek and Fletcher-Turner, 2001]. Furthermore, decreases in GDNF protein in the aged rat ventral midbrain have been reported [Yurek and Fletcher-Turner, 2001]. Comparing naïve GDNF levels in the young adult versus aged rat basal ganglia would be important to see if differences in endogenous levels of GDNF expression exist and should be considered in the interpretation of our results.

In addition, future studies using injected tissue for biochemical experiments should develop sensitive measures of quality control for injection placement and infusion success to exclude failed vector injections. In our study, outlier exclusion was only performed in the hemisphere designated for ELISA measurements. Quality control and outlier exclusion were attempted in the other hemisphere as well; however, no naïve striatal tissue was available for measurements of endogenous GDNF mRNA and

immunostaining for GDNF in the SNpr did not result in detectable overexpression to confirm injection success. Verifying injection placement and success is an important step in understanding transduction efficiency and needs to be performed so failed injections do not alter the results and interpretations of data.

Future studies should also increase the amount of vector injected by either titer or volume. This increase will be important for quality control and measuring downstream GDNF signaling activation in SNpc neurons. As mentioned previously, outlier exclusion was not performed in one hemisphere due to a lack of detectable GDNF overexpression in the SNpr using histological methods. Increasing the vector dose would allow visualization of GDNF overexpression in the SNpr for proper quality control using histology. In addition, this study failed to find any upregulation of GDNF neuroprotective signaling in the SNpc of young adult or aged rats. The procedure we used to measure GDNF signaling, however, has been performed previously on multiple occasions [Decressac *et al*, 2012; Chtarto *et al*, 2016]. Increasing the titer or volume of vector injection could induce detectable activation of downstream signaling and prevent these issues in future experiments.

Finally, future experiments should use other markers of downstream GDNF signaling cascades in the young adult versus aged brain. Naïve aged rats display significantly more pS6 in the SNpc than young adult rats, thereby making any comparisons in pS6 upregulation difficult in young adult versus aged rats following intervention with a construct like rAAV2/2 GDNF. Future experiments need to compare endogenous, naïve levels of proteins involved in GDNF neuroprotective signaling in the SNpc to determine how expression of these proteins changes with age. The proteins then found to be equivalent between the naïve young adult and aged brain should be used to measure GDNF signaling after rAAV2/2 GDNF intrastriatal injection.

III. Mechanism of the Transduction Deficiency

A list of the possible mechanisms of the AAV age-related transduction deficiency can be found in **Table 5**.

i. Receptors

In this dissertation, we hypothesize that an age-related decrease in cell surface receptors is the mechanism of the transduction deficiencies in the aged nigrostriatal and striatonigral systems. Although supported by the rAAV2 chimera study [Dissertation Chapter 5], it is not entirely clear whether the rescue of rAAV2/2 transduction by the addition of rAAV9 receptor binding motifs is mediated purely by increased binding to N-linked galactose. The age-related deficiency in rAAV2/2 transduction could be the result of alterations in other steps of transduction that might differ between AAV2- and AAV9-receptor binding, like internalization. As a result, additional investigations into age-related changes in cell surface receptors involved in viral transduction will be necessary.

Previous studies have reported decreases in 2,3-linked sialic acid receptors (the primary receptor for AAV5) in the hippocampus [Sato *et al*, 2001] and cerebellum [Sasaki *et al*, 2002] of aged as compared to young adult rats. We hypothesized that expression of other cell surface receptors necessary for viral vector transduction also decreased in the aged brain, thus causing the decreased transduction efficiency. We sought to investigate this possibility by quantifying levels of HSPG, 2,3-linked sialic acid, and N-Gal in the young adult versus aged brain for their role in the rAAV2/2, rAAV2/5, and rAAV2/9 transduction deficiencies, respectively. Multiple attempts were made to quantify these receptors using a variety of techniques (**Table 6**). Unfortunately, quantitation of these receptors was made difficult due to the fact that most of the receptors used for viral vector transduction require specific post-translational

Table 5. Potential Mechanisms of the AAV Age-Related Transduction Deficiency.

Mechanism	Rationale	Likelihood
Neutralizing Antibodies	Transduction: Neutralizing antibodies can block transduction of specific vector serotypes as they are specific to the vector capsid [Chrimule <i>et al</i> , 1999; Peden <i>et al</i> , 2009].	Unlikely. High titers of neutralizing antibodies would block transduction of the vector regardless of structure. Two of our vectors are deficient in one structure but not the other (Chapter 3).
	Age: Neutralizing antibody titers may increase with age and exposure to natural viruses [Mimuro <i>et al</i> , 2013].	
Astrocyte Sequestration	Transduction: Astrocytes can endocytose viral particles [Furman <i>et al</i> , 2012] and endocytosis by astrocytes can decrease the number of viral particles available for neuronal transduction.	Unlikely. Performed a stain to visualize viral genomes in neurons and astrocytes in the striatum of young adult and aged rats and saw genomes primarily in neurons and rarely in astrocytes (Chapter 3).
	Age: Astrocyte numbers double in the striatum with between young adult and aged rats [Yurek <i>et al</i> , 2015] and may be sequestering a large portion of the virions.	
Changes in ECM	Transduction: The virions need to spread from the site of injection to transduce the structure of interest. The degree of spread is dependent on interactions between the vector capsid and ECM [Ding <i>et al</i> , 2005].	Unlikely. Did not see age-related changes in vector spread with rAAV2/5 two weeks after injection (Chapter 2). Also did not see differences in spread one month after striatal injection for all vector constructs (Chapter 3)
	Age: Age-related changes in the composition of the ECM could impair vector spread from the site of injection [Morawski <i>et al</i> , 2014].	
Receptors and Co-Receptors	Transduction: Binding to receptors and co-receptors is an important step for viral attachment and internalization into cells and is capsid-dependent [Nonnenmacher and Weber, 2012].	Likely. Altering the ability of a virus to bind to receptors used by constructs that are not deficient with age eliminates the age-related transduction deficiency (Chapter 5). Receptor measurement experiments are ongoing.
	Age: Age-related decreases in receptors necessary for rAAV transduction have been observed in other brain structures [Sato <i>et al</i> , 2001; Walters <i>et al</i> , 2001; Sasaki <i>et al</i> , 2002].	
Endocytosis	Transduction: Viral particles are internalized via clathrin-mediated endocytosis or caveolar endocytosis [Nonnenmacher and Weber, 2012].	Possible. Has not been investigated. Could indirectly investigate by measuring age-related changes in proteins necessary for endocytosis.
	Age: Altered clathrin dynamics are observed in the aged brain [Park <i>et al</i> , 2001; Blanpied <i>et al</i> , 2003].	

Abbreviations: ECM, extracellular matrix; rAAV, recombinant adeno-associated virus; ssDNA, single stranded DNA; dsDNA, double stranded DNA; mRNA, messenger RNA; GFP, green fluorescent protein; SNpc, substantia nigra pars compacta; GDNF, glial cell line-derived neurotrophic factor; GFP+, GFP immunoreactive; TH+, tyrosine hydroxylase immunoreactive.

Table 5 (cont'd).

Mechanism	Rationale	Likelihood
Intracellular Trafficking and Degradation	Transduction: Intracellular trafficking and processing within endosomes is necessary for transporting virions to the nucleus and release from endosomes [Nonnenmacher and Weber, 2012]. Phosphorylation of tyrosine residues can lead to proteasomal degradation of the virions [Schultz and Chamberlain, 2008].	Possible. Has not been investigated. Could gain insight through the use of vector mutants that avoid proteasomal degradation pathways (Table 3).
	Age: Deficient trafficking due to mitochondrial dysfunction leading to energetics issues [Bender <i>et al</i> , 2006] or increased kinase activity leading to increased proteasomal degradation could impair transduction.	
Nuclear Translocation	Transduction: Internalization of vector particles into the nucleus is a rate-limiting step of transduction and dependent on nuclear localization signals on the capsid [Nicolson and Samulski, 2014].	Possible. Has not been investigated. Could gain insight through measures of cytoplasmic vs nuclear vector genomes using cell fractionation and qPCR for the vector promoter [Zaghloul <i>et al</i> , 2013].
	Age: The process may become slower and less efficient with age, causing a buildup of virions outside the nucleus.	
Conversion of ssDNA to dsDNA	Transduction: Conversion of ssDNA to dsDNA is a rate-limiting step of transduction [Sanlioglu <i>et al</i> , 2001].	Unlikely. The genome of each viral construct is identical, so deficiencies should be observed with all or no viruses. We see deficiencies in some, but not all viral constructs (Chapter 3).
	Age: Strand annealing or second strand synthesis via DNA repair mechanisms could be impaired with age [Lombard <i>et al</i> , 2005].	
Transcription	Transduction: Conversion of vector transgene dsDNA to mRNA is necessary for transduction [Schultz and Chamberlain, 2008].	Unlikely. The genome of each viral construct is identical, so deficiencies should be observed with all or no viruses. We see deficiencies in some, but not all viral constructs (Chapter 3).
	Age: Age-related impairments in transcription could lead to lower-efficiency transcription and lower measures of transduction [Lee <i>et al</i> , 2000; Gao <i>et al</i> , 2013].	
Translation	Transduction: Translation of vector genome mRNA to protein is necessary for end-stage transduction [Schultz and Chamberlain, 2008].	Unlikely. The genome of each viral construct is identical, so deficiencies should be observed with all or no viruses. We do not see this (Chapter 3). Also observed lower GFP mRNA two weeks post-injection in SNpc (Chapter 2).
	Age: Age-related impairments in protein synthesis could lead to lower measures of transduction [Smith <i>et al</i> , 1995; Ryazanov and Nefsky, 2002].	

Table 5 (cont'd).

Mechanism	Rationale	Likelihood
Protein Degradation	Transduction: Protein degradation leads to degradation of the virions and transgene protein in the cytoplasm [Schultz and Chamberlain, 2008].	Unlikely. The genome of each viral construct is identical, so deficiencies should be observed with all or no viruses. We see deficiencies in some, but not all viral constructs (Chapter 3). Could test degradation of the virions with the endosomal processing mutant (Table 3)
	Age: Rates of protein degradation in the aged brain are lower than rats in young adult brains due to impairments in proteasome and lysosome function [Smith <i>et al</i> , 1995; Ryazanov and Nefsky, 2002]	
Anterograde Transport	Transduction: Efficient anterograde transport of the transgene is necessary for accurate measures of transduction efficiency in the anterograde structure of the system (striatum in nigrostriatal system and SNpr in striatonigral system).	Possible. Deficiencies could be due to low levels of vector toxicity impairing transport without decreasing cell phenotype or initiating cell death.
	Age: Aged cells could have impaired anterograde transport resulting from impaired cellular processes with age [Viancour and Kreiter, 1993].	Unlikely due to observance of deficiencies at injection site with rAAV2 GDNF in the striatum (Chapter 4) and deficiencies in GFP+/TH+ counts in the SNpc (Chapter 3).

Table 6. Catalogued Attempts at Quantifying AAV2, AAV5, and AAV9 Receptor Levels.

Receptor	Tissue	Method	Attempt	Result
HSPG	N/A	IHC	Only rodent-reactive antibodies raised in rat	Unable to perform stain
	Unfixed, frozen punches	WB	No primary delete and multiple dilutions of antibody	No bands in HSPG wavelength in any attempt
	Unfixed, frozen punches	WB	Same as before with new secondary for HSPG	No bands in HSPG wavelength in any attempt
	Cryostat sectioned, acetone fixed, 10um	ZG	Ran analyses on tissue sections from multiple perfusion days and sectioning in Boston vs Grand Rapids	Relative abundances of post-translational modifications obtained. Will gather absolute abundances in new tissue set
2,3-linked sialic acid	Microtome sectioned, para post-fixed, 40um	LHC	No primary delete and multiple dilutions of lectin (DAB chromagen)	No staining in primary delete but stain very abundant and diffuse
	Microtome sectioned, para post-fixed, 40um	LHC	Multiple lectin incubation times (DAB chromagen)	Stain equivalent between different incubations. Very diffuse and seemingly non-specific
	Microtome sectioned, para post-fixed, 40um	LHC	Addition of neuraminidase control to remove receptors (DAB chromagen)	Neuraminidase did not remove any staining.
	Microtome sectioned, para post-fixed, 40um	LHC	Antigen retrieval using protocol provided by collaborator and testing of multiple lectin incubation times (DAB chromagen)	No difference in staining with antigen retrieval. Called lectin supplier and they said antigen retrieval will eliminate 2,3-linkages and staining.
	Cryostat sectioned, acetone fixed, 10um	LHC	No primary delete and multiple dilutions of lectin (DAB chromagen)	Staining starting to appear possibly neuronal in cortex. Very high background
	Cryostat sectioned, acetone fixed, 10um	LHC	No primary delete and multiple dilutions of lectin with TH counterstain (fluorescent)	Staining possibly more specific and displaying neuronal outlines
	Cryostat sectioned, acetone fixed, 10um	LHC	No primary delete, one dilution of lectin, and one treatment with sialidase to remove receptors. TH counterstain. (fluorescent)	No stain in primary delete, repeated stain with lectin addition, reduction of lectin staining with sialidase.

Abbreviations: HSPG, heparan sulfate proteoglycan; IHC, immunohistochemistry; WB, Western blot; ZG, Zia Glycomics method; DAB, 3,3'-diaminobenzadine; LHC, lectin histochemistry; TH, tyrosine hydroxylase; SNpc, substantia nigra pars compacta; BSA, bovine serum albumin.

Table 6 (cont'd).

Receptor	Tissue	Method	Attempt	Result
2,3-linked sialic acid	Cryostat sectioned, acetone fixed, 10um	LHC	Full run of tissue with one section from each brain treated with sialidase. TH counterstain (fluorescent)	Normalized stain to sialidase-treatment. No quantifiable difference between young adult and aged levels in the SNpc.
	Unfixed, frozen punches	WB	No primary delete and multiple dilutions of lectin	Bands in no primary control with streptavidin secondary. Bands exaggerated with lectin addition.
	Unfixed, frozen punches	WB	No primary delete, one test sample with one dilution of lectin tested, and BSA positive control added.	Bands in no primary control but not in BSA positive control. Complete smear in test sample with lectin.
	Cryostat sectioned, acetone fixed, 10um	ZG	Have not extracted or analyzed levels of receptor in tissue yet	Pending
N-linked galactose	Microtome sectioned, para post-fixed, 40um	LHC	Antigen retrieval using protocol provided by collaborator and testing of multiple lectin incubation times (DAB chromagen)	No staining in any group. Even with prolonged DAB incubation.
	Microtome sectioned, para post-fixed, 40um	LHC	Antigen retrieval using pressure cooker method (DAB chromagen)	No staining in tissue except background where tissue bubbled from antigen retrieval
	Cryostat sectioned, acetone fixed, 10um	LHC	Antigen retrieval using pressure cooker method with no primary delete and test dilution of lectin (DAB chromagen)	Some staining present but only in white matter tracks. Seems non-specific.
	Unfixed, frozen punches	WB	No primary delete and multiple dilutions of lectin	Bands in no primary control with streptavidin secondary. Additional bands with lectin that increase with lectin concentration
	Unfixed, frozen punches	WB	No primary delete, one test sample with one dilution of lectin tested, and BSA positive control added.	Bands in no primary control but not in BSA positive control. Additional bands in test sample with lectin addition but not where predicted
	Cryostat sectioned, acetone fixed, 10um	ZG	Ran analyses on tissue sections from Grand Rapids perfusion and sectioning	No levels of glycans detected in rat samples but detected in bovine cortex control.
	Cryostat sectioned, acetone fixed, 10um	ZG	Have not extracted or analyzed levels of receptor in new tissue set yet	Pending

modifications that cannot be detected by traditional antibodies. As a result, we attempted to quantify these receptors using immunohistochemistry, lectin histochemistry, and Western blotting but were unable to successfully achieve this goal. In addition, a newly discovered universal AAV receptor [Pillay et al, 2016] has been uncovered and it remains unclear whether the available antibodies will allow for accurate measurement of this receptor in brain tissue using Western blots.

Given our inability to accurately measure capsid receptors using the approaches described in Table 5, we have sought the expertise provided by an ongoing collaboration with Dr. Joseph Zaia of Boston University. Dr. Zaia is a glycomics expert who has recently developed a method for quantifying specific post-translational modifications and glycan signatures on proteins in fresh frozen tissue slices and punches (Figure 25) [Shao et al, 2013; Turiak et al, 2014]. In this collaboration, we have provided and will continue to provide Dr. Zaia with cryostat-sectioned tissue of the young adult and aged rat striatum and SNpc for glycan analyses. He will use multiple rounds of enzymatic digestions to serially extract our proteins and glycans of interest, followed by liquid chromatography-mass spectrometry to quantify the glycan signature within the samples. This is an ongoing collaboration and the need to troubleshoot tissue preparation and train a new student at Boston University has slowed data collection. Recently, Dr. Zaia was able to collect data providing the levels of relative abundance of the different post-translational modifications related to HSPG in the young adult and aged rat striatum, demonstrating feasibility of this approach (Figure 32). We will continue these investigations by collecting absolute abundances of HSPG, as well as levels of N-glycans (AAV9 receptor) and 2,3-linked sialic acid (AAV5 receptor), in the near future.

It is important to note that care should be taken when interpreting data from receptor-measurement experiments. Although HSPG, 2,3-linked sialic acid, and N-Gal have been shown to be necessary for viral

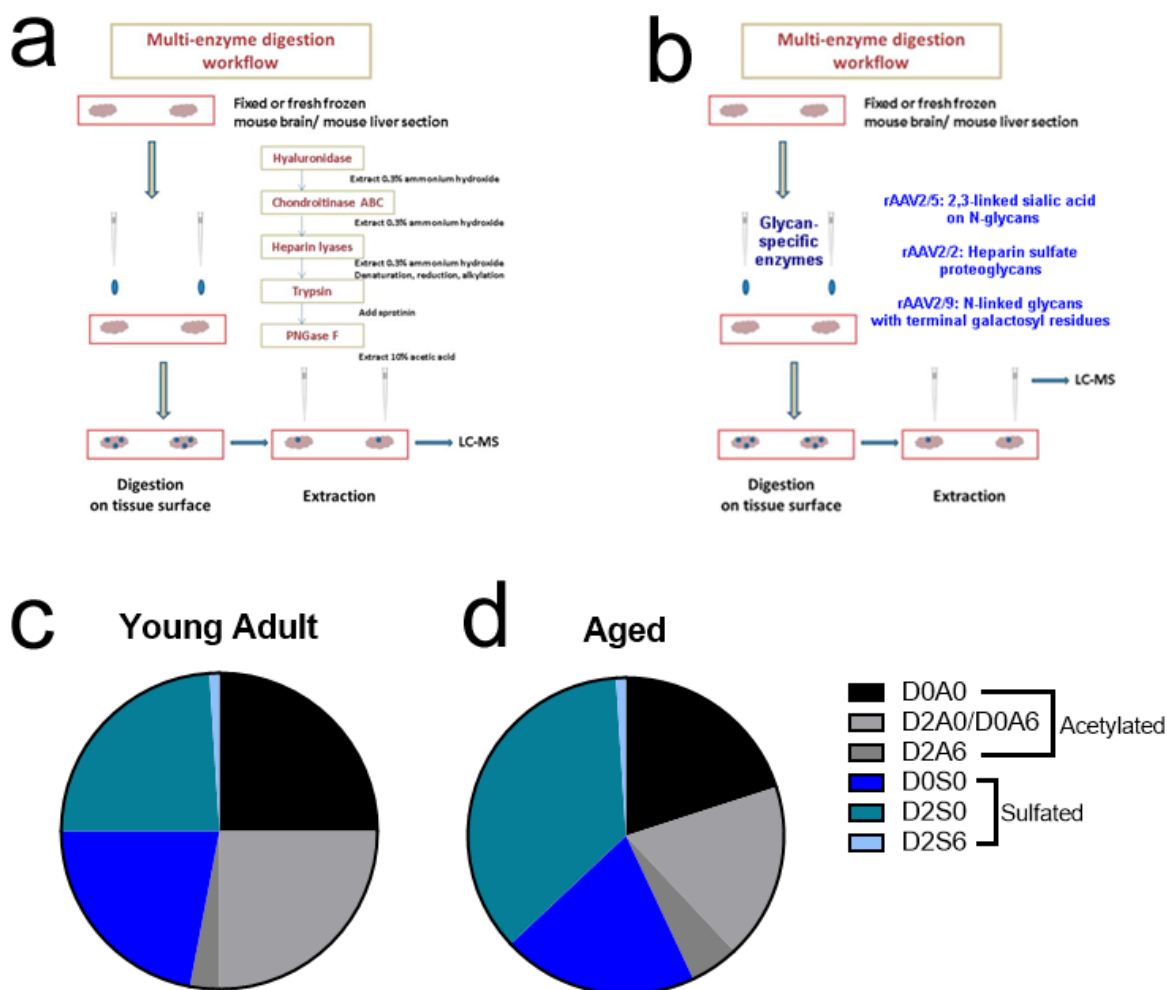


Figure 32. Workflow of the LC-MS proteomics and glycomics analyses by Dr. Joseph Zaia. General workflow provided by Dr. Zaia dictating a) the enzymes used or b) the extraction of receptors involved in AAV2, AAV5, and AAV9 transduction. Briefly, fresh frozen rat brain tissue from young and aged rats will be sectioned on a cryostat at 10 μ m and immediately mounted on a slide. Slides are then post-fixed with brief immersion in acetone and the structure of interest is outlined on the back of the slide. Tissue undergoes serial digestion with glycan-specific enzymes and digestates are extracted immediately after enzyme application for LC-MS quantitation of the individual glycans. Figure taken (a) or adapted (b) from Turiak *et al*, 2014. c-d) Relative abundances of different post-translational modifications on HSPG extracted from the striatum of (c) young adult or (d) aged rats. Acetylations are depicted in greyscale and sulfations are depicted in blue. Abbreviations: LC-MS, liquid chromatography mass spectrometry.

transduction [Summerford and Samulski, 1998; Walters *et al*, 2001; Shen *et al*, 2012], emerging evidence suggests virions may be able to infect cells using other mechanisms when primary receptors are absent [Boyle *et al*, 2006]. Changes in secondary receptors for these viral constructs could also be contributing to the deficiency rather than changes in the primary receptors [Dissertation Chapter 1, Table 1]. In addition, none of our receptor measurement studies investigate the number of cell surface receptors in our particular cell populations of interest. Although attempts were made to dual-label dopaminergic neurons of the SNpc with markers of cell surface receptors, these stains were not successful even after months of troubleshooting (**Table 6**). Although the glycomics experiments with Dr. Zaia allow for brain structure specificity, this technique does not allow the isolation of one cell population in particular and will collect levels of these receptors from the cell surface as well as the extracellular matrix. These factors should be considered when interpreting the results of receptor quantitation.

ii. Downstream Steps of Transduction

As previously mentioned, although our chimera study indicates a role for age-related changes in viron-receptor interactions in the transduction deficiency of viral vectors in the aged brain, it is still unclear what the exact mechanism of the transduction deficiency is and whether other steps of transduction are also impaired in the aged brain. For instance, although our chimera experiment indicates the AAV2 deficiency in the nigrostriatal system is most likely receptor-mediated, this does not rule out additional steps of endocytosis and intracellular trafficking as these are also controlled by receptors and could be contributing to the deficiency [Nonnenmacher and Weber, 2012]. In addition, the mechanism of the deficiency in the striatum is not necessarily identical to the mechanism of the deficiency in the SNpc. Cell fractionation experiments measuring viral particles in the membrane/endosomal, cytoplasmic, and

nuclear fractions would provide an interesting look into where age-related differences in virion numbers are present and may help investigate the mechanism of the transduction deficiency further.

Final Remarks

The need to develop better symptomatic and disease-modifying treatments for age-related diseases such as PD is more important now than ever due to the aging of the Baby Boomer generation leading to an increased prevalence of age-related neurodegenerative diseases. Although viral vector-mediated gene therapy is a promising strategy for altering progression of these diseases, this therapy needs to be optimized to efficiently deliver the transgene of interest to the aged brain. The findings presented in this dissertation highlight this need by uncovering robust age-related deficiencies in structures of the brain related to PD treatment. This information will hopefully guide optimization efforts and highlight the need to account for aging when studying treatments and modeling of diseases in the aged animal brain. Furthermore, clinical trials using viral vectors to treat age-related diseases like AD and PD can hopefully use this information to interpret past trials and inform the design of future trials that will be more successful in delivering genes to combat neurodegenerative disease symptoms or progression.

LITERATURE CITED

LITERATURE CITED

- Aslanidi, G.V., A.E. Rivers, L. Ortiz, L. Song, C. Ling, L. Govindasamy, K. Van Vliet, M. Tan, M. Agbandje-McKenna, and A. Srivastava. (2013). Optimization of the capsid of recombinant adeno-associated virus 2 (AAV2) vectors: the final threshold? *PLoS One*, **8(3)**: e59142.
- Bartus, R.T., C.D. Herzog, Y. Chu, A. Wilson, L. Brown, J. Siffert, E.M. Johnson Jr, C.W. Olanow, E.J. Mufson, and J.H. Kordower. (2011). Bioactivity of AAV2-neurturin gene therapy (CERE-120): differences between Parkinson's disease and nonhuman primate brains. *Mov Disord*, **26(1)**: 27-36.
- Bender, A., K.J. Krishnan, C.M. Morris, G.A. Taylor, A.K. Reeve, R.H. Perry, E. Jaros, J.S. Hersheson, J. Betts, T. Klopstock, R.W. Taylor, and D.M. Turnbull. (2006). High levels of mitochondrial DNA deletions in substantia nigra neurons in aging and Parkinson's disease. *Nat Gen*, **38(5)**: 515-517.
- Blanpied, T.A., D.B. Scott, and M.D. Ehlers. (2003). Age-related regulation of dendritic endocytosis associated with altered clathrin dynamics. *Neurobiol Aging*, **24**: 1095-1104.
- Boyle, M.P., R.A. Enke, J.B. Reynolds, P.J. Mogayzel, W.B. Guggino, and P.L. Zeitlin. (2006). Membrane-associated heparan sulfate is not required for AAV-2 infection of human respiratory epithelia. *Virology*, **3**: 29.
- Burger, C., O.S. Gorbatyuk, M.J. Velardo, C.S. Peden, P. Williams, S. Zolotukhin, P.J. Reier, R.J. Mandel, and N. Muzyczka. (2004). Recombinant AAV viral vectors pseudotyped with viral capsids from serotypes 1, 2, and 5 display differential efficiency and cell tropism after delivery to different regions of the central nervous system. *Mol Ther*, **10(2)**: 302-317.
- Cannon, J.R., T. Sew, L. Montero, E.A. Burton, and J.T. Greenamyre. (2011). Pseudotype-dependent lentiviral transduction of astrocytes or neurons in the rat substantia nigra. *Exp Neurol*, **228(1)**: 41-52.
- Chan, F., W.W. Hauswirth, T.G. Wensel, and J.H. Wilson. (2011). Efficient mutagenesis of the rhodopsin gene in rod photoreceptor neurons in mice. *Nucleic Acids Res*, **39(14)**: 5955-5966.
- Chirmule, N., K.J. Propert, S.A. Magosin, Y. Qian, R. Qian, and J.M. Wilson. (1999). Immune responses to adenovirus and adeno-associated virus in humans. *Gene Ther*, **6**: 1574-1583.
- Choudhury, S.R., E. Hudry, C.A. Maguire, M. Sena-Esteves, X.O. Breakefield, and P. Grandi. (2016). Viral vectors for therapy of neurologic diseases. *Neuropharmacology*, doi: 10.1016/j.neuropharm.2015.02.013.
- Chtarto, A., M. Humbert-Claude, O. Bockstael, A.T. Das, S. Boutry, L.S. Breger, B. Klaver, C. Melas, P. Barroso-Chinea, T. Gonzalez-Hernandez, R.N. Muller, O. DeWitte, M. Levivier, C. Lundberg, B. Berkhout, and L. Tenenbaum. (2016). A regulatable AAV vector mediated GDNF biological effects at clinically-approved sub-antimicrobial doxycycline doses. *Mol Ther Methods Clin Dev*, **5**: 16027.

- Ciesielska, A., G. Mittermeyer, P. Hadaczek, A.P. Kells, J. Forsayeth and K.S. Bankiewicz. (2011). Anterograde axonal transport of AAV2-GDNF in rat basal ganglia. *Mol Ther*, **19(5)**: 922-927.
- ClinicalTrials.gov. (2016). AAV2-GDNF for Advanced Parkinson s Disease (NCT01621581). <https://http://www.clinicaltrials.gov/ct2/show/NCT01621581?term=gdnf&rank=1>.
- Collier, T.J., Z. Dung Ling, P.M. Carvey, A. Fletcher-Turner, D.M. Yurek, J.R. Sladek Jr, and J.H. Kordower. (2005). Striatal trophic factor activity in aging monkeys with unilateral MPTP-induced parkinsonism. *Exp Neurol*, **191(Suppl 1)**: S60-S67.
- Damian-Matsumura, P., V. Zaga, A. Maldonado, C. Sanchez-Hernandez, C. Timossi, and A. Ulloa-Aguirre. (1999). Oestrogens regulate pituitary alpha2,3-sialyltransferase messenger ribonucleic acid levels in the female rat. *J Mol Endocrinol*, **23(2)**: 153-165.
- Davidson, B.L., C.S. Stein, J.A. Heth, I. Martins, R.M. Kotin, T.A. Derksen, J. Zabner, A. Ghodsi, and J.A. Chiorini. (2000). Recombinant adeno-associated virus type 2, 4, and 5 vectors: transduction of variant cell types and regions in the mammalian central nervous system. *PNAS*, **97(7)**: 3428-3432.
- Decressac, M., B. Kadkhodaei, B. Mattsson, A. Laguna, T. Perlmann, and A. Bjorklund. (2012). Alpha-synuclein-induced down-regulation of Nurr1 disrupts GDNF signaling in nigral dopamine neurons. *Science Trans Med*, **4(163)**: 163ra156.
- Ding, W., L. Zhang, Z. Yan, and J.F. Engelhardt. (2005). Intracellular trafficking of adeno-associated viral vectors. *Gene Ther*, **12**: 873-880.
- Dodiya, H.B., T. Bjorklund, J. Stansell III, R.J. Mandel, D. Kirik, and J.H. Kordower. (2010). Differential transduction following basal ganglia administration of distinct pseudotyped AAV capsid serotypes in nonhuman primates. *Mol Ther*, **18(3)**: 579-587.
- Emborg, M.E., J. Moirano, J. Raschke, V. Bondarenko, R. Zufferey, S. Peng, A.D. Ebert, V. Joers, B. Roitberg, J.E. Holden, J. Koprach, J. Lipton, J.H. Kordower, and P. Aebischer. (2009). Response of aged parkinsonian monkeys to in vivo gene transfer of GDNF. *Neurobiol Dis*, **36(2)**: 303-311.
- Fischer, D.L., S.E. Gombash, C.J. Kemp, F.P. Manfredsson, N.K. Polinski, M.F. Duffy, and C.E. Sortwell. (2016). Viral vector-based modeling of neurodegenerative disorders: Parkinson's disease. *Methods Mol Biol*, **1382**: 367-382.
- Furman, J.L., D.M. Smaa, J.C. Gant, T.L. Beckett, M.P. Murphy, A.D. Bachstetter, L.J. Van Eldik, and C.M. Norris. (2012). Targeting astrocytes ameliorates neurlogic changes in a mouse model of Alzheimer's disease. *J Neurosci*, **32(46)**: 16129-161240.
- Gao, G.P., M.R. Alvira, L. Wang, R. Calcedo, J. Johnston, and J.M. Wilson. (2002). Novel adeno-associated viruses from rhesus monkeys as vectors for human gene therapy. *PNAS*, **99(18)**: 11854-11859.
- Gao, L., M. Hidalgo-Figueroa, L.M. Escudero, J. Diaz-Martin, J. Lopez-Barneo, and A. Pascual. (2013). Age-mediated trascryptomic changes in adult mouse substantia nigra. *PLoSone*, **9(4)**: e62456.

- Gurda, B.L., C. Raupp, R. Popa-Wagner, M. Naumer, N.H. Olson, R. Ng, R. McKenna, T.S. Baker, J.A. Kleinschmidt, and M. Agbandje-McKenna. (2012). Mapping a neutralizing epitope onto the capsid of adeno-associated virus serotype 8. *J Virol*, **86(15)**: 7739-7751.
- Halder, S., K. Van Vliet, J.K. Smith, T.T. Duong, R. McKenna, J.M. Wilson, and M. Agbandje-McKenna. (2015). Structure of neurotropic adeno-associated virus AAVrh.8. *J Struct Biol*, **192(1)**: 21-36.
- Howard, D.B., K. Powers, Y. Wang, and B.K. Harvey. (2008). Tropism and toxicity of adeno-associated viral vector serotypes 1, 2, 5, 6, 7, 8, and 9 in rat neurons and glia in vitro. *Virology*, **372(1)**: 24-34.
- Klein, R.L., R.D. Datron, C.G. Diaczynsky, and D.B Wang. (2010). Pronounced microgliosis and neurodegeneration in aged rats after tau gene transfer. *Neurobiol Aging*, **31(12)**: 2091-2102.
- Lee, C., R. Weindruch, and T.A. Prolla. (2000). Gene-expression profile of the ageing brain in mice. *Nat Gen*, **25**: 294-297.
- Lombard, D.B., K.F. Chua, R. Mostoslavsky, S. Franco, M. Gostissa, and F.W. Alt. (2005). DNA repair, genome stability, and aging. *Cell*, **120(4)**: 497-512.
- Marks Jr., W.J., R.T. Bartus, J. Siffert, C.S. Davis, A. Lozano, N. Boulis, J. Vitek, M. Stacy, D. Turner, L. Verhagen, R. Bakay, R. Watts, B. Guthrie, J. Jankovic, R. Simpson, M. Tagliati, R. Alterman, M. Stern, G. Baltuch, P.A. Starr, P.S. Larson, J.L. Ostrem, J. Nutt, K. Kieburz, J.H. Kordower, and C.W. Olanow. (2010). Gene delivery of AAV2-neurturin for Parkinson's disease: a double-blind randomized, controlled trial. *Lancet*, **9**: 1164-1172.
- McCarty, D.M., H. Fu, P.E Monahan, C.E. Toulson, P. Naik, and R.J. Samulski. (2003). Adeno-associated virus terminal repeat (TR) mutant generates self-complementary vectors to overcome the rate-limiting step to transduction in vivo. *Gene Ther*, **10(26)**: 2112-2118.
- McCarty, D.M., P.E. Monahan, and R.J. Samulski. (2001). Self-complementary recombinant adeno-associated virus (scAAV) vectors promote efficient transduction independently of DNA synthesis. *Gene Ther*, **8(16)**: 1248-1254.
- McFarland, N.R., J. Lee, B.T. Hyman, and P.J. McLean. (2009). Comparison of transduction efficiency of recombinant AAV serotypes 1, 2, 5, and 8 in the rat nigrostriatal system. *J Neurochem*, **109**: 838-845.
- Mietzsch, M., F. Broecker, A. Reinhardt, P.H. Seeberger, and R. Heilbronn. (2014). Differential adeno-associated virus serotype-specific interaction patterns with synthetic heparins and other glycans. *J Virol*, **88(5)**: 2991-3003.
- Mimuro, J., H. Mizukami, M. Shima, T. Matsushita, M.Taki, S. Muto, S. Higasa, M. Sakai, T. Ohmori, S. Madoiwa, T. Ozawa, and Y. Sakata. (2013). The prevalence of neutralizing antibodies against adeno-associated virus capsids is reduced in young Japanese individuals. *Journal of Med Virol*, doi: 10.1002/jmv.23818.
- Morawski, M., M. Filippov, A. Tzinia, E. Tsilibary, and L. Vargova. (2014). ECM in brain aging and dementia. *Prog Brain Res*, **214**: 207-227.

- Mori, S., L. Wang, T. Takeuchi, and T. Kanda. (2004). Two novel adeno-associated viruses from cynomolgus monkey: pseudotyping characterization of capsid protein. *Virology*, **330(2)**: 375-383.
- Nicolson, S.C., and R.J. Samulski. (2014). Recombinant adeno-associated virus utilizes host cell nuclear import machinery to enter the nucleus. *J Virol*, **88(8)**: 4132-4144.
- Nonnenmacher, M., and T. Weber. (2012). Intracellular transport of recombinant adeno-associated virus vectors. *Gene Ther*, **19(6)**: 649-658.
- O'Connor, D.M., and N.M. Boulis. (2015). Gene therapy for neurodegenerative diseases. *Trends Mol Med*, **21(8)**: 504-512.
- Park, J., W. Park, K. Cho, D. Kim, B. Jhun, S. Kim, and S.C. Park. (2001). Down-regulation of amphiphysin-1 is responsible for reduced receptor-mediated endocytosis in the senescent cells. *FASEB J*, **15**: 1625-1627.
- Peden, C.S., F.P. Manfredsson, S.K. Reimsnider, A.E. Poirier, C. Burger, N. Muzyczka, and R.J. Mandel. (2009). Striatal readministration of rAAV vectors reveals an immune response against AAV2 capsids that can be circumvented. *Mol Ther*, **17(3)**: 524-537.
- Pillay, S., N.L. Meyer, A.S. Puschnik, O. Davulcu, J. Diep, Y. Ishikawa, L.T. Jae, J.E. Wosen, C.M. Nagamine, M.S. Chapman, and J.E. Carette. (2016). An essential receptor for adeno-associated virus infection. *Nature*, **530(7588)**: 108-112.
- Rafii, M.S., T.L. Baumann, R.A. Bakay, J.M. Ostrove, J. Siffert, A.S. Fleisher, C.D. Herzog, D. Barba, M. Pay, D.P. Slamon, Y. Chu, J.H. Kordower, K. Bishop, D. Keator, S. Potkin, and R.T. Bartus (2014). A phase1 study of stereotactic gene delivery of AAV2-NGF for Alzheimer's disease. *Alzheimer's Dement*, **10(5)**: 571-581.
- Raupp, C., M. Naumer, O.J. Muller, B.L. Gurda, M. Agbandje-McKenna, and J.A. Kleinschmidt. (2012). The threefold protrusions of adeno-associated virus type 8 are involved in cell surface targeting as well as postattachment processing. *J Virol*, **86(17)**: 9396-9408.
- Reimsnider, S., F.P. Manfredsson, N. Muzyczka, and R.J. Mandel. (2007). Time course of transgene expression after intrastriatal pseudotyped rAAV2/1, rAAV2/2, rAAV2/5, and rAAV2/8 transduction in the rat. *Mol Ther*, **15(8)**: 1504-1511.
- Ryazanov, A.G., and B.S. Nefsky. (2002). Protein turnover plays a key role in aging. *Mech Age Dev*, **123**: 207-213.
- Sanlioglu, S., M.M. Monick, G. Luleci, G.W. Hunninghake, and J.F. Engelhardt. (2001). Rate limiting steps of AAV transduction and implications for human gene therapy. *Curr Gene Ther*, **1**: 137-147.
- Sasaki, T., Y. Akimoto, Y. Sato, H. Kawakami, H. Hirano, and T. Endo. (2002). Distribution of sialoglycoconjugates in the rat cerebellum and its change with age. *J Histo Cyto*, **50(9)**: 1179-1186.

- Sato, Y., Y. Akimoto, H. Kawakami, H. Hirano, and T. Endo. (2001). Location of aialoglycoconjugates containing the sialyl- α 2-3Gal and sialyl- α 2-6Gal groups in the rat hippocampus and the effect of aging on their expression. *J Histo Cyto*, **49(10)**: 1311-1319.
- Schultz, B.R., and J.S. Chamberlain. (2008). Recombinant adeno-associated virus transduction and integration. *Mol Ther*, **16(7)**: 1189-1199.
- Shao, C., X. Shi, J.J. Phillips, and J. Zaia. (2013). Mass spectral profiling of glycosaminoglycans from histological tissue surfaces. *Anal Chem*, **85(22)**: 10984-10991.
- Shen, S., K.D. Bryant, S.M. Brown, S.H. Randell, and A. Asokan. (2011). Terminal N-linked galactose is the primary receptor for adeno-associated virus 9. *J Biol Chem*, **286**: 13532-13540.
- Smith, C.B., Y. Sun, and L. Sokoloff. (1995). Effects of aging on regional rates of cerebral protein synthesis in the Sprague-dawley rat: examination of the influence of recycling of amino acids derived from protein degradation into the precursor pool. *Neurochem Int*, **27(4/5)**: 407-416.
- Summerford, C., and R.J. Samulski. (1998). Membrane-associated heparan sulfate proteoglycan is a receptor for adeno-associated virus type 2 virions. *J Virol*, **72(2)**: 1438-1445.
- Turiak, L., C. Shao, L. Meng, K. Kharti, N. Leymarie, Q. Wang, H. Pantazopoulos, D.R. Leon, and J. Zaia. (2014). Workflow for combined proteomics and glycomics profiling from histological tissues. *Anal Chem*, **86(19)**: 9670-9678.
- Van der Perren, A., J. Toelen, J.M. Taymans, and V. Baekelandt. (2012). Using recombinant adeno-associated viral vectors for gene expression in the brain. *Neuromethods*, **65**: 47-68.
- Viancour, T.A., and N.A. Kreiter. (1993). Vesicular fast axonal transport rates in young and old rat axons. *Brain Res*, **628(1-2)**: 209-217.
- Walters, R.W., S.M. Yi, S. Keshavjee, K.E. Brown, M.J. Welsh, J.A. Chiorini, and J. Zabner. (2001). Binding of adeno-associated virus type 5 to 2,3-linked sialic acid is required for gene transfer. *J Biol Chem*, **276**: 20610-20616.
- Wu, K., C.A. Meyers, N.K. Guerra, M.A. King, and E.M. Meyer. (2004). The effects of rAAV2-mediated NGF gene delivery in adult and aged rats. *Mol Ther*, **9(2)**: 262-269.
- Xu, J., C. Ma, C. Bass, and E.F. Terwilliger. (2005). A combination of mutations enhances the neurotropism of AAV-2. *Virology*, **341(2)**: 203-214.
- Yurek, D.M. and A. Fletcher-Turner. (2001). Differential expression of GDNF, BDNF, and NT-3 in the aging nigrostriatal system following a neurotoxic lesion. *Brain Res*, **891**: 228-235.
- Yurek, D.M., U. Hasselrot, W.A. Cass, O. Sesenoglu-Laird, L. Padegimas, and M.J. Cooper. (2015). Age and lesion-induced increases of GDNF transgene expression in brain following intracerebral injections of DNA nanoparticles. *Neuroscience*, **284**: 500-512.

- Zaghlool, A., A. Ameer, L. Nyberg, J. Halvardson, M. Grabherr, L. Cavelioer, and L. Feuk. (2013). Efficient cellular fractionation improves RNA sequencing analysis of mature and nascent transcripts from human tissue. *BMC Biotech*, **13**: 99.
- Zhong, L., B. Li, G. Jayandharan, C.S. Mah, L. Govindasamy, M. Agbandje-McKenna, R.W. Herzog, A.K. Weigle-Van Aken, J.A. Hobbs, S. Zolotukhin, N. Muzyczka, and A. Srivastava. (2008). Tyrosine-phosphorylation of AAV2 vectors and its consequences on viral intracellular trafficking and transgene expression. *Virology*, **381(2)**: 194-202.